

This file is part of the following work:

Salehisaki, Mehdi (2018) *Synthesis and reactivity of rare earth complexes involving formamidates of moderate steric bulk*. PhD Thesis, James Cook University.

Access to this file is available from:

<https://doi.org/10.25903/5d7f19a9b0767>

Copyright © 2018 Mehdi Salehisaki.

The author has certified to JCU that they have made a reasonable effort to gain permission and acknowledge the owners of any third party copyright material included in this document. If you believe that this is not the case, please email

researchonline@jcu.edu.au

Synthesis and reactivity of Rare Earth complexes involving formamidinates of moderate steric bulk

A thesis submitted for the degree of

Doctor of Philosophy

by

Mehdi Salehisaki

M.S. (Master of Engineering)

Supervisors:

Prof. Peter C. Junk

Dr. Murray Davies

College of Science and Engineering

James Cook University (JCU)

August 2018

Dedicated to my loving parents

and

my wife, Nazli

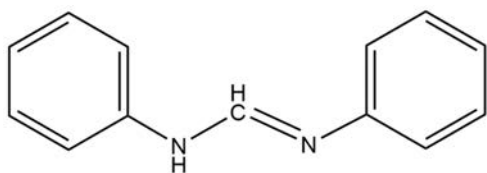
Table of Contents

Abstract	i
Declaration	iii
Acknowledgments	iv
Abbreviations	v
1 Introduction	2
1.1 Rare earth metals.....	2
1.2 Electron Configuration	3
1.3 Ligands.....	5
1.4 Organometallic chemistry of rare earth metals.....	5
1.5 Amidines.....	8
1.6 Formamidinate – metal compounds.....	12
1.6.1 <i>p</i> -TolFormH	12
1.6.2 <i>o</i> -TolFormH and HFPhF	15
1.6.3 MesFormH.....	20
1.6.4 Bulkier bis(aryl)formamidine ligands.....	24
1.7 Tishchenko reactions and reactivity.....	40
1.8 Conclusion	42
1.9 References.....	44
2 Synthesis and reactivity of RE-PhForm complexes	48
2.1 Introduction.....	48
2.2 Results and discussion.....	51
2.3 Reactivity as catalysts in Tishchenko reactions.....	67
2.4 Conclusions.....	69
2.5 Experimental	70
2.6 References.....	79
3 Rare earth- N,N'-bis(2,4-dimethyl phenyl)formamidinate (DMForm) complexes	82
3.1 Introduction.....	82
3.2 Results and discussion.....	89
3.2.1 Reactivity towards the Tishchenko reaction	100
3.3 Conclusions.....	102

3.4	Experimental	103
3.5	References.....	111
4	Synthesis and characterisation of some main group formamidinate complexes	113
4.1	Introduction.....	113
4.2	Results and discussion.....	120
4.2.1	Potassium formamidinate compounds.....	121
4.2.2	Sodium formamidinate compounds	125
4.2.3	Zinc formamidinate compound	130
4.2.4	Aluminium formamidinate compounds.....	135
4.3	Conclusions.....	137
4.4	Experimental	138
4.5	References.....	143
5	Concluding remarks.....	147
5.1	Concluding remarks.....	147
5.2	References.....	150
	Publications	151

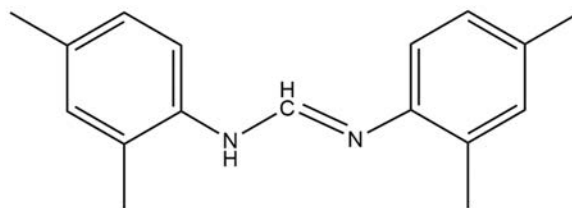
Abstract

This thesis explores the synthesis and characterisation of rare earth bis(aryl)formamidinate complexes of low to moderate steric bulk. Redox transmetallation/protolysis reactions were employed to synthesize the complexes. Reactivity of the compounds towards the Tishchenko reaction were studied using the standard reaction of benzaldehyde to form benzyl benzoate. Besides, some chemistry of Na, K, Zn and Al - bis(aryl)formamidinate complexes is also discussed. Metalation reactions of the formamidine using metal alkyls produced a range of compounds. The following bis(aryl)formamidine ligands were used for each chapter:



N,N'-(diphenyl)formamidine (PhFormH)

Chapters: 2,4



N,N'-bis(2,4-dimethyl)formamidine (DMFormH)

Chapters: 3,4

Ligands used throughout chapters two to four

Chapter **2** describes a series of rare earth PhForm complexes which were prepared by redox transmetallation/protolysis (RTP) using the rare earth metals (Tb, Ho, Er, Y, Pr, Nd, Sm, Gd, Dy and Lu), bis(pentafluorophenyl)mercury ($\text{Hg}(\text{C}_6\text{F}_5)_2$), PhFormH and using THF as solvent. Trivalent complexes with the general formula $[\text{Ln}(\text{PhForm})_3(\text{thf})_x].(\text{THF})_y$ were synthesized and characterized in this chapter. Investigation of reactivities towards the Tishchenko reaction revealed these compounds have promising catalytic properties and can be used for the Tishchenko reaction while $[\text{Y}(\text{PhForm})_3.(\text{thf})_2].(\text{THF})_3$ has the highest reactivity compared with the other compounds in this chapter.

Chapter **3** investigates rare earth DMForm complexes prepared by RTP reactions using the rare earth metals (Y, Lu, Pr, Ho, Sm, Gd and Er), bis(pentafluorophenyl)mercury ($\text{Hg}(\text{C}_6\text{F}_5)_2$) and DMFormH. Different solvents (THF, DME or DMF) were used for the reactions. As results,

trivalent complexes were synthesized with three chelating formaminate ligands about the metal centers. Study of reactivities towards the Tishchenko reaction shows the compounds in this chapter do indeed catalyse Tishchenko reaction. It was found that $[\text{Y}(\text{DMForm})_3(\text{thf})]$ has the highest reactivity towards this reaction among all the compounds synthesized in this research.

Chapter 4 is a small contribution to the main group chemistry involving PhFormH and DMFormH ligands. This chapter presents the synthesis and structural characterisation of the new complexes $[\text{K}(\text{DMForm})(\text{dme})]_{\infty}$, $[\text{K}_2(\text{PhForm})\text{N}(\text{SiMe}_3)_2]_{\infty}$, $[\text{Na}(\text{DMForm})(\text{dme})_2]$, $[\text{Na}(\text{PhForm})(\text{dme})]_2$, $[\text{Zn}_4(\text{PhForm})_6\text{O}]\cdot\text{THF}$ and $[\text{Al}(\text{PhForm})_3]$. These compounds can be used in future for metathesis and catalysis chemistry. This chapter shows decreasing steric effect of the ligand changes possible structures and bonding modes.

Overall this thesis contributes synthesis and reactivity of complexes involving formamidinates of moderate steric bulk to the fascinating field of metal-formamidinate chemistry.

Declaration

To the best of this author's knowledge, this thesis does not contain any material that has been accepted for the award of any other degree or diploma at any university or other institution, except where due reference is made in the text.

Mehdi Salehisaki

College of Science and Engineering

James Cook University

August 2018

Acknowledgments

I owe my deepest gratitude to my supervisor Prof. Peter C. Junk. Thank you for providing me with an opportunity to be part of your team. I want to thank you for helping me throughout the research and writing of this thesis. Your invaluable support during my Ph.D. made it possible to carry out this work. I am so grateful for all your patience, motivation, and immense knowledge.

I would like to express my gratitude to Prof. Glen B. Deacon (Monash University) for his valuable advice and support throughout my study. Many thanks to my secondary supervisor Dr. Murray Davies for all of his support and insightful comments and suggestions during this research. I would like to thank Dr. Jun Wang for introducing me to the techniques of working with air-sensitive chemistry in the Lab and helping with X-ray crystallography to get results of better quality.

Many thanks to all the group members (past and present), in particular, Dr. Elius, Areej, Dr. Bill, Aymeric and Dr. Safaa for your support and friendship over the years. Many thanks to the friends in office: Dr. Ioana Bowden, Dr. Simon Ho and Hannah King.

I would like to express my gratitude to the chemical staff in the discipline of chemistry at James Cook University, in particular: I would like to thank Dr. Bruce Bowden and Dr. Mark Robertson for aid with NMR experiments, to Dr. Winnie Lee and Dr. Dana Roberts for assistance with running IR.

I would like to thank James Cook University for supporting and providing me JCU Postgraduate Research Scholarship (JCUPRS), and the Australian Research Council (ARC) for funding our research project.

Last but not the least, I would like to thank my family: my parents and brother for their continuing support. Finally, I want to thank my wonderful wife and friend, Nazli, for always being by my side and for your endless love and support.

Abbreviations

PhFormH = N,N'-(diphenyl)formamidine

DMFormH = N,N'-bis(2,4-dimethyl)formamidine

RE = Rare earth (La-Lu, Sc, Y)

RTP = Redox transmetallation/protolysis

Ln = Lanthanoid metal

THF = tetrahydrofuran (solvent)

thf = tetrahydrofuran (coordinated)

DME = 1,2-dimethoxyethane (solvent)

dme = 1,2-dimethoxyethane (coordinated)

DMF = dimethylformamide (solvent)

dmf = dimethylformamide (coordinated)

Å = Angstrom, 10^{-10} m

Chapter1

Introduction

1 Introduction

Organometallic chemistry combines aspects of classical organic and inorganic chemistry. Organometallic chemistry studies involve the interactions between organic molecules and inorganic species containing metals.¹ Therefore, the number of possible organometallic compounds is almost unlimited. The suffix “metallic” in the term “organometallic” can be interpreted as the elements which are metallic (more electropositive) compared to carbon. According to this definition, derivatives of nitrogen (3.0), oxygen (3.5), sulfur (2.6), fluorine (4.0), chlorine (3.0), bromine (2.8) and iodine (2.7) are excluded from organometallic compounds because of their higher electronegativity than carbon (2.5). There is a long history regarding organometallic compounds in industry. The background refers to the 1849, when organozinc compounds discovered by Frankland² and early 1880s, when Ludwig Mond purified crude Ni with CO by heating the formed vapor of Ni(CO)₄ to deposit pure Ni. Many organometallic compounds are used as catalysts. The interest in studying organometallics is rising continuously to expand catalysis application ranges. The metal elements can be from the main group, consisting the *s* and *p* blocks or the transition metals of the *d* and *f* blocks of the periodic table. Organometallic chemistry of the transition metals, elements of groups 3–12 of the periodic table, is different from that of groups 1–2 and the *p*-block because of having electrons in their *d* valence shell.¹ The organometallic compounds consisting of rare earth metals are generally more effective toward polymerization and also Lewis acid catalysts compared to the organometallic compounds of other metals.^{1, 3, 4}

1.1 Rare earth metals

The Rare earth metals are a set of seventeen chemical elements in the periodic table, consisting of 15 lanthanoids, lanthanum to lutetium (Z=57 to 71), plus scandium and yttrium (Z=21 & 39).⁵ Scandium and yttrium exhibit similar chemical properties to lanthanoids and usually tend to occur in the same ore deposits as the lanthanoids, so they are considered as rare earth elements. Rare earth metals are attractive for organic synthesis because of their reactivity, low toxicity and availability at a moderate prices.⁶

Rare earth metals are also known by various names, such as rare earth elements (REEs), rare earth materials (REMs), rare earth oxides or yttrium based rare earth metals. Rare earth metals can be classified into two distinct categories: light rare earth elements (LREEs), consisting of lanthanum-europium, and heavy rare earth elements (HREEs), involving gadolinium-lutetium and yttrium.⁷

It has been found that the lighter lanthanoids are more abundant than the heavier ones and elements with even atomic number are more abundant than those with odd atomic number. Table 1-1 presents the abundance of the lanthanoids in the earth's crust and in the solar system.⁸

Table 1-1. Abundance of the lanthanoids in the earth's crust and in the solar system

	La	Ce	Pr	Nd	Pm	Sm	Eu	Gd	Tb	Dy	Ho	Er	Tm	Yb	Lu	Y
Crust (ppm)	35	66	9.1	40	0	7	2	6	1	5	1	4	1	3	1	31
Solar System (with respect to 107 atoms Si)	5	1.2	1.7	8.5	0	3	1	3	1	4	1	3	0	2	0	40

1.2 Electron Configuration

On crossing the series from La to Lu the basic concept is that there is a decrease in radius of the lanthanoid ion Ln^{3+} . The f orbitals of lanthanoids (and actinoids) are gradually filled. Lanthanum has the electron configuration $[\text{Xe}] 6s^2 5d^1$.⁸ In lanthanum, the $5d$ subshell is lower in energy than $4f$ so the $5d$ subshell fills before the $4f$. However, the $4f$ orbitals become more stable than the $5d$ by moving toward Lu.⁹ So electron configuration of $[\text{Xe}] 6s^2 5d^1 4f^1$ is expected for Ce. Considering the same trend, Pr has the arrangement $[\text{Xe}] 6s^2 4f^3$. For the metals Nd–Eu which have configurations $[\text{Xe}] 6s^2 4f^n$ ($n = 4-7$) this pattern continues. After europium, the next electron is added to the $5d$ orbital because of the stability of the half-filled f subshell. So, the electron configuration for Gd is $[\text{Xe}] 6s^2 5d^1 4f^7$. The earlier pattern is resumed for terbium to have the configuration $[\text{Xe}] 6s^2 4f^9$ and with the same trend, for succeeding elements to ytterbium the electron configuration is $[\text{Xe}] 6s^2 4f^n$ ($n = 10-14$). The electron configuration of $[\text{Xe}] 6s^2 5d^1 4f^{14}$ is expected for the last lanthanoid, lutetium, where the $4f$ subshell is now filled.⁸ Table 1-2 shows the electron configuration for lanthanoids and their common ions.

Table 1-2. Electron configuration of lanthanoids for their common ions

	Atom	Ln³⁺	Ln⁴⁺	Ln²⁺
La	[Xe] 5d ¹ 6s ²	[Xe]		
Ce	[Xe] 4f ¹ 5d ¹ 6s ²	[Xe] 4f ¹	[Xe]	
Pr	[Xe] 4f ³ 6s ²	[Xe] 4f ²	[Xe] 4f ¹	
Nd	[Xe] 4f ⁴ 6s ²	[Xe] 4f ³	[Xe] 4f ²	[Xe] 4f ⁴
Pm	[Xe] 4f ⁵ 6s ²	[Xe] 4f ⁴		
Sm	[Xe] 4f ⁶ 6s ²	[Xe] 4f ⁵		[Xe] 4f ⁶
Eu	[Xe] 4f ⁷ 6s ²	[Xe] 4f ⁶		[Xe] 4f ⁷
Gd	[Xe] 4f ⁷ 5d ¹ 6s ²	[Xe] 4f ⁷		
Tb	[Xe] 4f ⁹ 6s ²	[Xe] 4f ⁸	[Xe] 4f ⁷	
Dy	[Xe] 4f ¹⁰ 6s ²	[Xe] 4f ⁹	[Xe] 4f ⁸	[Xe] 4f ¹⁰
Ho	[Xe] 4f ¹¹ 6s ²	[Xe] 4f ¹⁰		
Er	[Xe] 4f ¹² 6s ²	[Xe] 4f ¹¹		
Tm	[Xe] 4f ¹³ 6s ²	[Xe] 4f ¹²		[Xe] 4f ¹³
Yb	[Xe] 4f ¹⁴ 6s ²	[Xe] 4f ¹³		[Xe] 4f ¹⁴
Lu	[Xe] 4f ¹⁴ 5d ¹ 6s ²	[Xe] 4f ¹⁴		

1.3 Ligands

Transition metals and rare earth elements can complete their subshells with electrons which can be provided by ligands to form more stable compounds. Ligands can be classified into two groups. The first group of ligands provide one or several electron pairs. This group of Lewis Base ligands is shown as L or L_n and n is the number of electron pairs donated to the metal. The bond involved in this type of ligand set is of the donor type. Therefore, L or L_n ligands do not accept valence electrons from metals. Ligands of this type are uncharged. However, the second ligands provide an odd number of electron to the metals. Ligands of this group are generally charged.

Ligands also can be classified considering their haptic number.¹⁰ Hapticity is the coordination of a ligand to a metal centre via a contiguous series of atoms.¹¹ The hapticity of a ligand is described with the η^n . Therefore, η^5 describes a ligand that coordinates through 5 contiguous atoms. According to this classification η^5 -cyclopentadienyl and η^5 -pentadienyl belong to the “-dienyl” group.¹⁰ The η -notation only applies when multiple atoms are coordinated. The maximum haptic number for unsaturated hydrocarbon ligands is equal to number of carbon atoms in an unsaturated system. In the case of coordination of one atom the κ -notation is used. Also, κ is used for describing denticity. If the ligand coordinates through multiple atoms that are not contiguous then this is considered as denticity.¹¹

1.4 Organometallic chemistry of rare earth metals

Organometallic compounds can be synthesized using different reactions. Metathesis (salt elimination) and protolysis are the common synthetic routes to prepare rare earth metal-organic compounds but redox transmetallation and redox transmetallation/protolysis are becoming more prevalent.

Metathesis reactions, according to the Equation 1-1, involve the treatment of a rare earth halide with an alkali metal form of the ligand.¹²⁻¹⁴



M = alkali metal

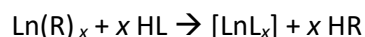
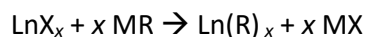
L = anionic ligand

X = halide

Equation 1-1.

In metathesis reactions the choice of lanthanoid halide and alkali metal salt as starting materials is important. For example, in many cases the use of lanthanoid trichlorides and lithium salts results in either low yields or unwanted side-products while LiCl has reasonable solubility in THF making isolation from the RE organometallic compounds difficult.¹⁴

Protolysis reaction includes treatment of a lanthanoid precursor (LnR_n) with protic agents (LH) (Equation 1-2) which is possible because of thermodynamic acidities.



R = usually $\text{N}(\text{SiMe}_3)_2$, $\text{N}(\text{SiHMe}_2)_2$ or C_6F_5

L = ligand $x = 2, 3$

X = halide

Equation 1-2.

Due to the high solubility of the reactants in common solvents, this reaction can be performed in the absence of coordinating/donor solvents.¹² Thus this route is a highly versatile approach for the synthesis of both heteroleptic and homoleptic lanthanoid complexes.¹⁵⁻¹⁷ Protolysis reactions involve two steps. The main drawback for this method is the number of steps for getting the final product. Each step often involves air and moisture sensitive compounds. Therefore, it can be difficult to get a pure product. The compounds also usually have to be prepared by metathesis with its drawbacks.

Another prominent method is redox transmetalation (Equation 1-3). This method benefits from a synthesis involving one step procedure followed by easy separation of the products.¹⁸

This method has been performed widely using different ligands like pyrazolates and phenolates^{19, 20} and using diarylmercurials as the oxidant.¹⁸



L = Anionic ligand
 n = 2, 3
 m = 1-4
 M = Usually Hg

Equation 1-3.

Redox transmetallation/protolysis (RTP) is another type of reaction for synthesizing rare earth metal-organic compounds. RTP is the reaction of a rare earth metal with a diarylmercurial such as diphenylmercury¹⁸ or bis(pentafluorophenyl)mercury^{18, 21-25} and a protic ligand (Equation 1-4).



R = C₆F₅, Ph
 L = ligand
 x = 2, 3

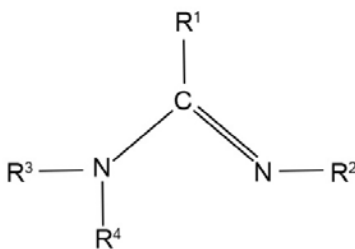
Equation 1-4.

This method is also a one-pot procedure like redox transmetallation. Therefore, compared to the metathesis and protolysis synthetic routes, it is more straightforward. Tetrahydrofuran (THF) or 1,2-dimethoxyethane (DME) are normally used in RTP reactions as the solvent. THF and DME are donor solvents. Reactions in a non-donor solvent like toluene generally need to be performed under more forcing conditions like refluxing.²⁶ Besides using mercury reagents, two or three drops of mercury can be used in the beginning of the reaction to activate the surface of rare earth metal. Involvement of mercury reagents is the main drawback of this type of reaction since it raises environmental concerns and it needs more care to perform the reaction and handling the precursors. Bis(pentafluorophenyl)mercury is a stronger oxidant compared with diphenylmercury. Performing RTP reactions using diphenylmercury is more

difficult than using $\text{Hg}(\text{C}_6\text{F}_5)_2$ due to lower reactivity, and requires activation of the metal (HgCl_2 or I_2) and heating.¹⁸

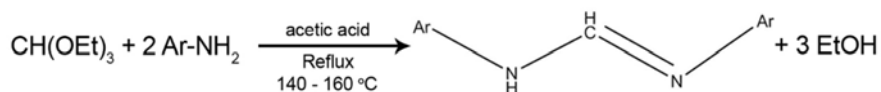
1.5 Amidines

Scheme 1-1 shows the general structure of an amidine ($\text{R}^4 = \text{H}$). Amidines are named based on the acid or amide obtained after hydrolysis.²⁷ When $\text{R}^1 = \text{CH}_3$ the compound is acetamidine; and $\text{R}^1 = \text{C}_6\text{H}_5$, benzamidine. In the case of using H as R^4 and R^1 , the compound is called a formamidine. N,N'-diarylformamidinates ($(\text{ArN})_2\text{CH}^-$, (ArForm^-)), have a special place amongst the amidinate ligands.



Scheme 1-1. The general structure of an amidine.

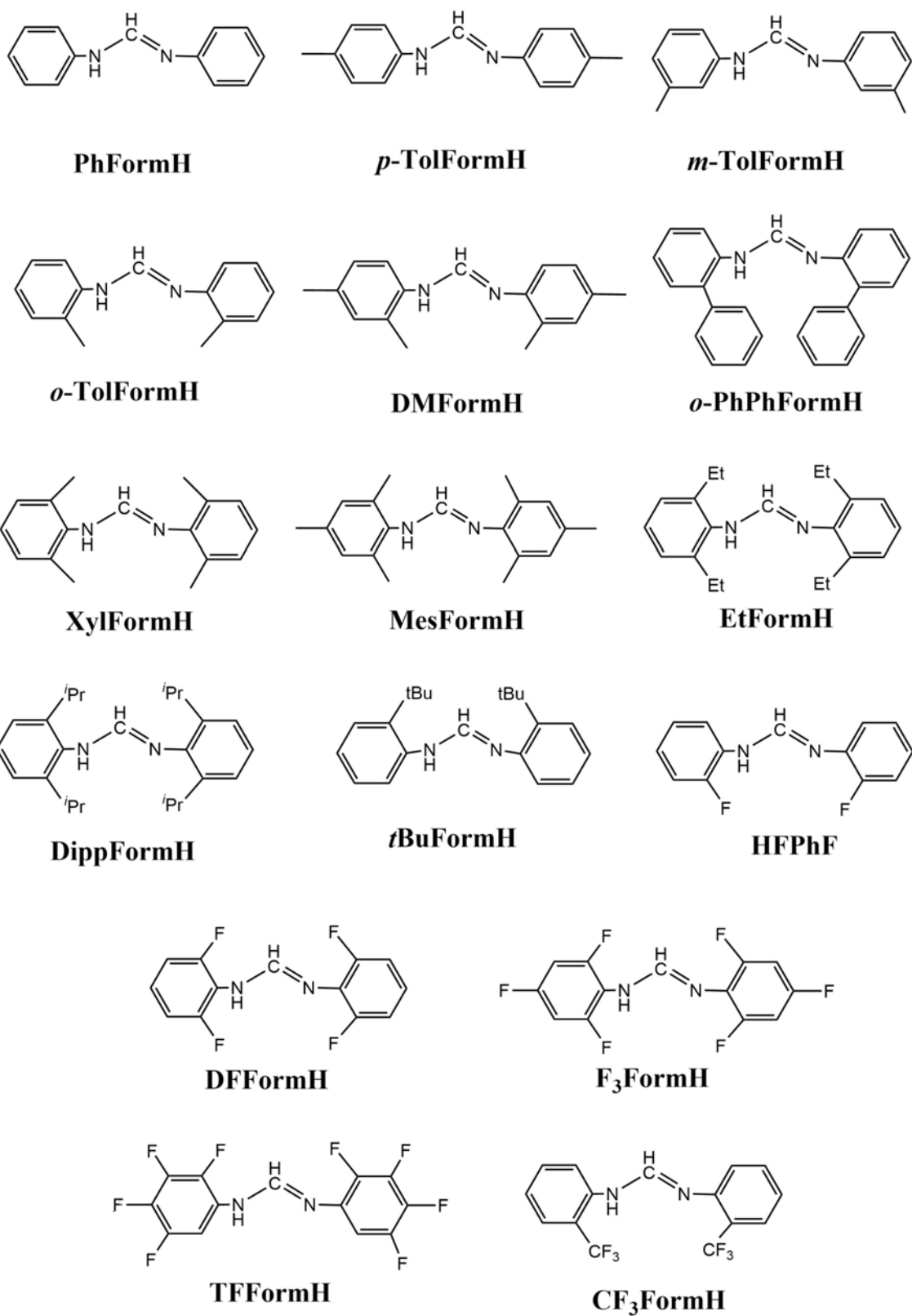
N,N'-Bis(aryl)formamidines ($\text{ArN}=\text{CH}-\text{NHAr}$ ($\text{Ar} = \text{aryl}$)) can be easily synthesized in high yields by heating to reflux one equivalent of triethyl orthoformate with two equivalents of the appropriate substituted aniline (Equation 1-5).²⁸ This reaction should be performed in the presence of acetic acid as the catalyst.



Equation 1-5.

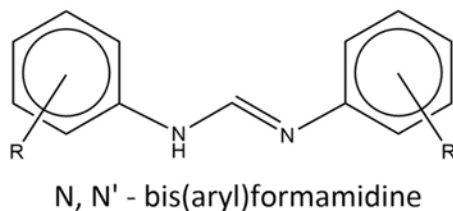
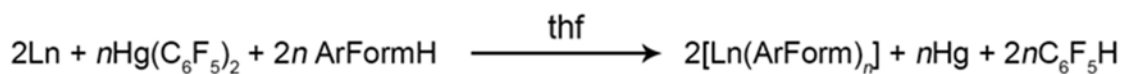
There has been a lot of interest toward using bis(aryl)formamidinates as ligands.²⁹ They can be used to kinetically stabilize group 13 hydride and low valent complexes by application of bulky variants of these ligands. Another reason is to sterically engineer carbon-fluorine bond activation. Also, they can act as anionic ligand supports for low valent compounds. These

ligands bind rare earth metals very well and they have the benefit of being able to vary the steric bulk and electronic functionality at the N donor atoms.³⁰ Moreover, rare earth amidinate complexes have a great versatility in material and chemical applications. For example, precursors that are used for atomic layer deposition of rare-earth oxide films³¹ or polymerization of olefins.³² Scheme 1-2 shows some important types of formamidine ligands. It can be seen by using different derivatives of aniline as the precursor, various formamidine ligands with different steric properties can be prepared. Therefore, different organometallic compounds with different coordination numbers can be synthesized by using different forms of formamidines which can lead to different reactivities.



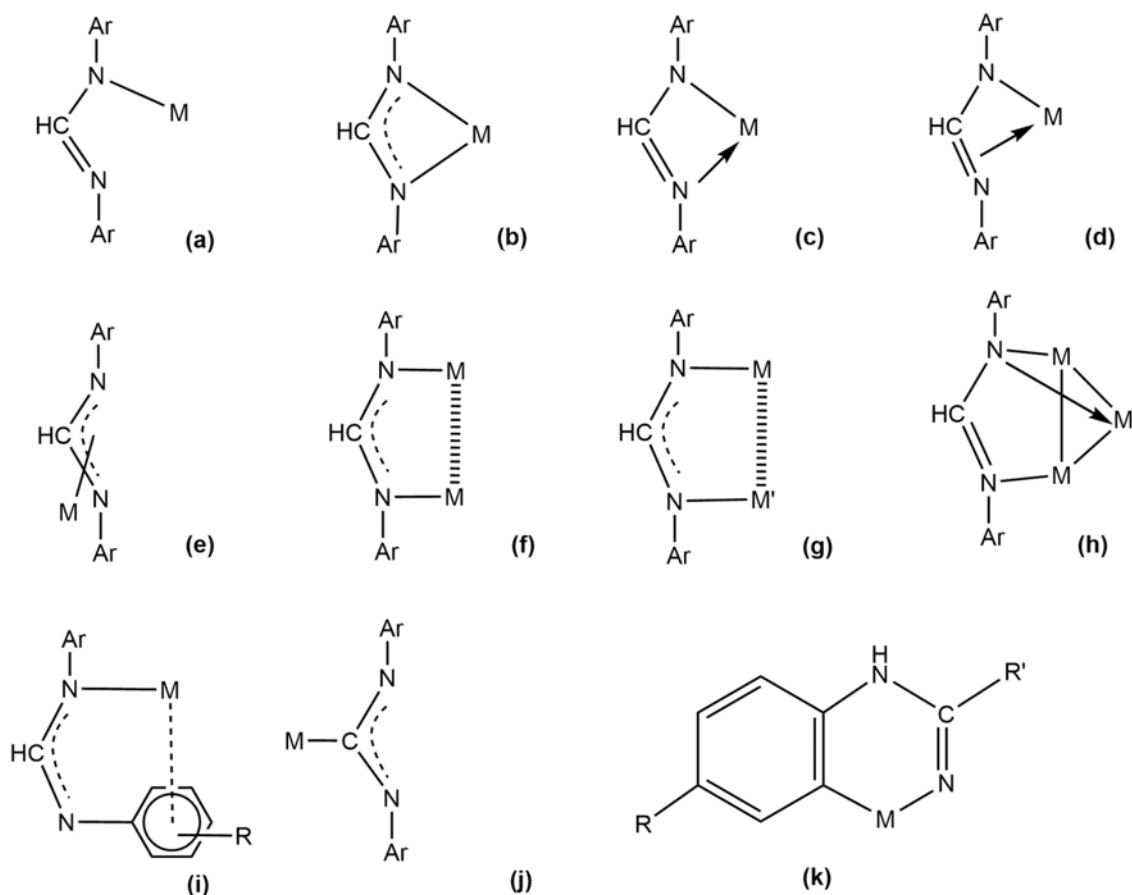
Scheme 1-2. Different formamidine ligands.

N,N'-diarylformamidinate precursors (ArFormH) have a straightforward synthesis route and their weakly acidic nature²⁹ enables them to be used in RTP reactions for producing rare earth formamidinate compounds (Equation 1-6).³⁰



Equation 1-6. Typical N,N'-bis(aryl)formamidinate ligands for using in RTP reactions.

Amidinate ligands can display various potential binding modes to metal centers. Infrared and NMR spectroscopies can be used for studying the coordination of a metal amidinate complex. However, when more than one binding mode is present and/or the complex exhibits fluxional coordination in solution, the use of these methods is complicated significantly.²⁹ Scheme 1-3 illustrates many of the possible bonding modes for the formamidinate ligands including monodentate (a), chelate (b-d), η^3 -allyl (e), bridging (f and g), capping (h), η^6 -bonding (i), C-bonded (j) and *ortho*-metallation (k).²⁷



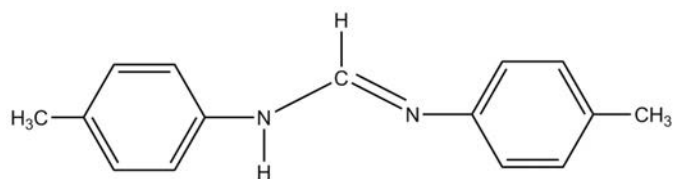
Scheme 1-3. Possible bonding modes for an amidinate ligand.

1.6 Formamidinate – metal compounds

Different formamidinate-metal compounds have been synthesized using different forms of formamidines. This chapter presents examples of using various formamidines to prepare formamidinate-metal compounds. The metals in the reviewed papers mainly involve rare earth metals and the compounds reported here in order of bulkiness of formamidinates.

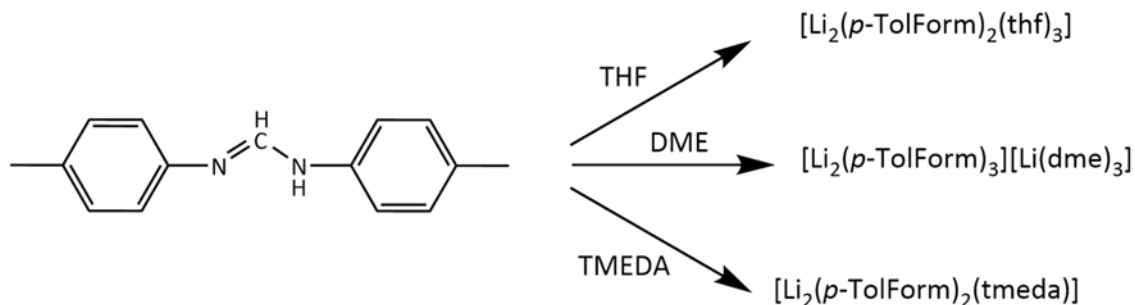
1.6.1 *p*-TolFormH

It has been found that the *N,N'*-di(*p*-tolyl)formamidine ligand, known as *p*-TolFormH (Scheme 1-4), is a versatile ligand for alkali metals and exhibits a wide variety of binding modes.³³



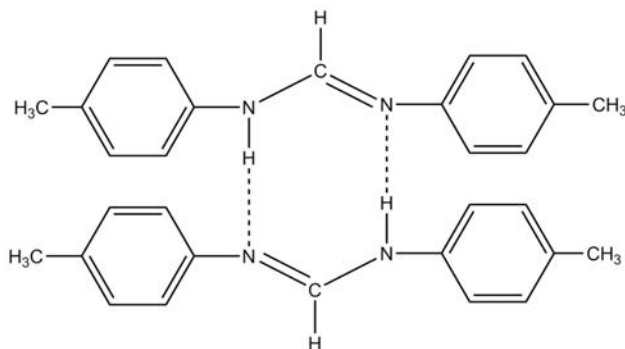
Scheme 1-4. Structure of *p*-TolFormH.

p-TolForm has been used as ligand with different metals. In 2002 *p*-TolFormH was used with LiBu^n using THF, DME and a non-coordinating solvent (hexane) in the presence of the potentially chelating amine *N,N,N',N'*-tetramethylethylene-1,2-diamine (TMEDA) (Scheme 1-5).



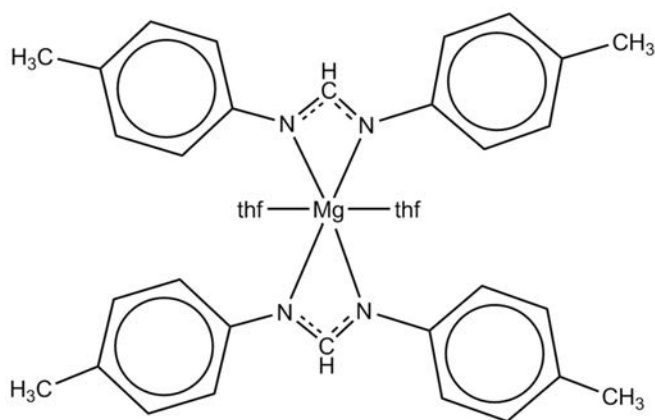
Scheme 1-5. Schematic reaction of *p*-TolFormH with LiBu^n using different solvents of THF, DME and TMEDA.

In this research *p*-TolFormH itself was recrystallized in the form of large colorless blocks from hexane. According to the X-ray crystallography, the molecules are dimers hydrogen bonded arising from $\text{N-H}\cdots\text{N}$ interactions between adjacent molecules (Scheme 1-6).



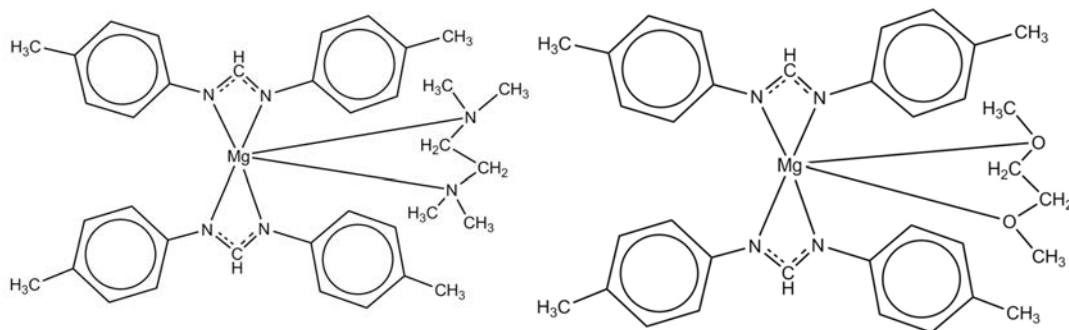
Scheme 1-6. Scheme of the hydrogen-bonded dimer *p*-TolFormH.

As an another example of using the *p*-TolForm ligand, MgBu₂ was employed to prepare [Mg(*p*-TolForm)₂(thf)₂], [Mg(*p*-TolForm)₂(dme)].DME and [Mg(*p*-TolForm)₂(TMEDA)] compounds using THF, DME and TMEDA (diluted in toluene) respectively. In the case of using THF, [Mg(*p*-TolForm)₂(thf)₂] compounds were produced in the form of colorless crystals in good yields (64%).³⁴ Scheme 1-7 displays schematic of the X-ray structure of [Mg(*p*-TolForm)₂(thf)₂].



Scheme 1-7. Schematic of the X-ray structure of [Mg(*p*-TolForm)₂(thf)₂].³⁴

The compounds which were synthesized using DME and TMEDA have two chelating ligands to the metal center (Scheme 1-8) as in [Mg(*p*-TolForm)₂(thf)₂].

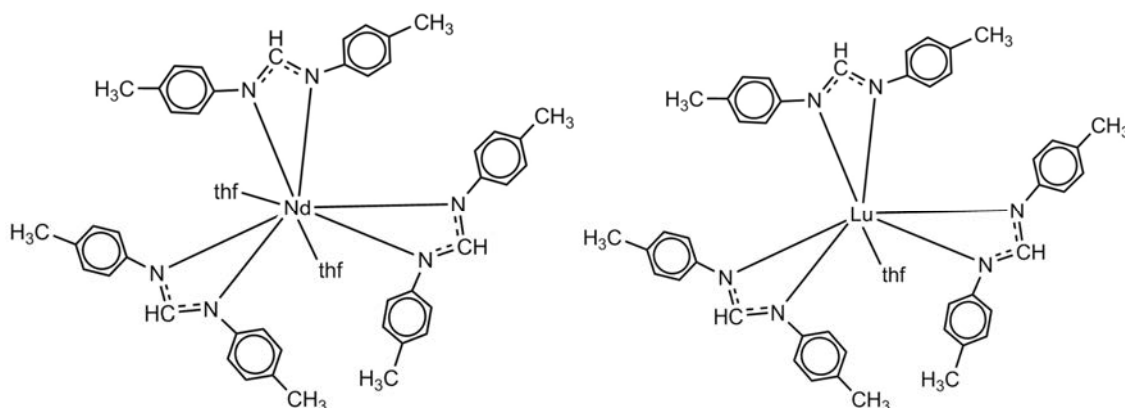


Scheme 1-8. Schematic X-ray structures for [Mg(*p*-TolForm)₂(TMEDA)] (left) and [Mg(*p*-TolForm)₂(DME)].DME (right) compounds.³⁴

Trivalent rare earth compounds with general form [Ln(*p*-TolForm)₃]₂ can be used as precursors to synthesize other N,N'-bis(aryl)formamidinates. This study shows treating [Sm(*p*-TolForm)₃]₂ with triphenylphosphine oxide (Ph₃PO) generates [Sm(*p*-TolForm)₃(Ph₃PO)₂].³⁰ The protolysis reaction of DFFormH on [Sm(*p*-TolForm)₃]₂ using PhMe is another example in

which three different complexes, $[\text{Sm}(\text{DFForm})_2(\textit{p}\text{-TolForm})(\text{thf})_2]$, $[\text{Sm}(\textit{p}\text{-TolForm})_3]_2$ and $[\text{Sm}(\text{DFForm})_3(\text{thf})_2]$ can be isolated.

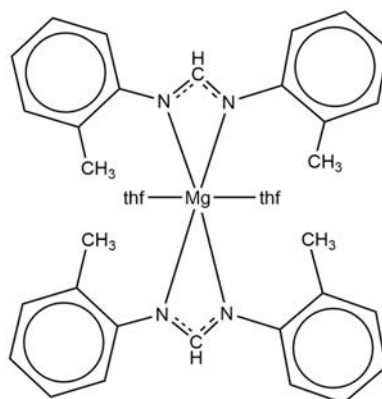
Scheme 1-9 shows the schematic structure of complexes in this study containing Nd and Lu.³⁰ The Nd atom is eight coordinated by three bidentate *p*-TolForm ligands and two transoid-THF ligands, in a distorted dodecahedral environment. The lutetium center is seven coordinated reflecting lanthanoid contraction effect. This compound has one symmetric and two asymmetric chelating *p*-TolForm ligands and one coordinated thf molecule.



Scheme 1-9. Schematic molecular structures of $[\text{Nd}(\textit{p}\text{-TolForm})_3(\text{thf})_2]\cdot\text{THF}$ (left) and $[\text{Lu}(\textit{p}\text{-TolForm})_3(\text{thf})]\cdot\text{THF}$ (right).³⁰

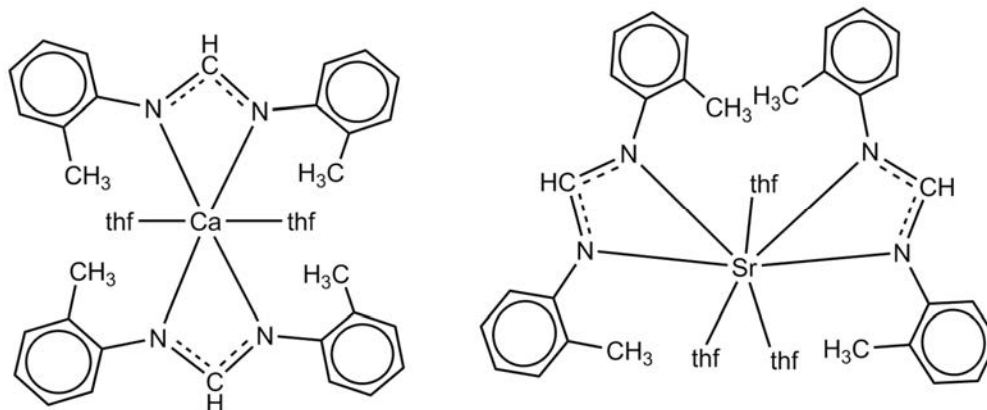
1.6.2 *o*-TolFormH and HFPhF

N,N'-bis(*o*-methylphenyl)formamidine (*o*-TolFormH) was used to prepare $[\text{Mg}(\textit{o}\text{-TolForm})_2(\text{thf})_2]$ from THF in the form of colorless crystals in good yield (62%) which has two chelating formamidinates.³⁴ Scheme 1-10 displays a schematic of the X-ray crystal structure of $[\text{Mg}(\textit{o}\text{-TolForm})_2(\text{thf})_2]$.



Scheme 1-10. Schematic X-ray structures of $[\text{Mg}(\text{o-TolForm})_2(\text{thf})_2]$ compounds.³⁴

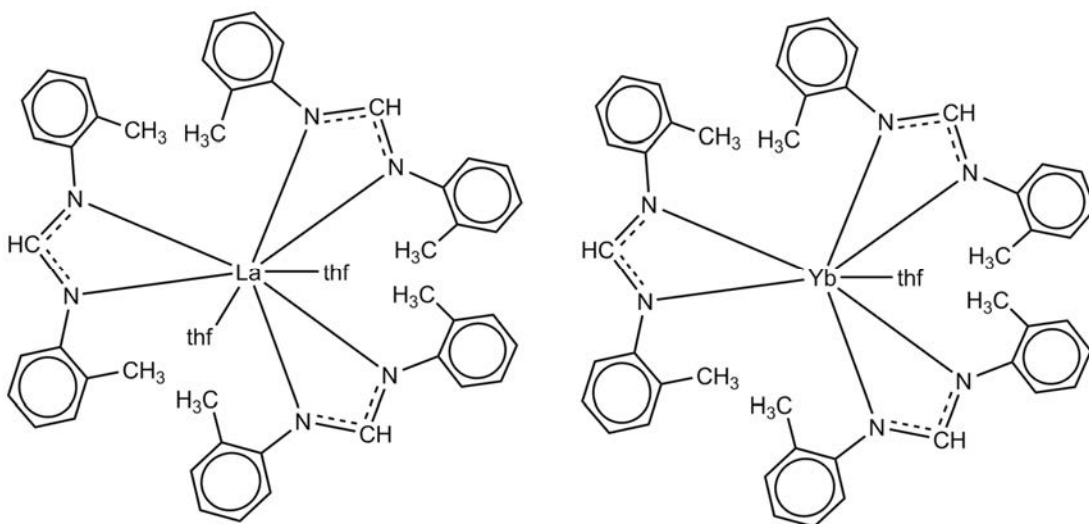
In another study involving RTP reactions, $[\text{Ca}(\text{o-TolForm})_2(\text{thf})_2]$ and $[\text{Sr}(\text{o-TolForm})_2(\text{thf})_3]$ compounds were synthesized by using calcium and strontium with two equivalents of *o*-TolFormH in the presence of one equivalent of $\text{Hg}(\text{C}_6\text{F}_5)_2$ in THF.³⁵ The crystals of $[\text{Ca}(\text{o-TolForm})_2(\text{thf})_2]$ and $[\text{Sr}(\text{o-TolForm})_2(\text{thf})_3]$ were colorless. X-ray data revealed that both of the compounds are mononuclear with two chelating formamidinate ligands (Scheme 1-11).



Scheme 1-11. Schematic molecular structures of $[\text{Ca}(\text{o-TolForm})_2(\text{thf})_2]$ (left) and $[\text{Sr}(\text{o-TolForm})_2(\text{thf})_3]$ (right).³⁵

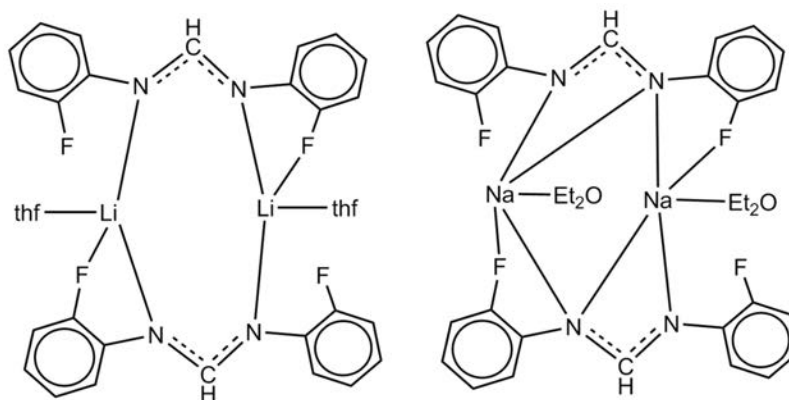
The coordination number for calcium in $[\text{Ca}(\text{o-TolForm})_2(\text{thf})_2]$ compound is six. This compound exhibits two *transoid* thf donor molecules and two formamidinate ligands. $[\text{Sr}(\text{o-TolForm})_2(\text{thf})_3]$ has three coordinating thf molecules in its structure and strontium is seven-coordinate reflecting the larger size of Sr compared with Ca. Er and La are two other metals that were used for performing RTP reactions with *o*-TolFormH to synthesize metal-organic compounds. As a result, $[\text{La}(\text{o-TolForm})_3(\text{thf})_2]$ and $[\text{Er}(\text{o-TolForm})_3(\text{thf})]$ were produced.²⁵ In

this study, $[\text{Yb}(o\text{-TolForm})_3(\text{thf})]$ was isolated from a metathesis reaction route since the RTP route consistently gave $[\{\text{Yb}(o\text{-TolForm})_2(\mu\text{-OH})\text{thf}\}_2]$. The coordination number of La metal center is eight and the molecular unit exhibits two *transoid* thf donor molecules (Scheme 1-12 left). The ytterbium center in $[\text{Yb}(o\text{-TolForm})_3(\text{thf})]$ has three chelating *o*-TolFormH ligands and one thf molecule which render a seven-coordinate ytterbium center (Scheme 1-12 right). The ionic radius of Yb^{3+} is smaller than La^{3+} due to the lanthanoid contraction and the lanthanum complex $[\text{La}(o\text{-TolForm})_3(\text{thf})_2]$ is eight-coordinate and the ytterbium complex $[\text{Yb}(o\text{-TolForm})_3(\text{thf})]$ is seven coordinate.³⁶



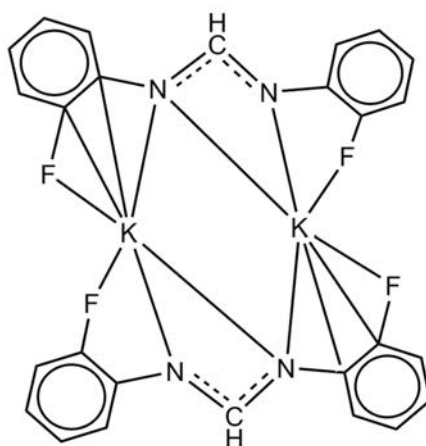
Scheme 1-12. Schematic molecular structures of $[\text{La}(o\text{-TolForm})_3(\text{thf})_2]$ (left) and $[\text{Yb}(o\text{-TolForm})_3(\text{thf})]$ (right).³⁶

Replacement of methyl groups in *o*-TolFormH ligand with fluoride gives N,N'-di-(ortho-fluorophenyl)formamidine (HFPhF) as another ligand which can be used for synthesizing metal-organic compounds. HFPhF has been used along with *n*-butyllithium, sodium bis(trimethylsilyl)amide and potassium bis(trimethylsilyl)amide to prepare the colorless crystalline formamidinate complexes $[\text{Li}(\text{FPhF})(\text{thf})]$, $[\text{Na}(\text{FPhF})(\text{thf})]$ and $[\text{K}(\text{FPhF})]$.³⁷ Also, in this study $[\text{Na}(\text{FPhF})(\text{Et}_2\text{O})]$ was prepared by a low-temperature reaction between sodium bis(trimethylsilyl)amide and HFPhF in diethyl ether. These compounds were the first non-chromium complexes of N,N'-di(ortho-fluorophenyl)formamidinate. Structures of $[\text{Li}(\text{FPhF})(\text{thf})]$ and $[\text{Na}(\text{FPhF})(\text{Et}_2\text{O})]$ compounds are dimeric including $\mu_2:\eta^2:\eta^1$ and $\mu_2:\eta^2:\eta^2$ formamidinate ligands bonded respectively (Scheme 1-13). It can be seen F is involved in coordination to metal center which can lead to C-F activation.

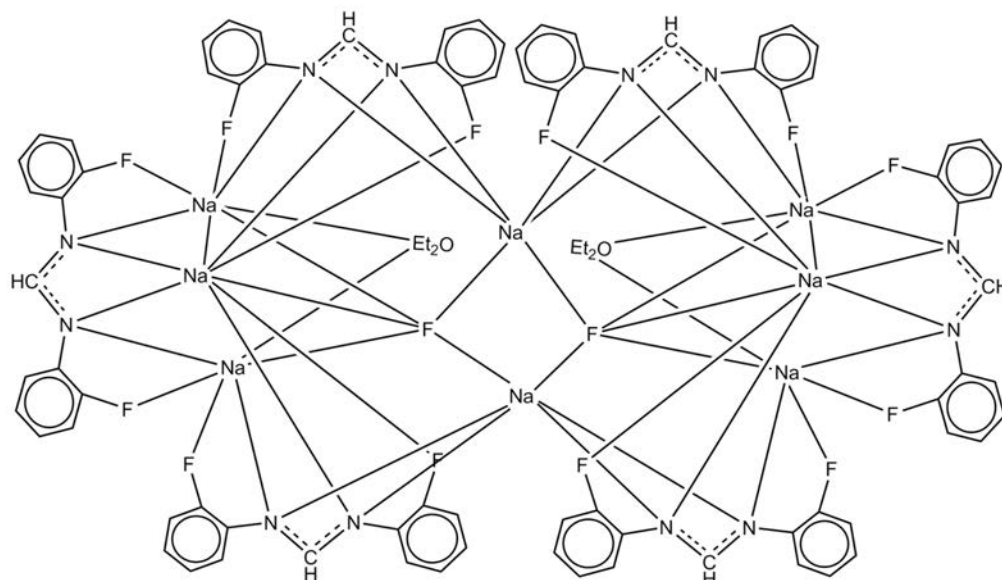


Scheme 1-13. Schematic structures of $[\{\text{Li}(\mu_2:\eta^2:\eta^1\text{-FPhF})(\text{thf})\}_2]$ (left) and $[\{\text{Na}(\mu^2:\eta^2:\eta^2\text{-FPhF})(\text{Et}_2\text{O})\}_2]$ (right).³⁷

Scheme 1-14 displays the structure of $[\text{K}(\text{FPhF})]$ which is dimeric and formamidinate ligands exhibit the $\mu_2:\eta^4:\eta^3$ -binding mode. It has been reported another dimeric $[\text{Na}_3(\text{FPhF})_3(\text{Et}_2\text{O})(\text{NaF})]$ compound was isolated during preparation of $[\{\text{Na}(\mu^2:\eta^2:\eta^2\text{-FPhF})(\text{Et}_2\text{O})\}_2]$ which is result of C-F activation. This compound also synthesized deliberately by reaction of sodium bis(trimethylsilyl)amide and HFPhF in Et_2O solution. $[\text{Na}_3(\text{FPhF})_3(\text{Et}_2\text{O})(\text{NaF})]$ contains two trisodium tris(formamidinate) units involving $\mu_2:\eta^2:\eta^2$ -FPhF ligands, a bridging diethyl ether moiety and an unprecedented $\mu_3:\eta^2:\eta^2:\eta^2$ -formamidinate donor. Together, these trinuclear units encapsulate two sodium fluoride units by η^2 -N,N-formamidinate chelation of the sodium cations (thereby creating further $\mu_3:\eta^2:\eta^2:\eta^2$ -bound formamidinates) and fluoride - sodium interactions which can be seen in Scheme 1-15.

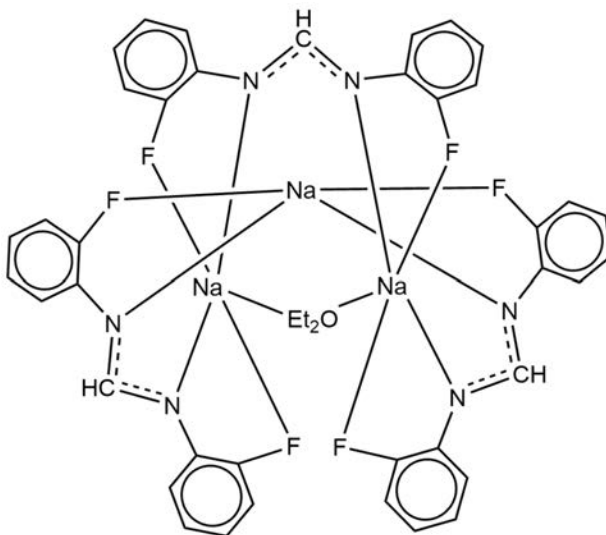


Scheme 1-14. Schematic molecular structure of a dimeric $\text{K}_2(\text{FPhF})$ unit.³⁷



Scheme 1-15. Schematic molecular structure of $\{[\text{Na}_3(\mu_3\text{:}\eta^2\text{:}\eta^2\text{:}\eta^2\text{-FPhF})_3(\mu_2\text{-Et}_2\text{O})(\text{NaF})]_2\}$.³⁷

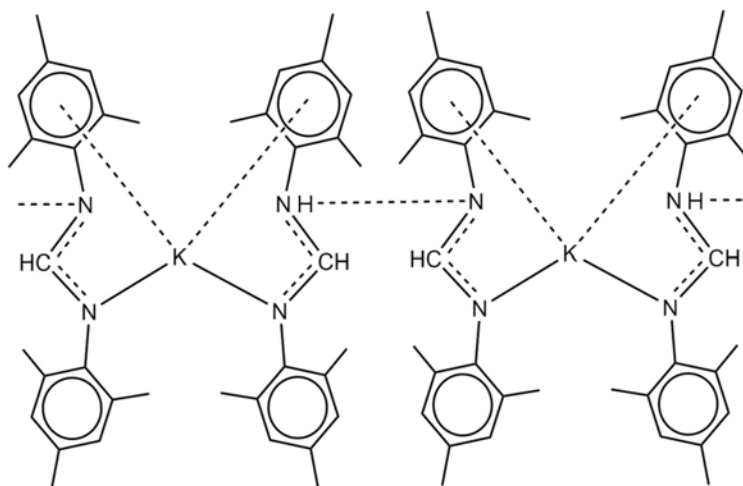
Formation of $[\text{Na}_3(\text{FPhF})_3(\text{Et}_2\text{O})(\text{NaF})]$ can be prevented by preparation of $[\text{Na}(\text{FPhF})(\text{Et}_2\text{O})]$ at lower temperatures ($-50\text{ }^\circ\text{C}$). This hypothesis was confirmed by the absence of resonance signals at $\delta = 7.08$ and 8.49 ppm in the ^1H NMR spectrum of the bulk product. $[\text{Na}_3(\text{FPhF})_3(\text{Et}_2\text{O})]$ is a trinuclear compound. This compound includes $\mu_2\text{:}\eta^2\text{:}\eta^2\text{-FPhF}$ and $\mu_3\text{:}\eta^2\text{:}\eta^2\text{:}\eta^2\text{-FPhF}$ bridging bonds and a $\mu_2\text{-Et}_2\text{O}$ bond (Scheme 1-16).



Scheme 1-16. Molecular structure of the trinuclear $[\text{Na}_3(\mu_2\text{:}\eta^2\text{:}\eta^2\text{-FPhF})_2(\mu_3\text{:}\eta^2\text{:}\eta^2\text{:}\eta^2\text{-FPhF})(\mu_2\text{-Et}_2\text{O})]$.³⁷

1.6.3 MesFormH

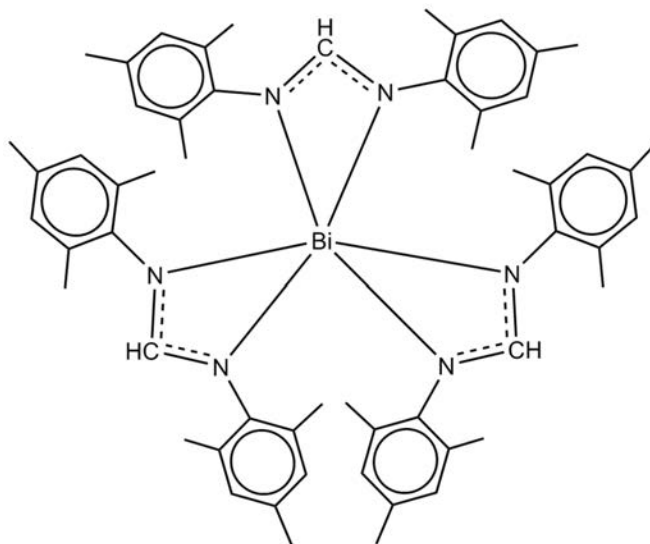
The first potassium formamidinate complex $[K(\text{MesForm})_2]$ was obtained at ambient temperature by treatment of the bulky N,N' -bis(2,4,6-trimethylphenyl)formamidine (MesFormH) with 0.5 or 1.0 equivalents of potassium hydride or potassium bis(trimethylsilyl)amide.³⁸ Scheme 1-17 shows the schematic X-ray monomeric structure of the compound.



Scheme 1-17. Schematic X-ray structure of $[K\{\{\eta^6\text{-MesForm}\}\text{-NC(H)N(MesForm)}\}]\{\{\eta^6\text{-MesForm}\}\text{NHC(H)N(MesForm)}\}$.³⁸

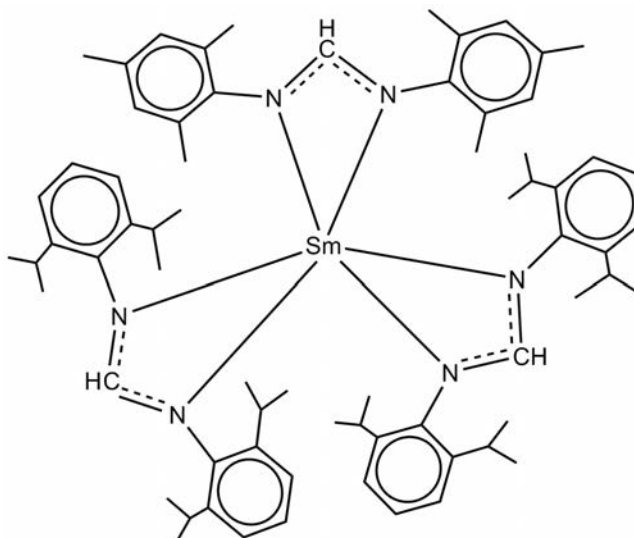
The RTP reaction of MesFormH with La, Nd, Sm, and Yb lanthanoid metals using $\text{Hg}(\text{C}_6\text{F}_5)_2$ in THF gave the tris(formamidinato)lanthanoid(III) complexes $[\text{Ln}(\text{MesForm})_3(\text{thf})_n]$.²⁵ It has been reported that $[\text{Nd}(\text{MesForm})_3(\text{thf})_n]$, $[\text{Sm}(\text{MesForm})_3(\text{thf})_n]$ and $[\text{Yb}(\text{MesForm})_3(\text{thf})_n]$ are homoleptic six-coordinate complexes.

Metathesis reactions between $\text{Li}(\text{MesForm})$ or $\text{K}(\text{MesForm})$ alkali metal complexes with BiCl_3 or BiBr_3 were studied in another research.³⁹ As the result of these reactions, $\text{Bi}(\text{MesForm})_3$ was synthesized. As it can be seen in Scheme 1-18, this compound is mononuclear with three chelating ligands.



Scheme 1-18. Schematic X-ray structure of $[\text{Bi}(\text{MesForm})_3]$.³⁹

The heteroleptic (mixed Form complex) $[\text{Sm}(\text{DippForm})_2(\text{MesForm})]$ was synthesized in a moderate yield by reaction of $[\text{Sm}(\text{DippForm})_2(\text{thf})_2]$ with MesFormH.⁴⁰ This compound is mononuclear and the Sm centre binds to three $\kappa^2\text{-N,N}'$ -formamidinate ligands (Scheme 1-19).

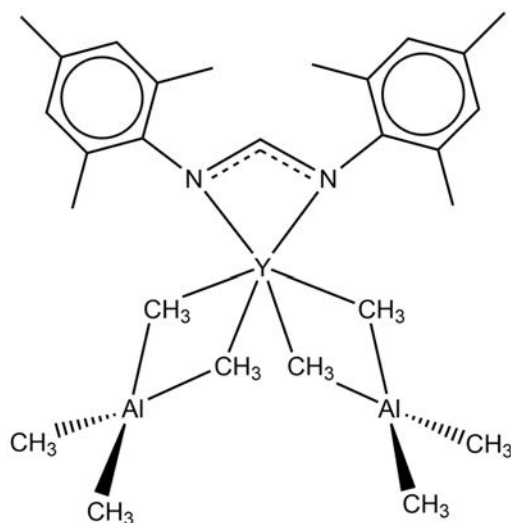


Scheme 1-19. Schematic X-ray structure of heteroleptic $[\text{Sm}(\text{DippForm})_2(\text{MesForm})]$.⁴⁰

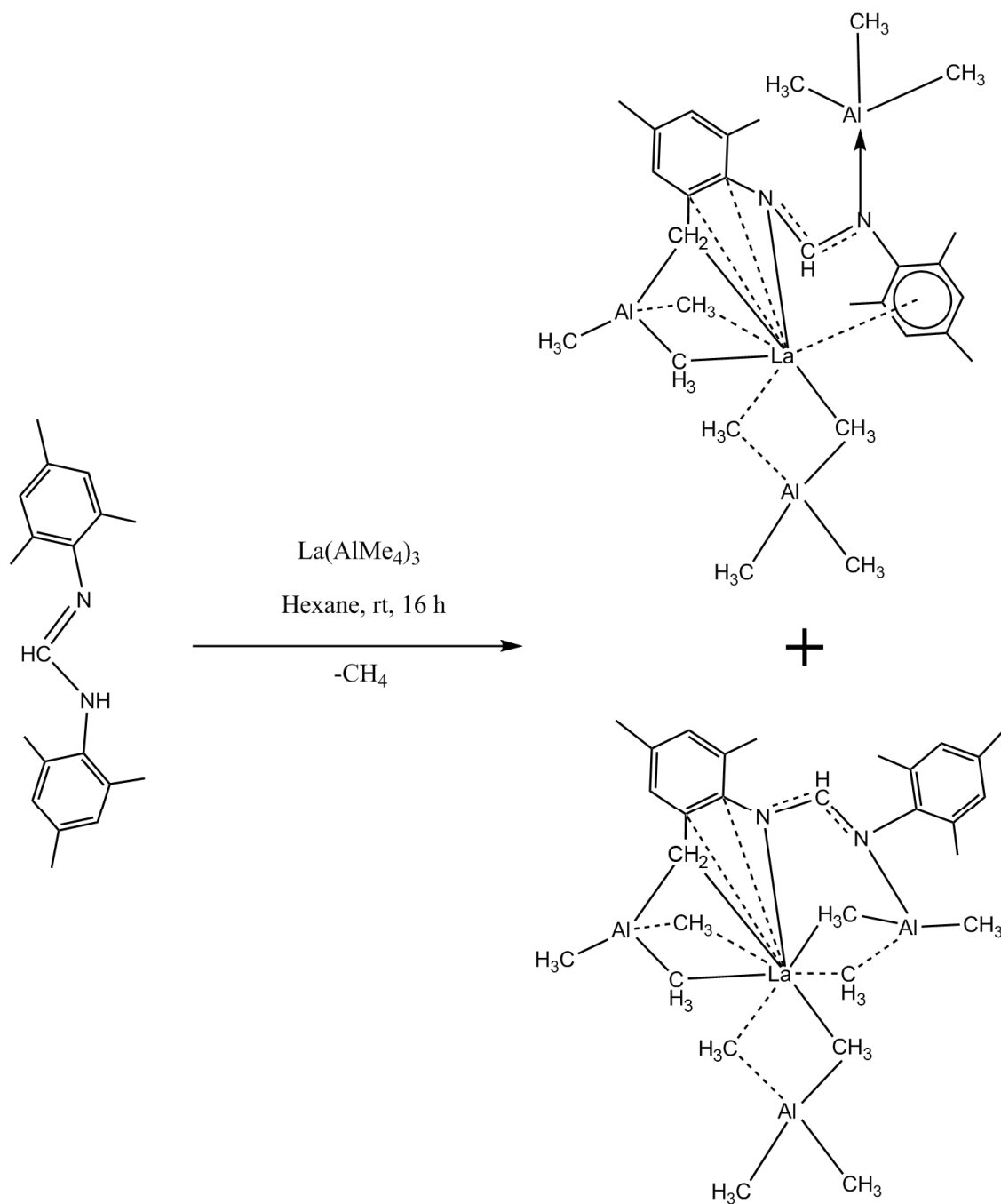
Divalent $[\text{Yb}(\text{MesForm})_2(\text{thf})_2]$ is another example of using the MesFormH ligand. This complex was synthesized using the RTP reaction using $\text{Hg}(\text{C}_6\text{F}_5)_2$ in THF.⁴¹ This compound is

monomeric and the coordination number for central metal is six. It has two chelating N,N'-Form ligands and two *cis*-thf donors.

The bimetallic formamidinate complex $[Y(\text{MesForm})(\text{AlMe}_4)_2]$ was obtained in a high yield by performing reaction between MesFormH and $Y(\text{AlMe}_4)_3$ (Scheme 1-20).¹⁷ By adding $\text{La}(\text{AlMe}_4)_3$ to 1 equivalent of MesFormH in hexane, the C-Me group of the mesityl moiety undergoes C-H activation and yields a yellow solution from which the complexes $[\text{La}\{\eta^1(\text{N}):\eta^6(\text{Ar})\text{-MesFormAlMe}_3\}(\text{AlMe}_3)(\text{AlMe}_4)]$ and $[\text{La}(\text{MesFormAlMe}_3)(\text{AlMe}_3)(\text{AlMe}_4)(\text{C}_6\text{H}_{14})_{1.5}]$ co-crystallised in a 1:1 ratio. Presence of a methylene ligand is the most interesting structural characteristic of this compound. The methylene ligand increases the coordination saturation of the lanthanum centre and helps the η^2 -binding of two aromatic carbon atoms (Scheme 1-21).



Scheme 1-20. Schematic X-ray structure of $[\text{Y}(\text{MesForm})(\text{AlMe}_4)_2]$.¹⁷

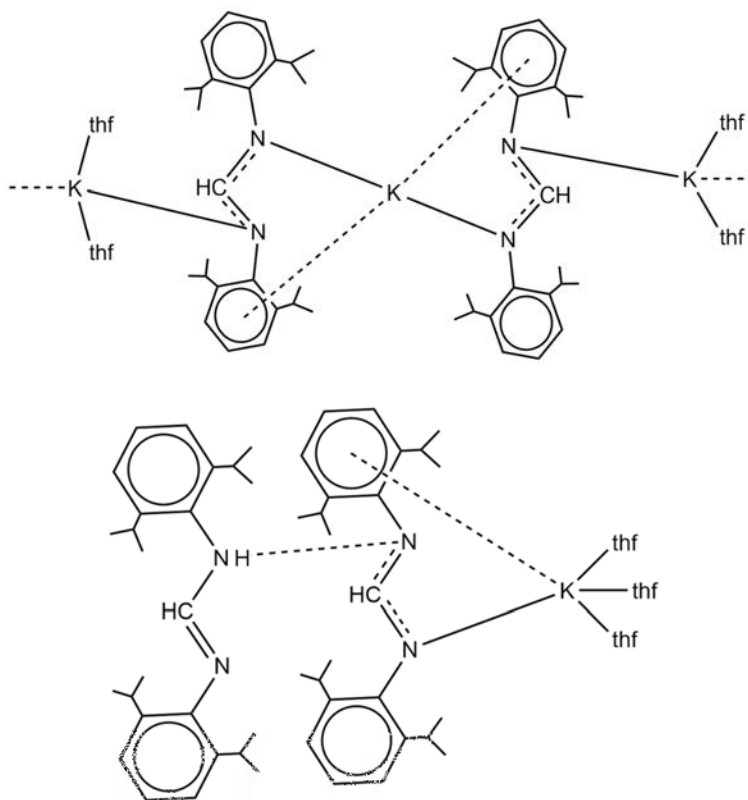


Scheme 1-21. Synthetic pathway and the products for $[\text{La}(\eta^1(\text{N})\text{:}\eta^6(\text{Ar})\text{-MesFormAlMe}_3)(\text{AlMe}_3)(\text{AlMe}_4)]_2(\text{C}_6\text{H}_{14})_{1.5}$ compound.¹⁷

The coordination number of the metal in $[\text{La}\{\eta^1(\text{N})\text{:}\eta^6(\text{Ar})\text{-MesFormAlMe}_3\}(\text{AlMe}_3)(\text{AlMe}_4)]$ is ten and this complex contains the $\eta^1(\text{N})\text{:}\eta^6(\text{Ar})$ binding mode of MesForm. The coordination number for the La centre in $[\text{La}(\text{MesFormAlMe}_3)(\text{AlMe}_3)(\text{AlMe}_4)]$ is nine and AlMe_3 bridges a nitrogen donor atom and the lanthanum atom via two methyl groups.

1.6.4 Bulkier bis(aryl)formamidinate ligands

Treatment of potassium bis(trimethylsilyl)amide with *N,N'*-bis(2,6-diisopropylphenyl)formamidinate (DippFormH) yields the formamidinate species $[\{K(\text{DippForm})_2K(\text{thf})_2\}]_n \cdot n\text{THF}$.⁴² DippFormH ligands in this compound participate in $\eta^6:\eta^1$ binding mode (Scheme 1-22). Also, it has been reported that by adding a further equivalent of DippFormH to this compound, $[K(\text{DippForm})(\text{thf})_3] \cdot \text{DippFormH}$ can be synthesized. According to the X-ray data, this compound has three thf ligands bound to a potassium centre, a single $\eta^6:\eta^1$ -DippForm ligand and a protonated DippFormH formamidinate (Scheme 1-22).



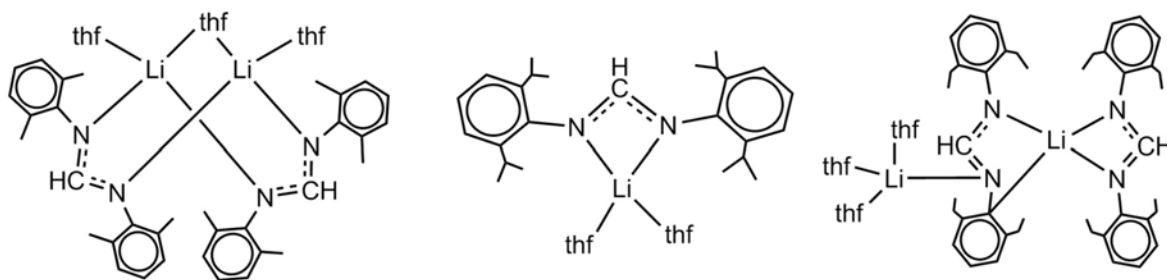
Scheme 1-22. Schematic structures of $[\{K(\text{DippForm})_2K(\text{thf})_2\}]_n \cdot n\text{THF}$ (top) and $[K(\text{DippForm})(\text{thf})_3] \cdot \text{DippFormH}$ (bottom).⁴²

n-Butyl lithium and sodium bis(trimethylsilyl)amide were used along with different solvents (DME and THF) and different *N,N'*-di(2,6-dialkylphenyl)formamidinate ligands containing alkyl

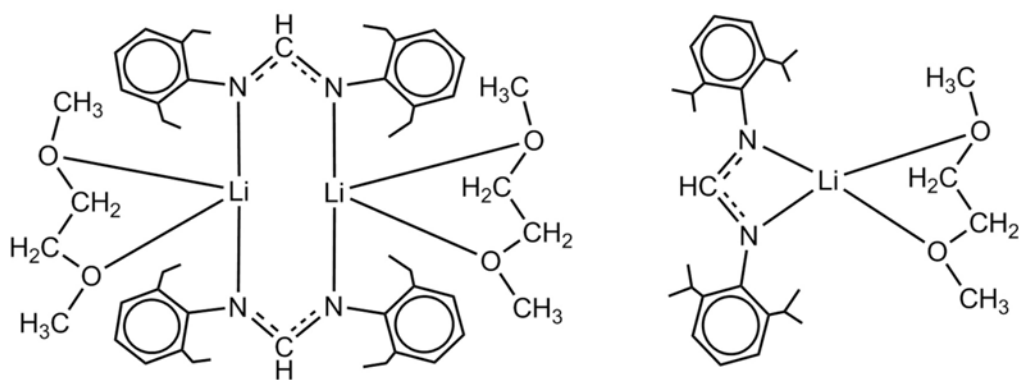
groups at the 2- and 6-aryl position (XylFormH, EtFormH and DippFormH) to provide a wide range of compounds.⁴³

Among the lithium complexes, X-ray structure data for the products of using XylFormH in DME has not been reported because of high solvent dependency and consistent twinning. Scheme 1-23 illustrates molecular structures of lithium complexes containing thf in this research. Various binding modes can be observed for the lithium compounds prepared in THF: two $\mu_2:\eta^1:\eta^1$ ligand binding modes with two terminals and one bridging thf (Scheme 1-23 left), $\mu_2:\eta^1:\eta^1:\eta^1$ ligand bond with three terminal thf connected to a lithium centre (Scheme 1-23 middle) and a monomer structure containing one chelating ligand and two thf molecules connected to the metal centre (Scheme 1-23 right). It can be found that bonding modes gradually change from bridging to chelating.

The schematic molecular structures of the DME solvated EtFormH and DippFormH are depicted in Scheme 1-24. The nuclearity of the complexes are different for these two compounds. The $[\text{Li}(\text{EtForm})(\text{dme})_2]$ compound is a dimer containing the $\mu_2:\eta^1:\eta^1$ bridging mode. Ligands with larger 2- and 6-position alkyl groups have a greater steric effect, resulting in formation of $[\text{Li}(\text{DippForm})(\text{dme})]$. Compound $[\text{Li}(\text{DippForm})(\text{dme})]$ is a monomeric structure which contains η^2 chelating mode.

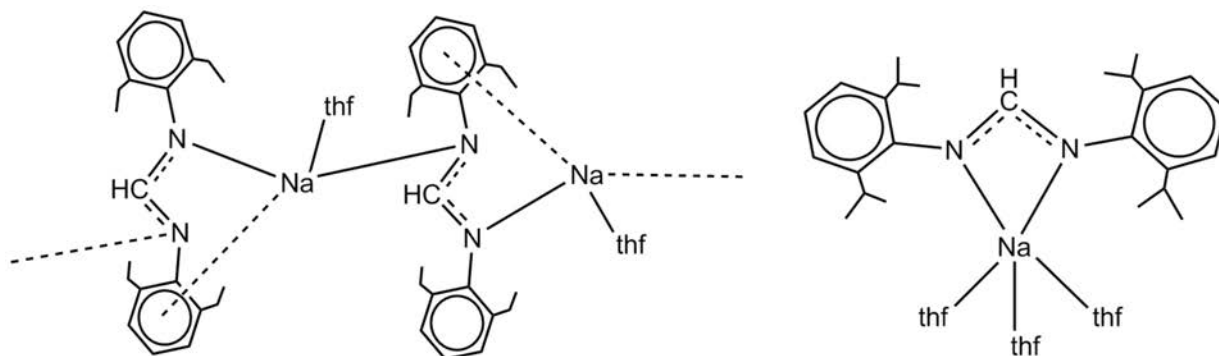


Scheme 1-23. Schematic structures of $[\text{Li}_2(\mu_2:\eta^1:\eta^1\text{-N,N'-XylForm})_2(\mu_2\text{-thf})(\text{thf})_2]$ (left), $[\text{Li}(\eta^2\text{-N,N'-DippForm})(\text{thf})_2]$ (middle) and $[\text{Li}(\text{thf})_3(\mu_2:\eta^1:\eta^1:\eta^1\text{-N,C,N'-EtForm})\text{Li}(\eta^2\text{-N,N'-EtForm})]$ (right).⁴³



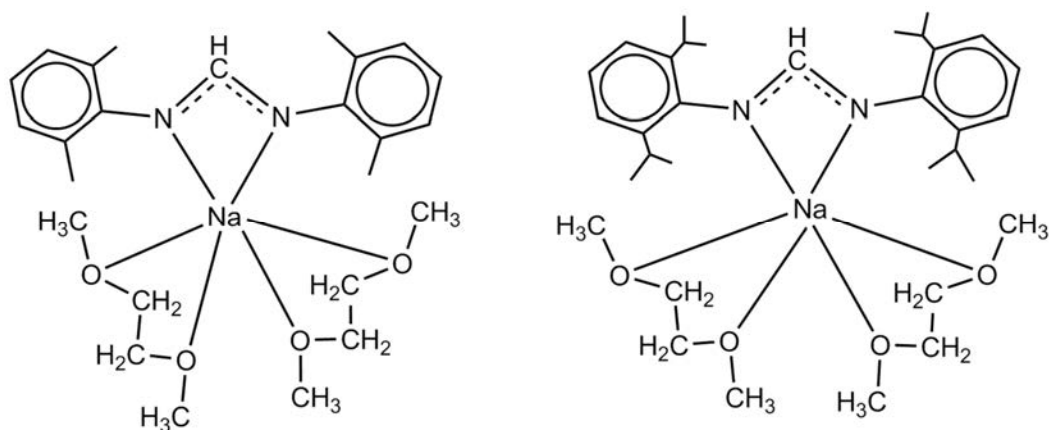
Scheme 1-24. Schematic structures of $[\text{Li}(\mu_2:\eta^1:\eta^1\text{-N,N'-EtForm})(\text{dme})_2]_2$ (left) and $[\text{Li}(\eta^2\text{-N,N'-DippForm})(\text{dme})]$ (right).⁴³

Different species were synthesized in this study using sodium bis(trimethylsilyl)amide as the metallic reagent in solvents of THF and DME. The structures of $[\{\text{Na}(\text{EtForm})(\text{thf})\}_n]$ and $[\text{Na}(\text{DippForm})(\text{thf})_3]$ are the same as their lithium analogues. Compound $[\text{Na}(\text{DippForm})(\text{thf})_3]$ is monomeric with three terminal thf molecules and an $\mu_2:\eta^1:\eta^1$ -chelate donor (Scheme 1-25).



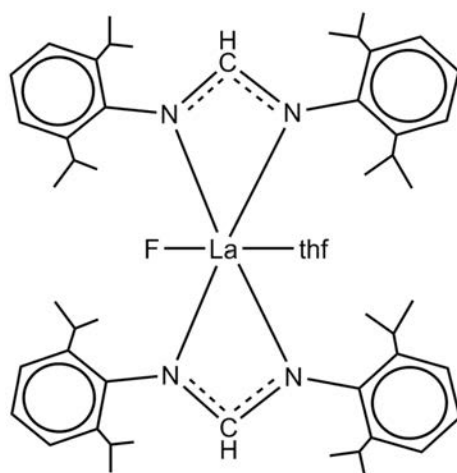
Scheme 1-25. Schematic structures of $[\{\text{Na}(\mu_2:\eta^6:\eta^1:\eta^1\text{-Ar,N,N'-EtForm})(\text{thf})\}_n]$ (left) and $[\text{Na}(\text{DippForm})(\text{thf})_3]$ (right).⁴³

The molecular structures of DME species for Na complexes are shown in Scheme 1-26. Unlike the related THF species, but similar to their lithium analogues, the steric constraints of DME reduce the number of possible ligand binding compared to the related THF examples. This can be seen in Scheme 1-26, which exhibit one chelating formamidinate and two chelating dme molecules.



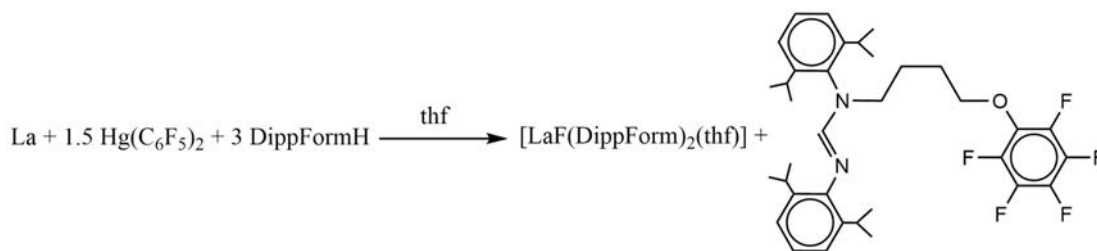
Scheme 1-26. Schematic structures of $[\text{Na}(\text{XylForm})(\text{dme})_2]$ (left) and $[\text{Na}(\text{DippForm})(\text{dme})_2]$ (right).⁴³

A functionalised formamidine, DippForm($(\text{CH}_2)_4\text{OC}_6\text{F}_4\text{H}-o$) and a rare terminal $\text{Ln}-\text{F}$ bond were the results for another study of using DippFormH as the ligand along with lanthanum.²⁴ In this study $\text{Hg}(\text{C}_6\text{F}_5)_2$ was used in an RTP reaction involving La metal and DippFormH. The resulting compound (Scheme 1-27) shows that lanthanum is six coordinate and there are two chelating *cisoid* DippForm ligands.



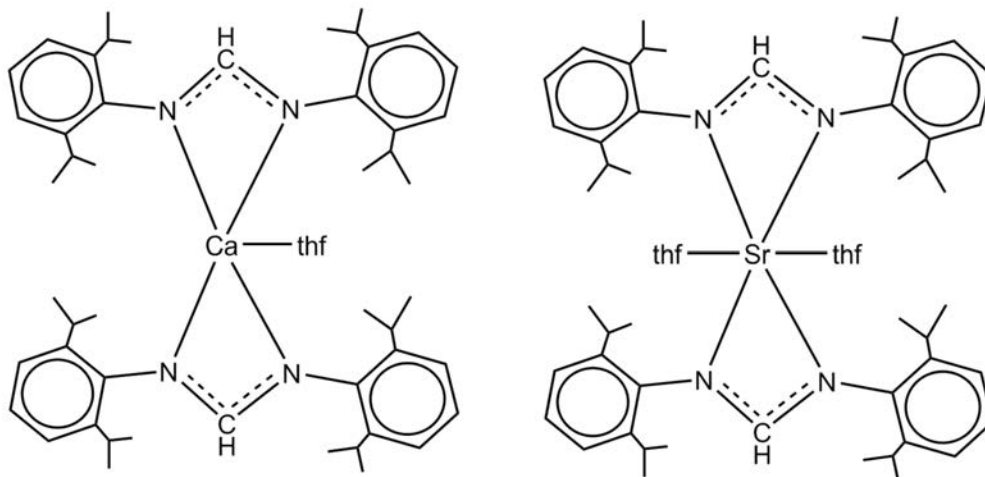
Scheme 1-27. Schematic of X-ray structure of $[\text{LaF}(\text{DippForm})_2(\text{thf})]$ compound.²⁴

This study proposes that the intermediate $[\text{La}(\text{C}_6\text{F}_5)(\text{DippForm})_2]$ compound in the RTP reaction undergoes C-F activation to yield $[\text{LaF}(\text{DippForm})_2(\text{thf})]$ and a unique functionalised formamidine, DippForm($(\text{CH}_2)_4\text{OC}_6\text{F}_4\text{H}-o$) derived from ring opened thf (Equation 1-7).



Equation 1-7.

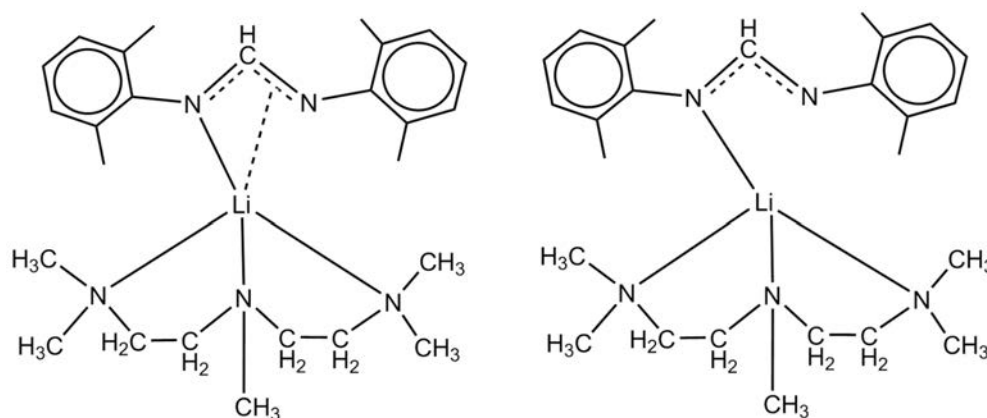
The heavy alkaline earth elements calcium, strontium and barium were used with two equivalents of DippFormH for another study and related products were reported.⁴⁴ As a result, $[\text{Ca}(\text{DippForm})_2(\text{thf})]$, $[\text{Sr}(\text{DippForm})_2(\text{thf})_2]$ and $[\text{Ba}(\text{DippForm})_2(\text{thf})_2]$ were formed in good to moderate yields and the X-ray structures were obtained (Scheme 1-28). All three species are mononuclear with two chelating DippForm ligands in the structure. $[\text{Ca}(\text{DippForm})_2(\text{thf})]$ has one terminal thf connected to the Ca center and calcium is five coordinate. Compounds $[\text{Sr}(\text{DippForm})_2(\text{thf})_2]$ and $[\text{Ba}(\text{DippForm})_2(\text{thf})_2]$ have two terminal thf molecules and the coordination number for the central metal is six for both of them.



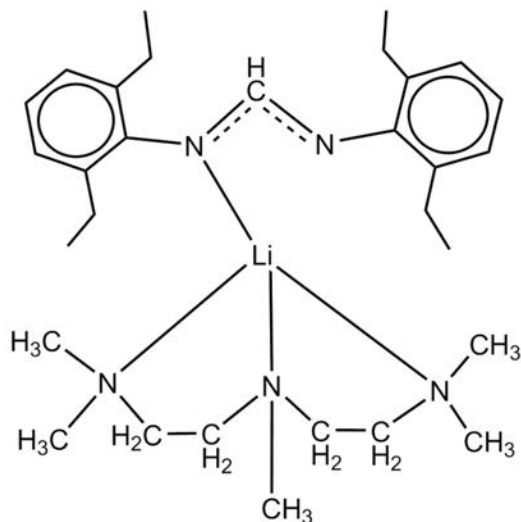
Scheme 1-28. Schematic of X-ray structures for $[\text{Ca}(\text{DippForm})_2(\text{thf})]$ (left) and $[\text{Sr}(\text{DippForm})_2(\text{thf})_2]$ (right).⁴⁴

The first examples of $\eta^2:\eta^1\text{-C}=\text{N},\text{N}'$ metal amidinate coordination were reported in 2005.⁴⁵ In this study the lithium complexes were synthesized using $\text{N},\text{N},\text{N}',\text{N}'',\text{N}'''$ -pentamethyldiethylenetriamine (pmdeta) with XylFormH, EtFormH and DippFormH ligands. *n*-Butyl lithium was used as the lithium source and THF was used as the solvent. As a result,

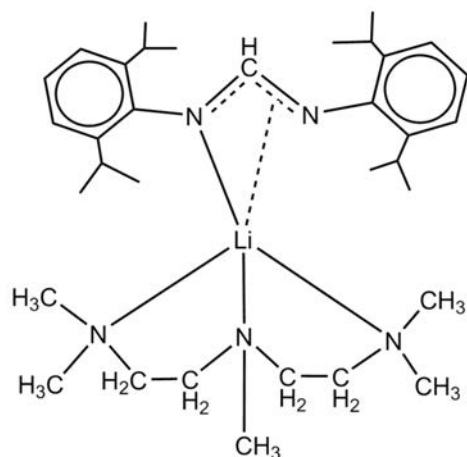
mononuclear compounds of [Li(XylForm)(pmdeta)], [Li(EtForm)(pmdeta)] and [Li(DippForm)(pmdeta)] were synthesized (Scheme 1-29 - Scheme 1-31). Two unique molecular units in the asymmetric unit were observed for [Li(XylForm)(pmdeta)]. One displays *E-anti* isomerism for the amidinate ligand (Scheme 1-29 left) and the other one displays *E-syn* isomerism (Scheme 1-29 right). The structures of [Li(DippForm)(pmdeta)] and *E-anti* isomer of [Li(XylForm)(pmdeta)] display coordination of the pendant amidinate imine. Thus, it can be considered as the first examples of $\eta^2:\eta^1\text{-C=N,N'}$ metal amidinate coordination.



Scheme 1-29. Schematic X-ray structures of [Li(XylForm)(pmdeta)] *E-anti* formamidinate (left) and *E-syn* formamidinate (right).⁴⁵

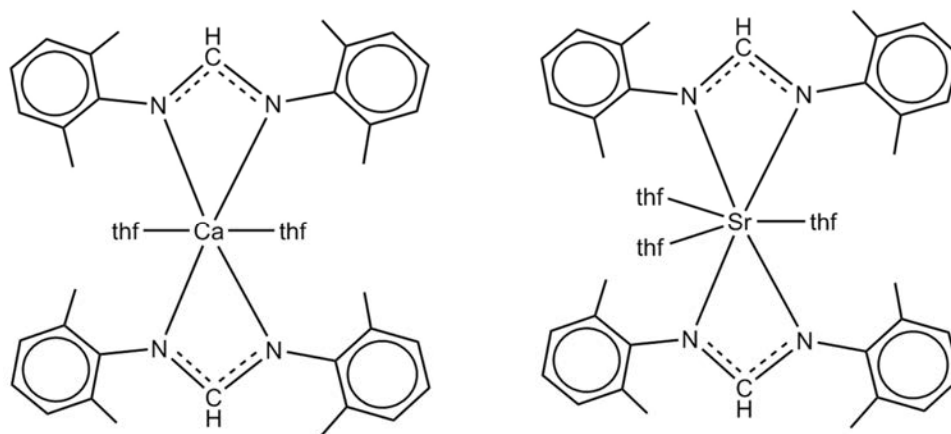


Scheme 1-30. Schematic X-ray structure of [Li(EtForm)(pmdeta)] compound.⁴⁵



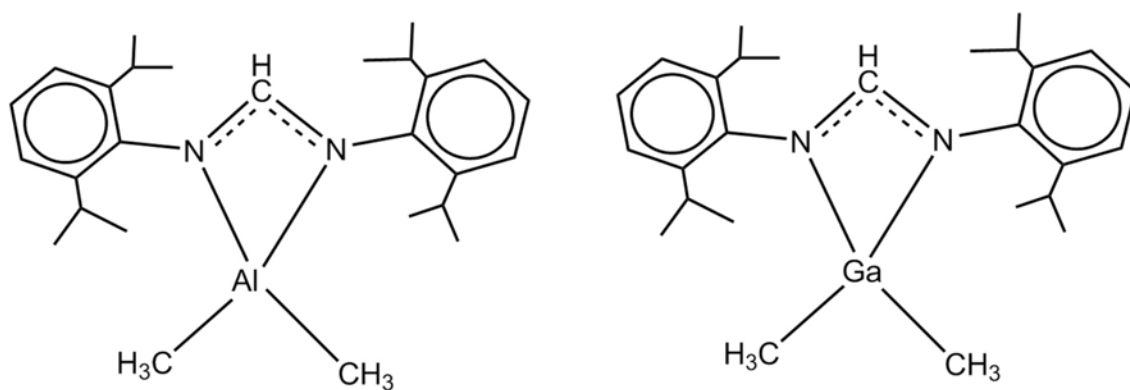
Scheme 1-31. Schematic X-ray structure of [Li(DippForm)(pmdeta)] compound.⁴⁵

Calcium or strontium metal with 2.0 equivalents of XylFormH in the presence of 1.0 equivalent of $\text{Hg}(\text{C}_6\text{F}_5)_2$ in THF were used to produce $[\text{Ca}(\text{XylForm})_2(\text{thf})_2]$ and $[\text{Sr}(\text{XylForm})_2(\text{thf})_3] \cdot 3\text{THF}$ (Scheme 1-32).³⁵ $[\text{Ca}(\text{XylForm})_2(\text{thf})_2]$ exhibits six-coordination about its metal centre and the metal centre is considered *cisoid* distorted trigonal prism. The strontium centre in $[\text{Sr}(\text{XylForm})_2(\text{thf})_3] \cdot 3\text{THF}$ is seven coordinate by two chelating formamidinates and three thf molecules.



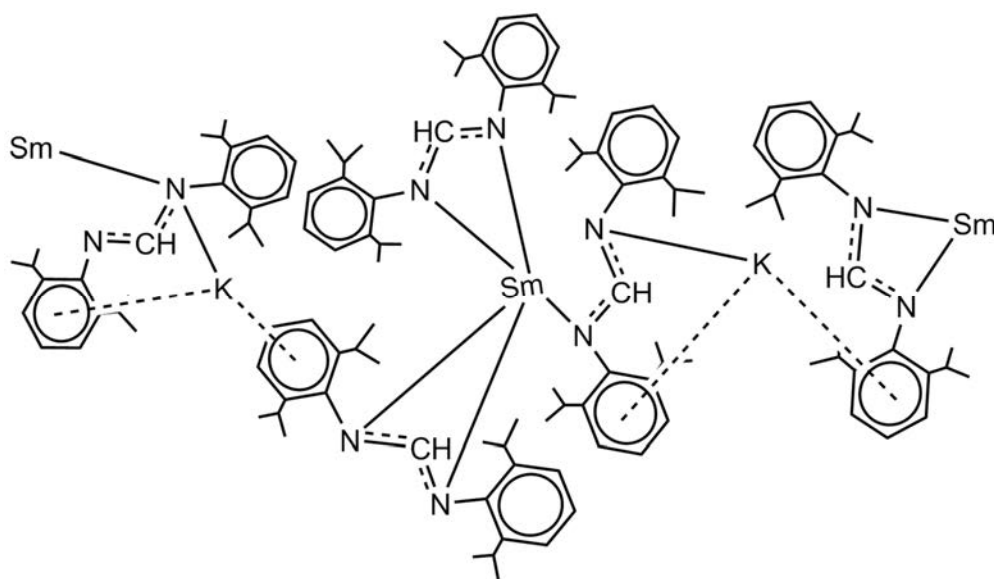
Scheme 1-32. Schematic X-ray structures of $[\text{Ca}(\text{XylForm})_2(\text{thf})_2]$ (left) and $[\text{Sr}(\text{XylForm})_2(\text{thf})_3] \cdot 3\text{THF}$ (right) compounds.³⁵

$[\text{Al}(\text{DippForm})\text{Me}_2]$, $[\text{Al}(\text{EtForm})\text{Me}_2]$ and $[\text{Ga}(\text{DippForm})\text{Me}_2]$ were prepared in high yields by the protonolysis reactions of AlMe_3 with DippFormH and EtFormH and GaMe_3 with DippFormH in 1:1 stoichiometry. The metal centres in $[\text{Al}(\text{DippForm})\text{Me}_2]$ and $[\text{Ga}(\text{DippForm})\text{Me}_2]$ are four coordinate (Scheme 1-33).



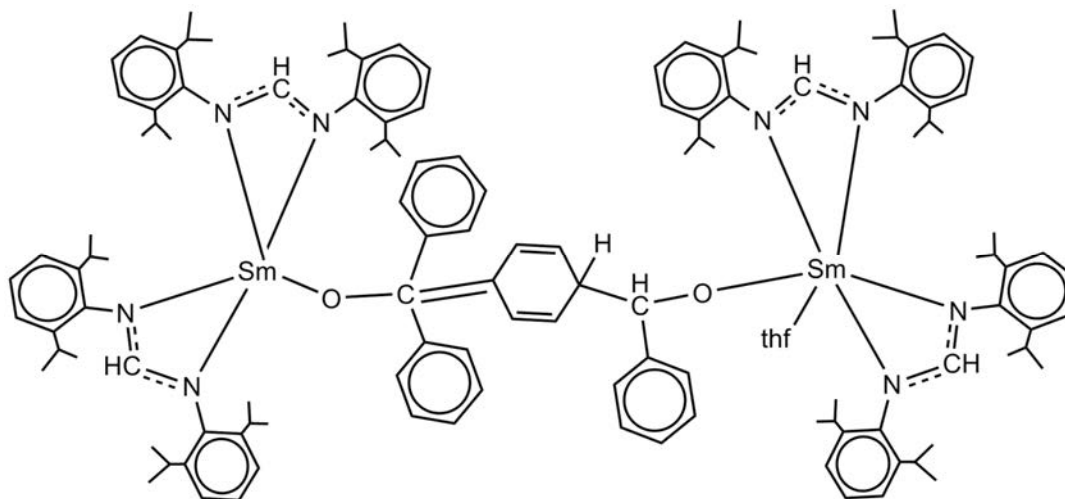
Scheme 1-33. Schematic X-ray structures of $[\text{Al}(\text{DippForm})\text{Me}_2]$ (left) and $[\text{Ga}(\text{DippForm})\text{Me}_2]$ (right) compounds.³⁵

Preparation of a new heterobimetallic samarium(II) formamidinate complex and selected reactions of samarium(II) complexes and one samarium(III) formamidinate complex with benzophenone or CS_2 were reported in 2014.⁴⁶ The heterobimetallic formamidinate samarium(II)/potassium complex $[\text{KSm}(\text{DippForm})_3]$ was synthesized by the reaction of $[\text{Sm}(\text{DippForm})_3]$ with potassium graphite in toluene at elevated temperature (Scheme 1-34). $[\text{KSm}(\text{DippForm})_3]$ and $[\text{Sm}(\text{DippForm})_2(\text{thf})_2]$ are the only known divalent formamidinate samarium species so far reported.⁴⁰ In this compound samarium is five coordinated by two chelating $\kappa(\text{N},\text{N}')$ formamidinate ligands and one formamidinate ligand binds to potassium by an η^6 -2,6-diisopropylphenyl group. The third formamidinate bridges Sm and K with μ -1 $\kappa(\text{N}):2\kappa(\text{N}')$ binding mode.



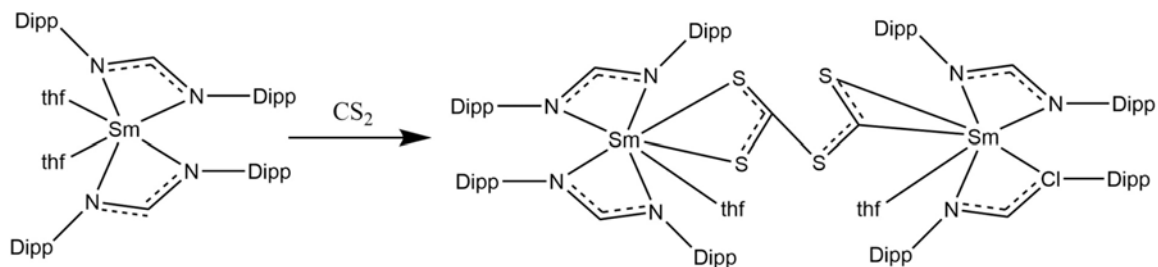
Scheme 1-34. Schematic of the X-ray structure of $[\text{KSm}(\text{DippForm})_3]^{40}$

The highly unusual $[\text{Sm}(\text{DippForm})_2(\text{thf})\{\mu\text{-OC}(\text{Ph})=(\text{C}_6\text{H}_5)\text{-C}(\text{Ph})_2\text{O}\}\text{Sm}(\text{DippForm})_2]$ ($\text{C}_6\text{H}_5 = 1,4\text{-cyclohexadiene-3-yl-6-ylidene}$) compound was reported in this study as the result of the reaction of $[\text{Sm}(\text{DippForm})_2(\text{thf})_2]$ with benzophenone. This compound contains rare C–C coupling between a carbonyl carbon and the carbon at the *para* position of a phenyl group of the OCPh_2 fragment (Scheme 1-35).

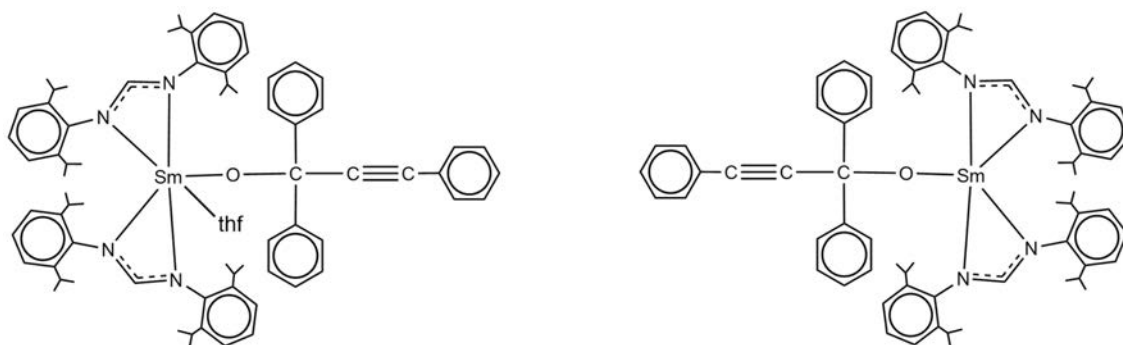


Scheme 1-35. Schematic X-ray structure of $[\text{Sm}(\text{DippForm})_2(\text{thf})\{\mu\text{-OC}(\text{Ph})=(\text{C}_6\text{H}_5)\text{-C}(\text{Ph})_2\text{O}\}\text{Sm}(\text{DippForm})_2]^{40}$

It was also reported that $[\text{Sm}(\text{DippForm})_2(\text{thf})_2]$ reacts with carbon disulfide to form a dinuclear $[\{\text{Sm}(\text{DippForm})_2(\text{thf})\}_2(\mu\text{-}\eta^2(\text{C,S}):\kappa(\text{S}',\text{S}'')\text{-SCSCS}_2)]$ complex via C–S coupling of CS_2 molecules (Scheme 1-36). $[\text{Sm}(\text{DippForm})_2(\text{CCPh})(\text{thf})]$ can activate the C=O bond of benzophenone and form $[\text{Sm}(\text{DippForm})_2\{\text{OC}(\text{Ph})_2\text{C}_2\text{Ph}\}(\text{thf})]$ with unsolvated $[\text{Sm}(\text{DippForm})_2\{\text{OC}(\text{Ph})_2\text{C}_2\text{Ph}\}]$ as a minor product. $\kappa(\text{N},\text{N}')$ bonding between a DippForm and samarium exists in all compounds (Scheme 1-37).

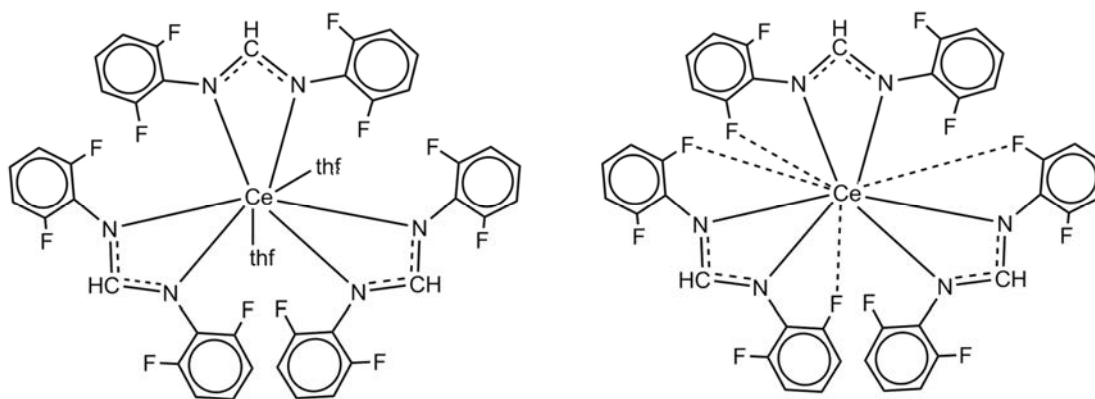


Scheme 1-36. Schematic X-ray structures of $[\{\text{Sm}(\text{DippForm})_2(\text{thf})\}_2(\mu\text{-}\eta^2(\text{C,S}):\kappa(\text{S}',\text{S}'')\text{-SCSCS}_2)]^{40}$



Scheme 1-37. Schematic X-ray molecular structures of $[[\text{Sm}(\text{DippForm})_2\{\text{OC}(\text{Ph})_2\text{C}_2\text{Ph}\}(\text{thf})]$ (left) and $[\text{Sm}(\text{DippForm})_2\{\text{OC}(\text{Ph})_2\text{C}_2\text{Ph}\}]$ (right).⁴⁰

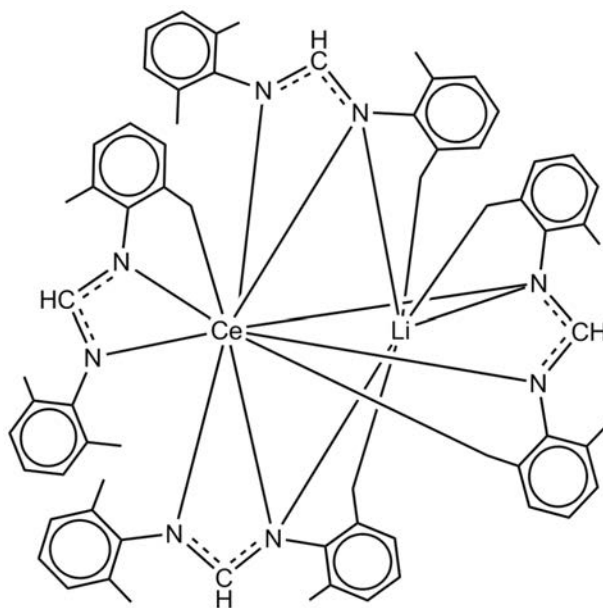
Three new cerium(III) formamidinate complexes comprising $[\text{Ce}(\text{DFForm})_3(\text{thf})_2]$, $[\text{Ce}(\text{DFForm})_3]$ and $[\text{Ce}(\text{EtForm})_3]$ are the results of another study using protonolysis reactions of $[\text{Ce}\{\text{N}(\text{SiMe}_3)_2\}_3]$ with N, N'-bis(2,6-difluorophenyl)formamidine (DFFormH) and EtFormH.⁴⁷ The unsolvated $[\text{Ce}(\text{DFForm})_3]$ complex was prepared and isolated from toluene. The THF solvated species $[\text{Ce}(\text{DFForm})_3(\text{thf})_2]$ can be formed by adding THF to $[\text{Ce}(\text{DFForm})_3]$ (Scheme 1-38).



Scheme 1-38. Schematic X-ray molecular structures of $[\text{Ce}(\text{DFForm})_3(\text{thf})_2]$ (left) and $[\text{Ce}(\text{DFForm})_3]$ (right).⁴⁷

Treating a mixture of $[\text{Ce}\{\text{N}(\text{SiHMe}_2)_2\}_3(\text{thf})_2]$ and $[\text{Li}\{\text{N}(\text{SiHMe}_2)_2\}]$ with four equivalents of DFFormH in toluene resulted in the bimetallic cerium/lithium complex $[\text{LiCe}(\text{DFForm})_4]$. The cerium–lithium bimetallic complex $[\text{LiCe}(\text{DFForm})_4]$ is the first reported trivalent rare-earth complex with four coordinating formamidinate ligands. The cerium atom is ten-coordinated, with eight nitrogens and two fluorine donor atoms (Scheme 1-39). This complex has one terminal formamidinate ligand bound to cerium and three formamidinate ligands bridging

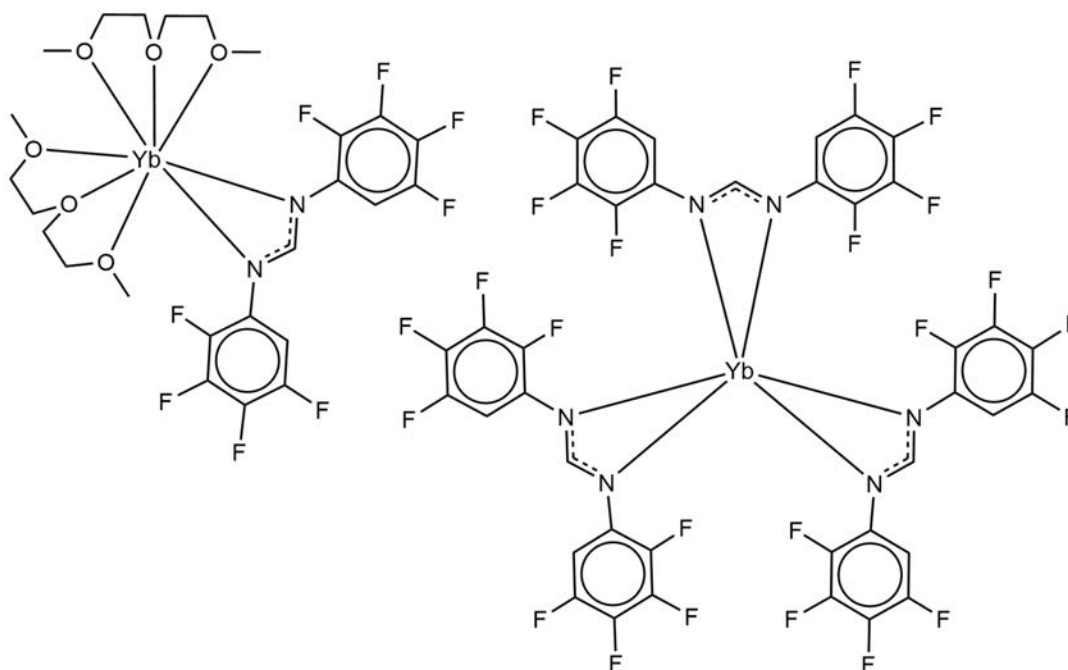
between cerium and lithium. The bridging formamidinate ligands have one $\mu\text{-}\kappa^1$, κ^1 nitrogen atom and one κ^1 .



Scheme 1-39. Schematic X-ray structure of $[\text{LiCe}(\text{DFForm})_4]$.⁴⁷

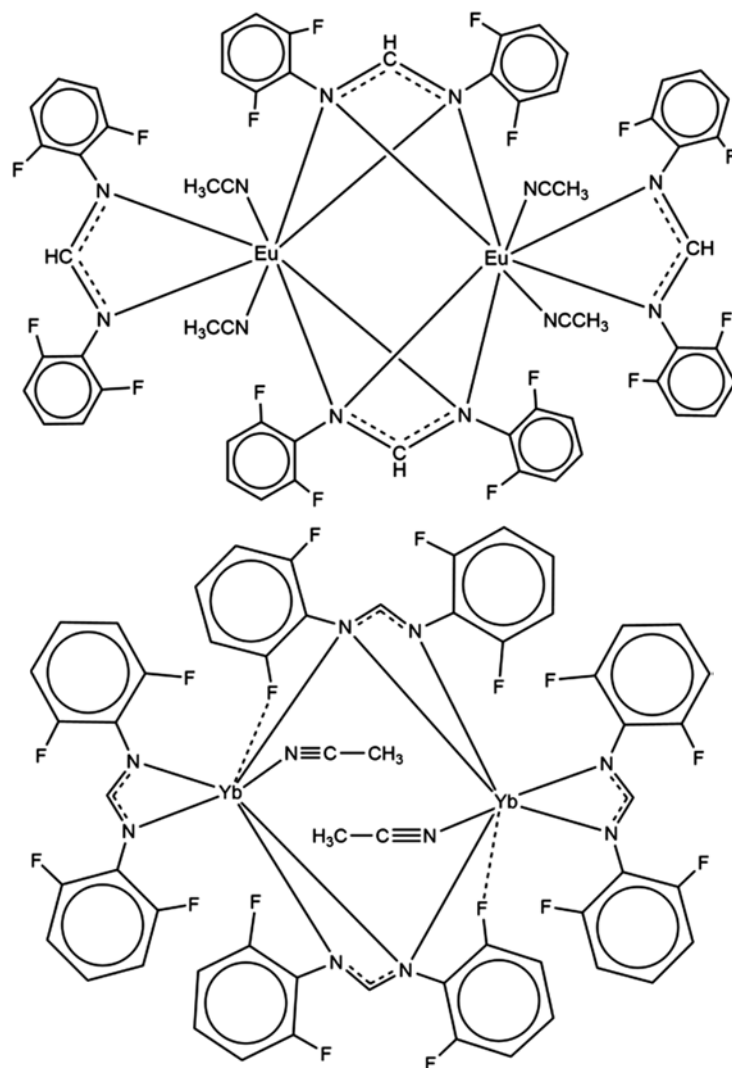
It has been reported that the product of the reaction of $[\text{Ce}\{\text{N}(\text{SiHMe}_2)_2\}_4]$ with DFFormH and EtFormH are cerium(IV) complexes which decompose before possible isolation.

Three different rare earth metals (La, Nd, Yb) and FFormH have been used in RTP reactions in another study to yield trivalent $[\text{La}(\text{FForm})_3(\text{thf})_2]\cdot\text{THF}$, $[\text{Nd}(\text{FForm})_3(\text{thf})_x]$, $[\text{Yb}(\text{FForm})_3(\text{thf})]$ complexes and a divalent $[\text{Yb}(\text{FForm})_2(\text{thf})_2]$ complex.⁴⁸ This study shows $[\text{Yb}(\text{FForm})_3(\text{thf})]$ is the product of the RTP reaction when a small amount of Yb is used and in the case of higher amounts of Yb the divalent complex of $[\text{Yb}(\text{FForm})_2(\text{thf})_2]$ can be isolated as the main product. Same products with different coordinated solvents ($[\text{La}(\text{FForm})_3(\text{dme})]$, $[\text{Yb}(\text{FForm})_2(\text{dme})_2]$ and $[\text{Nd}(\text{FForm})_3(\text{diglyme})]$) can be obtained by using DME or diglyme for recrystallization. $[\text{Yb}(\text{TFForm})(\text{diglyme})_2][\text{Yb}(\text{TFForm})_4]$ is the first crystallographically characterised trivalent ytterbium complex coordinating four discrete amidinate ligands and was synthesized by heating the previously reported $[\text{Yb}(\text{TFForm})_2(\text{thf})_3]$ complex in diglyme (Scheme 1-40).



Scheme 1-40. Schematic X-ray structure of $[\text{Yb}(\text{TFForm})(\text{diglyme})_2][\text{Yb}(\text{TFForm})_4]$.⁴⁸

Treating DippFormH or DFFormH with europium metal in CH_3CN has been reported as an efficient method to synthesize divalent complexes of $[\{\text{Eu}(\text{DFForm})_2\text{CN}\}_2]$ (Scheme 1-41 right) or $[\text{Eu}(\text{DippForm})_2(\text{CH}_3\text{CN})_4]$ which has the highest coordination number for divalent rare earth ArForm complexes.⁴⁹ The significance of this method is synthesizing without using an organomercurial co-oxidant as in RTP reactions. However, in the case of using Yb, addition of Hg^0 is required to activate the metal. $[\{\text{Yb}(\text{DFForm})_2(\text{CH}_3\text{CN})\}_2]$ (Scheme 1-41 left) or $[\text{Yb}(\text{DFForm})_2(\text{thf})_3]$ are two complexes that were isolated using this method with $\text{CH}_3\text{CN}/\text{THF}$ as the solvent. $[\{\text{Yb}(\text{DFForm})_2(\text{CH}_3\text{CN})\}_2]$ undergoes CH_3CN activation upon heating in $\text{PhMe}/\text{C}_6\text{D}_6$ and decomposes to trivalent products. Complexes $[\{\text{Eu}(\text{DFForm})_2\text{CN}\}_2]$ and $[\{\text{Yb}(\text{DFForm})_2(\text{CH}_3\text{CN})\}_2]$ exhibit unusual bridging forms with perpendicular $\mu\text{-}1\kappa(\text{N}:\text{N}')\text{:}2\kappa(\text{N}:\text{N}')$ or twisted $\mu\text{-}1\kappa(\text{N}:\text{N}')\text{:}2\kappa(\text{N}':\text{F}')$ ligands respectively.



Scheme 1-41. Schematic X-ray structures of $[\{\text{Eu}(\text{DFForm})_2(\text{CH}_3\text{CN})\}_2]$ (top) and $[\{\text{Yb}(\text{DFForm})_2(\text{CH}_3\text{CN})\}_2]$ (bottom).⁴⁹

In the case of using another compound, a homoleptic monomer $[\text{La}(\text{CF}_3\text{Form})_3]$, heating in non-coordinating solvents like PhMe or C_6D_6 can lead to C-F activation to produce LaF_3 and $[(\text{CF}_3\text{Form})_2(\text{thq})]$ (thq = tetrahydroquinazoline) as the major and $[(\text{CF}_3\text{Form})_2\text{Benz}]$ (Benz = benzamidine) as the minor products (Figure 1-1).⁵⁰ $[\text{Yb}(\text{CF}_3\text{Form})_3(\text{thf})]$ (Figure 1-2) is another example which undergoes C-F activation upon heating and gives the same organic compounds but with $[(\text{CF}_3\text{Form})_2\text{Benz}]$ as the major product.

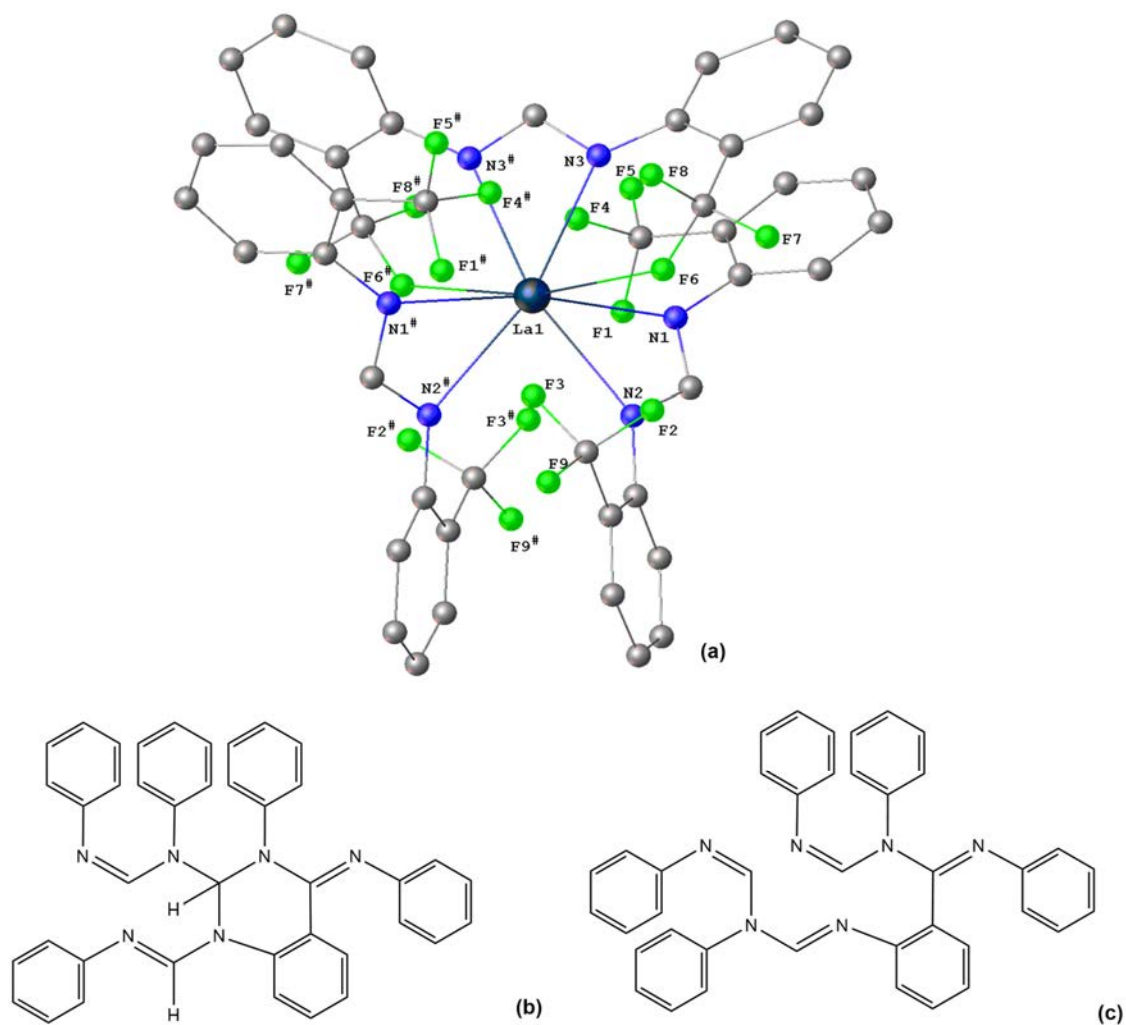


Figure 1-1. X-ray structure of a) $[\text{La}(\text{CF}_3\text{Form})_3]$ (25) and simplified structures of b) $[(\text{CF}_3\text{Form})_2(\text{thq})]$ c) $[(\text{CF}_3\text{Form})_2\text{Benz}]$. CF_3 groups removed for clarity and all phenyl groups in b) and c) represent *ortho*-trifluoromethylphenyl groups.⁵⁰

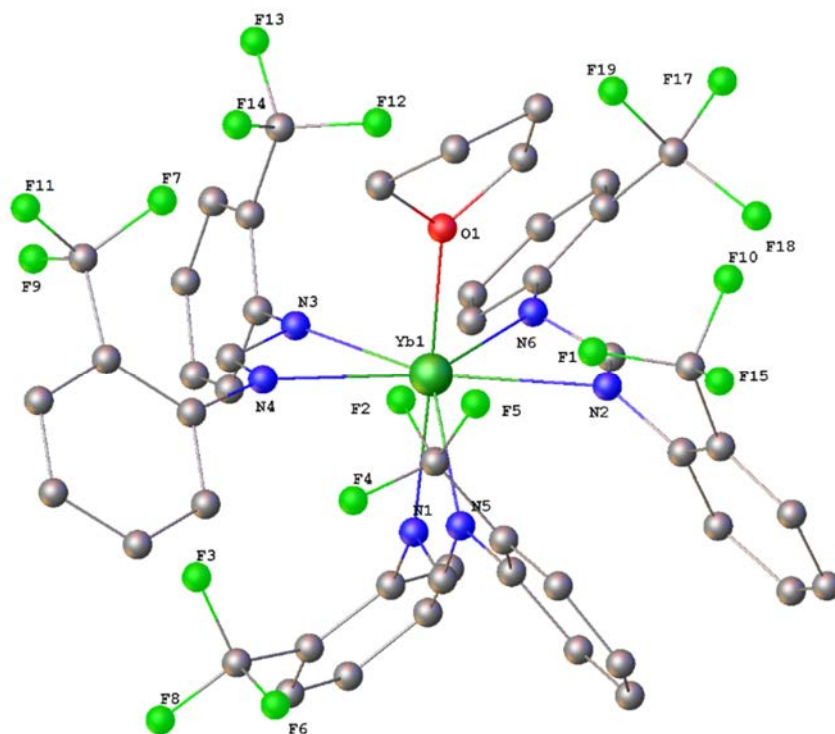
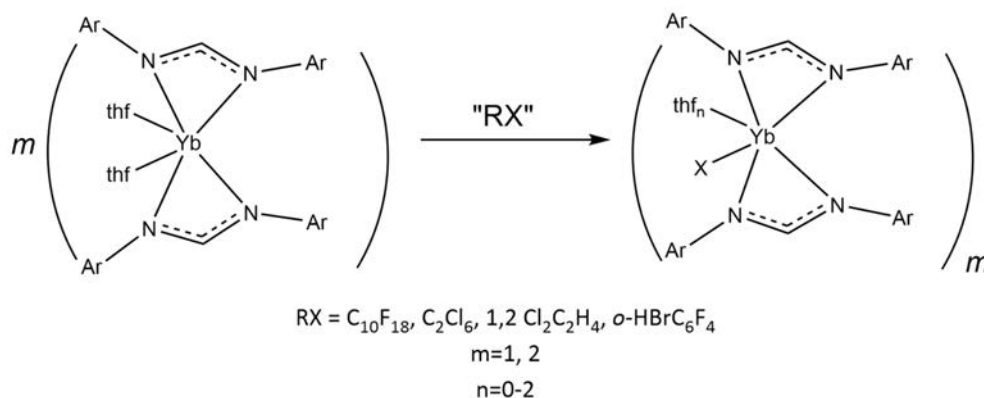


Figure 1-2. X-ray structure of $[\text{Yb}(\text{CF}_3\text{Form})_3(\text{thf})]$.⁵⁰

Divalent Yb complexes prepared by RTP reactions namely $[\text{Yb}(\text{Form})_2(\text{thf})_2]$ (Form = (DippForm, *o*-TolForm, EtForm, *o*-PhPhForm, TFForm and MesForm), have also been studied toward C-X (X=F, Cl, Br) activation reactions.⁴¹ Reaction of these compounds with perfluorodecalin, hexachloroethane or 1,2-dichloroethane, and 1-bromo-2,3,4,5-tetrafluorobenzene, yields $[\text{Yb}(\text{EtForm})_2\text{F}]_2$, $[\text{Yb}(\textit{o}\text{-PhPhForm})_2\text{F}]_2$, $[\text{Yb}(\textit{o}\text{-PhPhForm})_2\text{Cl}(\text{thf})_2]$, $[\text{Yb}(\text{DippForm})_2\text{Cl}(\text{thf})]$ and $[\text{Yb}(\text{DippForm})_2\text{Br}(\text{thf})]$ (Equation 1-8).



Equation 1-8.

The coordination number of Yb in $[\text{Yb}(\text{EtForm})_2\text{F}]_2$ is six same as in $[\text{Yb}(\text{DippForm})_2\text{Cl}(\text{thf})]$ and $[\text{Yb}(\text{DippForm})_2\text{Br}(\text{thf})]$ however it has a dimeric structure containing fluoride bridges (Figure 1-3).

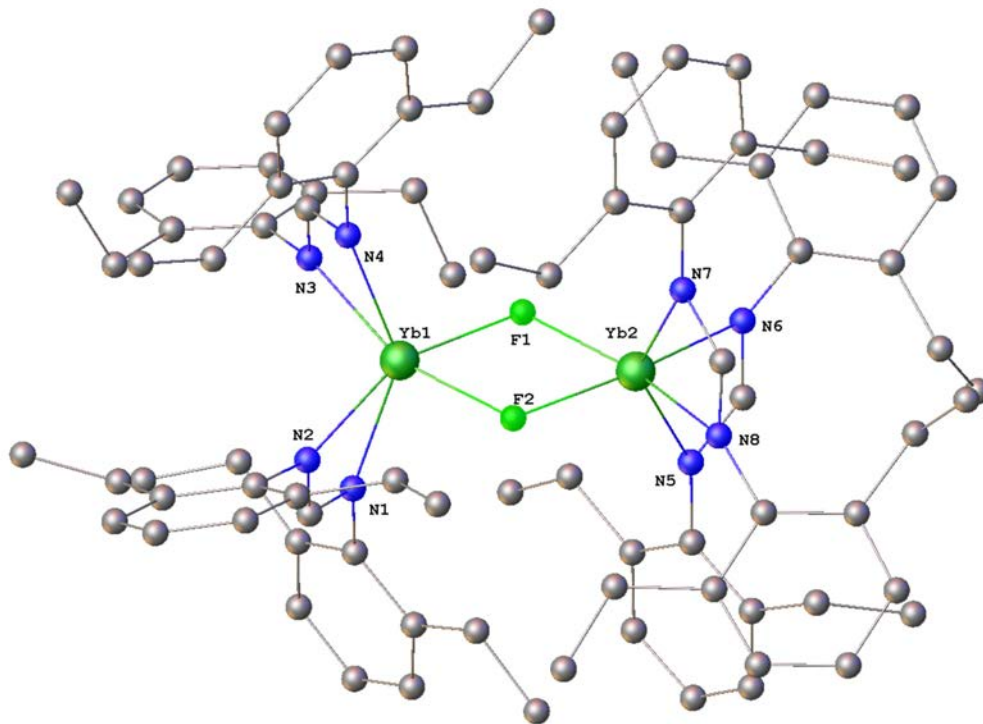
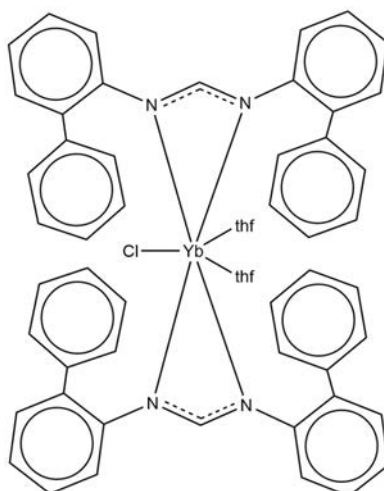


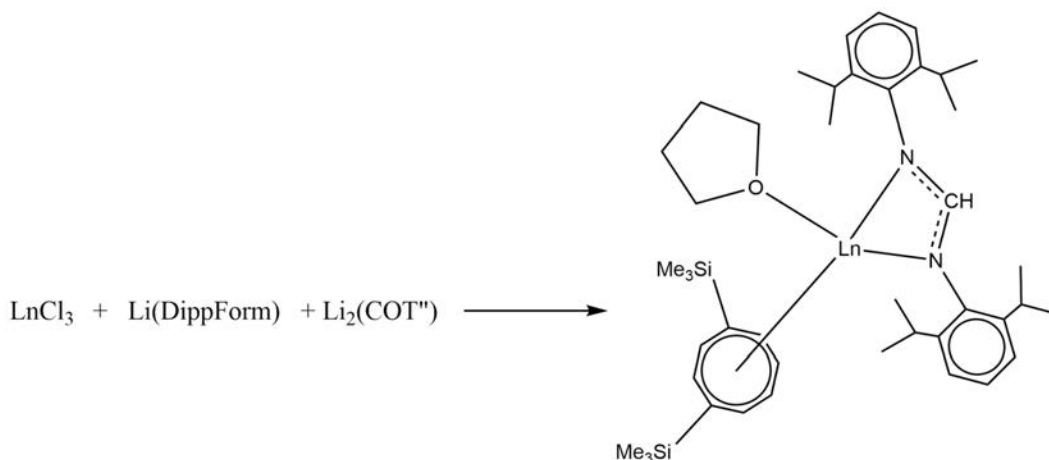
Figure 1-3. X-ray structure of $[\text{Yb}(\text{EtForm})_2\text{F}]_2$.⁴¹

The coordination number for monomeric $[\text{Yb}(o\text{-PhPhForm})_2\text{Cl}(\text{thf})_2]$ is seven and it has two chelating formamidinate ligands, a terminal chloride and two thf donor molecules (Scheme 1-42). This study shows in the case of using DippFormH and $\text{Hg}(2\text{-BrC}_6\text{F}_4)_2$ in RTP reactions, a series of complexes of the form $[\text{Ln}(\text{DippForm})_2\text{Br}(\text{thf})]$ ($\text{Ln} = \text{La}, \text{Nd}$) can be synthesized.



Scheme 1-42. Schematic X-ray structure of $[\text{Yb}(\text{o-PhPhForm})_2\text{Cl}(\text{thf})_2]$.⁴¹

Another studies show anhydrous samarium or ytterbium trichloride can be used with $\text{Li}(\text{DippForm})$ and $\text{Li}_2(\text{COT}'')$ [$\text{COT}'' = 1,4\text{-bis}(\text{trimethylsilyl})\text{cyclooctatetraenyl}$] in thf solution to yield $[\eta^8\text{-(COT}'')\text{Sm}(\text{DippForm})(\text{thf})]$ toluene monosolvate or $[(\text{COT}'')\text{Yb}(\text{DippForm})(\text{thf})]$ respectively (Scheme 1-43).^{51, 52}

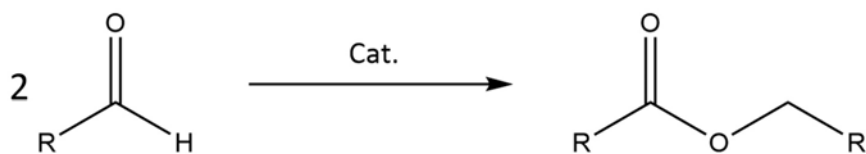


Scheme 1-43. Schematic of the reaction and X-ray structure of $[\text{Ln}(\text{DippForm})(\text{COT}'')(\text{thf})] \cdot \text{C}_7\text{H}_8$ complexes ($\text{Ln} = \text{Sm}, \text{Yb}$).⁵¹

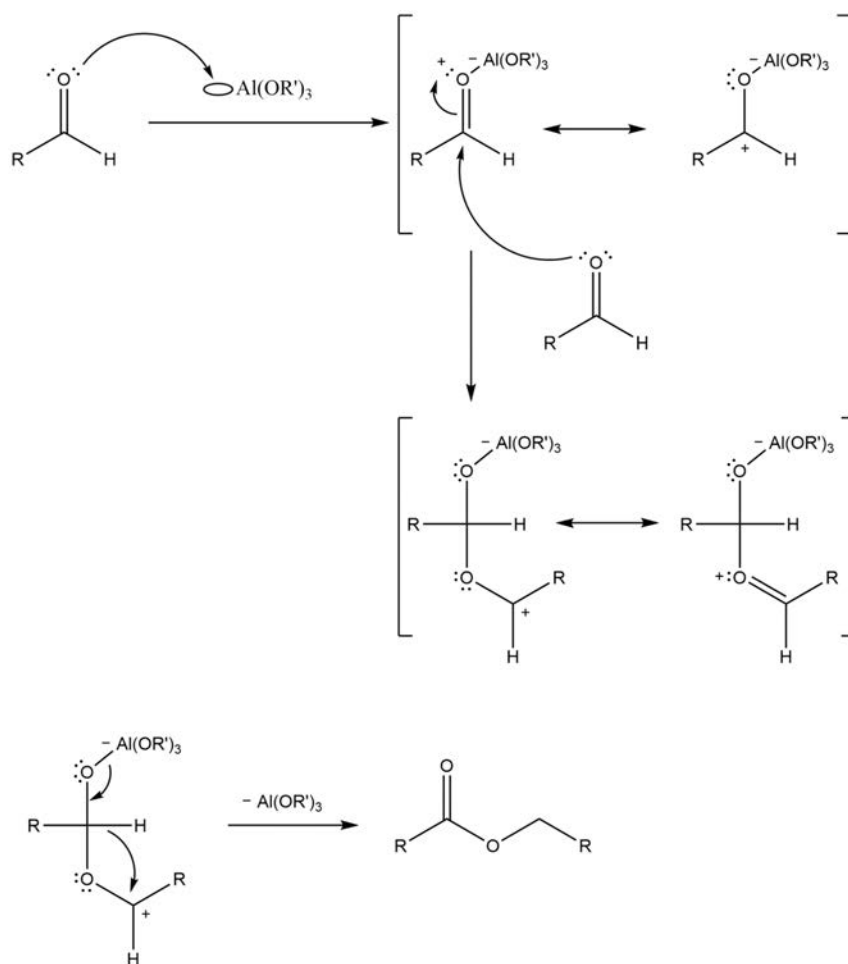
1.7 Tishchenko reactions and reactivity

The Tishchenko reaction is a disproportionation reaction that converts two aldehydes to the equivalent esters in the presence of a metal catalyst (Scheme 1-44) described by Russian organic chemist Vyacheslav Evgen'evich Tishchenko (Вячеслав Евгеньевич Тищенко) in

1906.⁵³ Aluminium alkoxides are traditional catalysts for this reaction.⁵⁴⁻⁵⁶ The catalyst acts as a Lewis acid and coordinates with one molecule of the aldehyde to facilitate the addition of a second equivalent of aldehyde (Scheme 1-45).



Scheme 1-44. Schematic of Tishchenko reaction.

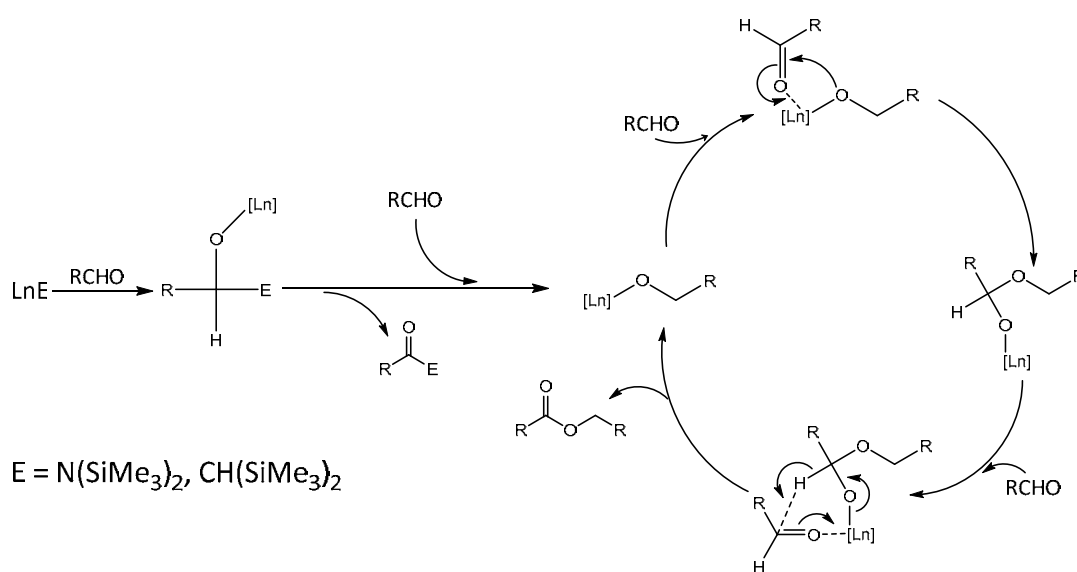


Scheme 1-45. Schematic mechanism of Aluminium alkoxides catalysed Tishchenko reaction.

Other catalysts such as transition metal complexes,⁵⁷ boric acid⁵⁸ or some Mg compounds,⁵⁹ have been used as the catalysts however it has been reported that the lanthanoid

formamidinate compounds are the most reactive catalyst system ever reported.⁵³ Reducing the steric effect of the formamidinate ligands can increase catalytic activity of the compounds and $[\text{La}(o\text{-TolForm})_3(\text{thf})_2]$ has been reported as the most reactive catalyst for the Tishchenko reaction.⁵³

$\text{Ln}[\text{N}(\text{SiMe}_3)_2]_3$ compounds ($\text{Ln} = \text{Sc}, \text{Y}$ and La) have been reported as highly active catalysts for the dimerization of aliphatic and aromatic aldehydes.⁶⁰ A similar mechanism as aluminium alkoxides has been proposed for these catalysts which involves formation of an intermediate lanthanoid(III) alkoxide (Scheme 1-46).



Scheme 1-46. Lanthanoid complexes catalysed Tishchenko reaction mechanism.

1.8 Conclusion

There is much interest in studying metal-organic compounds and expanding their structural ranges. The present literature review shows that a lot of attention has been paid to prepare metal-organic compounds using bis(aryl)formamidinate ligands which can show a variety of bonding modes and can be sterically modified. Among all the synthetic routes, the RTP reaction has been proven as an efficient method to synthesize rare earth formamidinate complexes. What is absent in this area is using formamidines of moderate bulk such as N,N' -di(diphenyl)formamidinate (PhFormH) or N,N' -di(2,4-dimethyl)formamidinate (DMFormH).

Based on the literature review, objectives of this research can be briefly summarized as below:

1. Synthesizing rare earth formamidinate complexes with moderate steric bulk.
2. Studying the structures and characterization of rare earth formamidinate complexes using microanalysis, IR spectra, X-ray crystallography, and NMR spectroscopy.
3. Studying the reactivity of the compounds towards the Tishchenko reaction.

1.9 References

1. R. Crabtree, *New York*, 2005, 104-111.
2. F. A. Cotton and G. Wilkinson, *Advanced inorganic chemistry*, Wiley New York, 1988.
3. R. H. Crabtree, *The Organometallic Chemistry of the Transition Metals*, Wiley, 2014.
4. R. C. Mehrotra, *Organometallic Chemistry*, New Age International (P) Limited, 2007.
5. E. C. Subbarao and W. E. Wallace, *Science and technology of rare earth materials*, Academic Press, 1980.
6. S. Kobayashi and R. Anwender, *Lanthanides: Chemistry and Use in Organic Synthesis*, Springer, 1999.
7. A. R. Jha, *Rare Earth Materials: Properties and Applications*, CRC Press, 2014.
8. S. Cotton, *Lanthanide and Actinide Chemistry*, Wiley, 2013.
9. H. Friedman Jr, G. Choppin and D. Feuerbacher, *J. Chem. Educ.*, 1964, **41**, 354.
10. P. Powell, *Principles of Organometallic Chemistry*, Springer, 1998.
11. A. D. McNaught, A. Wilkinson, I. U. o. Pure and A. Chemistry, *Compendium of Chemical Terminology: IUPAC Recommendations*, Blackwell Science, 1997.
12. T. J. Boyle and L. A. M. Ottley, *Chem. Rev.*, 2008, **108**, 1896-1917.
13. N. Bochkarev, L. N. Zakharov and G. S. Kalinina, *Organoderivatives of rare earth elements*, Kluwer Academic Publishers, 1995.
14. K. Izod, S. T. Liddle and W. Clegg, *Inorg. Chem.*, 2004, **43**, 214-218.
15. F. T. Edelmann, D. M. Freckmann and H. Schumann, *Chem. Rev.*, 2002, **102**, 1851-1896.
16. D. M. Barnhart, D. L. Clark, J. C. Gordon, J. C. Huffman, R. L. Vincent, J. G. Watkin and B. D. Zwick, *Inorg. Chem.*, 1994, **33**, 3487-3497.
17. S. Hamidi, L. N. Jende, H. Martin Dietrich, C. c. Maichle-Mössmer, K. W. Törnroos, G. B. Deacon, P. C. Junk and R. Anwender, *Organometallics*, 2013, **32**, 1209-1223.
18. G. B. Deacon, C. M. Forsyth and S. Nickel, *J. Organomet. Chem.*, 2002, **647**, 50-60.
19. G. B. Deacon, E. E. Delbridge, B. W. Skelton and A. H. White, *Eur. J. Inorg. Chem.*, 1998, **1998**, 543-545.
20. G. B. Deacon, E. E. Delbridge, B. W. Skelton and A. H. White, *Eur. J. Inorg. Chem.*, 1999, **30**, 751-761.
21. G. B. Deacon, P. C. Junk and A. Urbatsch, *Aust. J. Chem.*, 2012, **65**, 802-810.

22. M. L. Cole, G. B. Deacon, P. C. Junk and J. Wang, *Organometallics*, 2013, **32**, 1370-1378.
23. G. B. Deacon, M. G. Gardiner, P. C. Junk, J. P. Townley and J. Wang, *Organometallics*, 2012, **31**, 3857-3864.
24. M. L. Cole, G. B. Deacon, P. C. Junk and K. Konstas, *Chem. Commun.*, 2005, 1581-1583.
25. M. L. Cole, G. B. Deacon, C. M. Forsyth, P. C. Junk, K. Konstas and J. Wang, *Chem. Eur. J.*, 2007, **13**, 8092-8110.
26. G. B. Deacon, T. Feng, C. M. Forsyth, A. Gitlits, D. C. Hockless, Q. Shen, B. W. Skelton and A. H. White, *J. Chem. Soc., Dalton Trans.*, 2000, 961-966.
27. J. Barker and M. Kilner, *Coord. Chem. Rev.*, 1994, **133**, 219-300.
28. R. M. Roberts, *J. Org. Chem.*, 1949, **14**, 277-284.
29. P. C. Junk and M. L. Cole, *Chem. Commun.*, 2007, 1579-1590.
30. G. B. Deacon, P. C. Junk, L. K. Macreadie and D. Werner, *Eur. J. Inorg. Chem.*, 2014, 5240-5250.
31. B. S. Lim, A. Rahtu and R. G. Gordon, *Nat. Mater.*, 2003, **2**, 749-754.
32. F. T. Edelmann, *Chem. Soc. Rev.*, 2009, **38**, 2253-2268.
33. M. L. Cole, P. C. Junk and L. M. Louis, *J. Chem. Soc., Dalton Trans.*, 2002, 3906-3914.
34. M. L. Cole, D. J. Evans, P. C. Junk and L. M. Louis, *New. J. Chem.*, 2002, **26**, 1015-1024.
35. M. L. Cole, G. B. Deacon, C. M. Forsyth, K. Konstas and P. C. Junk, *Dalton Trans.*, 2006, 3360-3367.
36. R. Shannon, *Acta Crystallogr. A*, 1976, **32**, 751-767.
37. M. L. Cole, D. J. Evans, P. C. Junk and M. K. Smith, *Chem. Eur. J.*, 2003, **9**, 415-424.
38. J. Baldamus, C. Berghof, M. L. Cole, D. J. Evans, E. Hey-Hawkins and P. C. Junk, *J. Chem. Soc., Dalton Trans.*, 2002, 2802-2804.
39. M. Brym, C. M. Forsyth, C. Jones, P. C. Junk, R. P. Rose, A. Stasch and D. R. Turner, *Dalton Trans.*, 2007, 3282-3288.
40. M. L. Cole, G. B. Deacon, C. M. Forsyth, P. C. Junk, D. Polo-Cerón and J. Wang, *Dalton Trans.*, 2010, **39**, 6732-6738.
41. M. L. Cole, G. B. Deacon, C. M. Forsyth, P. C. Junk, K. Konstas, J. Wang, H. Bittig and D. Werner, *Chem. Eur. J.*, 2013, **19**, 1410-1420.
42. M. L. Cole and P. C. Junk, *J. Organomet. Chem.*, 2003, **666**, 55-62.
43. M. L. Cole, A. J. Davies, C. Jones and P. C. Junk, *J. Organomet. Chem.*, 2004, **689**, 3093-3107.

44. M. L. Cole and P. C. Junk, *New. J. Chem.*, 2005, **29**, 135-140.
45. M. L. Cole, A. J. Davies, C. Jones and P. C. Junk, *New. J. Chem.*, 2005, **29**, 1404-1408.
46. G. B. Deacon, P. C. Junk, J. Wang and D. Werner, *Inorg. Chem.*, 2014, **53**, 12553-12563.
47. D. Werner, G. B. Deacon, P. C. Junk and R. Anwander, *Chem. Eur. J.*, 2014, **20**, 4426-4438.
48. G. B. Deacon, P. C. Junk and D. Werner, *Polyhedron*, 2016, **103**, 178-186.
49. G. B. Deacon, P. C. Junk and D. Werner, *Chem. Eur. J.*, 2016, **22**, 160-173.
50. G. B. Deacon, P. C. Junk and D. Werner, *Eur. J. Inorg. Chem.*, 2015, 1484-1489.
51. A. Edelmann, C. G. Hrib, L. Hilfert, S. Blaurock and F. T. Edelmann, *Acta Crystallogr. E*, 2010, **66**, m1675-m1676.
52. A. Edelmann, V. Lorenz, C. G. Hrib, L. Hilfert, S. Blaurock and F. T. Edelmann, *Organometallics*, 2012, **32**, 1435-1444.
53. A. Zuyls, P. W. Roesky, G. B. Deacon, K. Konstas and P. C. Junk, *Eur. J. Org. Chem.*, 2008, **4**, 693-697.
54. E. Hawkins, D. Long and F. Major, *J. Chem. Soc.*, 1955, 1462-1468.
55. F. J. Villani and F. Nord, *J. Am. Chem. Soc.*, 1947, **69**, 2605-2607.
56. I. Lin and A. R. Day, *J. Am. Chem. Soc.*, 1952, **74**, 5133-5135.
57. K. Morita, Y. Nishiyama and Y. Ishii, *Organometallics*, 1993, **12**, 3748-3752.
58. P. R. Stapp, *J. Org. Chem.*, 1973, **38**, 1433-1434.
59. B. M. Day, W. Knowelden and M. P. Coles, *Dalton Trans.*, 2012, **41**, 10930-10933.
60. M. R. Bürgstein, H. Berberich and P. W. Roesky, *Chem. Eur. J.*, 2001, **7**, 3078-3085.

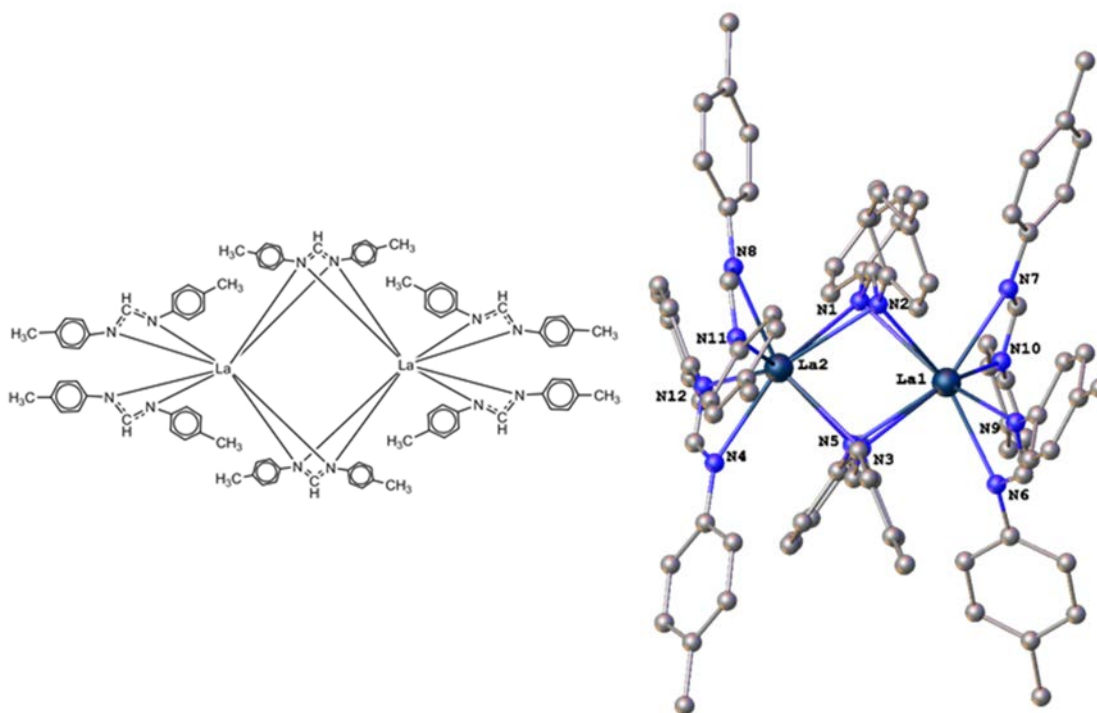
Chapter 2

Rare earth-N,N'-(diphenyl)formamidinate (PhForm) complexes

2 Synthesis and reactivity of RE-PhForm complexes

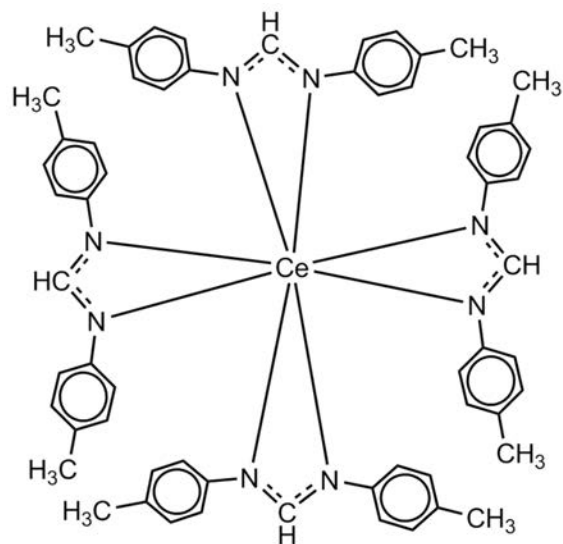
2.1 Introduction

This introduction shows some examples of lanthanoid formamidinate complexes and how versatile the less bulky bis(aryl)formamidinate ligands are e.g. *p*-TolFormH in producing compounds with variable coordination numbers and bonding modes. *p*-TolFormH can be used along with THF as the solvent in a RTP reaction to synthesize compounds with the general formula $[\text{Ln}(\textit{p}\text{-TolForm})_3(\text{thf})_2]$ (Ln = La, Ce, Nd, Sm).¹ The first $\mu\text{-}1\kappa(\text{N},\text{N}')\text{:}2\kappa(\text{N},\text{N}')$ coordination mode was observed in trivalent rare earth formamidinates by crystallizing them from non-coordinating solvents which liberates thf and yields compounds of general form $[\text{Ln}(\textit{p}\text{-TolForm})_3]_2$.¹ Considering the amidinate ligand class, especially non-bulky acetamidinate ligands, there are only a few examples of the $\mu\text{-}1\kappa(\text{N},\text{N}')\text{:}2\kappa(\text{N},\text{N}')$ binding mode.² However, it has been found using non-coordinating solvents has no effect on compounds with smaller RE metals such as lutetium, suggesting this trend highly depends on the size of metal. Structure of $[\text{La}(\textit{p}\text{-TolForm})_3]_2$ is identical to the structure of the Sm analogue (Scheme 2.1-1). In the case of Nd and Lu, the final structure is mononuclear.



Scheme 2.1-1. Schematic and X-ray structures of $[\text{La}(p\text{-TolForm})_3]_2$.¹

Cerium(III) formamidate $[\text{Ce}(p\text{-TolForm})_3]$ was prepared in good yield (96%) using a protonolysis reaction between $[\text{Ce}\{\text{N}(\text{SiMe}_3)_2\}_3]$ and $p\text{-TolFormH}$.³ Protonolysis between $[\text{Ce}\{\text{N}(\text{SiHMe}_2)_2\}_4]$ and four equivalents of $p\text{-TolFormH}$ led to the formation of $[\text{Ce}(p\text{-TolForm})_4]$ which is the first structurally characterized homoleptic cerium(IV) formamidate complex (Scheme 2.1-2). The Coordination number of cerium in this compound is eight with four chelating Form ligands.



Scheme 2.1-2. Schematic structure of $[\text{Ce}(p\text{-TolForm})_4]_3$.³

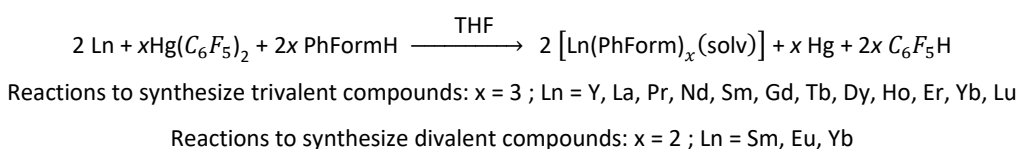
One of the bis(aryl)formamidine ligands that has been used to synthesize RE complexes for use in catalysts for the Tishchenko reaction is *o*-TolFormH.⁴ This ligand was used in RTP reactions to synthesize tris(formamidinato)lanthanoid(III) complexes, $[\text{La}(o\text{-TolForm})_3(\text{thf})_2]$ and $[\text{Er}(o\text{-TolForm})_3(\text{thf})]$.⁵ However, this route was not successful for preparing the Yb analogue in which consistently $[\{\text{Yb}(o\text{-TolForm})_2(\mu\text{-OH})(\text{thf})_2\}_2]$ was obtained. It has been reported Li(*o*-TolForm) and YbCl₃ can be used to synthesize $[\text{Yb}(o\text{-TolForm})_3(\text{thf})]$. Later, it was found that by using a larger Yb/Hg ratio in RTP reactions, the Yb(II) compound $[\text{Yb}(o\text{-TolForm})_2(\text{thf})_2]$ can be synthesized.⁶ Aluminium alkoxides are the traditional catalyst for the Tishchenko reaction.⁷⁻⁹ Recently, reactivity of lanthanide complexes, namely $[(\text{C}_5\text{Me}_5)_2\text{LaCH}(\text{SiMe}_3)_2]$ ¹⁰, $[\text{Ln}\{\text{N}(\text{SiMe}_3)_2\}_3]$ ^{11, 12} and $[\text{La}_2(\text{tBu}_2\text{pz})_6]$ (*t*Bu₂pz = 3,5-di-*tert*-butylpyrazolate)¹³, and homoleptic bis(trimethylsilyl)amides of the alkaline earth metals $[\text{M}\{\text{N}(\text{SiMe}_3)_2\}_2]$ (M= Ca, Sr, Ba)¹⁴ have been studied towards the Tishchenko reaction. However, it has been found that $[\text{La}(o\text{-TolForm})_3(\text{thf})_2]$ is the most effective in these reactions catalyzing the formation of esters from aldehydes.⁴

This chapter focuses on synthesis and reactivity of RE formamidinate complexes with moderate steric bulk effect. The aim is to increase reactivity by reducing bulkiness of the ligands about the metal center. Using PhForm⁻ (Scheme 1-2) as the ligand can decrease the steric effect and make the metal center more accessible for substrate. PhFormH was used in the present research as the ligand to synthesize RE-PhForm complexes for the first time. This ligand can be compared with *p*-TolFormH, *o*-TolFormH or *m*-TolFormH ligands which are

slightly bulkier. They have two methyl groups in *para*, *ortho* or *meta* positions respectively which make them slightly bulkier than PhFormH.

2.2 Results and discussion

RTP reactions using Ln⁰, Hg(C₆F₅)₂ and PhFormH in THF were performed to synthesize lanthanoid formamidinate complexes (Equation 2.2-1).



Equation 2.2-1.

One drop of mercury was used at the beginning of the reaction to activate the metal surface. Except in the case of La, Eu and Yb all other trivalent complexes were obtained in good yields (41% - 76%).

Single crystals suitable for X-ray crystallography were achieved by evaporation and concentration of the solutions (~5 ml) followed by cooling very slowly and keeping the samples in the fridge (~-5 °C) for several days. The IR spectra of all complexes are void of the 3300 cm⁻¹ absorption attributable to N-H stretching, suggesting complete consumption of PhFormH. ¹H NMR spectra (in C₆D₆) support the presence of PhForm with resonances at δ ≈ 9 ppm (NC(H)N). Metal analysis was performed on the crystals of compounds using EDTA before sending the sample to Metropolitan University in England for elemental analysis (C, H and N). Melting points of the compounds were measured using crystals of compounds in sealed glass capillaries under nitrogen and are uncalibrated.

A series of compounds with general formula of [Ln(PhForm)₃(thf)] was obtained using RTP reactions using Tb (**2.1**), Ho (**2.2**) and Er (**2.3**). These compounds were crystallized in the monoclinic space group *P*2₁/*c*, with the whole molecule occupying the asymmetric unit and geometry around the metal center can be described as distorted pentagonal bipyramidal. In

these compounds there are three chelating formamidinates and one coordinated thf molecule in the structure which gives coordination number of 7 to the metal center.

For Ln=La (**2.4**), Y (**2.5**), Pr (**2.6**), Nd (**2.7**), Sm (**2.8**), Gd (**2.9**), Dy (**2.10**) and Lu (**2.11**), the metal center has two coordinated *transoid*-thf molecules which gives coordination number of 8 to the metal center and general formula of $[\text{Ln}(\text{PhForm})_3(\text{thf})_2] \cdot (\text{THF})_m$ can be assigned to these compounds. All of these compounds except $[\text{La}(\text{PhForm})_3(\text{thf})_2]$ (**2.4**) and $[\text{Pr}(\text{PhForm})_3(\text{thf})_2]$ (**2.6**), were crystallized in the monoclinic space group $P2_1/c$, with the whole molecule occupying the asymmetric unit. $[\text{La}(\text{PhForm})_3(\text{thf})_2]$ (**2.4**) and $[\text{Pr}(\text{PhForm})_3(\text{thf})_2]$ (**2.6**) were crystallized in the orthorhombic space group $Pca2_1$, with the whole molecule occupying the asymmetric unit. The geometry around the metal center can be describe as distorted dodecahedral for these compounds. The compounds $[\text{Gd}(\text{PhForm})_3(\text{thf})_2] \cdot (\text{THF})_3$ (**2.9**), $[\text{Dy}(\text{PhForm})_3(\text{thf})_2] \cdot (\text{THF})_3$ (**2.10**), $[\text{Lu}(\text{PhForm})_3(\text{thf})_2] \cdot (\text{THF})_3$ (**2.11**) and $[\text{Y}(\text{PhForm})_3(\text{thf})_2] \cdot (\text{THF})_3$ (**2.5**) have three lattice THF molecules within asymmetric unit ($m=3$). The Figure 2.2-1 (a) and Figure 2.2-1 (b) show the structures of $[\text{Ho}(\text{PhForm})_3(\text{thf})]$ (**2.2**) and $[\text{Sm}(\text{PhForm})_3(\text{thf})_2]$ (**2.8**) respectively.

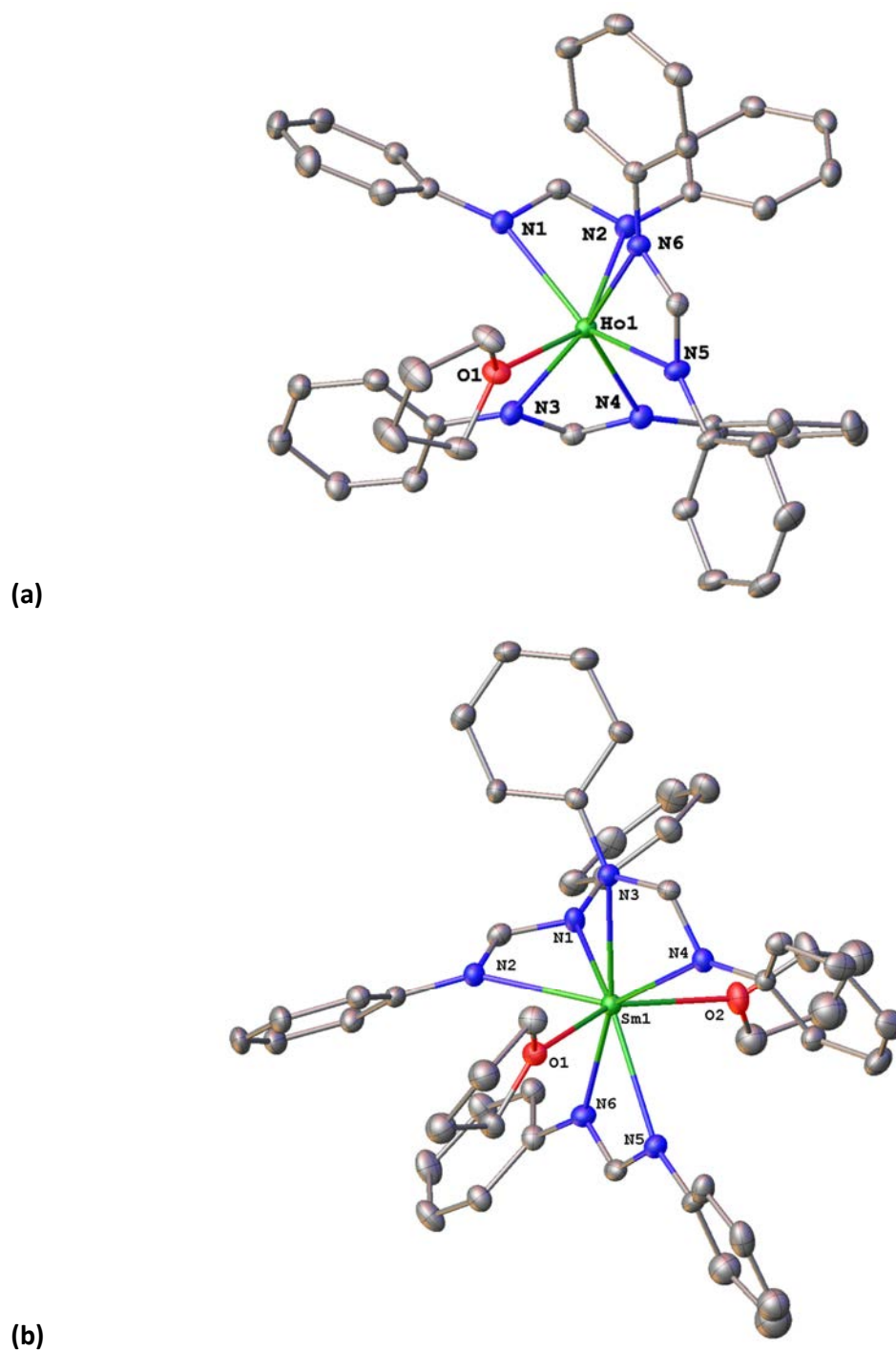


Figure 2.2-1. Molecular structures of (a) $[\text{Ho}(\text{PhForm})_3(\text{thf})]$ (**2.2**) and (b) $[\text{Sm}(\text{PhForm})_3(\text{thf})_2]$ (**2.8**). Hydrogen atoms removed for clarity.

The RTP reaction using Nd metal in THF following by evaporation and concentration did not give any crystals suitable for X-ray crystallography despite several attempts. Single crystals

suitable for X-ray crystallography were achieved by recrystallization from toluene. As a result, there is one lattice toluene within the asymmetric unit of $[\text{Nd}(\text{PhForm})_3(\text{thf})_2]\cdot\text{PhMe}$ (**2.7**).

Table 2.2-1 shows bond lengths of coordinated atoms from the metal centers for all compounds in this chapter. Figure 2.2-2 compares the bond length of Ln-N1 to Ln-N2. It can be seen in all of compounds, the chelation of ligands is symmetric. Figure 2.2-3 shows the distance of ligands to the metal center. For simplicity the back bone carbon was considered as the center of ligand in all compounds. It can be inferred from this figure that in all cases three ligands coordinated the metal center at equal distances. These two figures clearly show the lanthanide contraction effect. Moving from La to Lu, ionic radii of the metal center decreases as do the bond lengths of coordinating atoms and N-C-N centroid. It can be seen in these two graphs that the distances for $[\text{Tb}(\text{PhForm})_3(\text{thf})]$ (**2.1**), $[\text{Ho}(\text{PhForm})_3(\text{thf})]$ (**2.2**) and $[\text{Er}(\text{PhForm})_3(\text{thf})]$ (**2.3**) compounds are lower than other compounds. This can be attributed to the lower coordination number for these three compounds because of one less thf coordinated molecule in the structure. However, this figure shows shorter Ln-N bond lengths for $[\text{Tb}(\text{PhForm})_3(\text{thf})]$ (**2.1**) compared to the $[\text{Ho}(\text{PhForm})_3(\text{thf})]$ (**2.2**) and $[\text{Er}(\text{PhForm})_3(\text{thf})]$ (**2.3**) which have a same structure. This is an unusual feature observed for the compound (**2.2**). The average distance of the ligand from metal center is in good agreement with ionic radii of metal center and Figure 2.2-4 compares these values. Plotting the best fit between the values reveals that the average distance of the ligand and ionic radii follow almost a same trend and both of them decrease at a same rate because of lanthanide contraction effect.

Table 2.2-1. Bond length of coordinated atoms to the metal centers for different compounds

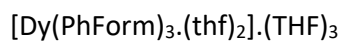
$[\text{Y}(\text{PhForm})_3(\text{thf})_2] \cdot (\text{THF})_3$			$[\text{La}(\text{PhForm})_3(\text{thf})_2]$		
Atom	Atom	Length/Å	Atom	Atom	Length/Å
Y1	N1	2.464(3)	La1	N1	2.504(17)
Y1	N2	2.434(3)	La1	N2	2.556(7)
Y1	N3	2.453(3)	La1	N3	2.549(7)
Y1	N4	2.466(3)	La1	N4	2.541(14)
Y1	N5	2.477(3)	La1	N5	2.544(8)
Y1	N6	2.418(3)	La1	N6	2.553(8)
Y1	O1	2.452(2)	La1	O1	2.531(7)
Y1	O2	2.390(2)	La1	O2	2.544(6)

$[\text{Pr}(\text{PhForm})_3(\text{thf})_2]$			$[\text{Nd}(\text{PhForm})_3(\text{thf})_2]$		
Atom	Atom	Length/Å	Atom	Atom	Length/Å
Pr1	N1	2.562(11)	Nd1	N1	2.534(5)
Pr1	N2	2.54(2)	Nd1	N2	2.525(5)
Pr1	N3	2.582(11)	Nd1	N3	2.519(5)
Pr1	N4	2.552(15)	Nd1	N4	2.571(5)
Pr1	N5	2.569(13)	Nd1	N5	2.545(5)
Pr1	N6	2.570(14)	Nd1	N6	2.539(5)
Pr1	O1	2.544(10)	Nd1	O1	2.483(4)
Pr1	O2	2.540(10)	Nd1	O2	2.502(4)

$[\text{Sm}(\text{PhForm})_3(\text{thf})_2]$			$[\text{Gd}(\text{PhForm})_3(\text{thf})_2] \cdot (\text{THF})_3$		
Atom	Atom	Length/Å	Atom	Atom	Length/Å
Sm1	N1	2.485(7)	Gd1	N1	2.471(6)
Sm1	N2	2.520(6)	Gd1	N2	2.500(6)
Sm1	N3	2.505(7)	Gd1	N3	2.460(6)
Sm1	N4	2.524(7)	Gd1	N4	2.535(7)
Sm1	N5	2.542(7)	Gd1	N5	2.514(6)
Sm1	N6	2.481(7)	Gd1	N6	2.488(6)
Sm1	O1	2.466(5)	Gd1	O1	2.480(6)
Sm1	O2	2.501(6)	Gd1	O2	2.437(5)



Atom	Atom	Length/Å
Tb1	N1	2.354(3)
Tb1	N2	2.350(2)
Tb1	N3	2.340(2)
Tb1	N4	2.408(2)
Tb1	N5	2.329(2)
Tb1	N6	2.382(2)
Tb1	O1	2.332(2)



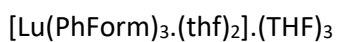
Atom	Atom	Length/Å
Dy1	N1	2.471(6)
Dy1	N3	2.427(6)
Dy1	N4	2.476(6)
Dy1	N5	2.475(6)
Dy1	N6	2.460(6)
Dy1	O1	2.402(5)
Dy1	O2	2.467(5)



Atom	Atom	Length/Å
Ho1	N1	2.421(2)
Ho1	N2	2.370(2)
Ho1	N3	2.390(2)
Ho1	N4	2.382(2)
Ho1	N5	2.375(2)
Ho1	N6	2.443(2)
Ho1	O1	2.3737(19)



Atom	Atom	Length/Å
Er1	N1	2.363(2)
Er1	N2	2.415(2)
Er1	N3	2.374(2)
Er1	N4	2.387(2)
Er1	N5	2.374(2)
Er1	N6	2.437(2)
Er1	O1	2.3620(18)



Atom	Atom	Length/Å
Lu1	N1	2.474(6)
Lu1	N2	2.455(6)
Lu1	N3	2.473(6)
Lu1	N4	2.489(6)
Lu1	N5	2.487(6)
Lu1	N6	2.450(6)
Lu1	O1	2.472(6)
Lu1	O2	2.424(5)

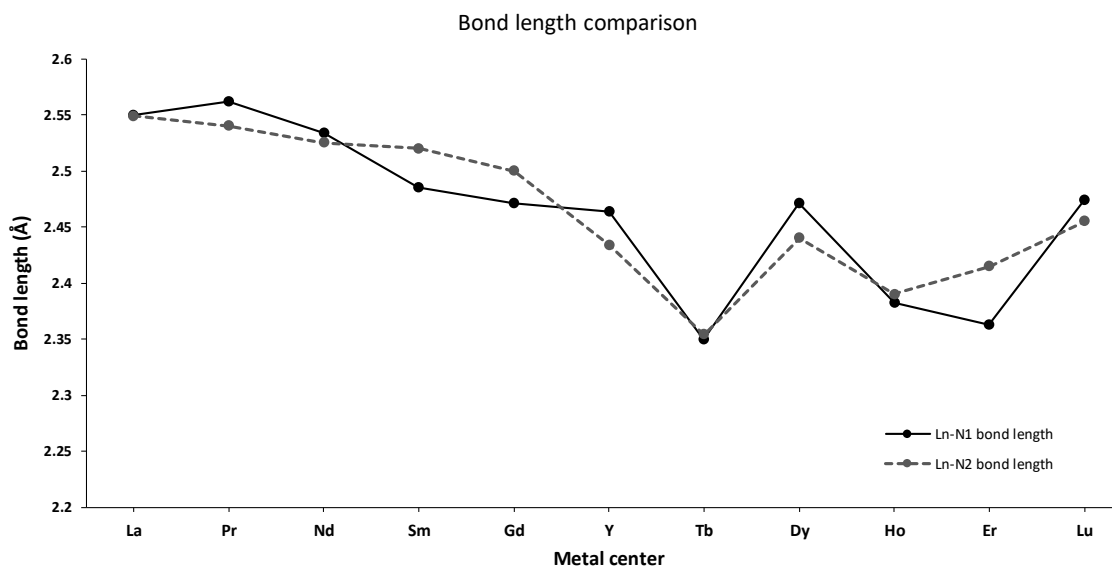


Figure 2.2-2. Comparison of Ln-N1 to Ln-N2 bond length for different metal centers of compounds.

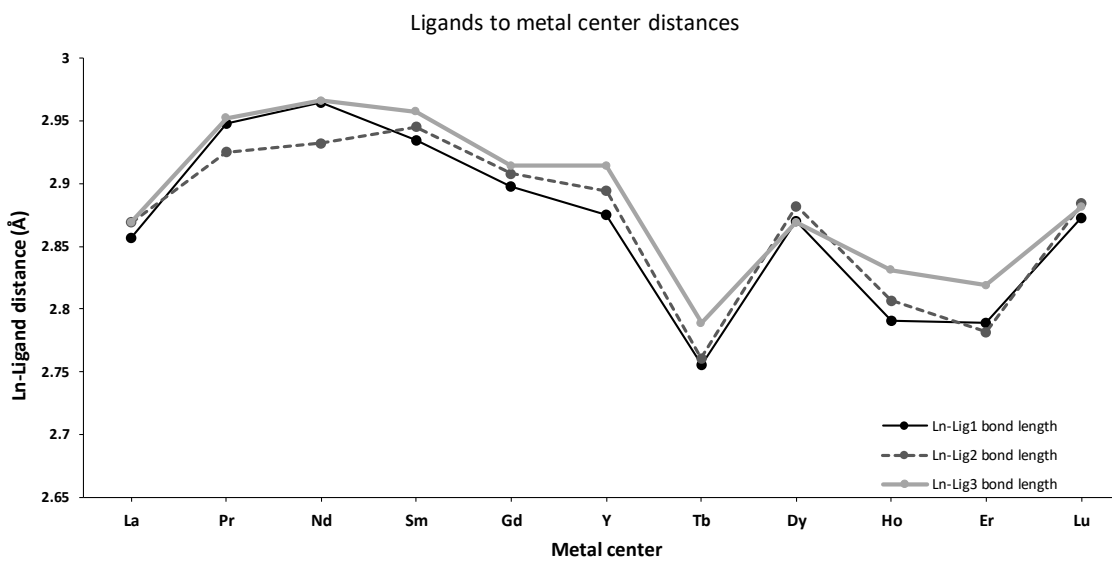


Figure 2.2-3. Comparison of Ln-Lig distances for different metal centers of compounds.

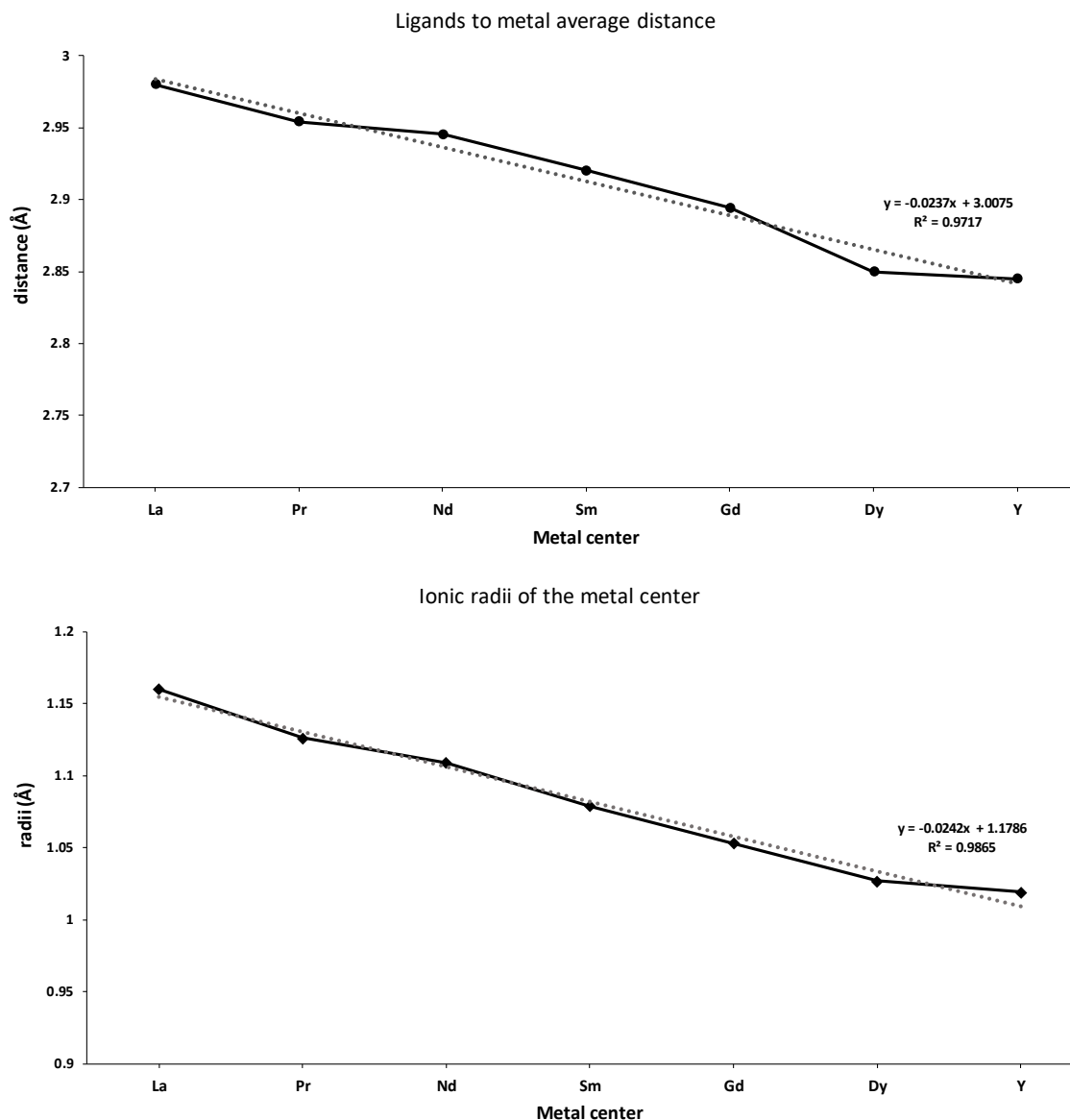


Figure 2.2-4. Comparison between average distances of ligand from metal center (up) and ionic radii of trivalent metal centers (down).

Table 2.2-2 shows the angles between the three ligands of each compound. For simplicity, the back bone carbon was considered as the center of ligand (Figure 2.2-5). If the three chelating ligands are considered as coplanar ligands, the sum of angles should be 360° . Except [Tb(PhForm)₃.(thf)] (**2.1**), [Ho(PhForm)₃.(thf)] (**2.2**) and [Er(PhForm)₃.(thf)] (**2.3**) compounds, the sum of angles are 360° in all compounds which suggesting coplanarity. For the Tb (**2.1**), Ho (**2.2**) and Er (**2.3**) complexes the sum of angles is about 351° which implies the ligands are not coplanar. This can be because of the lack of a coordinated thf molecule in the structure.

One more thf molecule in *trans* position related to other thf molecule, can push the non-coplanar ligand, and place it on the plane of two other ligands by steric force.

Table 2.2-2. Angles between the metal centers and chelating ligands

	C1-Ln-C2	C1-Ln-C3	C2-Ln-C3	Sum
Y	107.88°	106.56°	145.46°	359.9°
La	90.7°	132.2°	137°	359.9°
Pr	90.6°	131.6°	137.7°	359.9°
Nd	103.51°	110.56°	145.84°	359.91°
Sm	111°	104.7°	144.2°	359.9°
Gd	110.6°	104.7°	144.6°	359.9°
Tb	99.56°	138.31°	112.82°	350.69°
Dy	107.9°	106.5°	145.5°	359.9°
Ho	99.42°	138.76°	112.75°	350.93°
Er	99.33°	112.63°	138.73°	350.69°
Lu	108.2°	106.1°	145.6°	359.9°

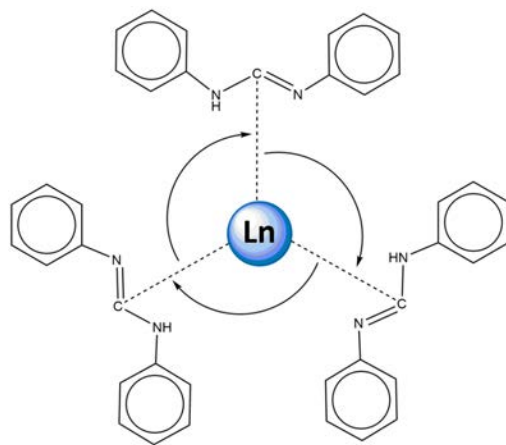
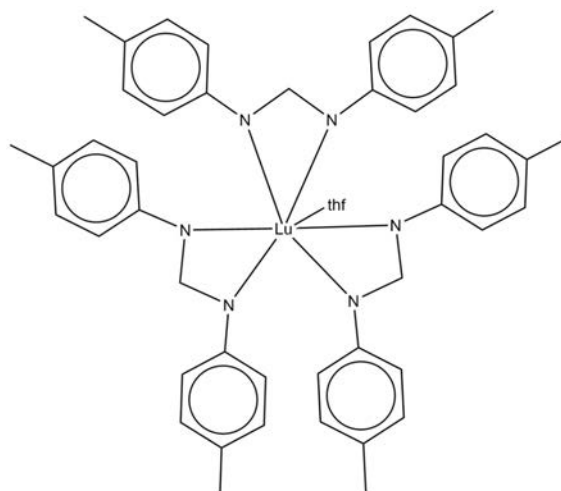


Figure 2.2-5. Schematic of the method has been used for measuring angles between three chelating ligands.

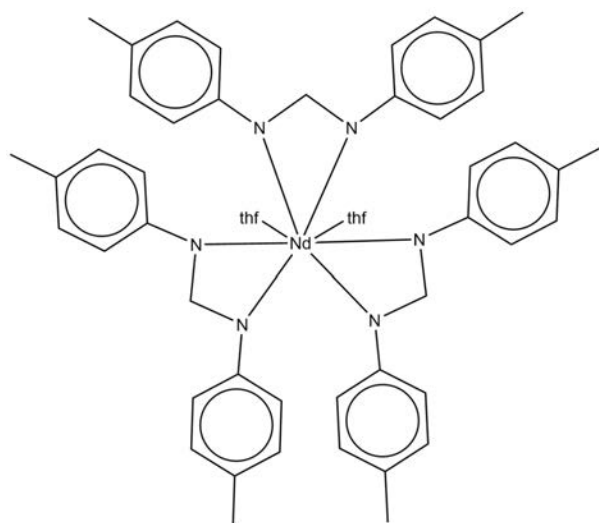
The main unusual feature of the Lu compound (**2.11**) is it has greater coordination number than Tb (**2.1**), Ho (**2.2**) and Er (**2.3**). Currently, there are only two other lutetium formamidinates that have been crystallographically characterized. One is $[\text{Lu}(p\text{-TolForm})_3\cdot\text{thf}]^1$ (Scheme 2.2-1) and the other one is $[\text{Lu}(\text{PhC}(\text{NC}_6\text{H}_3\text{iPr}_2\text{-2,6})_2)((t\text{Bu})\text{NCHN}(t\text{Bu}))(\text{thf})_2]^+.$ ¹⁵



Scheme 2.2-1. Schematic X-ray structure of $[\text{Lu}(p\text{-TolForm})_3.\text{thf}]$.¹

The coordination sphere of $[\text{Lu}(\text{PhForm})_3.(\text{thf})_2].(\text{THF})_3$ (**2.11**) is saturated with one more coordinate thf molecule compared with the $[\text{Lu}(p\text{-TolForm})_3.\text{thf}]$. This can be because of slightly greater steric effect of *p*-TolForm ligand that prevents coordination of another thf molecule. The extra methyl groups in *p*-TolForm are away from the metal center so the difference between steric effect of this ligand and PhForm expected to be minor however even this slight difference seems has influence on the coordination number of final structure. $[\text{Lu}(p\text{-TolForm})_3.\text{thf}]$ has lower coordination number so it is not unusual to see shorter Lu-N bond length and lower ligand to metal center distance compared with $[\text{Lu}(\text{PhForm})_3.(\text{thf})_2].(\text{THF})_3$ (**2.11**). The compound $[\text{Lu}(p\text{-TolForm})_3.\text{thf}]$ has the average Lu-N bond length of 2.3581(3) Å while this value is 2.4713(6) Å for $[\text{Lu}(\text{PhForm})_3.(\text{thf})_2].(\text{THF})_3$ (**2.11**). Comparing the Ln-N average length of $[\text{Lu}(p\text{-TolForm})_3.\text{thf}]$ with $[\text{Er}(\text{PhForm})_3.(\text{thf})]$ (**2.3**), which has same coordination number for the metal center, reveals that they are almost equal (2.3916(2) Å and 2.35816(3) Å respectively). The difference between the values is about 0.03 Å which can be attributed to the greater bulkiness of *p*-TolForm and the lower ionic radii of Lu. The mean distances of ligands to metal centers also follow the same trend. Similar to $[\text{Tb}(\text{PhForm})_3.(\text{thf})]$ (**2.1**), $[\text{Ho}(\text{PhForm})_3.(\text{thf})]$ (**2.2**) and $[\text{Er}(\text{PhForm})_3.(\text{thf})]$ (**2.3**) compounds, which have coordination number of seven, the three chelating ligands cannot be placed on a plane in $[\text{Lu}(p\text{-TolForm})_3.\text{thf}]$ compound and the sum of angles between the ligands is less than 360° (350.83° which is equal to the values for (**2.1**), (**2.1**) and (**2.1**) structures).

The structure of $[\text{Nd}(\text{PhForm})_3(\text{thf})_2]$ (**2.7**) is similar to the structure of the first reported eight coordinate neodymium formamidinate, $[\text{Nd}(p\text{-TolForm})_3(\text{thf})_2]\cdot\text{THF}$, which has been obtained by using $p\text{-TolFormH}$ ligand in a RTP reaction with Nd metal and $\text{Hg}(\text{C}_6\text{F}_5)_2$ in THF.¹ This complex crystallizes in the monoclinic space group $P2_1/n$, same as for $[\text{Nd}(\text{PhForm})_3(\text{thf})_2]$ (**2.7**), there are three bidentate ligands and two *transoid*-thf molecules ($[\text{O1-Nd-O2} = 153.61(6)^\circ]$)(Scheme 2.2-2). Searches within the Cambridge Structural database¹⁶ revealed that $[\text{Nd}(p\text{-TolForm})_3(\text{thf})_2]\cdot\text{THF}$ is the only crystallographically characterized eight coordinate neodymium formamidinate complex and $[\text{Nd}(\text{PhForm})_3(\text{thf})_2]\cdot\text{PhMe}$ (**2.7**) compound is the second one.



Scheme 2.2-2. Schematic X-ray structure of $[\text{Nd}(p\text{-TolForm})_3(\text{thf})_2]$.¹

The angle between the two *transoid*-thf molecules ($\text{O1-Nd-O2} = 153.61(6)^\circ$) is greater than usual values for $[\text{Ln}(\text{PhForm})_3(\text{thf})_2]$ compounds (Table 2.2-5). Three bulkier chelating $p\text{-TolForm}$ ligands in the structure of $[\text{Nd}(p\text{-TolForm})_3(\text{thf})_2]\cdot\text{THF}$ can exert greater influence to the two thf molecules more than the PhForm ligand so wider angles are expected for the *transoid*-thf molecules.

Mononuclear rare earth formamidinate structures with three chelating ligands is a common structural type for lanthanoid (III) complexes. Table 2.2-4 shows some other examples of these compounds with different homoleptic formamidinate ligands and their preparation reactions for comparison.

Table 2.2-3. Transoid-thf bond angles

Metal center	O1-Ln-O2
Y	148.92(9)
La	153.0(2)
Pr	153.2(3)
Nd	149.33(14)
Sm	149.7(2)
Gd	149.7(2)
Dy	149.00(19)
Lu	148.66(19)

Table 2.2-4. Trivalent mononuclear lanthanoid formamidinate complexes

CF₃FormH	[La(CF ₃ Form) ₃], ¹⁷	La + CF ₃ FormH + Hg(C ₆ F ₅) ₂ in THF
	[Yb(CF ₃ Form) ₃ (thf)], ¹⁷	Yb + CF ₃ FormH + Hg(C ₆ F ₅) ₂ in THF
DFFormH	[Yb(DFForm) ₃ (thf)], ¹⁸	Yb + DFFormH + Hg(C ₆ F ₅) ₂ in THF
	[Sm(DFForm) ₃ (thf) ₂], ¹	[Sm(p-TolForm) ₃] ₂ .1/2 thf + DFFormH in PhMe (crystallised from THF/Hexane mixture)
DippFormH	[Sm(DippForm) ₃], ¹⁹	Dissolution of [Na(THF) ₅][SmI ₂ (DippForm) ₂ (THF)] in hexane
o-TolFormH	[La(o-TolForm) ₃ (thf) ₂], ⁵	La + o-TolFormH + Hg(C ₆ F ₅) ₂ in THF
	[Er(o-TolForm) ₃ (thf)], ⁵	Er + o-TolFormH + Hg(C ₆ F ₅) ₂ in THF
XylFormH	[La(XylForm) ₃ (thf)], ⁵	La + XylFormH + Hg(C ₆ F ₅) ₂ in THF
	[Sm(XylForm) ₃], ⁵	Sm + XylFormH + Hg(C ₆ F ₅) ₂ in THF
MesFormH	[Ln(MesForm) ₃] (Ln = La, Nd, Sm and Yb), ⁵	Ln + MesFormH + Hg(C ₆ F ₅) ₂ in THF
EtFormH	[Ln(EtForm) ₃] (Ln = La, Nd, Sm, Ho and Yb), ⁵	Ln + EtFormH + Hg(C ₆ F ₅) ₂ in THF

Attempts for getting pure divalent or trivalent compounds involving PhForm and Yb or Eu using different stoichiometries, solvents and different crystallization methods were unsuccessful. Using Sm for obtaining divalent compounds always gave the mononuclear trivalent compound [Sm(PhForm)₃.(thf)₂] (**2.8**). Using PhFormH and Yb in a RTP reaction with Hg(C₆F₅)₂ in THF gave a red jelly product which could not be separated from other material in solution. A small amount of Yb solution (≈5 ml) was separated from the solution in one attempt and a layer of DMF was added. The solution was kept in the fridge (≈-5 °C) for a week. Very small crystals in a very low yield were observed on the wall of the Schlenk flask and

separated for X-ray crystallography. Figure 2.2-6 shows the crystal structure of the compound established as $[\{\text{Yb}(\text{PhForm})_2(\mu\text{-OH})(\text{dmf})_2\}_2]$ (**2.12**).

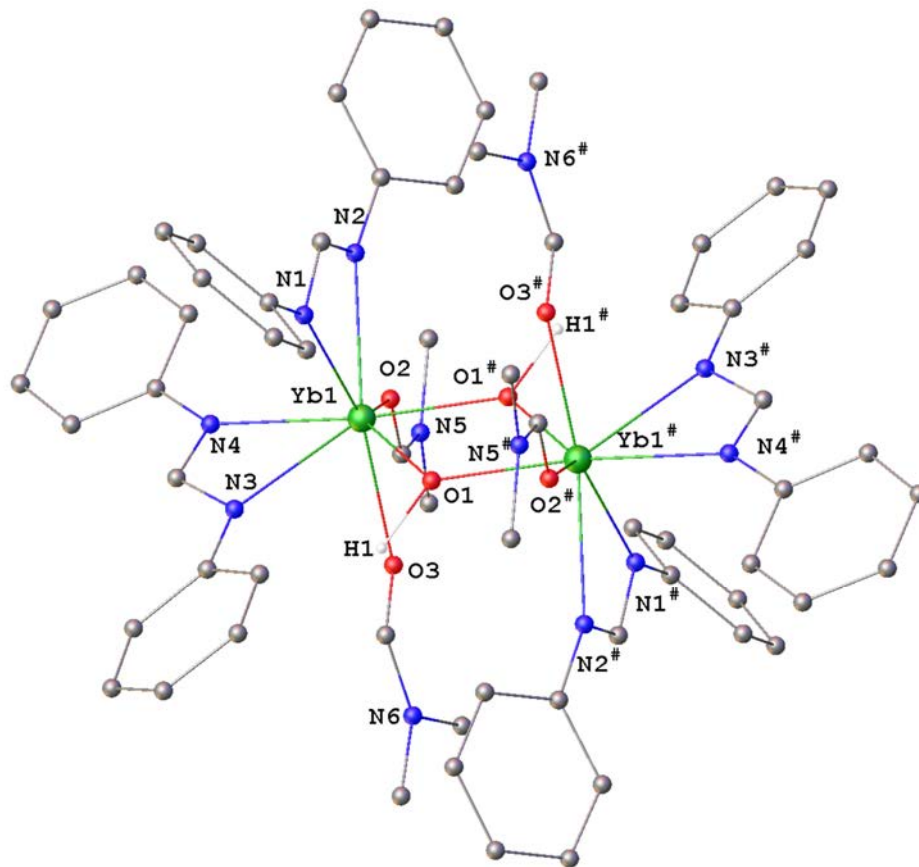


Figure 2.2-6. Molecular structure of $[\{\text{Yb}(\text{PhForm})_2(\mu\text{-OH})(\text{dmf})_2\}_2]$ (**2.12**). Hydrogen atoms except those for hydroxy bridge groups removed for clarity. Symmetry transformation used to generate “#” atoms: 1-X,1-Y,-Z.

This compound crystallizes in the monoclinic space group $P2_1/c$ with half of the molecule comprising the asymmetric unit. The compound is a dimer and has two trivalent Yb metal centers. Each metal center has two chelating PhForm ligands and two bound dmf molecules. The metal centers are connected by two coplanar bridging hydroxyl groups, which gives the coordination number of eight for each metal center. The geometries about the Yb^{3+} centers are best described as a distorted bicapped triangular prism (Figure 2.2-7). The two triangular faces of the capped triangular prism are distorted due to the bridging $\text{Yb}(\mu\text{-OH})_2\text{Yb}$ unit and NCN backbones of PhForm ligands.

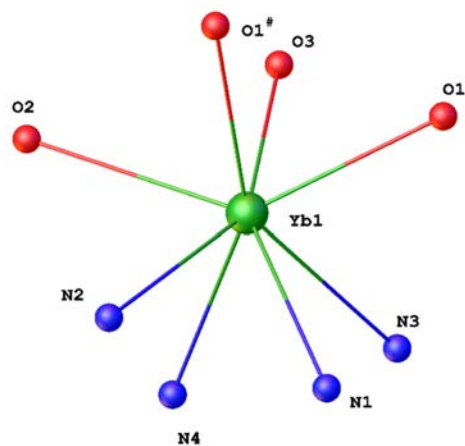


Figure 2.2-7. Yb coordination polyhedron of $[\{Yb(PhForm)_3(\mu-OH)(dmf)_2\}_2]$ (**2.12**).

Unfortunately, this compound has been not fully characterized because of its low yield and unsuccessful attempts to deliberately synthesize a pure compound. The structure of $[\{Yb(PhForm)_2(\mu-OH)(dmf)_2\}_2]$ (**2.12**) is very similar to $[\{Yb(o-TolForm)_2(\mu-OH)(thf)\}_2]$ which was reported in 2007 (Figure 2.2-8).⁵

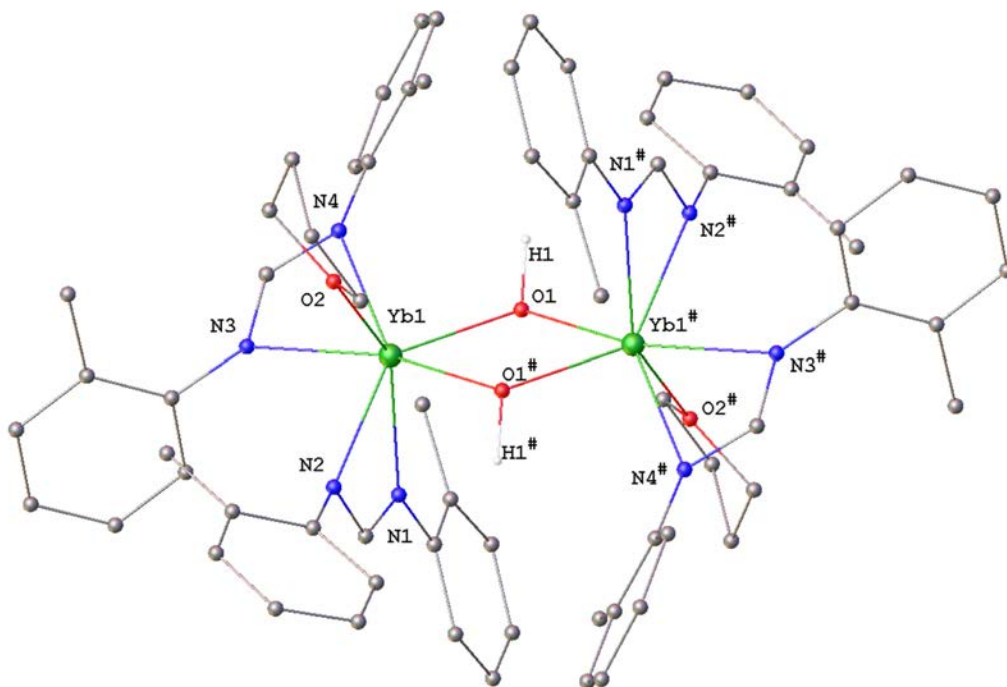


Figure 2.2-8. Molecular structure of $[\{Yb(o-TolForm)_2(\mu-OH)(thf)\}_2]$. Hydrogen atoms except those for hydroxy bridge groups removed for clarity. Symmetry transformation used to generate “#” atoms: 1-X,2-Y,1-Z.

As for compound **2.12**, this compound is dinuclear and crystallizes in the monoclinic space group $P2_1/c$ with half of the molecule comprising the asymmetric unit. The coordination number of metal centers is seven and they are bridged by two coplanar hydroxyl groups. The coordination number for each metal center is lower compared with the $[\{Yb(PhForm)_2(\mu-OH)(dmf)_2\}_2]$ (**2.12**) because of lack of one coordinated solvent molecule and this is presumably due to the steric influence of the *ortho* methyl group toward the metal center. There are two chelating formamidinates for each metal center. The geometry about the trivalent Yb metal centers are best described as distorted N(2) face capped triangular prisms (Figure 2.2-9).

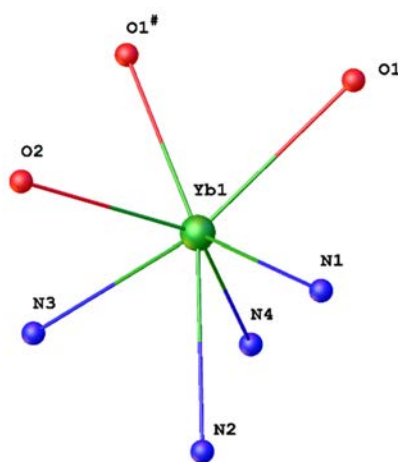


Figure 2.2-9. Yb coordination polyhedron of $[\{Yb(o-TolForm)_2(\mu-OH)(thf)\}_2]$ complex.

Comparing bond lengths of these two compounds (Figure 2.2-10) reveals generally **2.12** has longer bond lengths which can be attributed to the higher coordination number of the metal centers. This should be considered in relation to the steric effect of the ligands. Lower bond lengths are expected for **2.12** considering the lower steric effect of PhForm compared with the *o*-TolForm however Figure 2.2-10 suggests that the coordination number has more effect on the bond lengths. The longer bond lengths for **2.12** means the atoms are extended further away from the metal center so metal centers can come closer to each other which reduces the Yb-Yb[#] and Yb-OH distances. More obtuse in Yb-Yb[#] length pushes the hydroxyl groups away from each other resulting in higher angle of OH-Yb-OH[#] for **2.12** (Figure 2.2-11).

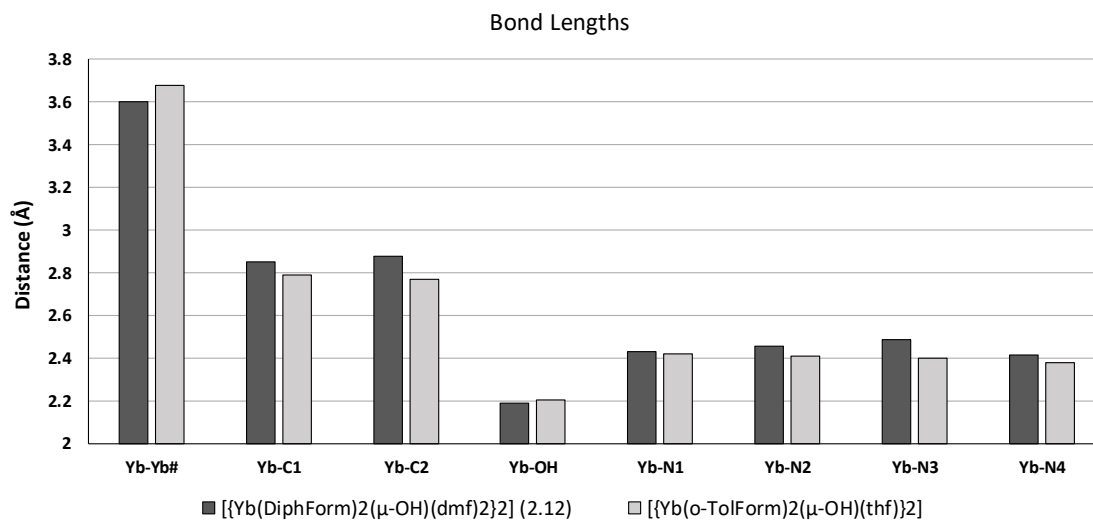


Figure 2.2-10. Comparison of bond lengths between $[\{Yb(PhForm)_2(\mu-OH)(dmf)_2\}_2]$ (**2.12**) and $[\{Yb(o-TolForm)_2(\mu-OH)(thf)_2\}_2]$.

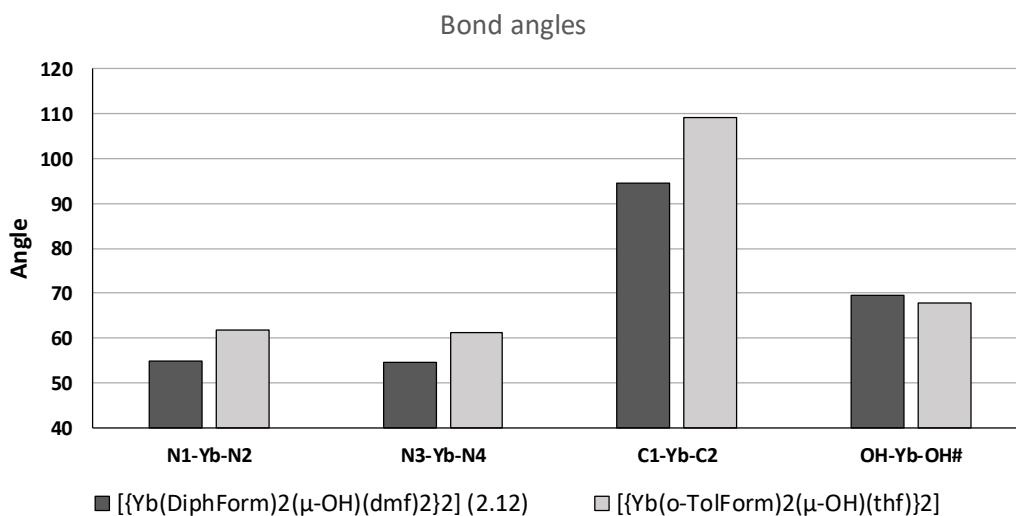
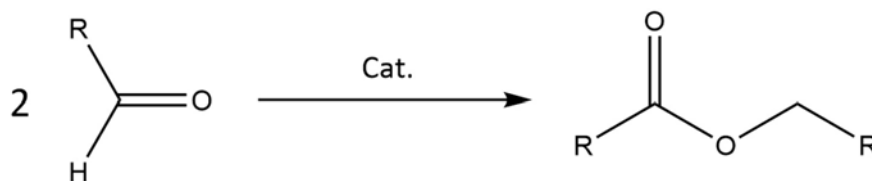


Figure 2.2-11. Comparison of bond angles between $[\{Yb(PhForm)_2(\mu-OH)(dmf)_2\}_2]$ (**2.12**) and $[\{Yb(o-TolForm)_2(\mu-OH)(thf)_2\}_2]$.

The attempts for getting crystals from the analogues reaction involving Eu was completely unsuccessful. It seems that the reactions of these two metals undergo polymerization reactions which give gel like products. In the case of Eu, the solution was dark yellow. DME was added hoping it may break up the assumed polymeric chain however the result was similar to the reaction using thf and a gel like product was obtained.

2.3 Reactivity as catalysts in Tishchenko reactions

Lanthanoid formamidinate compounds have been known as reactive catalysts toward the Tishchenko reaction⁴ (Scheme 2.3-1) and [La(*o*-TolForm)₃(thf)₂] has been reported as the most reactive catalyst for converting aldehydes to the corresponding esters. However, *ortho*-toluidine, the precursor for synthesizing *o*-TolFormH, has been reported as a restricted carcinogen.^{20, 21} The aim is to replace [La(*o*-TolForm)₃(thf)₂] with another lanthanoid formamidinate compound to avoid using carcinogen starting materials and increase the reactivity of the final compound. The idea is to use another ligand with less steric effect like PhFormH to increase the accessibility of the metal center for the reaction.



Scheme 2.3-1. Schematic of Tishchenko reaction.

The standard reaction of benzaldehyde to form benzyl benzoate was chosen to compare the activities of [Ho(PhForm)₃(thf)] (**2.2**), [Er(PhForm)₃(thf)] (**2.3**), [Y(PhForm)₃(thf)₂](THF)₃ (**2.5**), [Sm(PhForm)₃(thf)₂] (**2.8**), [Gd(PhForm)₃(thf)₂](THF)₃ (**2.9**) as catalysts in the Tishchenko reaction. The reactions were performed at room temperature using crystals of the compounds to ensure purity and ¹H NMR spectroscopy in C₆D₆ was used to determine the yields and progress of the reaction. The yields were evaluated based on 1 mol% of the catalyst. The reactions were monitored in different time intervals of 5 min, 1 hr, 24 hr, 48 hr, 72 hr, 96 hr and 120 hr after initiating the reaction. Decrease in the characteristic aldehyde proton signal (at 5.18 ppm) and increase in the intensity of the benzyl group proton signal (at 9.72 ppm) in the ¹H NMR spectra provide evidence for production of benzyl benzoate and the integration of these resonances were used to calculate the yield of the reaction at different time intervals. Figure 2.3-1 compares the reactivities of these compounds. It can be seen the best fitted logarithmic line for each compound has a good R² factor suggesting that kinetic of the reactions can be explained by logarithmic equations. Considering the ionic radius of the

metal centers²² and ligand distances from metal center (Figure 2.2-3 and Figure 2.2-4), higher reactivity is expected for [Sm(PhForm)₃(thf)₂] (**2.8**) and [Gd(PhForm)₃(thf)₂](THF)₃ (**2.9**) compared with [Ho(PhForm)₃(thf)] (**2.2**), [Er(PhForm)₃(thf)] (**2.3**) and [Y(PhForm)₃(thf)₂](THF)₃ (**2.5**), because higher ionic radius makes the metal center more accessible. Less reactivities of (**2.8**) and (**2.9**) can be attributed to higher coordination number of metal centers in these compounds. Considering compounds with the same metal center coordination numbers, higher reactivities have been observed for higher ionic radii. [Y(PhForm)₃(thf)₂](THF)₃ (**2.5**) compound is an exception and it is rather confusing to see highest reactivity for this compound despite of lower ionic radii compared with other compounds like [Sm(PhForm)₃(thf)₂] (**2.8**).

The results of reactivity experiments suggest that [La(*o*-TolForm)₃(thf)₂] is still the best catalyst towards the Tishchenko reaction.⁴ Compounds (**2.2**), (**2.3**), (**2.5**), (**2.8**) and (**2.9**) are sterically less hindered complexes compared with [La(*o*-TolForm)₃(thf)₂] and it was expected to see higher catalytic activities for these compounds. Even complexes with more sterically hindered formamidinates like [La(XylForm)₃(thf)] or [La(EtForm)₃] have greater catalytic reactivity compared with the (**2.2**), (**2.3**), (**2.5**), (**2.8**) and (**2.9**).⁴

The reason of less catalytic activities of these compounds is not clear yet. In previous studies, it has been found that the ionic radii of the involved lanthanoid atom plays the most important role in controlling the rate of catalytic conversion of aldehydes.²³ The aim was to compare the reactivity of compounds with the same metal centers however despite many attempts to repeat the RTP reaction involving La, PhFormH and Hg(C₆F₅)₂ to obtain La(PhForm)₃(thf)₂] (**2.8**), this compound could not be prepared in a pure form.

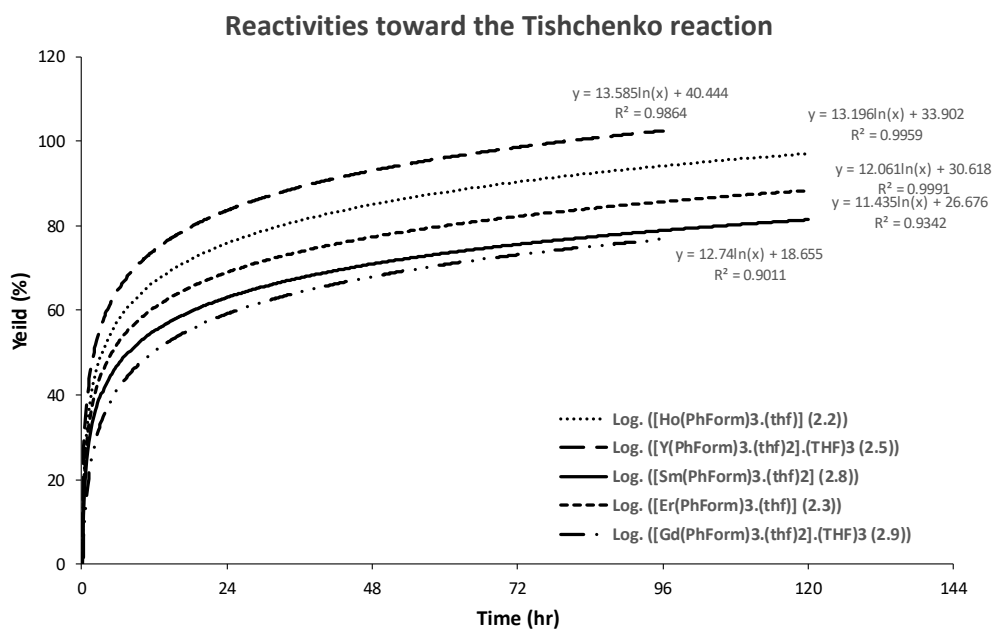


Figure 2.3-1. Comparison of catalytic reactivities for some of the compounds.

2.4 Conclusions

In this chapter PhFormH was used along with different lanthanoid metals in RTP reactions to synthesize a series of lanthanoid PhForm complexes. All the synthesized compounds were trivalent and PhFormH shows difficulties to use as the ligand for synthesizing divalent compounds. The resulted structures showed this ligand can bind lanthanoids very well and in most of the cases three chelating PhForm ligands bind to the metal center. Hoping to reduce the steric effect and increase the reactivity of the final compound toward the Tishchenko reaction, the compounds from this chapter were evaluated as the catalysts in the standard reaction of converting benzaldehyde to benzyl benzoate. The result of this study shows these compounds have catalytic properties and can be used for the Tishchenko reaction. The final reactivity of these compounds were less than previously reported [La(*o*-TolForm)₃.(thf)₂]. *Ortho*-toluidine, the precursor for synthesizing *o*-TolFormH, is a carcinogenic compound and this study demonstrated another compounds like [Y(PhForm)₃.(thf)₂].(THF)₃ (**2.5**) can be considered as a replacement. By comparing the reactivities of [La(*o*-TolForm)₃.(thf)₂], [La(XylForm)₃.(thf)], [La(EtForm)₃], (**2.2**), (**2.3**), (**2.5**), (**2.8**) and (**2.9**), it can be concluded that steric hindrance and the ionic radius of the metal center are two important parameters that

should be considered to produce an effective catalyst. $[\text{Y}(\text{PhForm})_3(\text{thf})_2](\text{THF})_3$ (**2.5**) has the highest catalytic activity compared with other compounds in this chapter suggesting there should be other factors that can affect the final reactivity.

2.5 Experimental

All the samples were prepared using a glove box, Schlenk flask and vacuum line techniques in an inert atmosphere since lanthanoid metals and their products are air-sensitive and moisture-sensitive. Sodium or sodium/benzophenone were used for refluxing and distillation of solvents to dry and deoxygenate them prior to use in reactions. The lanthanoid metal reagents were purchased either in form of fine powders or metal ingots from Rhone Poulenc or Santoku. In the case of metal ingots, they were freshly filed under an inert atmosphere into metal filings. PhFormH ligand either was purchased from Sigma-Aldrich or prepared by literature methods.²⁴ IR data were obtained from Nujol mulls for the region 4000-400 cm^{-1} with a Nicolet-Nexus FT-IR spectrometer. ^1H NMR spectra were recorded with a Bruker Avance 400 MHz spectrometer using dry degassed *deutero*-benzene (C_6D_6) as solvent, and resonances were referenced to the residual ^1H resonances of the deuterated solvent. Elemental analyses (C, H, N) were performed by the Micro analytical Laboratory, Science Centre, London Metropolitan University, England.

$[\text{Tb}(\text{PhForm})_3(\text{thf})]$ (**2.1**)

Terbium filings (0.30 g, 1.80 mmol), $\text{Hg}(\text{C}_6\text{F}_5)_2$ (0.62 g, 1.50 mmol) and PhFormH (0.60 g, 3.00 mmol) were added to a Schlenk flask and dissolved in THF (20 mL) with stirring at room temperature for one week. The resulting yellowish green solution was filtered through a filter cannula from the metal residue and evaporated under vacuum to 5 mL and cooled to $-5\text{ }^\circ\text{C}$ for several days. Small yellow crystals of (**2.1**) were produced. Yield = 0.51 g (63%); M.P. 160-163 $^\circ\text{C}$; IR (Nujol, cm^{-1}): $\nu = 1657$ (m), 1535 (s), 1455 (vs), 1377 (vs), 1291 (s), 1214 (s), 1169 (s), 1074 (m), 1023 (m), 985 (m), 938 (m), 893 (w), 807 (m), 756 (s), 723 (s), 693(s) cm^{-1} (wv); ^1H NMR (C_6D_6 , 303.2 K): Gives broad peaks due to the paramagnetic nature of this compound.

Elemental analysis calc. (%) for $C_{43}H_{41}N_6OTb$ ($M = 816.77 \text{ g.mol}^{-1}$): C 63.23, H 5.06, N 10.29; Found: C 55.43, H 5.09, N 9.88. Tb: 19.31; Found from titration: 19.41.

[Ho(PhForm)₃.(thf)] (**2.2**)

Holmium filings (0.30 g, 1.80 mmol), $Hg(C_6F_5)_2$ (0.62 g, 1.50 mmol) and PhFormH (0.60 g, 3.00 mmol) were added to a Schlenk flask and dissolved in THF (20 mL) with stirring at room temperature for one week. The resulting yellow solution was filtered through a filter cannula from the metal residue and evaporated under vacuum to 5 mL and cooled to -5 °C for several days. Small yellow crystals of (**2.2**) were produced. Yield = 0.46 g (57%); M.P. 167-170 °C; IR (Nujol, cm^{-1}): $\nu = 1932$ (w), 1661 (vw), 1591 (s), 1578 (s), 1464 (vs), 1377 (s), 1326 (s), 1283 (s), 1216 (s), 1171 (s), 1151 (s), 1076 (m), 1027 (m), 1012 (m), 996 (m), 987(s), 943 (s), 897 (w), 867(m), 757(s), 688(s), 622(vw), 603(m) cm^{-1} (wv); 1H NMR (C_6D_6 , 303.2 K): Gives broad peaks due to the paramagnetic nature of this compound. Elemental analysis calc. (%) for $C_{43}H_{41}N_6OHo$ ($M = 822.77 \text{ g.mol}^{-1}$): C 62.77, H 5.02, N 10.21. Found: C 62.43, H 5.10, N 10.04.

[Er(PhForm)₃.(thf)] (**2.3**)

Erbium filings (0.30 g, 1.79 mmol), $Hg(C_6F_5)_2$ (0.62 g, 1.50 mmol) and PhFormH (0.60 g, 3.00 mmol) were added to a Schlenk flask and dissolved in THF (20 mL) with stirring at room temperature for one week. The resulting dark pink solution was filtered through a filter cannula from the metal residue and evaporated under vacuum to 5 mL and cooled to -5 °C for several days. Small pink crystals of (**2.3**) were produced. Yield = 0.49 g (61%); 168-173 °C; IR (Nujol, cm^{-1}): $\nu = 1932$ (w), 1848 (vw), 1785 (vw), 1720 (vw), 1669 (w), 1590 (m), 1472 (vs), 1382 (vs), 1153 (s), 1077 (s), 942 (s), 893 (s), 808 (s), 721 (vs), 692 (s), 622(m), 603 (s) cm^{-1} (wv); 1H NMR (C_6D_6 , 303.2 K): Gives broad peaks due to the paramagnetic nature of this compound. $\delta = 0.66$ (br s, CH_2), 4.07 (br s, CH_2), 8.64 (br s, $NC(H)N$). Elemental analysis calc. (%) for $C_{43}H_{41}N_6OEr$ ($M = 825.10 \text{ g.mol}^{-1}$): C 62.60, H 5.01, N 10.19; Found: C 59.12, H 5.06, N 10.47. Er: 20.27; Found from titration: 20.31.

[La(PhForm)₃.(thf)₂] (**2.4**)

Lanthanum filings (0.30 g, 2.15 mmol), Hg(C₆F₅)₂ (0.62 g, 1.50 mmol) and PhFormH (0.60 g, 3.00 mmol) were added to a Schlenk flask and dissolved in THF (20 mL) with stirring at room temperature for one week. The resulting yellow solution was filtered through a filter cannula from the metal residue and evaporated under vacuum to 5 mL and cooled to -5 °C for several days. Small yellow crystals of (**2.4**) were produced. Yield ≈ 0.01 g (<20%);

[Y(PhForm)₃.(thf)₂].(THF)₃ (**2.5**)

Yttrium filings (0.30 g, 3.37 mmol), Hg(C₆F₅)₂ (0.62 g, 1.50 mmol) and PhFormH (0.60 g, 3.00 mmol) were added to a Schlenk flask and dissolved in THF (20 mL) with stirring at room temperature for one week. The resulting gray solution was filtered through a filter cannula from the metal residue and evaporated under vacuum to 5 mL and cooled to -5 °C for several days. Small crystals (almost colorless) of (**2.5**) were produced. Yield = 0.417 g (51%); M.P. 171-175 °C; IR (Nujol, cm⁻¹): ν = 1932 (w), 1656 (vw), 1529 (s), 1456 (vs), 1377 (vs), 1291 (s), 1216 (s), 1171 (s), 1152 (s), 1076 (m), 1026 (m), 987 (m), 890 (w), 943 (m), 896 (m), 865 (m), 806 (m), 756(s), 688(s), 621(m), 602(m) cm⁻¹ (wv); ¹H NMR (C₆D₆, 303.2 K): δ = 1.18 (br m, 20 H, CH₂), 3.40 (s, 20 H, CH₂) (loss of 2 THFs of solvation), 6.65–6.98 (br m, 30H; Ar-H), 8.71 (s, 3 H, NC(H)N). Elemental analysis calc. (%) for C₄₇H₄₉YN₆O₂ (loss of 3 THFs of solvation M = 818.30 g.mol⁻¹): C 68.85, H 6.02, N 10.51; Found: C 68.73, H 5.85, N 10.17.

[Pr(PhForm)₃.(thf)₂] (**2.6**)

Praseodymium filings (0.30 g, 2.12 mmol), Hg(C₆F₅)₂ (0.62 g, 1.50 mmol) and PhFormH (0.60 g, 3.00 mmol) were added to a Schlenk flask and dissolved in THF (20 mL) with stirring at room temperature for one week. The resulting yellow solution was filtered through a filter cannula from the metal residue and evaporated under vacuum to 5 mL and cooled to -5 °C for several days. Small yellowish green crystals of (**2.6**) were produced. Yield = 0.36 g (43%); M.P. 152-155 °C; IR (Nujol, cm⁻¹): ν = 1929 (w), 1864 (vw), 1756 (vw), 1719 (vw), 1673 (w), 1447 (vs), 1376 (vs), 1297 (s), 1170 (s), 1074 (s), 1022 (s), 986 (s), 934 (m), 889 (m), 806 (m), 755 (s), 693 (s), 619 (m), 597(m) cm⁻¹ (wv); ¹H NMR (C₆D₆, 303.2 K): Gives broad peaks due to

the paramagnetic nature of this compound. Elemental analysis calc. (%) for $C_{47}H_{49}PrN_6O_2$ ($M = 870.86 \text{ g}\cdot\text{mol}^{-1}$): C 64.82, H 5.67, N 9.65; Found: C 60.36, H 5.73, N 9.20. Pr: 16.18; Found from titration: 16.14.

[Nd(PhForm)₃.(thf)₂].PhMe (**2.7**)

Neodymium filings (0.30 g, 2.08 mmol), $Hg(C_6F_5)_2$ (0.62 g, 1.50 mmol) and PhFormH (0.60 g, 3.00 mmol) were added to a Schlenk flask and dissolved in THF (20 mL) with stirring at room temperature for one week. The resulting yellow solution was filtered through a filter cannula from the metal residue. The clear solution dried using vacuum and small amount of toluene ($\approx 5 \text{ ml}$) was added. The solution was cooled to $-5 \text{ }^\circ\text{C}$ for several days. Small white crystals of (**2.7**) were produced. Yield = 0.38 g (45%); M.P. 158-162 $^\circ\text{C}$; IR (Nujol, cm^{-1}): $\nu = 1665$ (vw), 1577 (m), 1535 (vs), 1508 (vs), 1463 (vs), 1377 (s), 1326 (m), 1307 (vs), 1217 (s), 1176 (m), 1151 (m), 1075 (m), 1023 (w), 996 (w), 985 (m), 936 (m), 901 (w), 888 (w), 801 (vw), 757 (s), 722 (vw), 693 (s), 618 (vw), 593 (w) cm^{-1} (wv); ^1H NMR (C_6D_6 , 303.2 K): Gives broad peaks due to the paramagnetic nature of this compound. Elemental analysis calc. (%) for $C_{47}H_{49}NdN_6O_2$ (loss of PhMe of solvation, $M = 874.19 \text{ g}\cdot\text{mol}^{-1}$): C 64.58, H 5.65, N 9.61; Found: C 64.09, H 5.88, N 9.67.

[Sm(PhForm)₃.(thf)₂] (**2.8**)

Samarium filings (0.30 g, 2.00 mmol), $Hg(C_6F_5)_2$ (0.62 g, 1.50 mmol) and PhFormH (0.60 g, 3.00 mmol) were added to a Schlenk flask and dissolved in THF (20 mL) with stirring at room temperature for one week. The resulting yellow solution was filtered through a filter cannula from the metal residue and evaporated under vacuum to 5 mL and cooled to $-5 \text{ }^\circ\text{C}$ for several days. Small yellow crystals of (**2.8**) were produced. Yield = 0.65 g (76%); M.P. 160-162 $^\circ\text{C}$; IR (Nujol, cm^{-1}): $\nu = 1660$ (w), 1464 (vs), 1377 (s), 1327 (s), 1286 (vs), 1216 (vs), 1171 (s), 1151 (s), 1075 (s), 1025 (m), 987 (s), 942 (m), 895 (m), 869 (m), 808 (w), 757 (vs), 692 (s), 621 (vw), 602 (m), 518 (s) cm^{-1} (wv); ^1H NMR (C_6D_6 , 303.2 K): Gives broad peaks due to the paramagnetic nature of this compound so the integration is not accurate. $\delta = 6.30 - 7.42$ (m br, Ar-H), 7.80 (s br, NC(H)N). Elemental analysis calc. (%) for $C_{47}H_{49}SmN_6O_2$ ($M = 880.31 \text{ g}\cdot\text{mol}^{-1}$):

¹): C 64.13, H 5.61, N 9.55; Found: C 63.66, H 5.90, N 9.42. Sm: 17.08; Found from titration: 16.99.

[Gd(PhForm)₃(thf)₂].(THF)₃ (**2.9**)

Gadolinium filings (0.30 g, 1.91 mmol), Hg(C₆F₅)₂ (0.62 g, 1.50 mmol) and PhFormH (0.60 g, 3.00 mmol) were added to a Schlenk flask and dissolved in THF (20 mL) with stirring at room temperature for one week. The resulting yellow solution was filtered through a filter cannula from the metal residue and evaporated under vacuum to 5 mL and cooled to -5 °C for several days. Small yellow crystals of (**2.9**) were produced. Yield = 0.62 g (72%); M.P. 161-163 °C; IR (Nujol, cm⁻¹): ν = 1651 (m), 1531 (vs), 1462 (vs), 1376 (vs), 1295 (vs), 1219 (s), 1170 (s), 1152 (m), 1074 (s), 1026 (s), 988 (m), 938 (m), 890 (m), 808 (m), 756 (s), 727 (vs), 694 (vs), 620 (m), 600 (m) cm⁻¹ (wv); ¹H NMR (C₆D₆, 303.2 K): Gives broad peaks due to the paramagnetic nature of this compound. δ = 1.26 (s br, CH₂), 4.84 (s br, CH₂), 7.16 (s br, Ar-H), 8.29 (s br, NC(H)N). Elemental analysis calc. (%) for C₄₇H₄₉GdN₆O₂ (loss of 3 THFs of solvation M = 887.20 g.mol⁻¹): C 63.63, H 5.57, N 9.47; Found: C 50.26, H 4.35, N 9.47. Gd: 14.25; Found from titration: 14.10.

[Dy(PhForm)₃(thf)₂].(THF)₃ (**2.10**)

Dysprosium filings (0.30 g, 1.85 mmol), Hg(C₆F₅)₂ (0.62 g, 1.50 mmol) and PhFormH (0.60 g, 3.00 mmol) were added to a Schlenk flask and dissolved in THF (20 mL) with stirring at room temperature for one week. The resulting yellow solution was filtered through a filter cannula from the metal residue and evaporated under vacuum to 5 mL and cooled to -5 °C for several days. Small yellow crystals of (**2.10**) were produced. Yield = 0.59 g (68%); M.P. 173-176 °C; IR (Nujol, cm⁻¹): ν = 1660 (w), 1464 (vs), 1377 (s), 1327 (m), 1286 (vs), 1216 (s), 1171 (s), 1151 (m), 1075 (m), 1025 (m), 987 (m), 942 (m), 895 (m), 869 (m), 808 (w), 757 (s), 692 (s), 621 (vw), 602 (m), 518 (s) cm⁻¹ (wv); ¹H NMR (C₆D₆, 303.2 K): Gives broad peaks due to the paramagnetic nature of this compound. δ = 7.14 (s br, Ar-H), 9.52 (s br, NC(H)N). Elemental analysis calc. (%) for C₄₃H₄₁DyN₆O₂ (loss of three THFs of solvation and one coordinated THF; M = 820.34 g.mol⁻¹): C 62.96, H 5.04, N 10.24; Found: C 57.00, H 5.29, N 10.21. Dy: 14.65; Found from titration: 15.06.

[Lu(PhForm)₃.(thf)₂].(THF)₃ (**2.11**)

Lutetium filings (0.30 g, 1.71 mmol), Hg(C₆F₅)₂ (0.62 g, 1.50 mmol) and PhFormH (0.60 g, 3.00 mmol) were added to a Schlenk flask and dissolved in THF (20 mL) with stirring at room temperature for one week. The resulting dark red solution was filtered through a filter cannula from the metal residue and evaporated under vacuum to 5 mL and cooled to -5 °C for several days. Small pale red crystals of (**2.11**) were produced. Yield = 0.36 g (41%); M.P. 204-208 °C; IR (Nujol, cm⁻¹): $\nu = 1932$ (vw), 1669 (vw), 1460 (vs), 1377 (vs), 1285 (vs), 1218 (s), 1304 (m), 1170 (s), 1076 (m), 1011 (m), 986 (m), 944 (m), 896 (w), 869 (w), 756 (s), 722 (s), 689 (s), 622 (vw) cm⁻¹ (wv); ¹H NMR (C₆D₆, 303.2 K): $\delta = 6.40$ – 7.17 (br m, 30H; Ar-H), 8.76 (s, 3 H, NC(H)N). Elemental analysis calc. (%) for C₅₉H₇₃LuN₆O₅ (loss of three THFs of solvation, M = 904.92 g.mol⁻¹): C 62.35, H 5.46, N 9.29; Found from microanalysis: C 57.87, H 5.26, N 10.01. Lu: 15.60; Found from titration: 16.12.

X-Ray crystallography

[Tb(PhForm)₃.(thf)] (**2.1**)

C₄₃H₄₁N₆OTb (M = 816.77 g/mol): monoclinic, space group P2₁/n (no. 14), $a = 11.997(2)$ Å, $b = 13.750(3)$ Å, $c = 22.224(4)$ Å, $\beta = 95.38(3)^\circ$, $V = 3649.9(13)$ Å³, $Z = 4$, $T = 100.15$ K, $\mu(\text{MoK}\alpha) = 1.978$ mm⁻¹, $D_{\text{calc}} = 1.411$ g/cm³, 41747 reflections measured ($3.488^\circ \leq 2\theta \leq 49.996^\circ$), 6285 unique ($R_{\text{int}} = 0.0428$, $R_{\text{sigma}} = 0.0264$) which were used in all calculations. The final R_1 was 0.0268 ($I > 2\sigma(I)$) and wR_2 was 0.0713 (all data).

[Ho(PhForm)₃.(thf)] (**2.2**)

C₄₃H₄₁HoN₆O (M = 822.77 g/mol): monoclinic, space group P2₁/n (no. 14), $a = 12.017(2)$ Å, $b = 13.841(3)$ Å, $c = 22.169(4)$ Å, $\beta = 94.98(3)^\circ$, $V = 3673.4(13)$ Å³, $Z = 4$, $T = 293(2)$ K, $\mu(\text{MoK}\alpha) = 2.196$ mm⁻¹, $D_{\text{calc}} = 1.488$ g/cm³, 60855 reflections measured ($3.472^\circ \leq 2\theta \leq 55.818^\circ$), 8744 unique ($R_{\text{int}} = 0.0345$, $R_{\text{sigma}} = 0.0176$) which were used in all calculations. The final R_1 was 0.0296 ($I > 2\sigma(I)$) and wR_2 was 0.0789 (all data).

[Er(PhForm)₃.(thf)] (2.3)

C₄₃H₄₁ErN₆O (*M* = 825.10 g/mol): monoclinic, space group *P2₁/n* (no. 14), *a* = 12.010(2) Å, *b* = 13.802(3) Å, *c* = 22.210(4) Å, *β* = 95.11(3)°, *V* = 3667.0(13) Å³, *Z* = 4, *T* = 100.15 K, *μ*(MoKα) = 6.850 mm⁻¹, *D*_{calc} = 1.997 g/cm³, 73067 reflections measured (3.478° ≤ 2θ ≤ 60.126°), 10719 unique (*R*_{int} = 0.0834, *R*_{sigma} = 0.0443) which were used in all calculations. The final *R*₁ was 0.0363 (*I* > 2σ(*I*)) and *wR*₂ was 0.0953 (all data).

[La(PhForm)₃.(thf)₂] (2.4)

C₄₇H₄₉LaN₆O₂ (*M* = 868.83 g/mol): orthorhombic, space group *Pca2₁* (no. 29), *a* = 21.3685(10) Å, *b* = 10.2707(5) Å, *c* = 19.5253(9) Å, *V* = 4285.2(4) Å³, *Z* = 4, *T* = 298.15 K, *μ*(MoKα) = 1.041 mm⁻¹, *D*_{calc} = 1.347 g/cm³, 100904 reflections measured (3.812° ≤ 2θ ≤ 55°), 9785 unique (*R*_{int} = 0.0947, *R*_{sigma} = 0.0513) which were used in all calculations. The final *R*₁ was 0.0430 (*I* > 2σ(*I*)) and *wR*₂ was 0.1276 (all data).

[Y(PhForm)₃.(thf)₂].(THF)₃ (2.5)

C₅₉H₇₃N₆O₅Y (*M* = 818.30 g/mol): monoclinic, space group *P2₁/c* (no. 14), *a* = 17.128(3) Å, *b* = 14.142(3) Å, *c* = 22.886(5) Å, *β* = 106.78(3)°, *V* = 5307(2) Å³, *Z* = 4, *T* = 173.15 K, *μ*(MoKα) = 1.088 mm⁻¹, *D*_{calc} = 0.224 g/cm³, 44235 reflections measured (3.428° ≤ 2θ ≤ 55.812°), 12547 unique (*R*_{int} = 0.0410, *R*_{sigma} = 0.0310) which were used in all calculations. The final *R*₁ was 0.0615 (*I* > 2σ(*I*)) and *wR*₂ was 0.1677 (all data).

[Pr(PhForm)₃.(thf)₂] (2.6)

C₄₇H₄₉N₆O₂Pr (*M* = 870.83 g/mol): orthorhombic, space group *Pca2₁* (no. 29), *a* = 21.355(3) Å, *b* = 10.2952(12) Å, *c* = 19.527(2) Å, *V* = 4293.1(9) Å³, *Z* = 4, *T* = 298.15 K, *μ*(MoKα) = 1.179 mm⁻¹, *D*_{calc} = 1.347 g/cm³, 53052 reflections measured (3.814° ≤ 2θ ≤ 54.996°), 9488 unique (*R*_{int} = 0.0981, *R*_{sigma} = 0.0750) which were used in all calculations. The final *R*₁ was 0.0615 (*I* > 2σ(*I*)) and *wR*₂ was 0.1834 (all data).

[Nd(PhForm)₃.(thf)₂].PhMe (2.7)

C₅₄H₅₄N₆NdO₂ (*M* = 963.27 g/mol): monoclinic, space group *P*2₁/*n* (no. 14), *a* = 17.553(4) Å, *b* = 14.216(3) Å, *c* = 20.855(4) Å, *β* = 107.18(3)°, *V* = 4971.9(19) Å³, *Z* = 4, *T* = 293(2) K, *μ*(MoKα) = 1.089 mm⁻¹, *D*_{calc} = 1.287 g/cm³, 83166 reflections measured (2.672° ≤ 2*θ* ≤ 55.888°), 11270 unique (*R*_{int} = 0.0695, *R*_{sigma} = 0.0333) which were used in all calculations. The final *R*₁ was 0.0613 (*I* > 2σ(*I*)) and *wR*₂ was 0.1880 (all data).

[Sm(PhForm)₃.(thf)₂] (2.8)

C₄₇H₄₉N₆O₂Sm (*M* = 880.31 g/mol): monoclinic, space group *P*2₁/*c* (no. 14), *a* = 17.140(7) Å, *b* = 14.769(9) Å, *c* = 23.284(11) Å, *β* = 104.013(16)°, *V* = 5718(5) Å³, *Z* = 4, *T* = 298.15 K, *μ*(MoKα) = 1.058 mm⁻¹, *D*_{calc} = 0.965 g/cm³, 14472 reflections measured (13.036° ≤ 2*θ* ≤ 49.994°), 8453 unique (*R*_{int} = 0.0590, *R*_{sigma} = 0.0791) which were used in all calculations. The final *R*₁ was 0.0646 (*I* > 2σ(*I*)) and *wR*₂ was 0.2144 (all data).

[Gd(PhForm)₃.(thf)₂].(THF)₃ (2.9)

C₅₉H₇₃GdN₆O₅ (*M* = 1067.32 g/mol): monoclinic, space group *P*2₁/*c* (no. 14), *a* = 17.055(3) Å, *b* = 14.644(2) Å, *c* = 23.155(4) Å, *β* = 104.122(3)°, *V* = 5608.2(15) Å³, *Z* = 4, *T* = 230.15 K, *μ*(MoKα) = 1.229 mm⁻¹, *D*_{calc} = 1.264 g/cm³, 33182 reflections measured (2.462° ≤ 2*θ* ≤ 55°), 12763 unique (*R*_{int} = 0.0698, *R*_{sigma} = 0.0839) which were used in all calculations. The final *R*₁ was 0.0573 (*I* > 2σ(*I*)) and *wR*₂ was 0.1675 (all data).

[Dy(PhForm)₃.(thf)₂].(THF)₃ (2.10)

C₅₉H₇₃DyN₆O₅ (*M* = 1107.72 g/mol): monoclinic, space group *P*2₁/*c* (no. 14), *a* = 17.124(3) Å, *b* = 14.155(3) Å, *c* = 22.873(5) Å, *β* = 106.70(3)°, *V* = 5310(2) Å³, *Z* = 4, *T* = 173.15 K, *μ*(MoKα) = 1.462 mm⁻¹, *D*_{calc} = 1.386 g/cm³, 64637 reflections measured (3.426° ≤ 2*θ* ≤ 55.832°), 11639 unique (*R*_{int} = 0.0349, *R*_{sigma} = 0.0208) which were used in all calculations. The final *R*₁ was 0.0710 (*I* > 2σ(*I*)) and *wR*₂ was 0.1907 (all data).

[Lu(PhForm)₃.(thf)₂].(THF)₃ (**2.11**)

C₅₉H₇₃LuN₆O₅ (*M* = 1120.19 g/mol): monoclinic, space group *P*2₁/*c* (no. 14), *a* = 17.122(3) Å, *b* = 14.195(3) Å, *c* = 22.883(5) Å, *β* = 106.71(3)°, *V* = 5327(2) Å³, *Z* = 4, *T* = 100.15 K, μ(MoKα) = 1.908 mm⁻¹, *D*_{calc} = 1.397 g/cm³, 62293 reflections measured (3.418° ≤ 2θ ≤ 50°), 8880 unique (*R*_{int} = 0.0254, *R*_{sigma} = 0.0136) which were used in all calculations. The final *R*₁ was 0.0641 (*I* > 2σ(*I*)) and *wR*₂ was 0.1588 (all data).

2.6 References

1. G. B. Deacon, P. C. Junk, L. K. Macreadie and D. Werner, *Eur. J. Inorg. Chem.*, 2014, 5240-5250.
2. M. N. Bochkarev, A. A. Maleev, T. V. Balashova, G. K. Fukin, E. V. Baranov, Y. A. Efimova, B. I. Petrov and V. A. Ilichev, *Inorg. Chim. Acta*, 2008, **361**, 2533-2539.
3. D. Werner, G. B. Deacon, P. C. Junk and R. Anwander, *Chem. Eur. J.*, 2014, **20**, 4426-4438.
4. A. Zuyls, P. W. Roesky, G. B. Deacon, K. Konstas and P. C. Junk, *Eur. J. Org. Chem.*, 2008, **4**, 693-697.
5. M. L. Cole, G. B. Deacon, C. M. Forsyth, P. C. Junk, K. Konstas and J. Wang, *Chem. Eur. J.*, 2007, **13**, 8092-8110.
6. M. L. Cole, G. B. Deacon, C. M. Forsyth, P. C. Junk, K. Konstas, J. Wang, H. Bittig and D. Werner, *Chem. Eur. J.*, 2013, **19**, 1410-1420.
7. E. Hawkins, D. Long and F. Major, *J. Chem. Soc.*, 1955, 1462-1468.
8. W. Child and H. Adkins, *J. Am. Chem. Soc.*, 1923, **45**, 3013-3023.
9. F. J. Villani and F. Nord, *J. Am. Chem. Soc.*, 1947, **69**, 2605-2607.
10. S.-y. Onozawa, T. Sakakura, M. Tanaka and M. Shiro, *Tetrahedron*, 1996, **52**, 4291-4302.
11. M. R. Bürgstein, H. Berberich and P. W. Roesky, *Chem. Eur. J.*, 2001, **7**, 3078-3085.
12. M. R. Bürgstein, H. Berberich and P. W. Roesky, *Organometallics*, 1998, **17**, 1452-1454.
13. G. B. Deacon, T. Feng, C. M. Forsyth, A. Gitlits, D. C. Hockless, Q. Shen, B. W. Skelton and A. H. White, *J. Chem. Soc., Dalton Trans.*, 2000, 961-966.
14. M. R. Crimmin, A. G. Barrett, M. S. Hill and P. A. Procopiou, *Org. Lett.*, 2007, **9**, 331-333.
15. J. Cheng and Z. Hou, *Chem. Commun.*, 2012, **48**, 814-816.
16. F. H. Allen, *Acta Crystallogr. B*, 2002, **58**, 380-388.
17. G. B. Deacon, P. C. Junk and D. Werner, *Eur. J. Inorg. Chem.*, 2015, 1484-1489.
18. G. B. Deacon, P. C. Junk and D. Werner, *Chem. Eur. J.*, 2016, **22**, 160-173.
19. M. L. Cole and P. C. Junk, *Chem. Commun.*, 2005, 2695-2697.
20. C. Watanabe, T. Egami, K. Midorikawa, Y. Hiraku, S. Oikawa, S. Kawanishi and M. Murata, *Environ. Health Prev. Med.*, 2010, **15**, 319.

21. Y. Ohkuma, Y. Hiraku, S. Oikawa, N. Yamashita, M. Murata and S. Kawanishi, *Arch. Biochem. Biophys.*, 1999, **372**, 97-106.
22. R. Shannon, *Acta Crystallogr. A*, 1976, **32**, 751-767.
23. H. Berberich and P. W. Roesky, *Angew. Chem. Int. Ed.*, 1998, **37**, 1569-1571.
24. R. M. Roberts, *J. Org. Chem.*, 1949, **14**, 277-284.

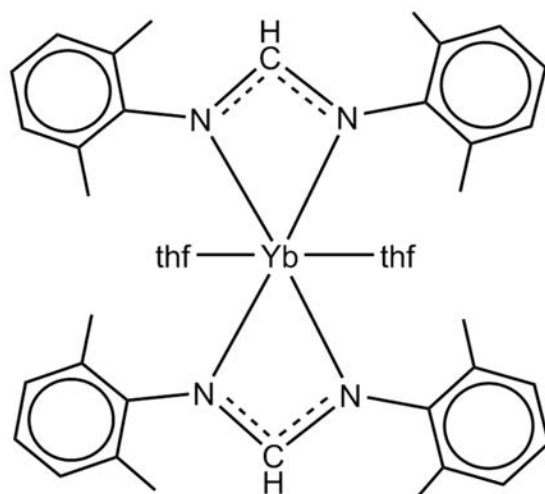
Chapter 3

Rare earth- N,N'-bis(2,4-dimethyl phenyl)formamidinate (DMForm) complexes

3 Rare earth- N,N'-bis(2,4-dimethyl phenyl)formamidinate (DMForm) complexes

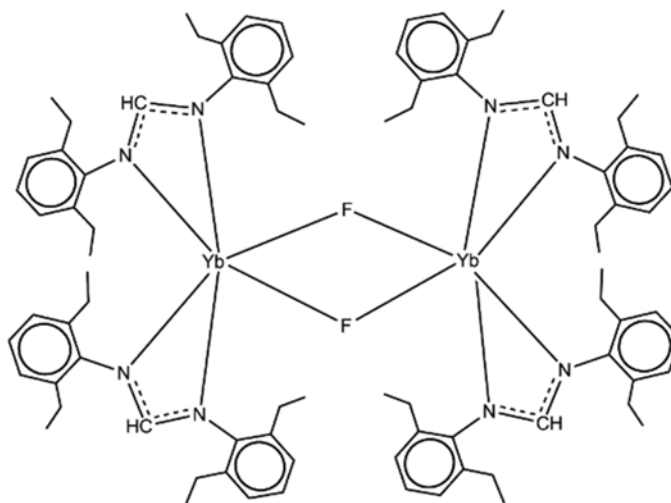
3.1 Introduction

Different lanthanoid formamidinate complexes of $[\text{Yb}(\text{XylForm})_2(\text{thf})_2]$, $[\text{Yb}(\text{EtForm})_2(\text{thf})_2]$, $[\text{Yb}(o\text{-PhPhForm})_2(\text{thf})_2]$, $[\text{Yb}(\text{DippForm})_2(\text{thf})_2]$ and $[\text{Eu}(\text{DippForm})_2(\text{thf})_2]$ have been previously prepared by RTP reactions between an excess of the lanthanoid metal, $\text{Hg}(\text{C}_6\text{F}_5)_2$ and the corresponding formamidinate ligand.¹ All the compounds are mononuclear and the metal center is six coordinate. The resulting compounds also have chelating N,N'-Form ligands and *cis*-thf donors (Scheme 3.1-1).

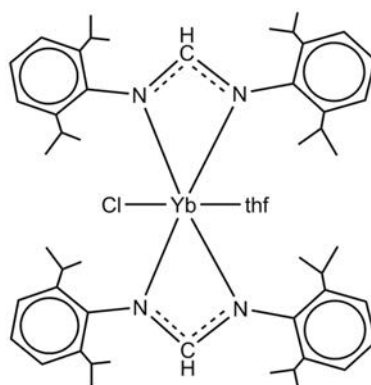


Scheme 3.1-1. Schematic X-ray structure of $[\text{Yb}(\text{XylForm})_2(\text{thf})_2]$ compound.¹

These complexes underwent C-X (X=F, Cl, Br) activation reactions with perfluorodecalin, hexachloroethane or 1,2-dichloroethane, and 1-bromo-2,3,4,5-tetrafluorobenzene, giving $[\text{Yb}(\text{EtForm})_2\text{F}]_2$, $[\text{Yb}(o\text{-PhPhForm})_2\text{F}]_2$, $[\text{Yb}(o\text{-PhPhForm})_2\text{Cl}(\text{thf})_2]$, $[\text{Yb}(\text{DippForm})_2\text{Cl}(\text{thf})]$ and $[\text{Yb}(\text{DippForm})_2\text{Br}(\text{thf})]$. The coordination number for Yb in $[\text{Yb}(\text{EtForm})_2\text{F}]_2$, $[\text{Yb}(\text{DippForm})_2\text{Cl}(\text{thf})]$ and $[\text{Yb}(\text{DippForm})_2\text{Br}(\text{thf})]$ is six. $[\text{Yb}(\text{EtForm})_2\text{F}]_2$ has dimeric structure containing fluoride-bridged mode (Scheme 3.1-2). However, $[\text{Yb}(\text{DippForm})_2\text{Cl}(\text{thf})]$ and $[\text{Yb}(\text{DippForm})_2\text{Br}(\text{thf})]$ are mononuclear. $[\text{Yb}(o\text{-PhPhForm})_2\text{Cl}(\text{thf})_2] \cdot 2\text{THF}$ is a seven coordinated monomeric complex with two chelating formamidinate ligands, a terminal chloride and two THF donors (Scheme 3.1-3).



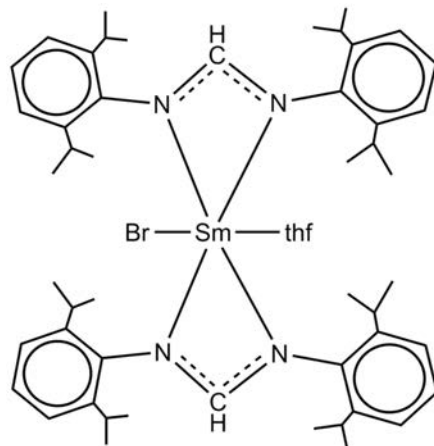
Scheme 3.1-2. Schematic X-ray structure of $[\text{Yb}(\text{EtForm})_2(\mu\text{-F})_2]$ compound.¹



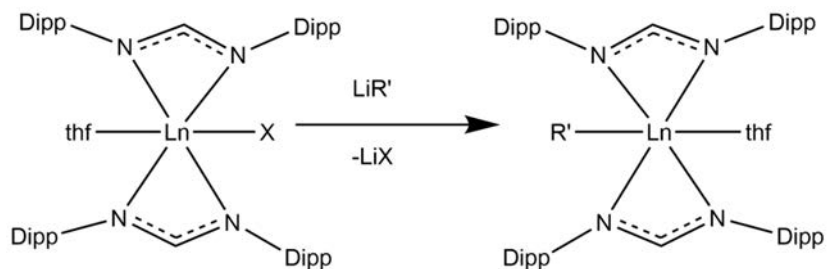
Scheme 3.1-3. Schematic X-ray structure of $[\text{Yb}(\text{DippForm})_2\text{Cl}(\text{thf})]$.THF compound.¹

The oxidation of $[\text{Sm}(\text{DippForm})_2(\text{thf})_2]$ by tert-butyl chloride, 1,2-dibromoethane and iodine at ambient temperature led to the formation of the samarium(III) halide complexes $[\text{Sm}(\text{DippForm})_2\text{Cl}(\text{thf})]$, $[\text{Sm}(\text{DippForm})_2\text{Br}(\text{thf})]$ (Scheme 3.1-4) and $[\text{Sm}(\text{DippForm})_2\text{I}(\text{thf})]$ in good yields.² The subsequent metathesis reaction of $[\text{Sm}(\text{DippForm})_2\text{Cl}(\text{thf})]$ and $[\text{La}(\text{DippForm})_2\text{F}(\text{thf})]$ with LiMe and $\text{LiCH}_2\text{SiMe}_3$ (Scheme 3.1-5) resulted in the formation of samarium alkyl complexes $[\text{Sm}(\text{DippForm})_2\text{Me}(\text{thf})]$, $[\text{Sm}(\text{DippForm})_2\text{CH}_2\text{SiMe}_3(\text{thf})]$ (Scheme 3.1-6) and $[\text{La}(\text{DippForm})_2\text{Me}(\text{thf})]$ (Scheme 3.1-7) which contains a rare terminal methyl ligand. This chemistry has been extended to the lanthanum halide complex $[\text{La}(\text{DippForm})_2\text{F}(\text{thf})]$ to isolate $[\text{La}(\text{DippForm})_2\text{Me}(\text{thf})]$. Unexpectedly, the homoleptic tris-(formamidinato)lanthanum complex $[\text{La}(\text{DippForm})_3]$ (Scheme 3.1-8) in a very low yield was

synthesized by the ligand exchange reaction of $[\text{La}(\text{DippForm})_2\text{Me}(\text{thf})]$ with 1,2,3,4-tetraphenylcyclopentadiene.



Scheme 3.1-4. Schematic X-ray structure of $[\text{Sm}(\text{DippForm})_2\text{Br}(\text{thf})]$.²

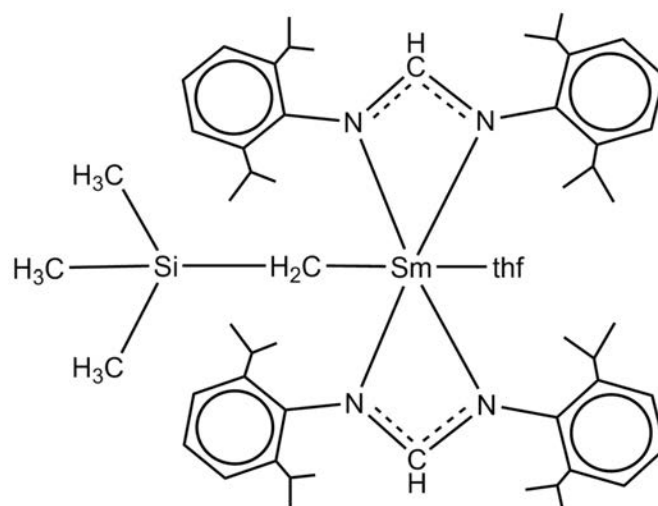


$\text{Ln}=\text{Sm}$, $\text{X}=\text{Cl}$, $\text{R}'=\text{Me}$

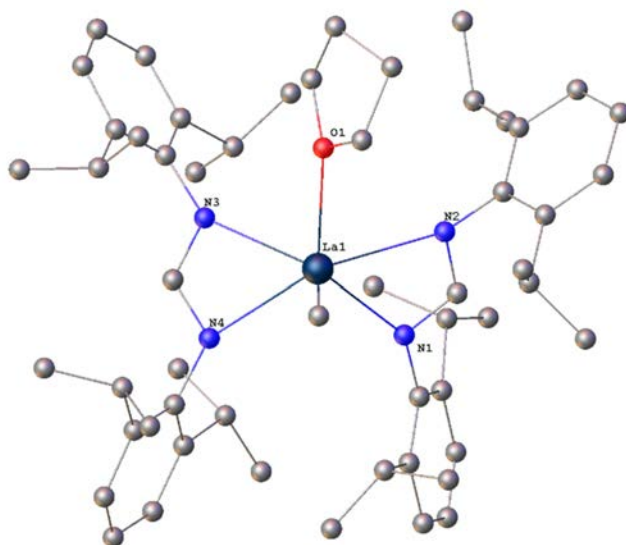
$\text{Ln}=\text{Sm}$, $\text{X}=\text{Cl}$, $\text{R}'=\text{CH}_2\text{SiMe}_3$

$\text{Ln}=\text{La}$, $\text{X}=\text{F}$, $\text{R}'=\text{Me}$

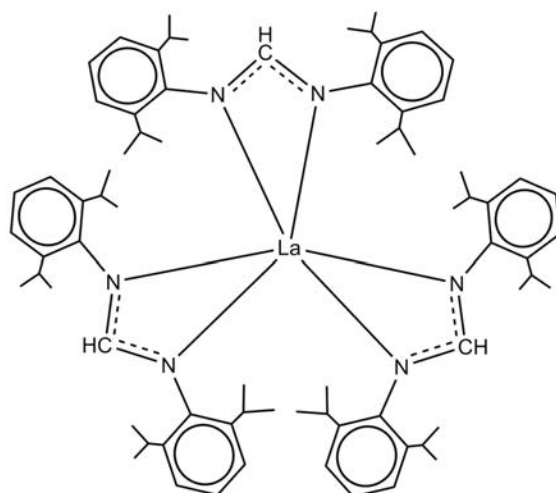
Scheme 3.1-5. Schematic of the X-ray structure of $[\text{Ln}(\text{DippForm})_2\text{R}'(\text{thf})]$ ($\text{Ln}=\text{Sm}$, $\text{X}=\text{Cl}$, $\text{R}'=\text{Me}$, $\text{Ln}=\text{Sm}$, $\text{X}=\text{Cl}$, $\text{R}'=\text{CH}_2\text{SiMe}_3$, $\text{Ln}=\text{La}$, $\text{X}=\text{F}$, $\text{R}'=\text{Me}$).²



Scheme 3.1-6. Schematic X-ray structure of $[\text{Sm}(\text{DippForm})_2\text{CH}_2\text{SiMe}_3(\text{thf})]_2$.²



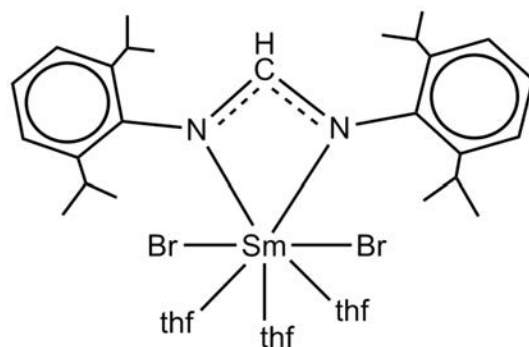
Scheme 3.1-7. X-ray structure of $[\text{La}(\text{DippForm})_2\text{Me}(\text{thf})]_2$.²



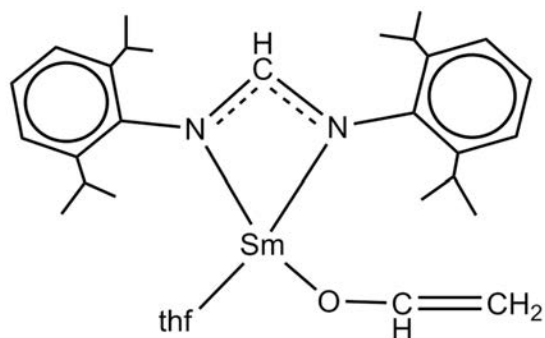
Scheme 3.1-8. Schematic X-ray structure of $[La(DippForm)_3]$.²

The RTP reaction was used in this study for reaction of samarium metal with bis(2-bromo-3,4,5,6-tetrafluorophenyl)mercury and DippFormH in THF. The mono(formamidinato)samarium(III) complex $[Sm(DippForm)Br_2(thf)_3]$ (Scheme 3.1-9) was synthesized as the result. Also, $[Sm(DippForm)_2(OCH=CH_2)(thf)]$ (Scheme 3.1-10) was synthesized by redox reaction of the divalent samarium complex $[Sm(DippForm)_2(thf)_2]$ with diphenylmercury and arises from the ring-opening of THF solvent.

$[Sm(DippForm)_2Cl(thf)]$, $[Sm(DippForm)_2Br(thf)]$, $[Sm(DippForm)_2Me(thf)]$, $[Sm(DippForm)_2CH_2SiMe_3(thf)]$, $[Sm(DippForm)_2(OCH=CH_2)(thf)]$ and $[La(DippForm)_2Me(thf)]$ are mononuclear and the coordination number of the central metal is six for all of them. Formamidinate ligands connect via κ^2 -bonding to the metal atom through two nitrogen donor atoms in these compounds.

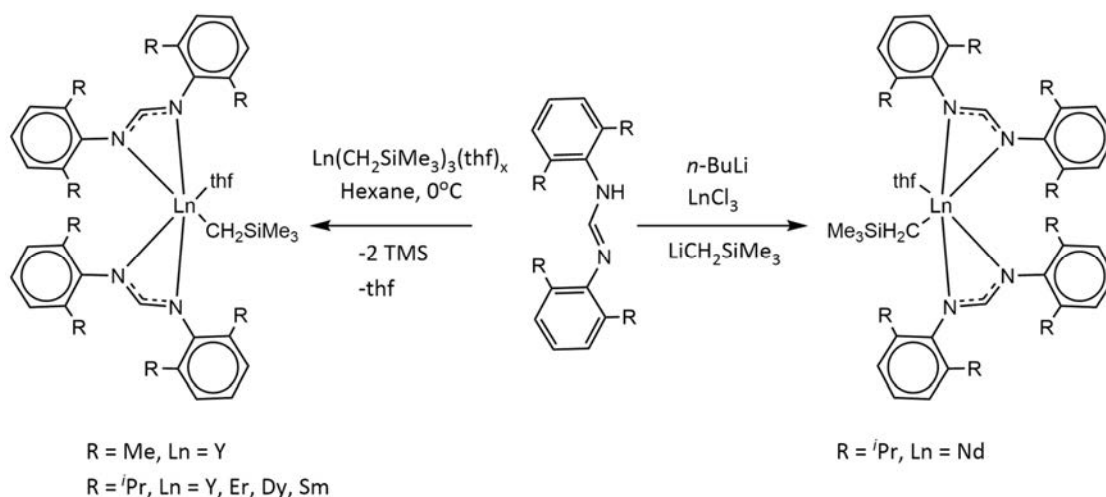


Scheme 3.1-9. Schematic X-ray structure of $[\text{Sm}(\text{DippForm})\text{Br}_2(\text{thf})_3]$.²



Scheme 3.1-10. Schematic X-ray structure of $[\text{Sm}(\text{DippForm})_2(\text{OCH}=\text{CH}_2)(\text{thf})]$.²

Similar rare-earth metal monoalkyl complexes of formamidinates have been reported in another study.³ In this study $[\text{LnL}_2\text{CH}_2\text{SiMe}_3.\text{thf}]$, $[\text{L}_2 = (\text{XylForm})_2, \text{Ln}=\text{Y}; \text{L}_2 = (\text{DippForm})_2, \text{Ln}=\text{Y}, \text{Er}, \text{Dy}, \text{Sm}$ and $\text{Nd}]$ compounds were synthesized by alkyl elimination or salt metathesis reactions in good yields (64–73%) (Scheme 3.1-11).

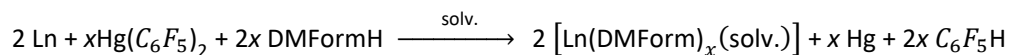


Scheme 3.1-11. Schematic structure of $\text{LnL}_2\text{CH}_2\text{SiMe}_3\cdot\text{thf}$ [$\text{L}_2 = (\text{XylForm})_2$, $\text{Ln} = \text{Y}$; $\text{L}_2 = (\text{DippForm})_2$, $\text{Ln} = \text{Y}, \text{Er}, \text{Dy}, \text{Sm}$ and Nd].³

This chapter shows researches that have been performed using DMFormH (scheme 1-2) as another less bulky form of the bis(aryl)formamidinate ligand to synthesize a set of lanthanoid formamidinate complexes and compare their reactivities. DMFormH is slightly bulkier than *o*-TolFormH and *p*-TolFormH particularly because of two extra methyl groups in *ortho* positions of the structure. However, this ligand is among less bulky types of bis(aryl)formamidinate ligands compared with XylFormH, MesFormH, EtFormH or DippFormH since it has only one methyl group *ortho* to the N-attachment site and therefore limited steric bulk.

3.2 Results and discussion

As per the previous chapter, RTP reactions between lanthanoids, $\text{Hg}(\text{C}_6\text{F}_5)_2$ and DMFormH as the ligand were used to synthesize lanthanoid formamidinate complexes (Equation 3.2-1).



To synthesize trivalent compounds: $x = 3$; Ln = Y, La, Pr, Nd, Sm, Gd, Tb, Dy, Ho, Er, Yb, Lu

To synthesize divalent compounds: $x = 2$; Ln = Sm, Eu, Yb

solv. = THF, DME

Equation 3.2-1.

At the beginning of the reaction one drop of mercury was used to activate the metal surface. All the obtained complexes were trivalent in moderate to low isolated yields (21% - 46%). All the reactions were performed with an extra care to obtain pure compounds however poor repeatability of the RTP reactions using DMFormH was the main problem of this part of the research. Compounds $[\text{Y}(\text{DMForm})_3(\text{thf})]$ **(3.1)**, $[\text{Lu}(\text{DMForm})_3(\text{thf})]$ **(3.2)**, $[\text{Pr}(\text{DMForm})_3(\text{DMFormH})]$ **(3.3)**, $[\text{Ho}(\text{DMForm})_3(\text{DMFormH})]$ **(3.4)**, $[\text{Sm}(\text{DMForm})_3(\text{dme})]$ **(3.5)**, $[\text{Gd}(\text{DMForm})_3(\text{dme})]$ **(3.6)** and $[\text{Er}(\text{DMForm})_3(\text{dmf})]$ **(3.7)** were obtained as the result of these reactions. In most of the cases, reactions had to be repeated many times to obtain enough pure sample for all the required analysis. The compounds were continually contaminated with starting materials and separation was difficult based on solubility. Additionally, obtaining good quality crystalline material was problematic and generally required recrystallization from varying solvents. We were able to obtain very pure crystalline materials to ensure our reactivity studies were based on pure compounds. Single crystals suitable for X-ray crystallography were achieved by evaporation and concentration of the solutions (~5 ml) followed by cooling down very slowly and keeping the samples in the fridge for several of days. The IR spectra of all complexes are void of the 3300 cm^{-1} absorption for all compounds suggesting complete consumption of DMFormH, except for $[\text{Pr}(\text{DMForm})_3(\text{DMFormH})]$ **(3.3)** and $[\text{Ho}(\text{DMForm})_3(\text{DMFormH})]$ **(3.4)** attributable to N-H stretching. The result of ^1H NMR spectra (in C_6D_6) supports the presence of DMForm with resonances at $\delta \approx 9 \text{ ppm}$ (NC(H)N). EDTA was used for metal analyse performed on crystals of compounds. Crystals of samples were sent to Metropolitan University in England for

elemental analysis (C, H and N). Most of the compounds have poor elemental analysis results despite of many attempts. Considering the result of other analysis methods, the poor elemental analysis results can be attributed to the incomplete combustion or carbides formation. Melting points of the compounds were measured using crystals of compounds in sealed glass capillaries under nitrogen and are uncalibrated.

All of the compounds except $[\text{Er}(\text{DMForm})_3(\text{dmf})]$ (**3.7**) crystallized in the monoclinic space group $P2_1/c$, with the whole molecule occupying the asymmetric unit. The molecular geometry about the metal centers of these compounds can be described as distorted tetrahedral (the N-C-N binding site is considered a sole point of attachment).

Figure 3.2-1 shows the X-ray crystal structure of $[\text{Y}(\text{DMForm})_3(\text{thf})]$ (**3.1**). This compound is mononuclear and has three chelating ligands and one coordinated solvent molecule which gives the metal center a coordination number of seven. Table 3-1 compares the bond lengths of metal center to nitrogen atoms which suggests symmetric formamidinate chelation.

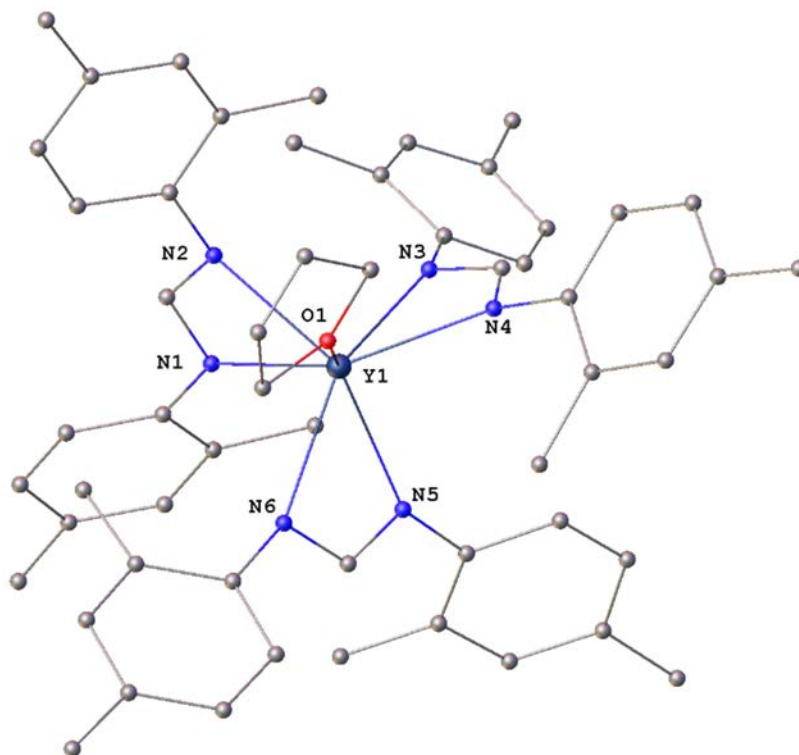


Figure 3.2-1. Molecular structure of $[\text{Y}(\text{DMForm})_3(\text{thf})]$ (**3.1**). Hydrogen atoms removed for clarity.

Table 3-1. Y-N bond lengths for [Y(DMForm)₃(thf)] (**3.1**)

Atom	Atom	Length/Å
Y1	N1	2.439(2)
Y1	N2	2.357(3)
Y1	N3	2.430(2)
Y1	N4	2.375(2)
Y1	N5	2.373(2)
Y1	N6	2.429(2)

In this compound, formamidinate ligands have equal distances from the metal center (2.789 Å). For simplicity the back bone carbon was considered as the point of attachment for all compounds. This compound can be compared with [Y(PhForm)₃(thf)₂](THF)₃ (**2.5**). The coordination number of the metal center in (**3.1**) is less than in (**2.5**) because of the lack of one coordinated solvent molecule which can be attributed to the higher steric effect of DMForm. The average Y-N bond length for (**2.5**) is 2.452(7) Å which is longer than the average Y-N bond length for (**3.1**) (2.400(2) Å). The same trend can be observed for the average of ligand to metal center distances which suggests that although DMForm is bulkier than PhForm, one more coordinated solvent molecule for (**2.5**) has more effect on increasing the radius of the coordination sphere around the metal center. There are few examples of yttrium formamidinate complexes in the literature and all of them are reported using more bulky forms of formamidinates.³⁻⁵ Compounds (**2.5**) and (**3.1**) are the least bulky yttrium formamidinate complexes that have been crystallographically characterized.

Table 3-2 shows the bond lengths of [Lu(DMForm)₃(thf)] (**3.2**). This compound has the same structure as [Y(DMForm)₃(thf)] (**3.1**) however the bond lengths are slightly shorter as expected since Lu³⁺ has a smaller ionic radius than Y³⁺.⁶ The only difference between (**3.2**) and (**3.1**) is the metal center so any differences in bond lengths can be attributed to the ionic radii of metal centers. Same as (**3.1**) the chelation of the formamidinates are symmetrical in this compound.

Table 3-2. Bond lengths of [Lu(DMForm)₃(thf)] (**3.2**)

Atom	Atom	Length/Å
Lu1	O1	2.375(2)
Lu1	N1	2.348(2)
Lu1	N2	2.399(2)
Lu1	N3	2.421(3)
Lu1	N4	2.320(3)
Lu1	N5	2.393(3)
Lu1	N6	2.350(2)

This compound has an average Lu-N bond length of 2.371(3) Å and can be compared with [Lu(PhForm)₃(thf)₂](THF)₃ (**2.11**) which has an average Lu-N bond length of 2.4713(6) Å. The lower steric effect of PhForm makes (**2.11**) able to have a higher coordination number and it has one more coordinated thf molecule to the metal center. Although DMForm is bulkier than PhForm, the lower coordination number in (**3.2**) makes (**3.2**) less bulky than (**2.11**). So, coordinated molecules can become closer to the metal center which gives a smaller coordination sphere around the metal center and slightly shorter bond lengths. The same trend can be observed for Lu-O bond lengths in (**3.2**) compared with (**2.11**). Compound (**3.2**) has a similar structure to other crystallographically characterized lutetium formamidinates [Lu(*p*-TolForm)₃(thf)].⁷ This compound has an average Lu-N bond length of 2.3581(3) Å which is shorter than the average value for (**3.2**) (2.371(3) Å) because of the lower steric effect of *p*-TolForm. The same trend can be observed for Lu-O bond length.

Compound [Pr(DMForm)₃(DMFormH)] (**3.3**) has the same structure as (**3.1**) however instead of a solvent molecule, it has one coordinated DMFormH ligand which is not deprotonated (Figure 3.2-2). The presence of this terminal ligand has been confirmed by IR and ¹H NMR spectra.

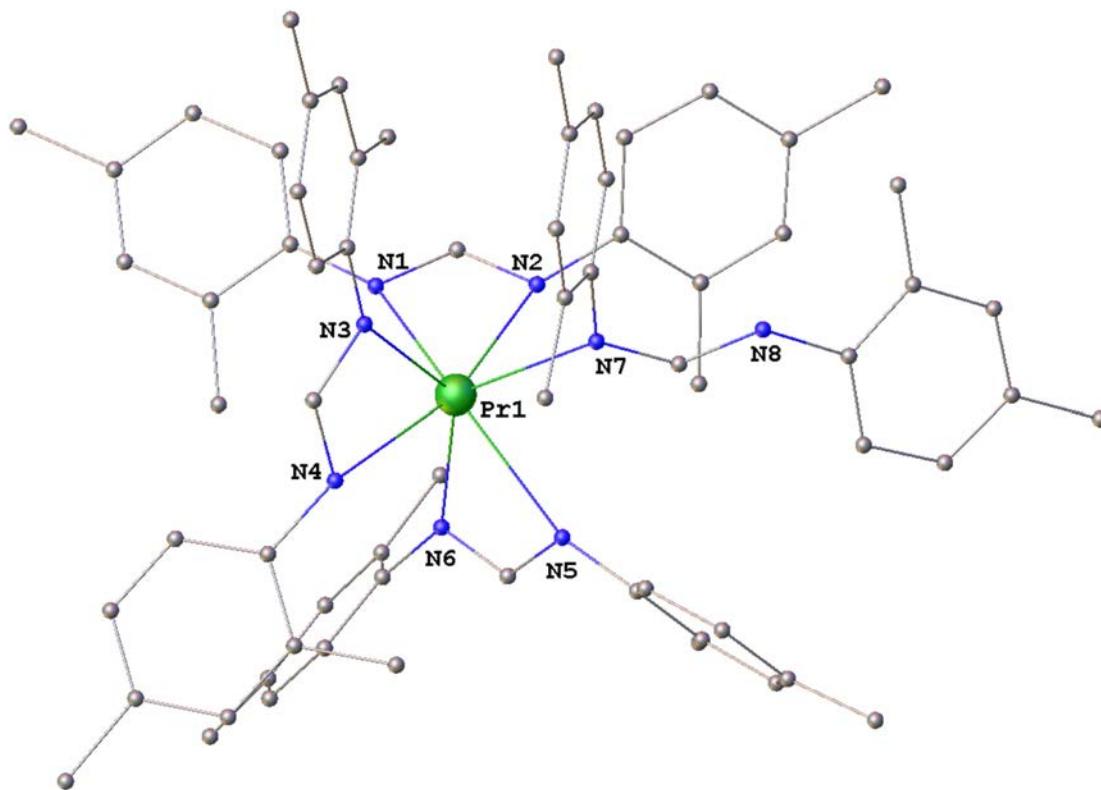


Figure 3.2-2. Molecular structure of [Pr(DMForm)₃(DMFormH)] (**3.3**). Hydrogen atoms removed for clarity.

Table 3-3 compares Pr-N bond lengths of this compound. The distances suggest chelation of formamidinates are symmetrical. Although Pr has longer ionic radius than Y,⁶ the average of Pr-N lengths is 2.5475(9) Å which is higher than the average Y-N distance of [Y(DMForm)₃(thf)] (**3.1**) because of one DMFormH in the structure which is more bulky than one coordinated thf molecule. Since the bulky hindrance of thf is less than DMFormH ligand, it can become closer to the metal center and gives the Y-O distance of 2.409(2) Å which is smaller than Pr-N7 distance (2.604(7) Å).

Table 3-3. Pr-N bond lengths of [Pr(DMForm)₃(DMFormH)] (**3.3**)

Atom	Atom	Length/Å
Pr1	N1	2.554(9)
Pr1	N2	2.524(8)
Pr1	N3	2.526(9)
Pr1	N4	2.564(9)
Pr1	N5	2.542(10)
Pr1	N6	2.519(8)
Pr1	N7	2.604(7)

Compound $[\text{Ho}(\text{DMForm})_3(\text{DMFormH})]$ (**3.4**) has a similar structure to $[\text{Pr}(\text{DMForm})_3(\text{DMFormH})]$ (**3.3**). It is a mononuclear compound and has a coordination number of seven about the Ho center. Figure 3.2-3 compares the bond lengths of this compound with (**3.3**). It can be seen (**3.4**) has shorter bond lengths due to the lanthanoid contraction effect.

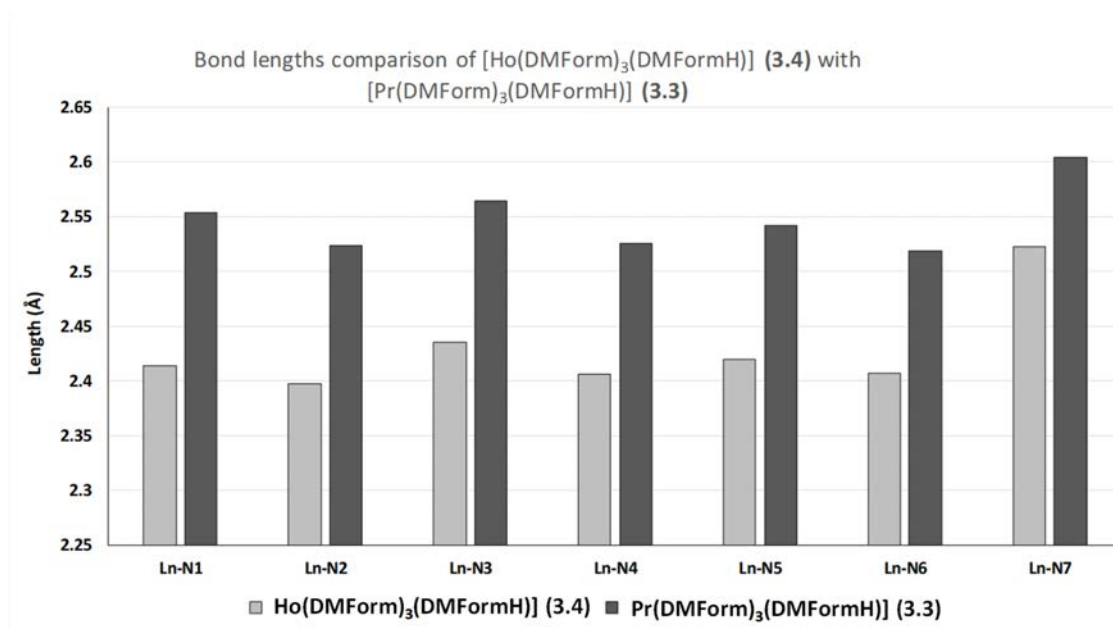


Figure 3.2-3. Bond lengths comparison of $[\text{Ho}(\text{DMForm})_3(\text{DMFormH})]$ (**3.4**) with $[\text{Pr}(\text{DMForm})_3(\text{DMFormH})]$ (**3.3**).

Attempts to get a pure compound from a RTP reaction of Sm with DMFormH and $\text{Hg}(\text{C}_6\text{F}_5)_2$ in THF or recrystallization from various solvents was failed. A pure product of $[\text{Sm}(\text{DMForm})_3(\text{dme})]$ (**3.5**) in the form of yellow crystals was obtained in one RTP reaction using DME as the solvent. Figure 3.2-4 shows X-ray crystal structure of $[\text{Sm}(\text{DMForm})_3(\text{dme})]$ (**3.5**). Table 3-4 shows the bond lengths of this structure. It can be seen the chelation of formamidinates and dme are symmetrical. This compound has an average Sm-N length of 2.500(5) Å.

Table 3-4. Bond lengths of [Sm(DMForm)₃(dme)] (**3.5**)

Atom	Atom	Length/Å
Sm1	O1	2.566(5)
Sm1	O2	2.671(5)
Sm1	N1	2.541(5)
Sm1	N2	2.473(5)
Sm1	N3	2.519(6)
Sm1	N4	2.461(5)
Sm1	N5	2.448(5)
Sm1	N6	2.562(6)

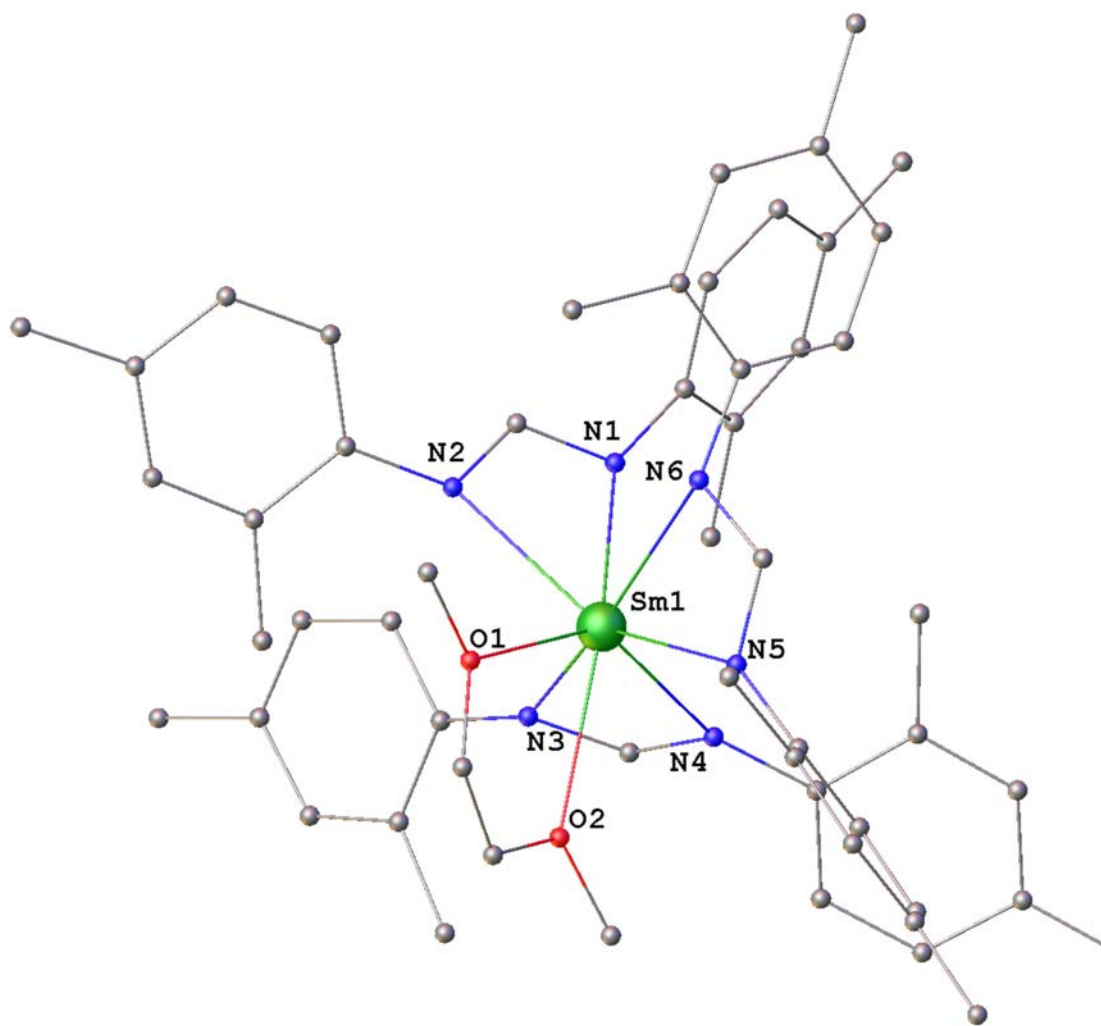


Figure 3.2-4. Molecular structure of [Sm(DMForm)₃(dme)] (**3.5**). Hydrogen atoms removed for clarity.

Compound [Gd(DMForm)₃(dme)] (**3.6**) has the same structure as [Sm(DMForm)₃(dme)] (**3.5**) however the bond lengths in (**3.6**) are slightly shorter than (**3.5**) (Table 3-5) which can be attributed to the lanthanoid contraction effect and smaller ionic radius of Gd compared with Sm.⁶

Table 3-5. Bond lengths of [Gd(DMForm)₃(dme)] (**3.6**)

Atom	Atom	Length/Å
Gd1	O1	2.512(18)
Gd1	O2	2.639(18)
Gd1	N1	2.435(18)
Gd1	N2	2.492(19)
Gd1	N3	2.527(2)
Gd1	N4	2.456(19)
Gd1	N5	2.544(2)
Gd1	N6	2.436(2)

Compound [Er(DMForm)₃(dmf)] (**3.7**) was crystallized in the monoclinic space group $P2_1$ with the whole molecule occupying the asymmetric unit. This compound has a similar structure to (**3.1**) with one coordinated dmf molecule in place of the thf molecule in (**3.1**). Figure 3.2-5 and Table 3-6 shows the X-ray structure and bond lengths of this compound respectively.

Table 3-6. Bond lengths of [Er(DMForm)₃(dmf)] (**3.7**)

Atom	Atom	Length/Å
Er1	N1	2.451(2)
Er1	N2	2.389(2)
Er1	N3	2.409(2)
Er1	N4	2.360(2)
Er1	N5	2.498(2)
Er1	N6	2.375(2)
Er1	O1	2.2964

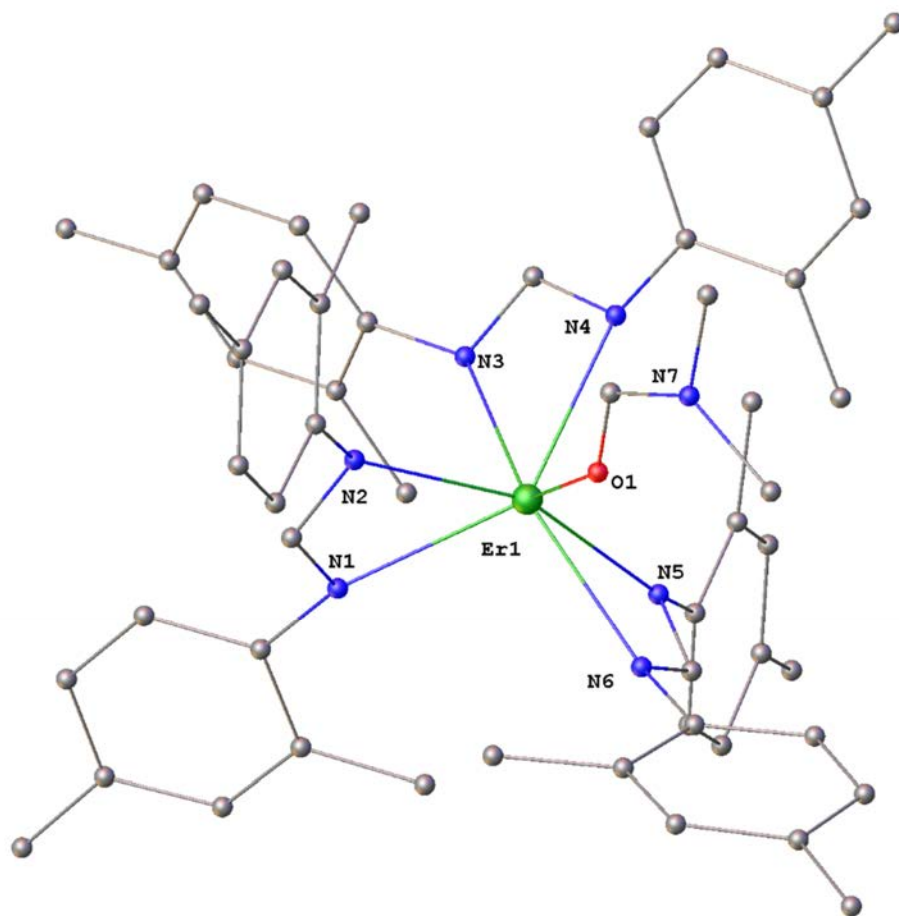


Figure 3.2-5. Molecular structure of $[\text{Er}(\text{DMForm})_3(\text{dmff})]$ (**3.7**). Hydrogen atoms removed for clarity.

In one of the attempts using Er as the metal and THF as the solvent, very few crystals of $[\text{Er}(\text{DMForm})_3(\text{thf})]$ (**3.8**) were obtained. The metal center in this structure is seven coordinated and the structure is similar to $[\text{Y}(\text{DMForm})_3(\text{thf})]$ (**3.1**), $[\text{Tb}(\text{PhForm})_3(\text{thf})]$ (**2.1**), $[\text{Ho}(\text{PhForm})_3(\text{thf})]$ (**2.2**), $[\text{Er}(\text{PhForm})_3(\text{thf})]$ (**2.3**) and $[\text{Lu}(p\text{-TolForm})_3(\text{thf})]$.⁷ Figure 3.2-6 compares the Ln-O and average Ln-N bond lengths of these compounds.

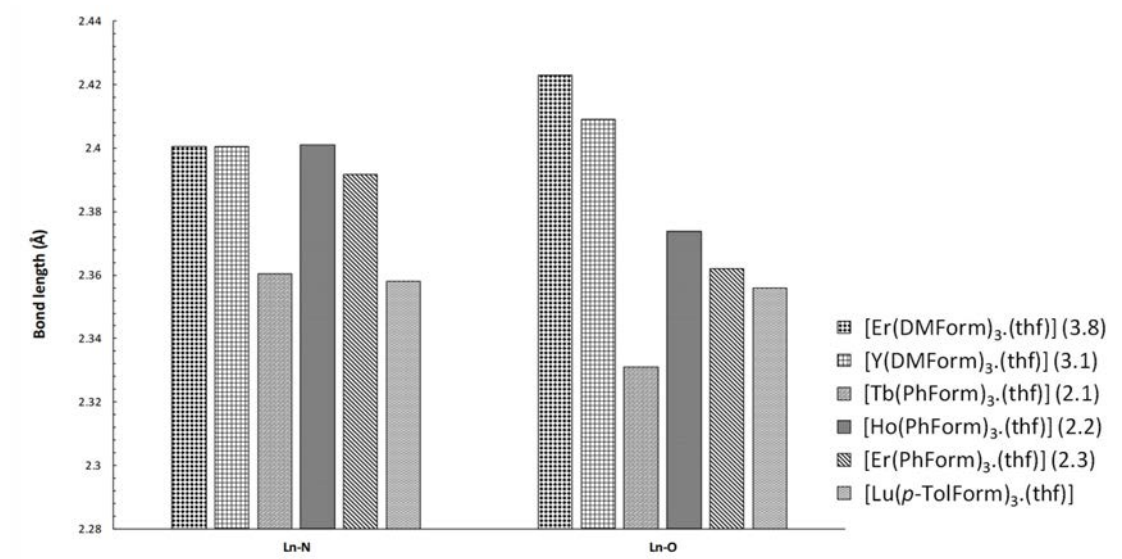


Figure 3.2-6. Comparison of average Ln-N and Ln-O bond lengths for [Er(DMForm)₃.(thf)] (**3.8**), [Y(DMForm)₃.(thf)] (**3.1**), [Tb(PhForm)₃.(thf)] (**2.1**), [Ho(PhForm)₃.(thf)] (**2.2**) and [Er(PhForm)₃.(thf)] (**2.3**) and [Lu(*p*-TolForm)₃.(thf)].

Unfortunately, further attempts to get more pure products of this compound to complete the characterization were failed. In one of these attempts another compound $[\{\text{Er}(\text{DMForm})_2(\mu\text{-OH})(\text{thf})_2\} \cdot (\text{THF})_2]$ (**3.9**) was obtained in a very low yield. Figure 3.2-7 shows the X-ray crystal structure of this compound. The structure of this compound is similar to $[\{\text{Yb}(\text{PhForm})_2(\mu\text{-OH})(\text{dmf})_2\}_2]$ (**2.12**) and $[\{\text{Yb}(o\text{-TolForm})_2(\mu\text{-OH})(\text{thf})_2\}_2]$.⁸ However, this compound crystallized in the triclinic space group *P*-1 with half of the molecule comprising the asymmetric unit. Same as $[\{\text{Yb}(o\text{-TolForm})_2(\mu\text{-OH})(\text{thf})_2\}_2]$, the geometry about the trivalent Er metal centers can be best described as a distorted N(2) face capped triangular prism.⁸ Figure 3.2-8 compares the bond lengths of (**3.9**) with $[\{\text{Yb}(o\text{-TolForm})_2(\mu\text{-OH})(\text{thf})_2\}_2]$. Generally, because of lower steric hindrance of *o*-TolForm, coordinated atoms can approach closer to the metal center so shorter bond lengths can be observed for $[\{\text{Yb}(o\text{-TolForm})_2(\mu\text{-OH})(\text{thf})_2\}_2]$ complex. Longer formamidinate-metal center distances are the main reason for lower bite angles in (**3.9**).

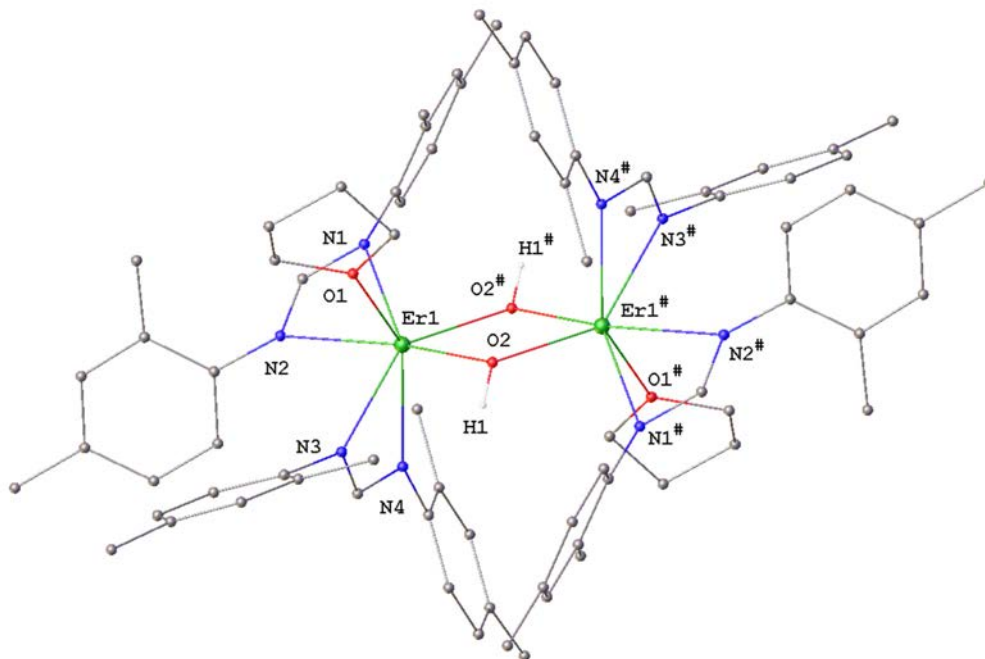


Figure 3.2-7. Molecular structure of $[\{\text{Er}(\text{DMForm})_2(\mu\text{-OH})(\text{thf})\}_2] \cdot (\text{THF})$ (**3.9**). Hydrogen atoms removed for clarity. Symmetry transformation used to generate “#” atoms: 1-X,1-Y,1-Z.

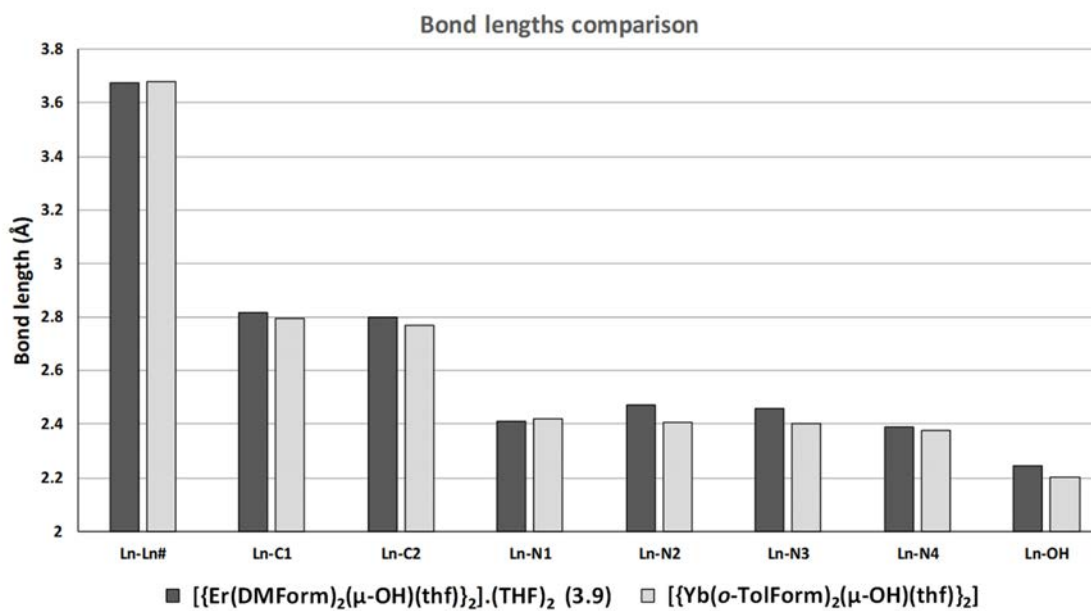


Figure 3.2-8. Comparison of bond lengths between $[\{\text{Er}(\text{DMForm})_2(\mu\text{-OH})(\text{thf})\}_2] \cdot (\text{THF})_2$ (**3.9**) and $[\{\text{Yb}(\text{o-TolForm})_2(\mu\text{-OH})(\text{thf})\}_2]$ compounds.

With the aim of getting compounds similar to [Er(DMForm)₃(dmf)] (**3.7**) with general formula of [Ln(DMForm)₃(dmf)_x], a series of RTP reactions with different lanthanoids in THF were performed and DMF was used as the recrystallization solvent. As the result of these reactions, compounds [Tb(DMForm)₃(dmf)] (**3.10**) and [Lu(DMForm)₃(dmf)] (**3.11**) were isolated. However, the yield of reactions was very low and only few small crystals could be collected for X-ray crystallography. Many reactions with different stoichiometries were performed to get pure compounds in good yield however, they were unsuccessful. Comparing average Ln-N bond lengths of (**3.7**), (**3.10**) and (**3.11**), compound (**3.11**) has the shorter (Ln-N_(avg.) = 2.381 Å) and (**3.10**) has the longest (Ln-N_(avg.) = 2.446 Å) values due to the lanthanoid contraction effect.

3.2.1 Reactivity towards the Tishchenko reaction

Hoping to find more reactive catalysts than those previously reported ones,⁹⁻¹⁶ the standard reaction of benzaldehyde to form benzyl benzoate was chosen to compare reactivities of the compounds with the aid of ¹H NMR spectroscopy (Scheme 2.3-1). Crystals of compounds were used as the pure products to perform the reactions at room temperature. The yields were evaluated based on 1 mol% of the catalyst. The yields were calculated in different time intervals of 5 min, 1 hr, 24 hr, 48 hr, 72 hr, 96 hr and 120 hr after starting the reaction. Increase in the intensity of the benzyl group proton signal (at 9.72 ppm) and decrease in the characteristic aldehyde proton signal (at 5.18 ppm) in the ¹H NMR spectrums provide good evidence for production of benzyl benzoate. Figure 3.2-9 compares the reactivities of [Pr(DMForm)₃(DMFormH)] (**3.3**), [Ho(DMForm)₃(DMFormH)] (**3.4**) and [Er(DMForm)₃(dmf)] (**3.7**) complexes. Integrating the signal was not possible for [Gd(DMForm)₃(dme)] (**3.6**) because it gave broad signals due to the paramagnetic nature of this compound.

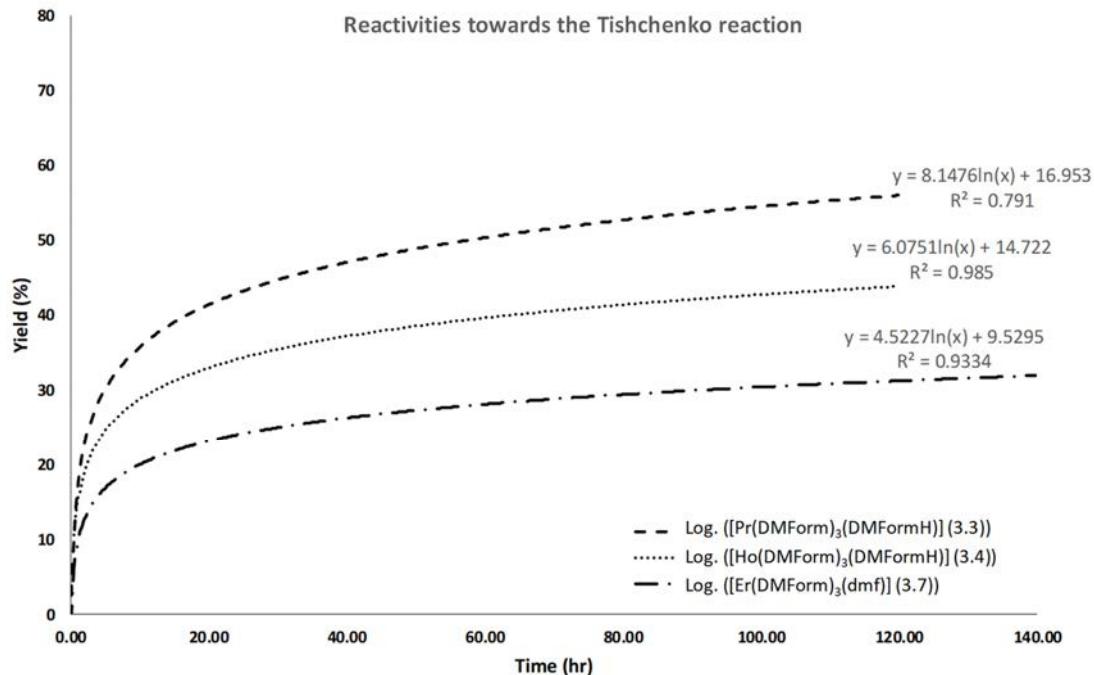


Figure 3.2-9. Comparison of catalytic reactivities for some of the compounds.

[Y(DMForm)₃(thf)] (**3.1**) was the most reactive catalyst since it completed the reaction within 24 hr. The yield of benzyl benzoate after 5 minutes from starting the reaction was ca. 70%. However, the result of reactivities show less reactivity toward Tishchenko reaction for these compounds compared with other reported catalysts like [La(*o*-TolForm)₃(thf)₂] complex.¹⁷ It should be noted that for better comparison about the reactivities, the same metal centers (i.e. same ionic radii) should be compared with each other. Comparing [Y(DMForm)₃(thf)] (**3.1**), [Ho(DMForm)₃(DMFormH)] (**3.4**) and [Er(DMForm)₃(dmf)] (**3.7**) with [Y(PhForm)₃(thf)₂](THF)₃ (**2.5**), [Ho(PhForm)₃(thf)] (**2.2**) and [Er(PhForm)₃(thf)] (**2.3**) shows higher reactivities for compounds with less steric effect (Figure 3.2-10). Compounds (**2.2**), (**2.3**) and (**2.5**) have less steric effect so the metal center is presumably more accessible for the substrate to gain access to the metal. Except (**3.1**), the reactivity of all other compounds follows a dependence on the ionic radius of the metal center.¹⁸

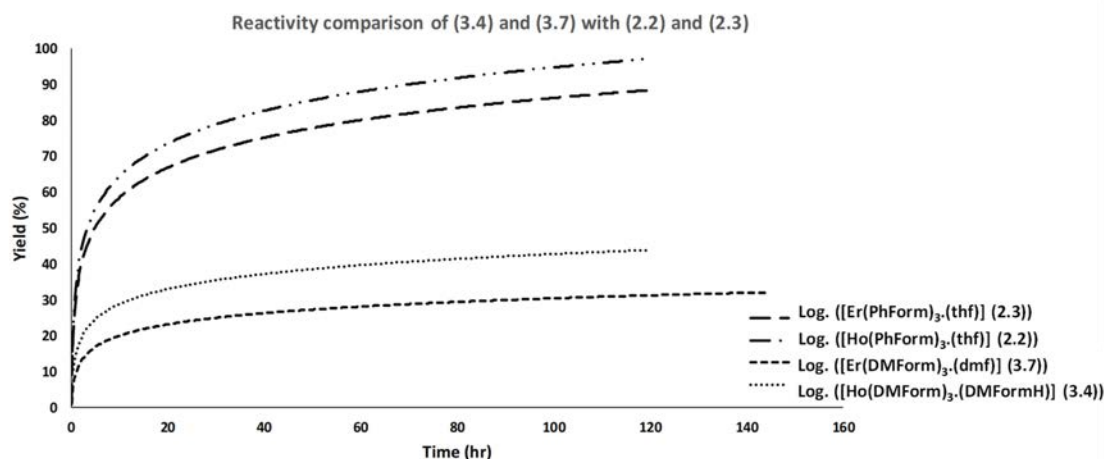


Figure 3.2-10. Comparison of reactivities of [Ho(DMForm)₃(DMFormH)] (**3.4**) and [Er(DMForm)₃(dmf)] (**3.7**) with [Ho(PhForm)₃.(thf)] (**2.2**) and [Er(PhForm)₃.(thf)] (**2.3**) compounds.

Almost no considerable catalytic reactivity for the Tishchenko reaction was observed for [Lu(DMForm)₃(thf)] (**3.2**). This can perhaps be attributed to the smaller ionic radius and so higher steric effect of the compound which makes the metal center less accessible for the substrate.

3.3 Conclusions

In this chapter DMFormH was engaged to synthesize a set of lanthanoid formamidinate complexes using Ln = Y, Pr, Sm, Gd, Ho, Er and Lu. All the resultant compounds were trivalent with three chelating formamidinate ligands about the metal centers. The results show DMFormH can bind rare earth elements very well and is a suitable ligand to synthesize organo-lanthanoid compounds. However, most of the yields were low and isolating a pure product was relatively difficult compared with PhFormH. The study of catalytic reactivity towards the Tishchenko reaction shows [Y(DMForm)₃(thf)] (**3.1**) can be introduced as a possible replacement for the highly catalytically active [La(*o*-TolForm)₃.(thf)₂] (where *o*-toluidine, the starting material for the synthesis of *o*-TolFormH is a registered carcinogen). The reason for the higher reactivity of [Y(DMForm)₃(thf)] (**3.1**) than other bis(aryl)formamidinate compounds in this research is not clear yet. However, in all the studied

compounds in this research, compounds with Y as the metal center showed higher reactivity than the analogous compounds.

3.4 Experimental

All samples were prepared using a glove box, Schlenk flask and vacuum line techniques in an inert atmosphere since lanthanoid metals and their products are air-sensitive and moisture-sensitive. Sodium or sodium/benzophenone were used for refluxing and distillation of solvents to dry and deoxygenate them prior to use in reactions. The lanthanoid metal reagents were purchased either in form of fine powders or metal ingots from Rhone Poulenc or Santoku. In the case of metal ingots, they were freshly filed under an inert atmosphere into metal filings. DMFormH was prepared by literature methods.¹⁹ IR data were obtained from Nujol mulls for the region 4000-400 cm^{-1} with a Nicolet-Nexus FT-IR spectrometer. ^1H NMR spectra were recorded with a Bruker Avance 400 MHz spectrometer using dry degassed *deutero*-benzene (C_6D_6) as solvent, and resonances were referenced to the residual ^1H resonances of the deuterated solvent. Elemental analyses (C, H, N) were performed by the Micro Analytical Laboratory, Science Centre, London Metropolitan University, England.

[Y(DMForm)₃(thf)] (**3.1**)

Yttrium filings (0.30 g, 3.3 mmol), $\text{Hg}(\text{C}_6\text{F}_5)_2$ (0.62 g, 1.50 mmol) and DMFormH (0.75 g, 3.00 mmol) were added to a Schlenk flask and dissolved in THF (20 mL) with stirring at room temperature for one week. The resulting yellowish solution was filtered through a filter cannula from the metal residue and evaporated under vacuum to 5 mL and cooled to $-5\text{ }^\circ\text{C}$ for several days. Small colorless crystals of (**3.1**) were produced. Yield = 0.62 g (68%); M.P.: 196-200 $^\circ\text{C}$. IR (Nujol, cm^{-1}): $\nu = 1870$ (vw), 1753 (vw), 1732 (vw), 1658 (m), 1610 (w), 1455 (vs), 1377 (vs), 1293 (vs), 1214 (vs), 1157 (s), 1119 (s), 998 (s), 951 (vs), 900 (m), 874 (s), 814 (s), 724 (m), 666 (w), 612 (m) and 560 (m) cm^{-1} (wv); ^1H NMR (C_6D_6 , 303.2 K): $\delta = 0.91$ (s, 4H; CH_2), 2.16-2.25 (d, 36H; CH_3), 3.56 (s, 4H; CH_2), 6.75–7.15 (m, 18H; Ar-H), 8.61 (s, 3 H, NC(H)N). Elemental analysis calc. (%) for $\text{C}_{55}\text{H}_{65}\text{N}_6\text{OY}$ ($M = 915.07\text{ g}\cdot\text{mol}^{-1}$): C 72.19, H 7.16, N 9.18; Found: C 68.79, H 5.85, N 10.15. Y: 9.71; Found from titration: 9.70.

[Lu(DMForm)₃(thf)] (**3.2**)

Lutetium filings (0.30 g, 1.70 mmol), Hg(C₆F₅)₂ (0.62 g, 1.50 mmol) and DMFormH (0.75 g, 3.00 mmol) were added to a Schlenk flask and dissolved in THF (20 mL) with stirring at room temperature for one week. The resulting yellowish solution was filtered through a filter cannula from the metal residue and evaporated under vacuum to 5 mL and cooled to -5 °C for several days. Small colorless crystals of (**3.2**) were produced. Yield = 0.63 g (63%); M.P.: 211-212 °C; IR (Nujol, cm⁻¹): ν = 1754 (vw), 1660 (w), 1611 (vw), 1454 (vs), 1377 (vs), 1292 (vs), 1215 (vs), 1158 (s), 1119 (s), 1033 (s), 998 (s), 952 (s), 932 (m), 901 (m), 875 (s), 812 (s), 775 (w), 724 (m), 655 (vw), 613 (m), 560 (s), cm⁻¹ (wv); ¹H NMR (C₆D₆, 303.2 K): δ = 1.15 (s, 4H; CH₂), 2.15-2.24 (d, 36H; CH₃), 3.56 (s, 4H; CH₂), 6.68–7.16 (m, 18H; Ar-H), 8.68 (s, 3 H, NC(H)N). Elemental analysis calc. (%) for C₅₅H₆₅N₆OLu (M = 1001.13 g.mol⁻¹): C 65.99, H 6.54, N 8.39; Found: C 67.94, H 7.51, N 9.50. Lu: 17.47; Found from titration: 17.50.

[Pr(DMForm)₃(DMFormH)] (**3.3**)

Praseodymium filings (0.30 g, 2.1 mmol), Hg(C₆F₅)₂ (0.62 g, 1.50 mmol) and DMFormH (0.75 g, 3.00 mmol) were added to a Schlenk flask and dissolved in THF (20 mL) with stirring at room temperature for one week. The resulting green solution was filtered through a filter cannula from the metal residue and evaporated under vacuum to 5 mL and cooled to -5 °C for several days. Small green crystals of (**3.3**) were produced. Yield = 0.72 g (63%); M.P.: 210-213 °C; IR (Nujol, cm⁻¹): ν = 1873 (w), 1817 (vw), 1756 (vw), 1724 (vw), 1701 (vw), 1632 (vs), 1608 (s), 1439 (vs), 1377 (vs), 1297 (vs), 1211 (vs), 1154 (s), 1119 (s), 998 (s), 948 (s), 896 (m), 872 (m), 811 (vs), 771 (m), 722 (s), 656 (m), 632 (m), 610 (m) cm⁻¹ (wv); ¹H NMR (C₆D₆, 303.2 K): Gives broad peaks due to the paramagnetic nature of this compound. Elemental analysis calc. (%) for C₆₈H₇₇N₈Pr (M = 1147.33 g.mol⁻¹): C 71.18, H 6.76, N 9.76; Found: C 77.00, H 7.35, N 9.48. Pr: 12.28; Found from titration: 12.29.

[Ho(DMForm)₃(DMFormH)] (**3.4**)

Holmium filings (0.30 g, 1.80 mmol), Hg(C₆F₅)₂ (0.62 g, 1.50 mmol) and DMFormH (0.75 g, 3.00 mmol) were added to a Schlenk flask and dissolved in THF (20 mL) with stirring at room temperature for one week. The resulting yellow solution was filtered through a filter cannula

from the metal residue and evaporated under vacuum to 5 mL and cooled to -5 °C for several days. Small yellow crystals of **(3.4)** were produced. Yield = 0.86 g (48%); M.P.: 215-217 °C; IR (Nujol, cm^{-1}): $\nu = 3457$ (w), 3375 (m), 1883 (w), 1828 (vw), 1733 (w), 1632 (vs), 1608 (vs), 1435 (vs), 1369 (vs), 1285 (vs), 1155 (vs), 1119 (vs), 1033 (vs), 957 (s), 899 (s), 872 (s), 811 (vs), 772 (s), 722 (vs), 659 (m), 637 (m), 612 (m), cm^{-1} (wv); ^1H NMR (C_6D_6 , 303.2 K): Gives broad peaks due to the paramagnetic nature of this compound. Elemental analysis calc. (%) for $\text{C}_{68}\text{H}_{78}\text{N}_8\text{Ho}$ ($M = 1172.36 \text{ g}\cdot\text{mol}^{-1}$): C 69.73, H 6.63, N 9.57; Found: C 65.56, H 7.58, N 8.55. Ho: 14.06; Found from titration: 14.10.

[Sm(DMForm)₃(dme)] **(3.5)**

Samarium filings (0.30 g, 1.9 mmol), $\text{Hg}(\text{C}_6\text{F}_5)_2$ (0.62 g, 1.50 mmol) and DMFormH (0.75 g, 3.00 mmol) were added to a Schlenk flask and dissolved in DME (20 mL) with stirring at room temperature for one week. The resulting yellow solution was filtered through a filter cannula from the metal residue and evaporated under vacuum to 5 mL and cooled to -5 °C for several days. Small yellow crystals of **(3.5)** were produced. Yield = 0.55 g (56%); M.P.: 181-183 °C; IR (Nujol, cm^{-1}): $\nu = 1663$ (w), 1609 (w), 1540 (vs), 1489 (s), 1464 (s), 1376 (m), 1296 (vs), 1245 (m), 1210 (s), 1153 (w), 1119.49 (m), 1057 (s), 1010 (m), 998 (m), 948 (vw), 898 (vw), 864 (m), 814 (s), 721.33 (vw) cm^{-1} (wv); ^1H NMR (C_6D_6 , 303.2 K): Gives broad peaks due to the paramagnetic nature of this compound. Elemental analysis calc. (%) for $\text{C}_{55}\text{H}_{67}\text{N}_6\text{O}_2\text{Sm}$ ($M = 994.54 \text{ g}\cdot\text{mol}^{-1}$): C 66.42, H 6.79, N 8.45; Found: C 66.78, H 6.19, N 8.34.

[Gd(DMForm)₃(dme)] **(3.6)**

Gadolinium filings (0.30 g, 1.90 mmol), $\text{Hg}(\text{C}_6\text{F}_5)_2$ (0.62 g, 1.50 mmol) and DMFormH (0.75 g, 3.00 mmol) were added to a Schlenk flask and dissolved in DME (20 mL) with stirring at room temperature for one week. The resulting yellow solution was filtered through a filter cannula from the metal residue and evaporated under vacuum to 5 mL and cooled to -5 °C for several days. Small yellow crystals of **(3.6)** were produced. Yield = 0.57 g (57%); M.P.: 184 °C; IR (Nujol, cm^{-1}): $\nu = 1867.94$ (vw), 1659.7 (s), 1607.65 (m), 1540.37 (s), 1466.79 (vs), 1376.76 (vs), 1296.65 (vs), 1243.14 (s), 1207.57 (vs), 1151.8 (m), 1119.97 (s), 1056.05 (m), 1034.56 (m), 1009.17 (m), 997.38 (m), 945.87 (vw), 935.2 (w), 880.9 (w), 866.19 (w), 814.8 (s), 776.79 (m),

720.06 (m), 604.81 (vw), cm^{-1} (wv); ^1H NMR (C_6D_6 , 303.2 K): Gives broad peaks due to the paramagnetic nature of this compound. Elemental analysis calc. (%) for $\text{C}_{55}\text{H}_{67}\text{N}_6\text{O}_2\text{Gd}$ (M = 1001.43 $\text{g}\cdot\text{mol}^{-1}$): C 65.97, H 6.74, N 8.39; Found: C 77.81, H 8.28, N 10.84. Gd: 15.70; Found from titration: 15.75.

[Er(DMForm)₃(dmf)] (**3.7**)

Erbium filings (0.30 g, 1.80 mmol), $\text{Hg}(\text{C}_6\text{F}_5)_2$ (0.62 g, 1.50 mmol) and DMFormH (0.75 g, 3.00 mmol) were added to a Schlenk flask and dissolved in THF (20 mL) with stirring at room temperature for one week. The resulting pale red solution was filtered through a filter cannula from the metal residue and completely dried. Resulting pink solid was dissolved in dried DMF (15 mL) and cooled to $-5\text{ }^\circ\text{C}$ for a day. Small pink crystals of (**3.7**) were produced. Yield = 0.49 g (51%); M.P.: 200-202 $^\circ\text{C}$; IR (Nujol, cm^{-1}): ν = 1878 (vw), 1762 (vw), 1734 (vw), 1647 (vs), 1608 (w), 1443 (vs), 1377 (vs), 1293 (vs), 1206 (s), 1154 (s), 1118 (s), 990 (m), 948 (m), 907 (m), 874 (m), 811 (s), 723 (vs), 684 (m), 614 (m), 558 (s), cm^{-1} (wv); ^1H NMR (C_6D_6 , 303.2 K): Gives broad peaks due to the paramagnetic nature of this compound. Elemental analysis calc. (%) for $\text{C}_{54}\text{H}_{64}\text{N}_7\text{OEr}$ (M = 994.5 $\text{g}\cdot\text{mol}^{-1}$): C 65.25, H 6.48, N 9.86; Found: C 64.62, H 7.00, N 9.67. Er: 16.81; Found from titration: 16.88.

[Er(DMForm)₃(thf)] (**3.8**)

Erbium filings (0.30 g, 1.80 mmol), $\text{Hg}(\text{C}_6\text{F}_5)_2$ (0.62 g, 1.50 mmol) and DMFormH (0.75 g, 3.00 mmol) were added to a Schlenk flask and dissolved in THF (20 mL) with stirring at room temperature for one week. The resulting red to pink solution was filtered through a filter cannula from the metal residue and evaporated under vacuum to 5 mL and cooled to $-5\text{ }^\circ\text{C}$ for several days. Small pink crystals of (**3.8**) were produced. Yield < 0.1 g (<10%);

[{Er(DMForm)₂(μ -OH)(thf)}₂].(THF)₂ (**3.9**)

Erbium filings (0.30 g, 1.80 mmol), $\text{Hg}(\text{C}_6\text{F}_5)_2$ (0.62 g, 1.50 mmol) and DMFormH (0.75 g, 3.00 mmol) were added to a Schlenk flask and dissolved in THF (20 mL) with stirring at room temperature for one week. The resulting red to pink solution was filtered through a filter

cannula from the metal residue and evaporated under vacuum to 5 mL and cooled to -5 °C for several days. Small pink crystals of **(3.9)** were produced. Yield \approx 0.1 g (<10%);

[Tb(DMForm)₃(dmf)] **(3.10)**

Terbium filings (0.30 g, 1.80 mmol), Hg(C₆F₅)₂ (0.62 g, 1.50 mmol) and DMFormH (0.75 g, 3.00 mmol) were added to a Schlenk flask and dissolved in THF (20 mL) with stirring at room temperature for one week. The resulting green yellowish solution was filtered through a filter cannula from the metal residue and completely dried. Resulting yellowish solid was dissolved in dried DMF (15 mL) and cooled to -5 °C for a day. Small yellow crystals of **(3.10)** were produced. Yield < 0.1 g (<10%);

[Lu(DMForm)₃(dmf)] **(3.11)**

Lutetium filings (0.30 g, 1.70 mmol), Hg(C₆F₅)₂ (0.62 g, 1.50 mmol) and DMFormH (0.75 g, 3.00 mmol) were added to a Schlenk flask and dissolved in THF (20 mL) with stirring at room temperature for one week. The resulting yellow solution was filtered through a filter cannula from the metal residue and completely dried. Resulting white solid was dissolved in dried DMF (15 mL) and cooled to -5 °C for a day. Small yellow crystals of **(3.11)** were produced. Yield \approx 0.1 g (<10%);

X-Ray crystallography

[Y(DMForm)₃(thf)] **(3.1)**

C₅₅H₆₅N₆OY (*M* = 915.04 g/mol): monoclinic, space group P2₁/n (no. 14), *a* = 12.889(3) Å, *b* = 17.537(4) Å, *c* = 21.661(4) Å, β = 100.31(3)°, *V* = 4817.1(17) Å³, *Z* = 4, *T* = 293(2) K, μ (MoK α) = 1.256 mm⁻¹, *D*_{calc} = 1.262 g/cm³, 87954 reflections measured (3.008° \leq 2 θ \leq 63.744°), 13890 unique (*R*_{int} = 0.0736, *R*_{sigma} = 0.0412) which were used in all calculations. The final *R*₁ was 0.0617 (*I* > 2 σ (*I*)) and *wR*₂ was 0.1818 (all data).

[Lu(DMForm)₃(thf)] (3.2)

C₅₅H₆₅LuN₆O (*M* = 998.07 g/mol): monoclinic, space group P2₁/n (no. 14), *a* = 12.993(3) Å, *b* = 17.631(4) Å, *c* = 21.624(4) Å, *β* = 99.32(3)°, *V* = 4888.3(17) Å³, *Z* = 4, *T* = 293(2) K, *μ*(MoKα) = 2.064 mm⁻¹, *D*_{calc} = 1.356 g/cm³, 89058 reflections measured (2.996° ≤ 2θ ≤ 63.76°), 13876 unique (*R*_{int} = 0.0448, *R*_{sigma} = 0.0255) which were used in all calculations. The final *R*₁ was 0.0441 (*I* > 2σ(*I*)) and *wR*₂ was 0.1551 (all data).

[Pr(DMForm)₃(DMFormH)] (3.3)

C₆₈H₇₇N₈Pr (*M* = 1144.26 g/mol): monoclinic, space group P2₁/c (no. 14), *a* = 10.717(2) Å, *b* = 21.627(4) Å, *c* = 27.219(5) Å, *β* = 94.820(11)°, *V* = 6286(2) Å³, *Z* = 4, *T* = 296.15 K, *μ*(MoKα) = 0.820 mm⁻¹, *D*_{calc} = 1.209 g/cm³, 48878 reflections measured (2.408° ≤ 2θ ≤ 50°), 10207 unique (*R*_{int} = 0.1410, *R*_{sigma} = 0.3068) which were used in all calculations. The final *R*₁ was 0.0680 (*I* > 2σ(*I*)) and *wR*₂ was 0.1959 (all data).

[Ho(DMForm)₃(DMFormH)] (3.4)

C₆₈H₇₄N₈Ho (*M* = 1168.28 g/mol): monoclinic, space group P2₁/n (no. 14), *a* = 16.4175(5) Å, *b* = 22.2459(7) Å, *c* = 20.1078(6) Å, *β* = 91.5140(10)°, *V* = 7341.2(4) Å³, *Z* = 4, *T* = 296.15 K, *μ*(MoKα) = 1.116 mm⁻¹, *D*_{calc} = 1.057 g/cm³, 115726 reflections measured (2.73° ≤ 2θ ≤ 55°), 16816 unique (*R*_{int} = 0.1046, *R*_{sigma} = 0.1082) which were used in all calculations. The final *R*₁ was 0.0745 (*I* > 2σ(*I*)) and *wR*₂ was 0.2893 (all data).

[Sm(DMForm)₃(dme)] (3.5)

C₅₅H₆₀N₆O₂Sm (*M* = 987.44 g/mol): monoclinic, space group P2₁/n (no. 14), *a* = 11.2836(14) Å, *b* = 25.826(3) Å, *c* = 17.941(2) Å, *β* = 97.734(7)°, *V* = 5180.9(11) Å³, *Z* = 4, *T* = 296.15 K, *μ*(MoKα) = 1.178 mm⁻¹, *D*_{calc} = 1.266 g/cm³, 58265 reflections measured (2.782° ≤ 2θ ≤ 49.998°), 9113 unique (*R*_{int} = 0.1597, *R*_{sigma} = 0.1421) which were used in all calculations. The final *R*₁ was 0.0567 (*I* > 2σ(*I*)) and *wR*₂ was 0.1344 (all data).

[Gd(DMForm)₃(dme)] **(3.6)**

C₅₅H₆₇GdN₆O₂ (*M* = 1001.39 g/mol): monoclinic, space group P2₁/n (no. 14), *a* = 11.070(2) Å, *b* = 25.475(5) Å, *c* = 17.869(4) Å, *β* = 97.82(3)°, *V* = 4992.3(18) Å³, *Z* = 4, *T* = 293(2) K, *μ*(MoKα) = 1.375 mm⁻¹, *D*_{calc} = 1.332 g/cm³, 91925 reflections measured (2.802° ≤ 2θ ≤ 63.9°), 14379 unique (*R*_{int} = 0.0492, *R*_{sigma} = 0.0275) which were used in all calculations. The final *R*₁ was 0.0375 (*I* > 2σ(*I*)) and *wR*₂ was 0.1152 (all data).

[Er(DMForm)₃(dmf)] **(3.7)**

C₅₄H₆₄N₇OEr (*M* = 994.5 g/mol): monoclinic, space group P2₁ (no. 4), *a* = 10.350(2) Å, *b* = 18.139(4) Å, *c* = 12.726(3) Å, *β* = 95.47(3)°, *V* = 2378.3(8) Å³, *Z* = 8, *T* = 293 K, *μ*(Mo Kα) = 1.810 mm⁻¹, *D*_{calc} = 1.3843 g/cm³, 43430 reflections measured (3.92° ≤ 2θ ≤ 63.8°), 11749 unique (*R*_{int} = 0.0457, *R*_{sigma} = 0.0372) which were used in all calculations. The final *R*₁ was 0.0285 (*I* > 2σ(*I*)) and *wR*₂ was 0.0857 (all data).

[Er(DMForm)₃(thf)] **(3.8)**

C₅₅H₆₅ErN₆O (*M* = 993.42 g/mol): monoclinic, space group P2₁/n (no. 14), *a* = 15.192(3) Å, *b* = 17.961(4) Å, *c* = 21.234(4) Å, *β* = 103.24(3)°, *V* = 5640(2) Å³, *Z* = 4, *T* = 293(2) K, *μ*(MoKα) = 1.526 mm⁻¹, *D*_{calc} = 1.169 g/cm³, 102107 reflections measured (3.004° ≤ 2θ ≤ 63.714°), 15960 unique (*R*_{int} = 0.0494, *R*_{sigma} = 0.0282) which were used in all calculations. The final *R*₁ was 0.0536 (*I* > 2σ(*I*)) and *wR*₂ was 0.1648 (all data).

[{Er(DMForm)₂(μ-OH)(thf)}₂].(THF)₂ **(3.9)**

C₄₆H₆₂ErN₄O₄ (*M* = 881.06 g/mol): triclinic, space group P-1 (no. 2), *a* = 13.046(3) Å, *b* = 14.116(3) Å, *c* = 14.301(3) Å, *α* = 61.37(3)°, *β* = 77.51(3)°, *γ* = 73.23(3)°, *V* = 2203.8(10) Å³, *Z* = 2, *T* = 173.15 K, *μ*(MoKα) = 1.948 mm⁻¹, *D*_{calc} = 1.323 g/cm³, 23025 reflections measured (3.488° ≤ 2θ ≤ 49.992°), 7174 unique (*R*_{int} = 0.0251, *R*_{sigma} = 0.0224) which were used in all calculations. The final *R*₁ was 0.0335 (*I* > 2σ(*I*)) and *wR*₂ was 0.1065 (all data).

[Tb(DMForm)₃(dmf)] (3.10)

C₅₄H₆₄N₇OTb (*M* = 986.06 g/mol): monoclinic, space group P2₁ (no. 4), *a* = 10.427(2) Å, *b* = 18.114(4) Å, *c* = 12.684(3) Å, *β* = 95.58(3)°, *V* = 2384.3(8) Å³, *Z* = 2, *T* = 293 K, μ(Mo Kα) = 1.529 mm⁻¹, *D*_{calc} = 1.3692 g/cm³, 43424 reflections measured (5.78° ≤ 2θ ≤ 63.7°), 11909 unique (*R*_{int} = 0.0473, *R*_{sigma} = 0.0401) which were used in all calculations. The final *R*₁ was 0.0315 (*I* ≥ 2*u*(*I*)) and *wR*₂ was 0.0922 (all data).

[Lu(DMForm)₃(dmf)] (3.11)

C₅₄H₆₄LuN₇O (*M* = 1002.10 g/mol): monoclinic, space group P2₁ (no. 4), *a* = 10.333(2) Å, *b* = 18.156(4) Å, *c* = 12.740(3) Å, *β* = 95.29(3)°, *V* = 2379.9(8) Å³, *Z* = 2, *T* = 293 K, μ(Mo Kα) = 2.120 mm⁻¹, *D*_{calc} = 1.3941 g/cm³, 42400 reflections measured (3.92° ≤ 2θ ≤ 63.4°), 13072 unique (*R*_{int} = 0.0428, *R*_{sigma} = 0.0360) which were used in all calculations. The final *R*₁ was 0.0492 (*I* ≥ 2*u*(*I*)) and *wR*₂ was 0.1621 (all data).

3.5 References

1. M. L. Cole, G. B. Deacon, C. M. Forsyth, P. C. Junk, K. Konstas, J. Wang, H. Bittig and D. Werner, *Chem. Eur. J.*, 2013, **19**, 1410-1420.
2. M. L. Cole, G. B. Deacon, P. C. Junk and J. Wang, *Organometallics*, 2013, **32**, 1370-1378.
3. L. Guo, X. Zhu, S. Zhou, X. Mu, Y. Wei, S. Wang, Z. Feng, G. Zhang and B. Deng, *Dalton Trans.*, 2014, **43**, 6842-6847.
4. S. Hamidi, L. N. Jende, H. Martin Dietrich, C. c. Maichle-Mössmer, K. W. Törnroos, G. B. Deacon, P. C. Junk and R. Anwender, *Organometallics*, 2013, **32**, 1209-1223.
5. X. Zhu, S. Zhou, S. Wang, Y. Wei, L. Zhang, F. Wang, S. Wang and Z. Feng, *Chem. Commun.*, 2012, **48**, 12020-12022.
6. R. Shannon, *Acta Crystallogr. A*, 1976, **32**, 751-767.
7. G. B. Deacon, P. C. Junk, L. K. Macreadie and D. Werner, *Eur. J. Inorg. Chem.*, 2014, 5240-5250.
8. M. L. Cole, G. B. Deacon, C. M. Forsyth, P. C. Junk, K. Konstas and J. Wang, *Chem. Eur. J.*, 2007, **13**, 8092-8110.
9. E. Hawkins, D. Long and F. Major, *J. Chem. Soc.*, 1955, 1462-1468.
10. W. Child and H. Adkins, *J. Am. Chem. Soc.*, 1923, **45**, 3013-3023.
11. F. J. Villani and F. Nord, *J. Am. Chem. Soc.*, 1947, **69**, 2605-2607.
12. S.-y. Onozawa, T. Sakakura, M. Tanaka and M. Shiro, *Tetrahedron*, 1996, **52**, 4291-4302.
13. M. R. Bürgstein, H. Berberich and P. W. Roesky, *Chem. Eur. J.*, 2001, **7**, 3078-3085.
14. M. R. Bürgstein, H. Berberich and P. W. Roesky, *Organometallics*, 1998, **17**, 1452-1454.
15. G. B. Deacon, T. Feng, C. M. Forsyth, A. Gitlits, D. C. Hockless, Q. Shen, B. W. Skelton and A. H. White, *J. Chem. Soc., Dalton Trans.*, 2000, 961-966.
16. M. R. Crimmin, A. G. Barrett, M. S. Hill and P. A. Procopiou, *Org. Lett.*, 2007, **9**, 331-333.
17. A. Zuyls, P. W. Roesky, G. B. Deacon, K. Konstas and P. C. Junk, *Eur. J. Org. Chem.*, 2008, **4**, 693-697.
18. H. Berberich and P. W. Roesky, *Angew. Chem. Int. Ed.*, 1998, **37**, 1569-1571.
19. R. M. Roberts, *J. Org. Chem.*, 1949, **14**, 277-284.

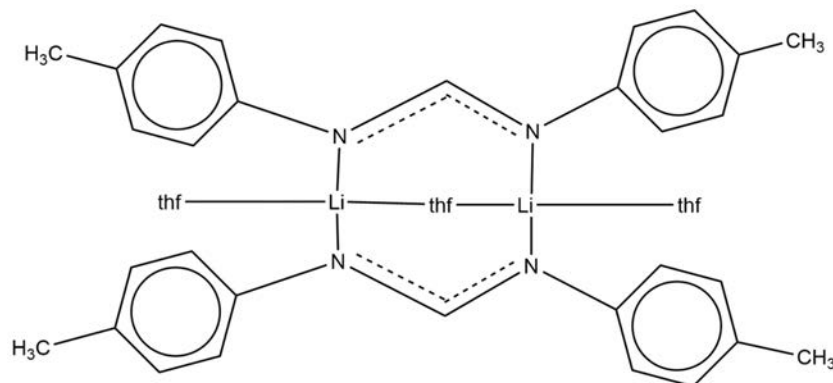
Chapter 4

Synthesis and characterisation of some main group formamidinate complexes

4 Synthesis and characterisation of some main group formamidinate complexes

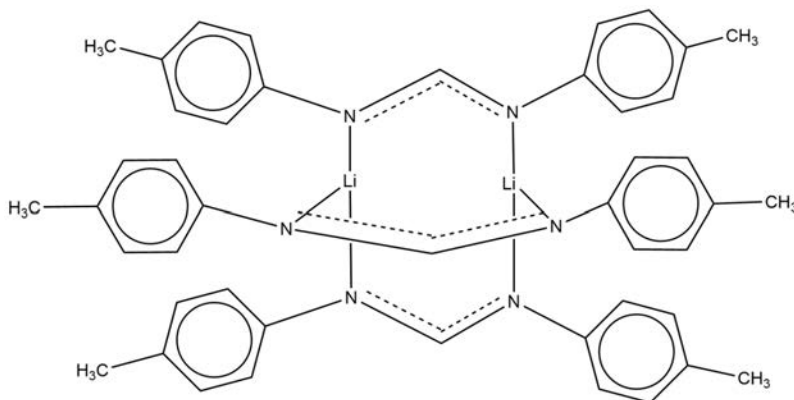
4.1 Introduction

Interest in lithium organometallic chemistry emerges from their importance as strong Bronsted bases or nucleophiles in organic synthesis and as synthetic reagents in inorganic chemistry.¹⁻³ There are a great range of studies using amidines in transition metal,⁴⁻⁶ Group 2,⁷ Group 13^{8,9}, Group 14^{10,11} and lanthanoid (see chapters 1-3) chemistry. Much attention has been paid to bis(aryl)formamidinate ligands in transition metal chemistry since they have vast structural diversity.¹² Cotton and co-workers were among the first groups to have studied Group 1 formamidinate chemistry.¹³⁻¹⁷ These ligands can bridge transition metal centers and the resultant complexes have good magnetic properties.^{18,19} $[\text{Li}(\textit{p}\text{-TolForm})(\text{Et}_2\text{O})_2]_2$ was the first structurally characterized Group 1 formamidinate.²⁰ In this compound the formamidinate ligand chelates and bridges two different lithium centers. Compounds of $[\text{Li}_2(\textit{p}\text{-TolForm})_2(\text{thf})_3] \cdot 2\text{THF}$, $[\text{Li}(\text{dme})_3][\text{Li}_2(\textit{p}\text{-TolForm})_3]$ and $[\{\text{Li}_2(\textit{p}\text{-TolForm})_2(\text{tmeda})\}_\infty]$ were obtained as the result of clean deprotonation of the amino group which was confirmed by spectroscopic evidence.¹² X-ray data indicates that $[\text{Li}_2(\textit{p}\text{-TolForm})_2(\text{thf})_3] \cdot 2\text{THF}$ crystallizes with two lithium centers bound by two terminal thf ligands, one bridging thf and two nitrogen centers of two different *p*-TolForm ligands. The lithium centers are four coordinate in a distorted tetrahedral geometry. Scheme 4.1-1 shows the structure of $[\text{Li}_2(\textit{p}\text{-TolForm})_2(\text{thf})_3] \cdot 2\text{THF}$.



Scheme 4.1-1. Schematic X-Ray crystal structure of the dinuclear $[\text{Li}_2(\textit{p}\text{-TolForm})_2(\text{thf})_3] \cdot 2\text{THF}$.¹²

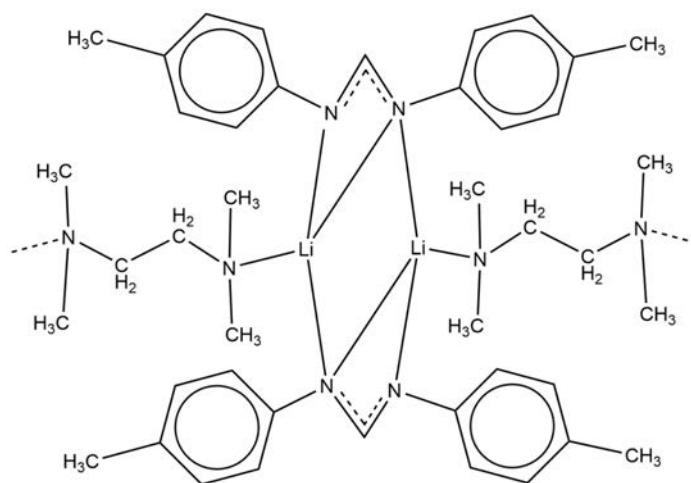
The formamidinate ligands bond two lithium atoms in a $\mu\text{-}\eta^1,\eta^1$ -mode and act in a bridging mode. The ligand has a potentially chelating NCN fragment. However, no chelation is observed in the structure. The interest for using DME solvent was to move from a monodentate THF solvent to potentially chelating solvent and determining structural changes. Scheme 4.1-2 shows that lithiation of *p*-TolFormH in DME resulted in the ionic complex $[\text{Li}(\text{dme})_3][\text{Li}_2(\textit{p}\text{-TolForm})_3]$ and the anion only is presented.



Scheme 4.1-2. Schematic X-ray crystal structure of the dinuclear anion in $[\text{Li}(\text{dme})_3][\text{Li}_2(\textit{p}\text{-TolForm})_3]$.¹²

$[\text{Li}(\text{dme})_3][\text{Li}_2(\textit{p}\text{-TolForm})_3]$ crystallizes with the anion consisting of two lithium centers and three formamidinate ligands which form a binuclear species. Two lithium centers are connected in a $\mu\text{-(Form)}_3$ binding mode by *N,N'*-di(*para*-tolyl)formamidinate as the bridging ligand. The cation has a distorted octahedral geometry about the metal center and the lithium center is solvated by three dme molecules. It should be noted that only three formamidinate ligands are able to orientate themselves around the lithium centers. However, for the transition metal complexes four formamidinate ligands can attach themselves to the central metals because the lithium is smaller than most transition metals.^{12, 21}

Using a non-coordinating solvent such as hexane for lithiating *p*-TolFormH led to generation of an insoluble precipitate. The precipitate dissolves by adding a potentially chelating amine TMEDA, to this mixture. In this study crystals of $[\{\text{Li}_2(\textit{p}\text{-TolForm})_2(\text{tmeda})\}_\infty]$ were isolated from the resulting solution. X-Ray crystal structure analysis showed that the TMEDA ligand bridges the binuclear lithium centers and each lithium center possesses a distorted tetrahedral geometry (Scheme 4.1-3).

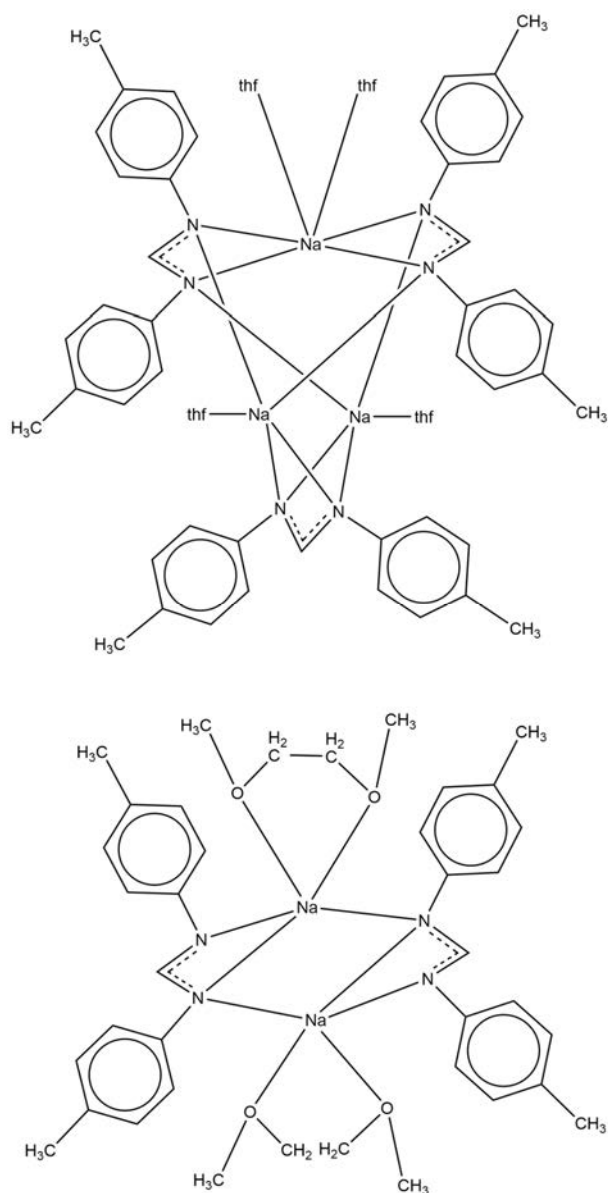


Scheme 4.1-3. Schematic X-ray crystal structure of $[\{Li_2(p\text{-TolForm})_2(tmeda)\}_\infty]$.¹²

It has been found in this study that the lithium–carbon (backbone) distance is in the range of 2.365(6) Å which is in the range of most accepted lithium–carbon bonds distance (2.1–2.37 Å) so contact with the carbon atom of the NCN backbone is appreciable in this case.

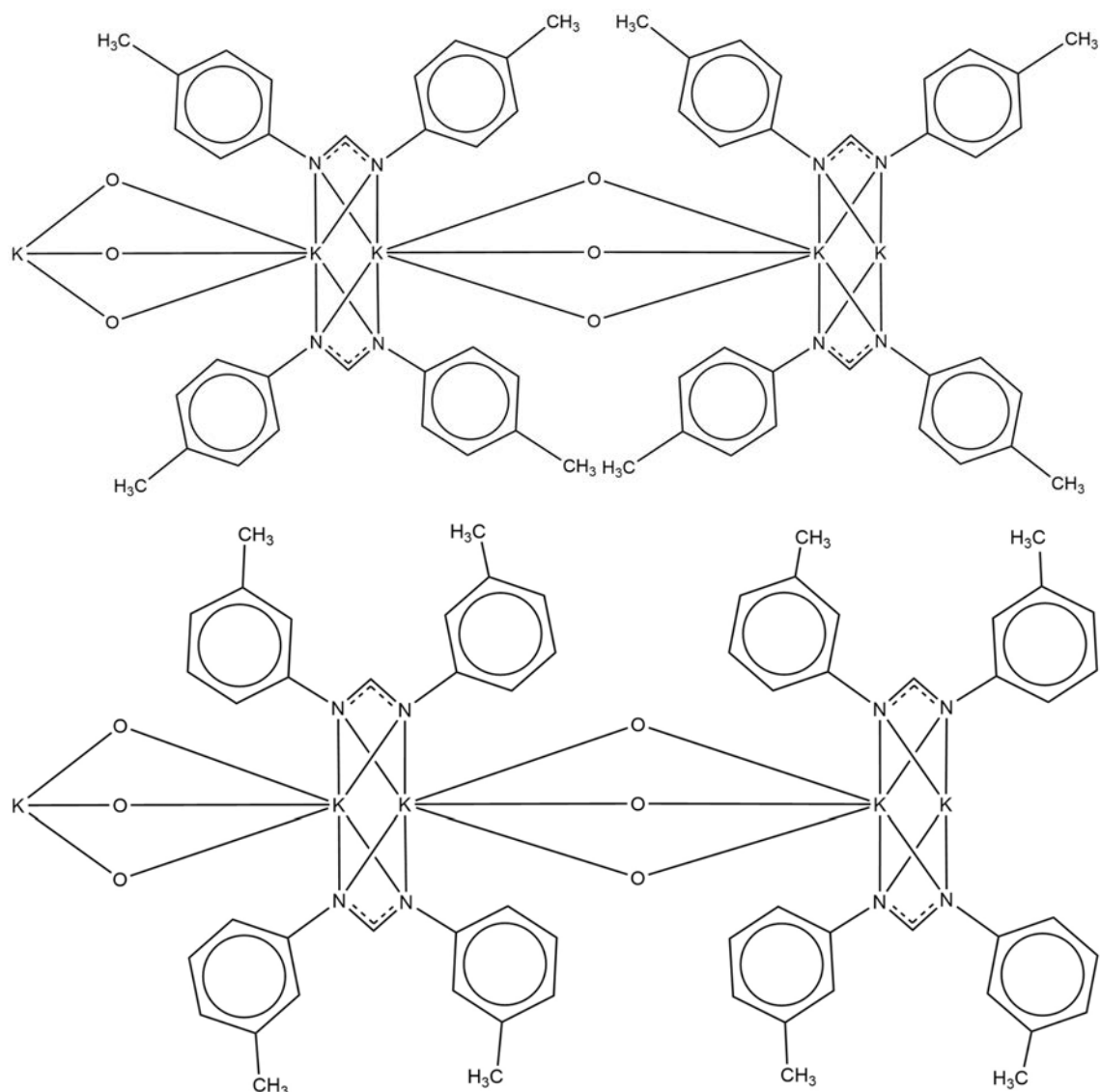
Sodium amides have gained less attention compared with lithium compounds in organic synthesis because they are more difficult to handle. However, incorporation of LiX (X = halide) can be problematic in lanthanoid halide²² metathesis reactions which makes the sodium reagents to be considered as an alternative. Therefore, a detailed study has previously been performed. $[Na_3(p\text{-TolForm})_3(thf)_4]$ and $[Na_2(p\text{-TolForm})_2(dme)_2]$ compounds were synthesized in good yield using two methods of treating *p*-TolFormH with either sodium hydride or by transamination using sodium bis(trimethylsilyl)amide.¹² Reactions can be performed using sodium hydride since it is much cheaper than bis(trimethylsilyl)amine. However, NMR spectroscopy shows that besides being a simpler synthetic method, a cleaner reaction is another advantage of using the bis(trimethylsilyl)amide reagent. Scheme 4.1-4 shows the structures for both sodium compounds. According to the X-ray data (Scheme 4.1-4 (top)), $[Na_3(p\text{-TolForm})_3(thf)_4]$ is a trinuclear compound with two structurally distinct sodium environments. Na(3) is bound to two terminal thf ligands and the metal is six-coordinate. There are two bidentate formamidinate ligands in a $\mu_3\text{-}\eta^2\text{:}\eta^1\text{:}\eta^1$ -binding mode. The other metal centers, Na(1) and Na(2) are five-coordinate, being bound by a monodentate thf, a bidentate (chelating) formamidinate and two monodentate (bridging) formamidinate ligands in a distorted square pyramidal geometry. The complex obtained using *p*-TolFormH and

sodium hydride in DME is a dinuclear compound (Scheme 4.1-4 (bottom)). X-ray data shows that this compound includes chelating dme molecules and formamidinate ligands showing chelating (from one $\mu\text{-}\eta^2\text{:}\eta^1\text{-}$ ligand) and monodentate bridging bonds (from another $\mu\text{-}\eta^2\text{:}\eta^1\text{-}$ ligand). Each sodium center sits in a five coordinate distorted trigonal bipyramidal geometry with a chelating bidentate dme molecule.



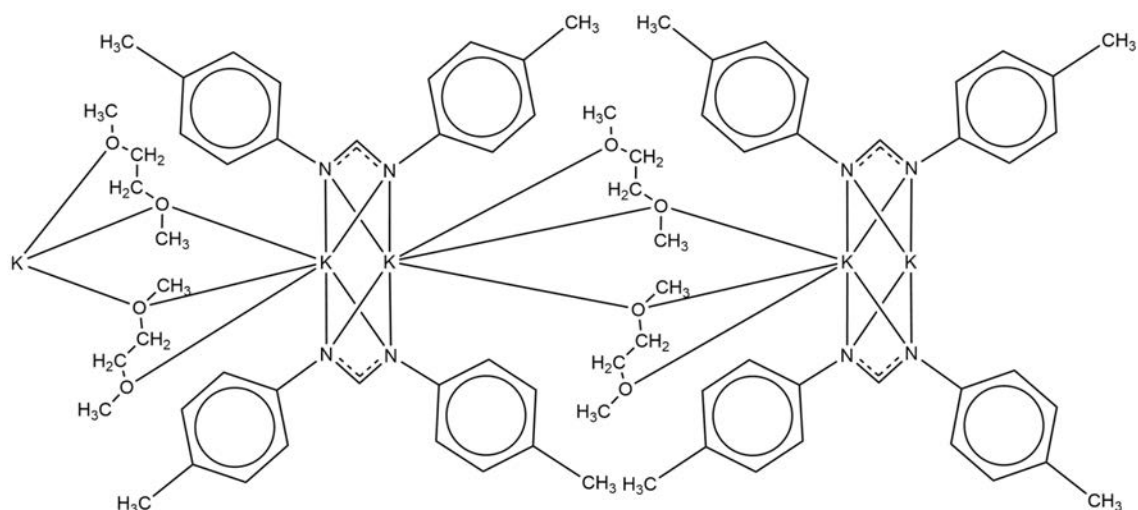
Scheme 4.1-4. Schematic X-ray crystal structures of trinuclear cluster of $[\text{Na}_3(p\text{-TolForm})_3(\text{thf})_4]$ (top) and dinuclear complex $[\text{Na}_2(p\text{-TolForm})_2(\text{dme})_2]$ (bottom).¹²

In another report, potassium hydride was used along with *p*-TolFormH and also the *meta*-tolyl form of N,N'-di(tolyl)formamidines (*m*-TolFormH).²³ Using THF as the solvent led to the formation of colorless crystals of $[\{K_2(p\text{-TolForm})_2(\text{thf})_3\}_\infty]$ and $[\{(K_2(m\text{-TolForm})_2(\text{thf})_3).\text{THF}\}_\infty]$ formamidinate complexes. Two other $[\{K(p\text{-TolForm})(\text{dme})\}_\infty]$ and $[K(p\text{-TolForm})(18\text{-crown-6})]$ compounds were synthesized using DME and toluene followed by stoichiometric addition of 18-crown-6 respectively. The solid-state compounds resulted from THF and DME exhibit $\mu\text{-}\eta^2\text{:}\eta^2$ -coordinated formamidinates and display one-dimensional polymeric structures. Compound $[K(p\text{-TolForm})(18\text{-crown-6})]$ was the first example of a polyether crown adducted monomeric Group 1 amidinate and exhibits both inter- and intramolecular C–H \cdots O hydrogen bonding in the solid-state which makes $[K(p\text{-TolForm})(18\text{-crown-6})]$ to be a two-dimensional hydrogen-bonded polymer. Scheme 4.1-5 shows schematic of the crystal structures for $[\{K_2(p\text{-TolForm})_2(\text{thf})_3\}_\infty]$ and $[\{(K_2(m\text{-TolForm})_2(\text{thf})_3).\text{THF}\}_\infty]$. Their molecular structures include discrete $K_2(\text{formamidinate})_2$ units linked to two adjacent $K_2(\text{formamidinate})_2$ units. Within these units the formamidinate ligands coordinate in a $\mu\text{-}\eta^2\text{:}\eta^2$ -binding mode without supplementary inter-unit contacts. For $[\{(K_2(m\text{-TolForm})_2(\text{thf})_3).\text{THF}\}_\infty]$ there is one THF molecule of solvation.



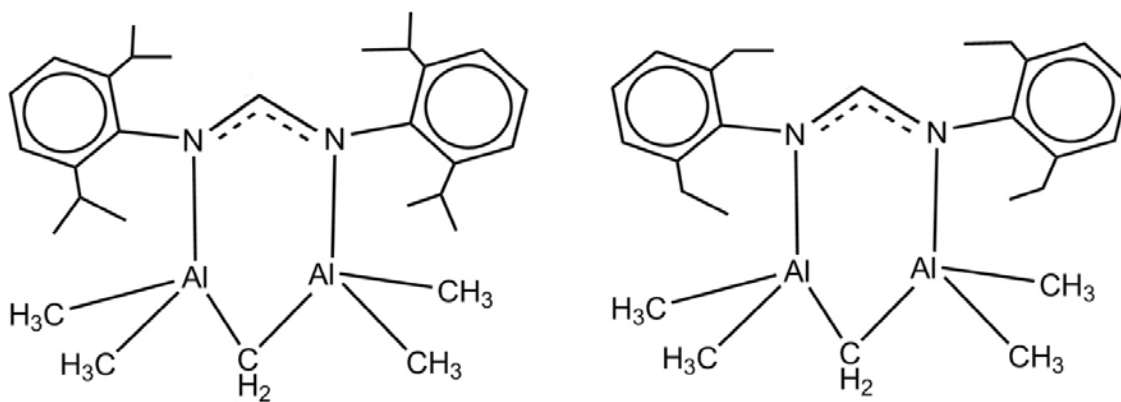
Scheme 4.1-5. Schematic X-ray crystal structures of $[\{K_2(p\text{-TolForm})_2(\text{thf})_3\}_\infty]$ (top) and $[\{(K_2(m\text{-TolForm})_2(\text{thf})_3).\text{THF}\}_\infty]$ (bottom). CH_2 of thf molecules removed for clarity in both structures.²³

This paper reports the mean NCN backbone angles of 121.4° for $[\{K_2(p\text{-TolForm})_2(\text{thf})_3\}_\infty]$ and 120.3° for $[\{(K_2(m\text{-TolForm})_2(\text{thf})_3).\text{THF}\}_\infty]$. Also, considering the intra-ligand tolyl–tolyl plane torsion angles of $52.92(6)^\circ$ for $[\{K_2(p\text{-TolForm})_2(\text{thf})_3\}_\infty]$ and $32.25(6)^\circ$ for $[\{(K_2(m\text{-TolForm})_2(\text{thf})_3).\text{THF}\}_\infty]$, it has been suggested greater steric strain for the $[\{(K_2(m\text{-TolForm})_2(\text{thf})_3).\text{THF}\}_\infty]$. It should be noted that it was the first time that a triple-thf-bridged unit was reported. The other compound, $[K(p\text{-TolForm})(\text{dme})]$, was obtained by the treatment of $p\text{-TolFormH}$ with potassium hydride in DME (Scheme 4.1-6).



Scheme 4.1-6. Schematic X-ray crystal structure of $[\{K(\mu\text{-}\eta^2\text{:}\eta^2\text{-}p\text{-TolForm})(\text{dme})\}]_{\infty}$.²³

The group of Jordan were pioneers in aluminium amidinate studies.²⁴⁻²⁶ It has been found aluminium amidinate complexes can be used as reagents in organic synthesis or as excellent catalysts toward olefin polymerization.^{24, 26-31} $[\text{AlMe}(\text{DippForm})_2]$, $[\text{AlCl}(\text{DippForm})_2]$, $[\text{AlCl}(\text{EtForm})_2]$, and $[\text{AlMe}(\text{EtForm})_2]$ ³²⁻³⁴ are some of the recent examples of aluminium bis(aryl)formamidinate complexes. DippFormH and EtFormH ligands were used with trimethylaluminum in a 1:3 stoichiometry to produce dialuminum formamidinate complexes $[\text{Me}_2\text{Al}(\mu\text{-DippForm})(\mu\text{-Me})\text{AlMe}_2]$ and $[\text{Me}_2\text{Al}(\mu\text{-EtForm})(\mu\text{-Me})\text{AlMe}_2]$ in good yields of 76% and 82% respectively.³⁵ Both of the compounds are dinuclear and each of them has one bridging ligand (Scheme 4.1-7).



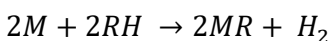
Scheme 4.1-7. Schematic X-ray crystal structures of $[\text{Me}_2\text{Al}(\mu\text{-DippForm})(\mu\text{-Me})\text{AlMe}_2]$ (left) and $[\text{Me}_2\text{Al}(\mu\text{-EtForm})(\mu\text{-Me})\text{AlMe}_2]$ (right) compounds.³⁵

The aim of this chapter is to extend the study of main group compounds involving two types of bis(aryl)formamidinates. PhFormH and DMFormH were used in this study as two formamidinate with low steric effect.

4.2 Results and discussion

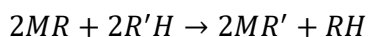
Organoalkali metal complexes can be synthesized by using different methods such as direct synthesis,^{36, 37} metalation³⁸⁻⁴⁰, transmetallation⁴⁰⁻⁴⁴ or metal-halogen exchange. The metallation method (Equation 4-2) was used to synthesize various compounds in this work. The route replaces hydrogen by an alkali metal. The final compound can be obtained via three ways depending on the substituent organic group:

(1) Direct reaction:



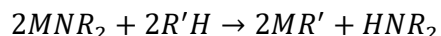
Equation 4-1.

(2) Using an organoalkali compound:



Equation 4-2.

(3) Using organoamido or organoalkali reagents with an acidic organic complex:



Equation 4-3.

Single crystals suitable for X-ray crystallography were achieved by evaporation and concentration of the solutions (~5 ml) followed by cooling very slowly and keeping the samples in the fridge for several days. The IR spectra of all complexes are void of the 3300 cm⁻¹ absorption attributable to N-H stretching, suggesting complete consumption of PhFormH or DMFormH. The result of ¹H NMR spectra (in C₆D₆) supports the presence of PhForm or DMForm with resonances at δ ≈ 9 ppm for NC(H)N. Repeated attempts to get good elemental analysis data repeatedly failed for some of the compounds synthesized in this study, presumably because they decomposed on trip to London.

4.2.1 Potassium formamidinate compounds

As result of reaction between a solution of DMFormH in THF and potassium bis(trimethylsilyl)amide (KN(SiMe₃)₂), [K(DMForm)(dme)]_∞ (**4.1**) was synthesized in good yield (59.3%). This compound crystallized in the triclinic, space group *P*-1, with half of the molecule occupying the asymmetric unit. Figure 4.2-1 shows the X-ray structure of this compound. The coordination number of the metal centre is six and searching in the Cambridge Structural database⁴⁵ revealed that this compound is the first six coordinated potassium formamidinate. The metal center is bonded by one chelating formamidinate ligand, one bridging (μ - η^2 : η^1) formamidinate ligand, one chelating dme and one bridging dme. The geometry around the metal centers can be described as distorted tetrahedral considering backbone carbon of the DMForm ligand as the point of attachment (Scheme 4.2-1). The chelation of DMForm is symmetrical for the formamidinate, however it is not symmetrical for the coordinated dme molecule. Table 4-1 shows the bond lengths of coordinated atoms to the metal center.

Table 4-1. Bond lengths of coordinated atoms in [K(DMForm)(dme)]₃ (**4.1**)

Atom...Atom	Length (Å)
K1...N1	2.8229(13)
K1...N2	2.8825(15)
K1...N1 [#]	2.9119(15)
K1...O1	2.8931(14)
K1...O2	2.7667(16)
K1...O1 [#]	2.9163(14)

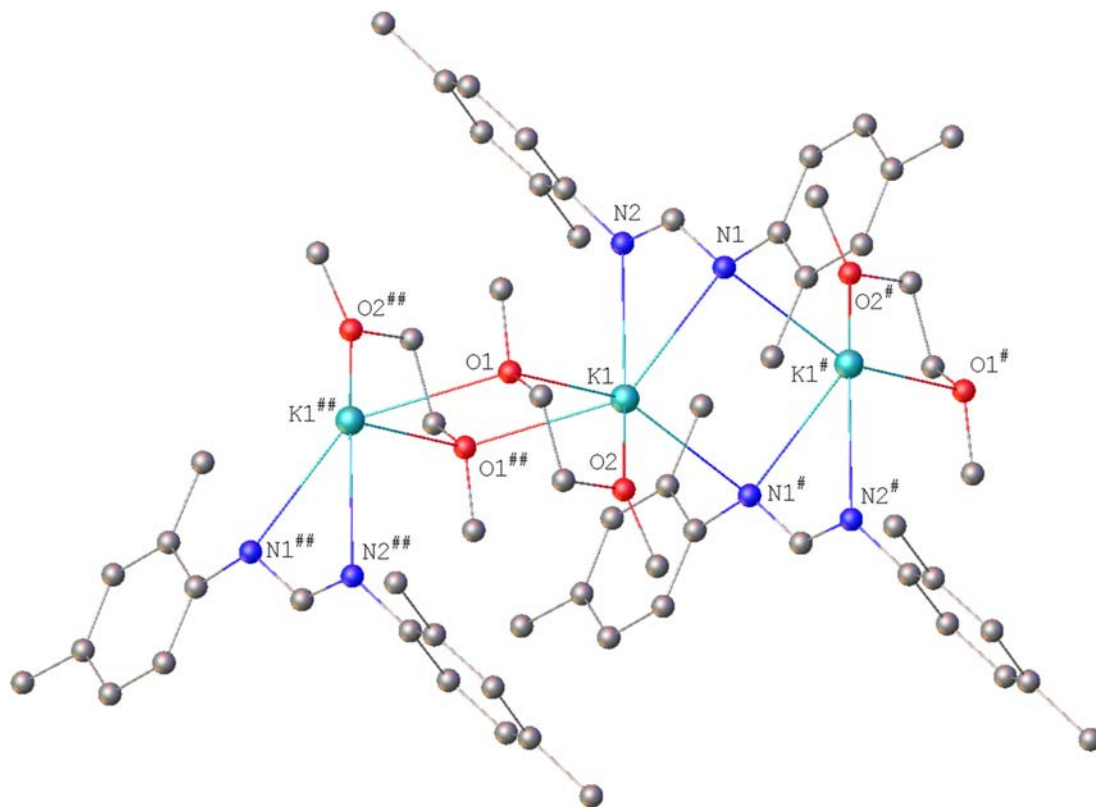
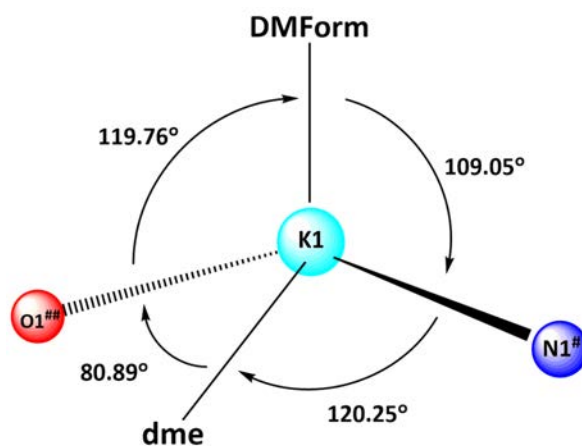


Figure 4.2-1. X-ray molecular structure of $[K(\text{DMForm})(\text{dme})]_{\infty}$ (**4.1**). Hydrogen atoms removed for clarity. Symmetry transformation used to generate “#” atoms: 1-X,1-Y,1-Z and “##” atoms: -X,1-Y,1-Z.



Scheme 4.2-1. Molecular geometry around metal centres of $[K(\text{DMForm})(\text{dme})]_{\infty}$ (**4.1**).

There are a few examples of potassium bis(aryl)formamidinate compounds in the literature.^{23, 45-48} Compound (**4.1**) can be compared with $[K(p\text{-TolForm})(\text{dme})]_{\infty}$ (Scheme 4.1-6) as discussed in the introduction.²³ The formamidinate ligands bridge metal centers via a $\mu\text{-}\eta^2\text{:}\eta^2$ bonding mode however the bridging mode in compound (**4.1**) is $\mu\text{-}\eta^2\text{:}\eta^1$. Compound (**4.1**) and

$[K(p\text{-TolForm})(dme)]_\infty$ have almost equal average K-N bond lengths (2.872(15) Å and 2.906(3) Å respectively). A same trend can be observed for the K-O bond lengths for **(4.1)** and $[K(p\text{-TolForm})(dme)]_\infty$ (2.858(16) Å and 2.804(3) Å respectively). Compound $[Na_2(p\text{-TolForm})_2(dme)_2]$ (Scheme 4.1-4 (down)) has the same structure as **(4.1)**.²² longer metal...N bond lengths (average length = 2.872 (15) Å) can be seen for compound **(4.1)** compared with $[Na_2(p\text{-TolForm})_2(dme)_2]$ (average length = 2.480(2) Å) because of larger ionic radius of potassium.²¹

Treating one equivalent of PhFormH with two equivalents of $KN(SiMe_3)_2$ resulted in formation of another polymeric structure, compound $[K_2(PhForm)N(SiMe_3)_2]_\infty$ **(4.2)**. This compound crystallized in the triclinic space group *P*-1 with one whole molecule occupying the asymmetric unit (Figure 4.2-2). There are one chelating formamidinate (which bridges to metal centers) and one $N(SiMe_3)_2$ fragment in the structure. The formamidinate ligand bridges metal centers in a $\mu_3\text{-}\eta^6:\eta^2:\eta^2$ bonding mode. The geometry around the metal center can be described as distorted trigonal planar (Scheme 4.2-2), if the backbone carbon of PhForm is considered as the point of attachment. Table 4-2 shows bond lengths of coordinated atoms to the metal center for this compound.

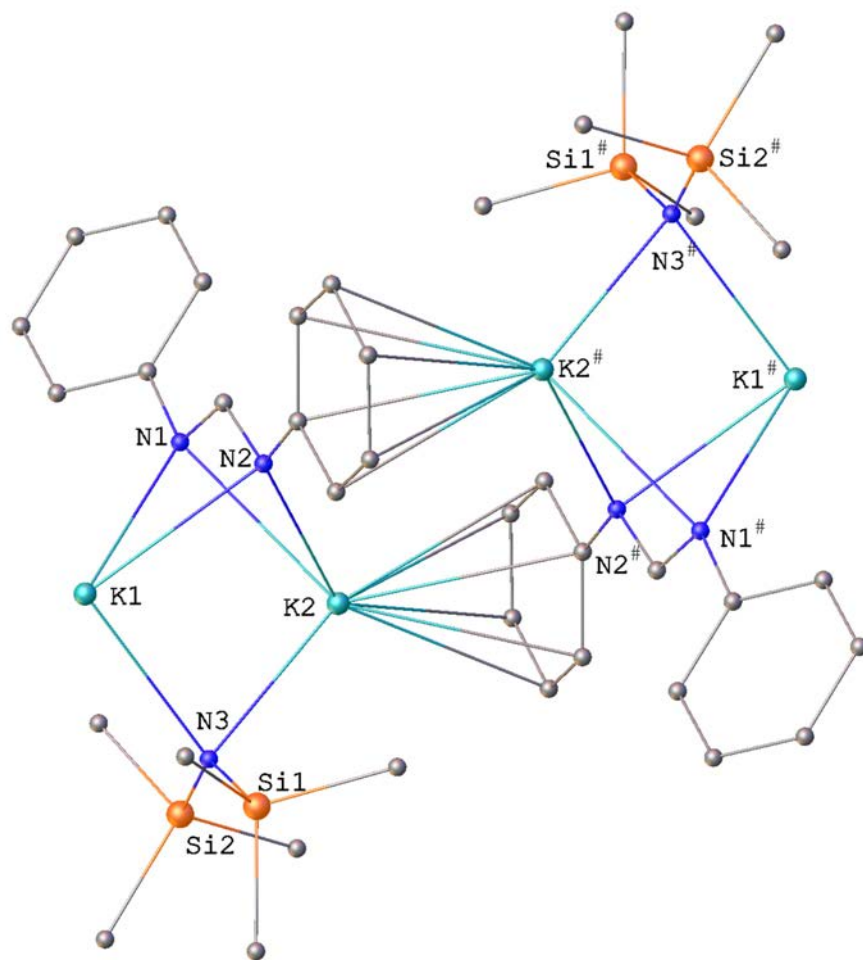
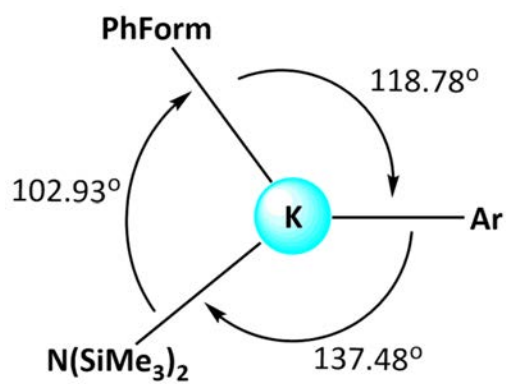


Figure 4.2-2. X-ray molecular structure of $[K_2(\text{PhForm})N(\text{SiMe}_3)_2]_\infty$ (**4.2**). Hydrogen atoms removed for clarity. Symmetry transformation used to generate “#” atoms: 1-X,1-Y,1-Z.



Scheme 4.2-2. Molecular geometry around metal center of $[K_2(\text{PhForm})N(\text{SiMe}_3)_2]_\infty$ (**4.2**).

Table 4-2. Bond lengths of coordinated atoms to metal centres in $[K_2(\text{PhForm})N(\text{SiMe}_3)_2]_\infty$ (**4.2**)

Atom...Atom	Length (Å)
K2...N1	2.932(3)
K2...N2	2.782(3)
K2...N3	2.764(3)
K2...Ar	2.931 (3)

Comparing this compound with $[K_2(p\text{-TolForm})_2(\text{thf})_3]_\infty$ (Scheme 4.1-5 (up)), reveals the average K-N bond distance is shorter in (**4.2**) (2.857(3) Å and 2.975(2) Å respectively). This can be because of slightly lower steric hindrance of PhForm compared with *p*-TolForm. The η^6 -bonding mode has been reported before for other potassium bis(aryl)formamidinate compounds⁴⁷⁻⁴⁹ however (**4.2**) is the first potassium bis(aryl)formamidinate compound that has a $\mu_3\text{-}\eta^6\text{:}\eta^2\text{:}\eta^2$ bonding mode. This can be attributed to the lower steric hindrance of PhForm which allows this ligand to be closer to the metal centers and bridge them via the $\mu_3\text{-}\eta^6\text{:}\eta^2\text{:}\eta^2$ bonding mode.

4.2.2 Sodium formamidinate compounds

Using sodium bis(trimethylsilyl)amide, DMFormH and the same preparation method, $[\text{Na}(\text{DMForm})(\text{dme})_2]$ (**4.3**) was synthesized. This compound crystallized in the monoclinic, space group *C2/c* with the whole molecule occupying the asymmetric unit. Figure 4.2-3 shows the X-ray crystal structure of this compound. The coordination number of the metal centre is six and there are one chelating formamidinate and two coordinated bidentate dme molecules. The geometry of the molecule around the metal centre can be described as distorted trigonal planar if the formamidinate attachment is considered midway between the N-C-N fragment (Scheme 4.2-3). The sum of the angles in Scheme 4.2-3 is 360.07° which suggests DMForm and two coordinated dme molecules are in the same plane. Table 4-3 shows bond lengths of the coordinated atoms in this compound.

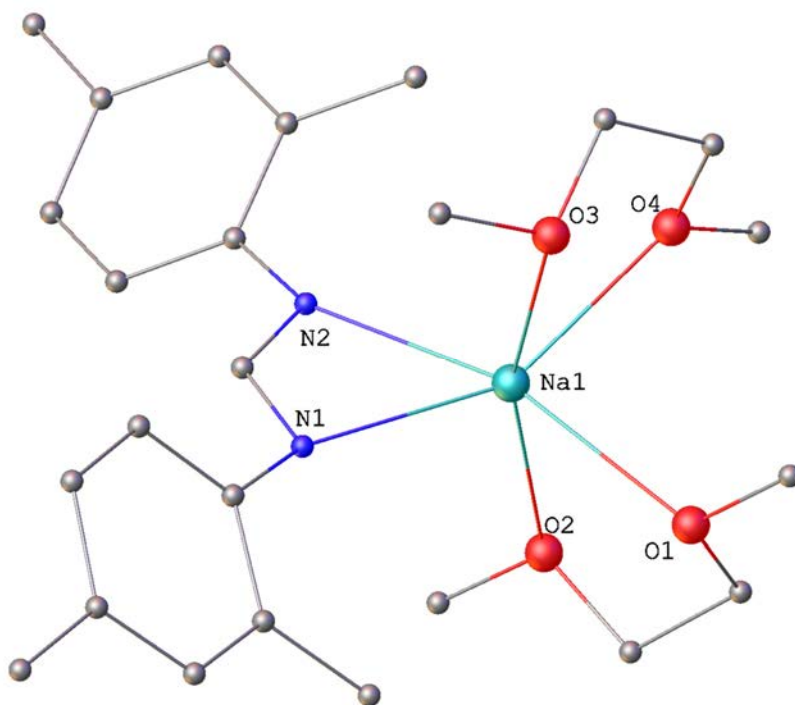
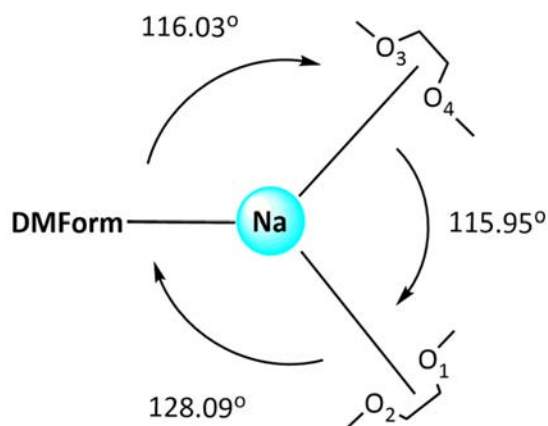


Figure 4.2-3. X-ray molecular structure of $[\text{Na}(\text{DMForm})(\text{dme})_2]$ (**4.3**). Hydrogen atoms removed for clarity.



Scheme 4.2-3. Molecular geometry around metal centres of $[\text{Na}(\text{DMForm})(\text{dme})_2]$ (**4.3**).

As mentioned in the introduction, structures have been reported using XylFormH and DippFormH as ligands.⁵⁰ $[\text{Na}(\text{XylForm})(\text{dme})_2]$ and $[\text{Na}(\text{DippForm})(\text{dme})_2]$ exhibit singular η^2 -N,N'-donors and two chelated dme donors same as $[\text{Na}(\text{DMForm})(\text{dme})_2]$ (**4.3**). The average Na-N bond distances for $[\text{Na}(\text{XylForm})(\text{dme})_2]$, $[\text{Na}(\text{DippForm})(\text{dme})_2]$ and (**4.3**) are 2.779(2) Å, 2.761(4) Å and 2.447(11) Å respectively. The lower steric effect of DMForm allows this ligand to become closer to the metal centre so the average Na-N distance is smaller for (**4.3**). Almost equal distances from the metal centre can be observed for coordinated dme

molecules in these compounds. The average Na-O bond distances for [Na(XylForm)(dme)₂], [Na(DippForm)(dme)₂] and **(4.3)** are 2.400(17) Å, 2.413(3) Å and 2.431(11) Å respectively. It seems the steric constraints of DME reduce the number of possible binding ligands and reduce the coordination number of the metal center. Using smaller monodentate solvent molecules like THF or less bulkier forms of bis(aryl)formamidinate can increase the coordination number of the metal center.^{12, 46, 50} [{Na(EtForm)(thf)}_∞] and [Na(DippForm)(thf)₃] are two examples of using THF which show higher coordination numbers for the metal center.⁵⁰

Table 4-3. Bond lengths of coordinated atoms in [Na(DMForm)(dme)₂] **(4.3)**

Atom...Atom	Length (Å)
Na1...N1	2.4102(11)
Na1...N2	2.4839(11)
Na1...O1	2.4928(11)
Na1...O2	2.3686(13)
Na1...O3	2.4410(15)
Na1...O4	2.4217(11)

Compound [Na(PhForm)(dme)]₂ **(4.4)** was synthesized by adding one equivalent of Sodium bis(trimethylsilyl)amide (NaN(SiMe₃)₂) to one equivalent of PhFormH in DME solution. This compound was crystallized in the monoclinic space group *P*2₁/*n* with half the molecule occupying the asymmetric unit (Figure 4.2-4). The coordination number of the metal center is five and there are one chelating formamidinate, one bridging formamidinate and one coordinated dme molecule about the metal center. The formamidinate ligands bridge the metal center in a μ-η²:η¹ bonding mode. The geometry around the metal center can be described as distorted trigonal planar (Scheme 4.2-4), if the backbone carbon of PhForm is considered as the attachment point of the formamidinate. Table 4-4 shows bond lengths of coordinated atoms to the metal center for this compound.

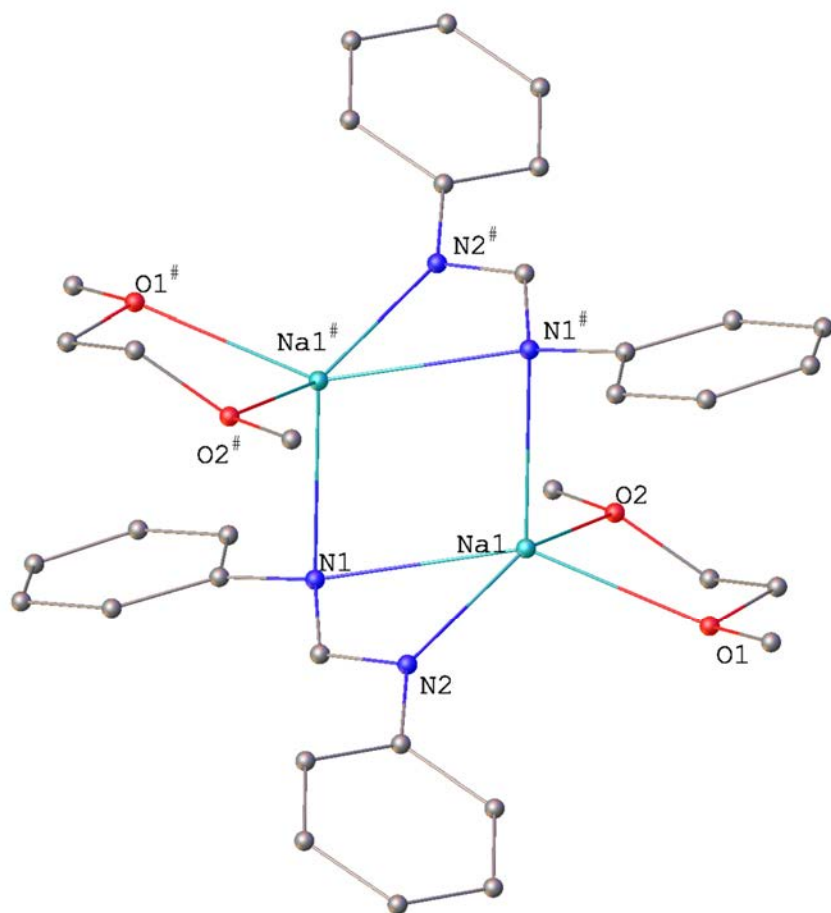
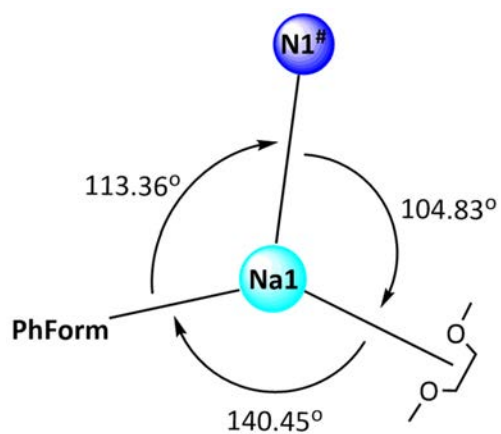


Figure 4.2-4. X-ray molecular structure of $[\text{Na}(\text{PhForm})(\text{dme})]_2$ (**4.4**). Hydrogen atoms removed for clarity. Symmetry transformation used to generate “#” atoms: 1-X,1-Y,1-Z.



Scheme 4.2-4. Molecular geometry around the Na1 metal center of $[\text{Na}(\text{PhForm})(\text{dme})]_2$ (**4.4**).

Table 4-4. Bond lengths of coordinated atoms to metal centre in $[\text{Na}(\text{PhForm})(\text{dme})_2]$ (**4.4**)

Atom...Atom	Length (Å)
Na1...N1	2.577(2)
Na1...N2	2.393(2)
Na1...N1 [#]	2.463(2)
Na1...O1	2.379(2)
Na1...O2	2.379(2)

Comparing this compound with (**4.3**) clearly shows the lower steric effect of the formamidinate can increase the number of coordinated ligands. Compound (**4.4**) has one more bridging formamidinate in the structure which prevents binding more dme molecules to the metal center. Because of one less coordinated dme molecule, the coordination number of the metal center in (**4.4**) is smaller than (**4.3**). The average Na-N bond length of (**4.4**) is 2.471(2) Å which is longer than the corresponding distance in (**4.3**) (2.447(11) Å). However, this compound has a lower average Na-O bond length (2.379(2) Å) compared with (**4.3**) (2.431(15) Å). Compound (**4.4**) and $[\text{Na}_2(p\text{-TolForm})_2(\text{dme})_2]$ have similar structures (Scheme 4.1-4 (bottom)). Compound $[\text{Na}_2(p\text{-TolForm})_2(\text{dme})_2]$ has a Na-N average distance of 2.462(3) Å which is slightly shorter than 2.471(2) Å for compound (**4.4**). This can be attributed to the longer Na1-N1[#] distance (2.470(3) Å) in $[\text{Na}_2(p\text{-TolForm})_2(\text{dme})_2]$ compared with (**4.4**) (2.463(2) Å) which suggests the corresponding ligand is further away from metal center allowing the other fomamidinate to closer approach the metal center.

4.2.3 Zinc formamidinate compound

$[\text{Zn}_4(\text{PhForm})_6\text{O}]\cdot\text{THF}$ (**4.5**) compound is the result of reaction between PhFormH and ZnEt_2 in THF (Figure 4.2-5). This compound crystallized in the triclinic space group *P*-1 with one whole molecule occupying the asymmetric unit. The compound has four metal centres and the coordination number of each centre is four. Resonances at $\delta = 8.71$ ppm which is for NC(H)N confirms the presence of six formamidinates in the structure. There is an oxygen at the centre of the cage which is connected to the four metal centres and gives an oxide cage structure to this compound. The source of the oxygen is not clear as the reaction was repeated with an extra care to avoid any possibility for presence of oxygen during the reaction. However, the reaction constantly gave an oxygen at the centre of the structure and presumably arises from ring opening of thf. Elemental analysis result confirms the purity of this compound. The geometry around each metal centre and the oxygen can be described as distorted tetrahedral (Scheme 4.2-5, Table 4-5 and Table 4-6).

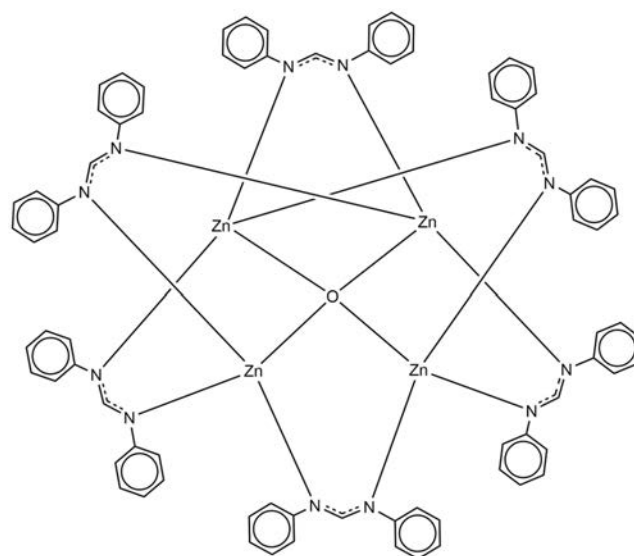
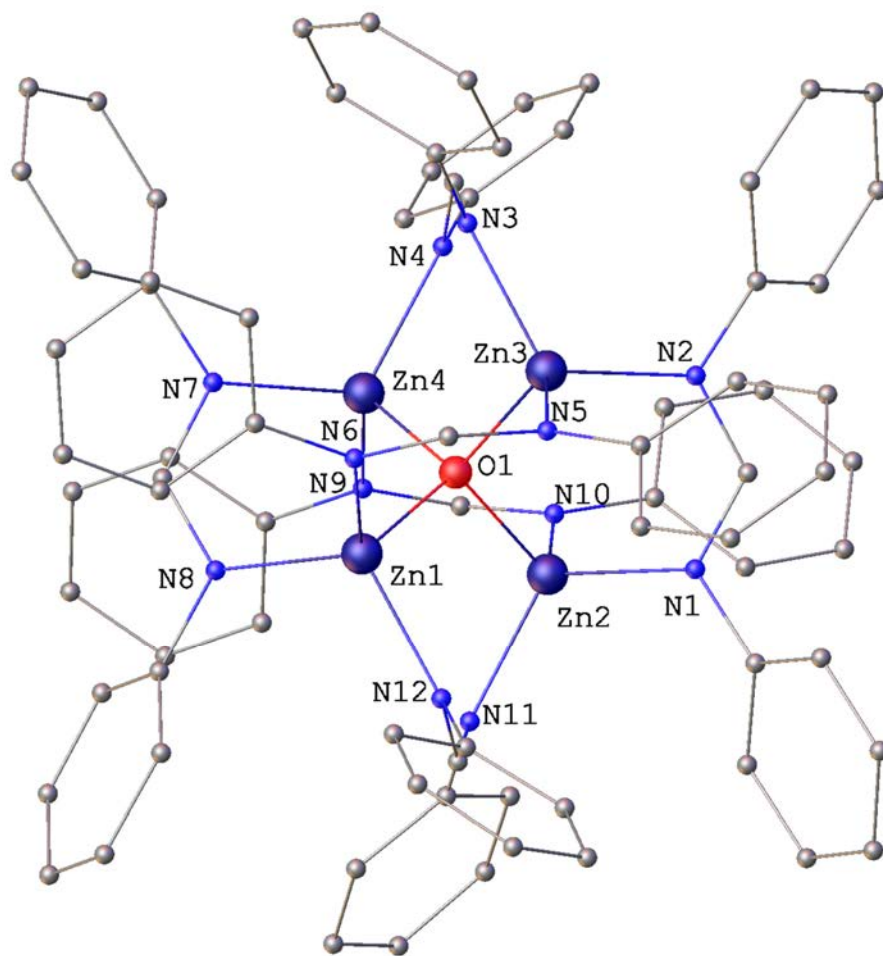
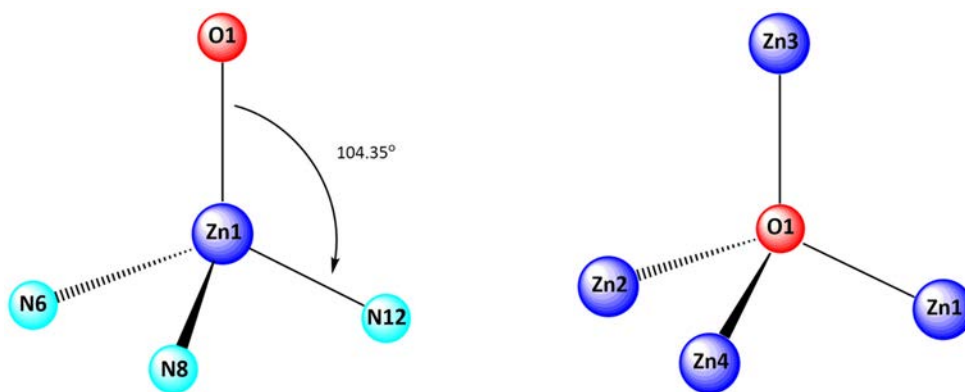


Figure 4.2-5. X-ray (top) and schematic (bottom) molecular structure of $[Zn_4(PhForm)_6O].THF$ (**4.5**). Hydrogen atoms and THF molecule removed for clarity.



Scheme 4.2-5. Molecular geometry around metal centres and the oxygen in $[\text{Zn}_4(\text{PhForm})_6\text{O}]\cdot\text{THF}$ (4.5).

Table 4-5. Bond angles for Zn1 metal center in $[\text{Zn}_4(\text{PhForm})_6\text{O}]\cdot\text{THF}$ (4.5)

Atom...O1...Atom	Angle (°)
O1...Zn1...N6	104.90(17)
O1...Zn1...N8	104.81(18)
O1...Zn1...N12	104.35(17)
N8...Zn1...N6	114.3(2)
N12...Zn1...N6	114.0(2)
N12...Zn1...N8	113.07(19)

Table 4-6. Bond angles for center oxygen atom in $[\text{Zn}_4(\text{PhForm})_6\text{O}]\cdot\text{THF}$ (4.5)

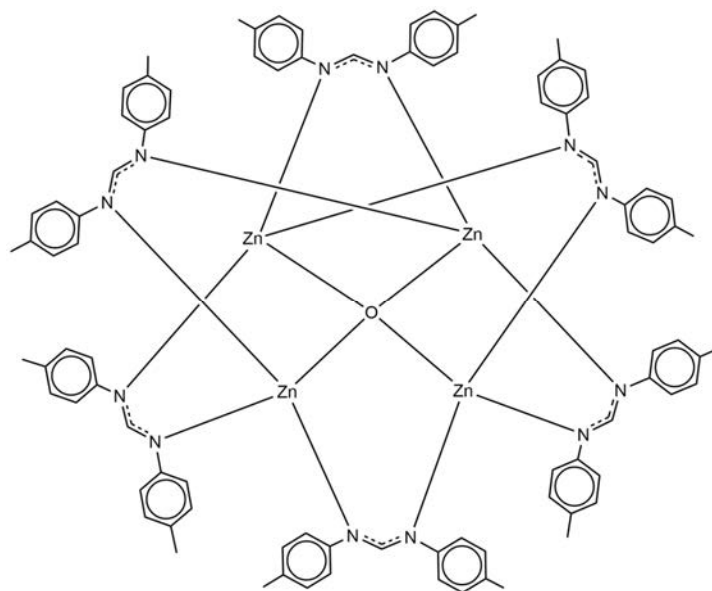
Atom...O1...Atom	Angle (°)
Zn2...O1...Zn1	109.43(18)
Zn2...O1...Zn3	110.1(2)
Zn2...O1...Zn4	108.51(19)
Zn3...O1...Zn1	108.76(19)
Zn3...O1...Zn4	110.76(18)
Zn4...O1...Zn1	109.25(19)

Table 4-7 shows the bond lengths of coordinated atoms to the metal centres for this compound. It can be seen the six formamidinate ligands bridge four metal centres in equal distances and the average length of Zn-N bond is 2.02(5) Å. The same trend can be seen for the bond lengths between metal centres and the caged oxygen with average bond length of 1.921(4) Å.

Table 4-7. Bond lengths of coordinated atoms to metal centres in [Zn₄(PhForm)₆O].THF (**4.5**)

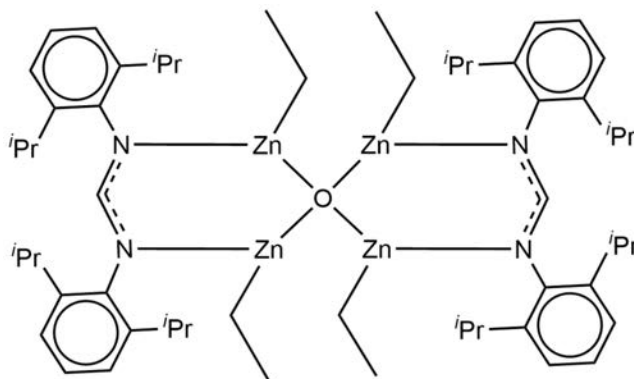
Atom...Atom	Length (Å)
Zn1...N6	2.017(5)
Zn1...N8	2.017(5)
Zn1...N12	2.008(5)
Zn2...N1	2.023(5)
Zn2...N10	2.026(5)
Zn2...N11	2.014(5)
Zn3...N2	2.014(5)
Zn3...N3	2.025(5)
Zn3...N5	2.030(5)
Zn4...N4	2.019(5)
Zn4...N7	2.023(5)
Zn4...N9	2.028(5)
Zn1...O1	1.926(4)
Zn2...O1	1.914(4)
Zn3...O1	1.921(4)
Zn4...O1	1.923(4)

It has been reported that the same structure can be synthesised using *p*-TolFormH ligand (Scheme 4.2-6).⁵¹ The steric effect of *p*-TolForm and PhForm are almost the same so average Zn-N bond lengths are expected for this compound compared with (**4.5**) (2.031(6) Å and 2.020(5) Å respectively).



Scheme 4.2-6. Schematic X-ray crystal structure of $[Zn_4(p\text{-TolForm})_6O]$.

It has been reported using Zn with a bulkier formamidinate like DippFormH can result in different structures.³³ $[Zn(\text{DippForm})_2]$ can be synthesized by using one equivalent of $ZnEt_2$ and two equivalents of DippFormH. The average Zn-N bond length of **(4.5)** can be compared well with $[Zn(\text{DippForm})_2]$ (2.020(5) Å and 2.024(2) Å). Complex $[Zn(\text{DippForm})(\text{Et})_4(O)]$ can be synthesized by using equal equivalents of $ZnEt_2$ and DippFormH. This compound has a Zn_4O core and the coordination number of metal center is three (Scheme 4.2-7).



Scheme 4.2-7. Schematic X-ray structure of $[Zn(\text{DippForm})(\text{Et})_4(O)]$.

There are two bridging formamidinates in $[Zn(\text{DippForm})(\text{Et})_4(O)]$ compared with **(4.5)** which has four bridging PhForm ligands. PhForm has lower steric bulk compared with DippForm so a larger number of PhForm ligands can be expected around the coordination sphere of Zn.

Compound $[\text{Zn}(\text{DippForm})(\text{Et})_4(\text{O})]$ has an average Zn-N bond length of 1.972(2) Å which is shorter than average Zn-N distance in **(4.5)** (2.020(5) Å). There are two bridging formamidinates in $[\text{Zn}(\text{DippForm})(\text{Et})_4(\text{O})]$ giving less steric hindrance compared with **(4.5)** so formamidinates can come closer to the metal center and decrease Zn-N distances. Compound **(4.5)** has shorter Zn-O bond lengths compared with $[\text{Zn}(\text{DippForm})(\text{Et})_4(\text{O})]$ (Average Zn...O = 1.921(4) Å and 1.959(2) Å respectively).

4.2.4 Aluminium formamidinate compounds

Performing a reaction between AlMe_3 and PhFormH with different stoichiometries of 1:1, 1:2 and 1:3 gave the same result for each experiment and compound $[\text{Al}(\text{PhForm})_3]$ **(4.6)** was synthesized. This compound crystallized in the orthorhombic space group Pccn and half of the molecule occupies the asymmetric unit (Figure 4.2-6). There are three chelating PhForm ligands connected to the metal center which gives it coordination number of six. If the backbone carbon of the formamidinates be considered as the point of binding, the geometry around the metal center can be described as distorted trigonal planar (Scheme 4.2-8). The average Al-N bond length is 2.00(11) Å and the formamidinate chelating is not symmetrical in this compound (Table 4-8).

Table 4-8. Bond lengths of coordinated atoms to metal centres in $[\text{Al}(\text{PhForm})_3]$ **(4.6)**

Atom...Atom	Length (Å)
Al1...N1	1.9956(11)
Al1...N2	2.0350(11)
Al1...N3	1.9800(11)
Al1...N1 [#]	1.9956(11)
Al1...N2 [#]	2.0351(11)
Al1...N3 [#]	1.9800(11)

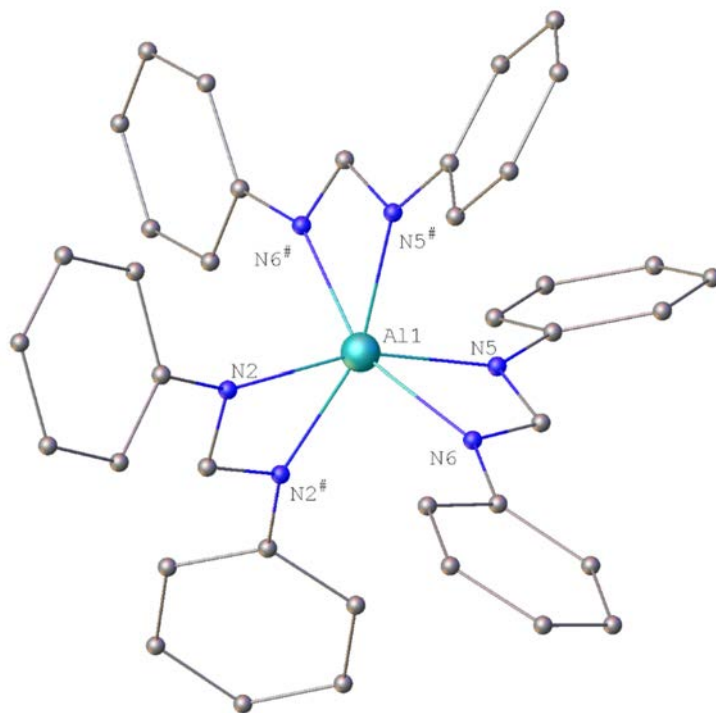
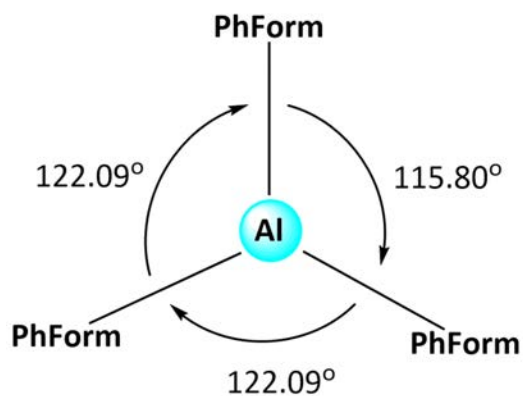


Figure 4.2-6. X-ray Molecular structure of $[\text{Al}(\text{PhForm})_3]$ (**4.6**). Hydrogen atoms removed for clarity. Symmetry transformation used to generate “#” atoms: $1/2-X, 3/2-Y, +Z$.



Scheme 4.2-8. Molecular geometry around metal center of $[\text{Al}(\text{PhForm})_3]$ (**4.6**).

Compound (**4.6**) is the first aluminium bis(aryl)formamidinate compound that has three chelating formamidinates in the structure.⁴⁵ Using bulkier ligands like DippFormH or XylFormH can decrease the number of coordinated formamidinates (Scheme 4.1-7) as expected for this small metal.^{33, 35, 52}

4.3 Conclusions

The research in this chapter is a small contribution to the main group chemistry involving two types of bis(aryl)formamidinates and presents several compounds that can be used in future, particularly in metathesis chemistry (K, Na) or in catalysis (Zn, Al). PhFormH and DMFormH were used in this study as two formamidinates with a low steric effect. Preparation and characterization of $[\text{K}(\text{DMForm})(\text{dme})]_{\infty}$ (**4.1**), $[\text{K}_2(\text{PhForm})\text{N}(\text{SiMe}_3)_2]_{\infty}$ (**4.2**), $[\text{Na}(\text{DMForm})(\text{dme})_2]$ (**4.3**), $[\text{Na}(\text{PhForm})(\text{dme})_2]$ (**4.4**), $[\text{Zn}_4(\text{PhForm})_6\text{O}].\text{THF}$ (**4.5**), and $[\text{Al}(\text{PhForm})_3]$ (**4.6**) complexes are discussed in this chapter. $[\text{K}(\text{DMForm})(\text{dme})]_{\infty}$ (**4.1**) is the first six coordinated potassium bis(aryl)formamidinate crystallographically characterized.⁴⁵ It has been found that both of the DMFormH and PhFormH can form polymeric potassium-formamidinate compounds ((**4.1**) and (**4.2**)). Decreasing the ligand steric effect led to a different bonding mode of η^6 in (**4.2**). $[\text{Na}(\text{DMForm})(\text{dme})_2]$ (**4.3**) was synthesized from DMFormH and $\text{NaN}(\text{SiMe}_3)_2$ and it was found that by using a ligand with lower steric effect (PhFormH) can give a different compound $[\text{Na}(\text{PhForm})(\text{dme})_2]$ (**4.4**), which exhibits different bonding mode of $\mu\text{-}\eta^2\text{:}\eta^1$. $[\text{Zn}_4(\text{PhForm})_6\text{O}].\text{THF}$ (**4.5**) has a oxide cage structure and comparing with other studies using different formamidinates, $[\text{Zn}(\text{DippForm})(\text{Et})_4(\text{O})]$,³³ more formamidinates can be fitted in the structure because of the lower steric effect of PhForm. Surprisingly, using PhFormH and Al in metalation reactions, gave only $[\text{Al}(\text{PhForm})_3]$ (**4.6**) despite using different stoichiometries of 1:1, 1:2 and 1:3 (AlMe_3 : PhFormH).

4.4 Experimental

All samples were prepared using a glove box, Schlenk flask and vacuum line techniques in an inert atmosphere since lanthanoid metals and their products are air-sensitive and moisture-sensitive. Sodium or sodium/benzophenone were used for refluxing and distillation of solvents to dry and deoxygenate them prior to use in reactions. PhFormH was purchased from Aldrich and DMFormH was prepared by literature methods.⁵³ Trimethylaluminium (AlMe₃), sodium bis(trimethylsilyl)amide (NaN(SiMe₃)₂), diethylzinc (ZnEt₂) and potassium bis(trimethylsilyl)amide (KN(SiMe₃)₂) were purchased from Aldrich and used as received. IR data were obtained from Nujol mulls for the region 4000-400 cm⁻¹ with a Nicolet-Nexus FT-IR spectrometer. ¹H NMR spectra were recorded with a Bruker Avance 400 MHz spectrometer using dry degassed *deutero*-benzene (C₆D₆) as solvent, and resonances were referenced to the residual ¹H resonances of the deuterated solvent. Melting points of the compounds were measured using crystals of compounds in sealed glass capillaries under nitrogen and are uncalibrated. Elemental analyses (C, H, N) were performed by the Micro analytical Laboratory, Science Centre, London Metropolitan University, England.

[K(DMForm)(dme)]_∞ (4.1)

Potassium bis(trimethylsilyl)amide (KN(SiMe₃)₂) (10 mL of a 0.5 M solution in toluene; 5 mmol) was added by a syringe to a stirring solution of DMFormH (1.25g; 5 mmol) in DME (20mL) using Schlenk line. After 1 hr stirring, the solution was concentrated to ~10 mL, colorless crystals of the product formed in room temperature after 1 hr. Yield = 1.26 g (59.3%); M.P. 240-246 °C; IR (crystal oil): ν = 1868 (vw), 1768 (vw), 1659 (s), 1606 (m), 1537 (m), 1458 (vs), 1377 (vs), 1298 (vs), 1241 (m), 1203 (vs), 1151 (m), 1120 (m), 1080 (m), 1033 (m), 1008 (s), 996 (m), 936 (m), 887 (m), 849 (w), 815 (s), 771 (m), 720 (m), 610 (m) and 553 (s) cm⁻¹; ¹H NMR (C₆D₆, 303.2 K): δ = 2.16-2.25 (d, 12H; CH₃), 2.80 (s, 6H; DME-CH₃), 2.91 (s, 4H; DME-CH₂), 6.75–6.97 (m, 6H; Ar-H), 8.15 (s, 1H, NC(H)N). Elemental analysis calcd. (%) for C₂₁H₂₉KN₂O₂ (*M* = 380.56 g/mol): C 66.28, H 7.68, N 7.36; Found from microanalysis: C 53.63, H 7.57, and N 7.26.

$[K_2(\text{PhForm})N(\text{SiMe}_3)_2]_\infty$ (**4.2**)

Potassium bis(trimethylsilyl)amide ($\text{KN}(\text{SiMe}_3)_2$) (10 mL of a 0.5 M solution in toluene; 5 mmol) was added by a syringe to a stirring solution of PhFormH (0.49 g; 2.5 mmol) in THF (20mL) using Schlenk line. After 1 hr stirring, the solution was concentrated to ~10 mL, colourless crystals of the product formed in room temperature after 1 hr. Yield = 0.37g (85.3%); M.P. 233-237 °C; IR (crystal oil): $\nu = 1796$ (w), 1721 (vw), 1666 (vw), 1590 (s), 1458 (vs), 1378 (vs), 1168 (vs), 1074 (s), 975 (s), 918 (s), 887 (s), 803 (s), 725 (s), 697 (s), 644 (s) and 591 (s) cm^{-1} ; $^1\text{H NMR}$ (C_6D_6 , 303.2 K): $\delta = 0$ (s, 18H; CH_3), 6.97–7.03 (br m, 10H; Ar-H), 8.45 (s, 1 H; $\text{NC}(\text{H})\text{N}$). Elemental analysis calcd. (%) for $\text{C}_{19}\text{H}_{29}\text{K}_2\text{N}_3\text{Si}_2$ ($M = 433.83$ g/mol): C 52.6, H 6.73, N 9.68; Found from microanalysis: C 52.7, H 6.59, N 9.52.

$[\text{Na}(\text{DMForm})(\text{dme})_2]$ (**4.3**)

Sodium bis(trimethylsilyl)amide ($\text{NaN}(\text{SiMe}_3)_2$) (5 mL of a 0.6 M solution in toluene; 3 mmol) was added by a syringe to a stirring solution of DMFormH (0.76g; 3 mmol) in DME (20mL) using Schlenk line. After 1 hr stirring, the solution was concentrated to ~10 mL, and cooled overnight causing the formation of colourless crystals of (**4.3**). Yield = 0.67 g (49.1%); M.P. 221-223 °C; IR (crystal oil): $\nu = 1869$ (vw), 1859 (vw), 1740 (vw), 1712 (vw), 1540 (s), 1458 (vs), 1376 (vs), 1320 (s), 1192 (s), 1154 (s), 1081 (vs), 1030 (vs), 940 (m), 893 (m), 860 (vs), 812 (s), 773 (s), 728 (w), 717 (w), 660 (w), 612 (m), 563 (s) and cm^{-1} ; $^1\text{H NMR}$ (C_6D_6 , 303.2 K): $\delta = 2.16$ -2.25 (d, 12H; CH_3), 2.80 (s, 12H; DME-CH_3), 2.91 (s, 8H; DME-CH_2), 6.75–6.97 (m, 6H; Ar-H), 8.15 (s, 1H, $\text{NC}(\text{H})\text{N}$). Elemental analysis calcd. (%) for $\text{C}_{25}\text{H}_{39}\text{N}_2\text{NaO}_4$ ($M = 223.27$ g.mol $^{-1}$): C 65.91, H 8.85, N 6.15; Found from microanalysis: C 53.13, H 7.27, N 7.56.

$[\text{Na}(\text{PhForm})(\text{dme})_2]$ (**4.4**)

Sodium bis(trimethylsilyl)amide ($\text{NaN}(\text{SiMe}_3)_2$) (5 mL of a 0.6 M solution in toluene; 3 mmol) was added by a syringe to a stirring solution of PhFormH (0.588g; 3 mmol) in DME (20mL) using Schlenk line. After 1 hr stirring, the solution was concentrated to ~10 mL, and cooled overnight causing the formation of colourless crystals. Yield = 0.43 g (46.5%); M.P. 220-223 °C; IR (crystal oil): $\nu = 1847$ (vw), 1784 (vw), 1722 (vw), 1675 (vw), 1648 (m), 1586 (s), 1533

(vs), 1455 (vs), 1377 (vs), 1313 (vs), 1205 (s), 1169 (s), 1075 (s), 1023 (s), 985 (s), 922 (m), 892 (m), 839 (m), 802 (s), 762 (s), 722 (s), 693 (s), 618 (w) and 594 (m) cm^{-1} ; ^1H NMR (C_6D_6 , 303.2 K): δ = 1.53-1.81 (m, 4 H, DME- CH_2), 2.7-2.86 (m, 6 H, DME- CH_3), 6.65–6.98 (br m, 10H; Ar-H), 8.71 (s, 1 H, NC(H)N). Elemental analysis calcd. (%) for $\text{C}_{17}\text{H}_{21}\text{N}_2\text{NaO}_2$ (M = 308.35 g/mol): C 66.21, H 6.86, N 9.08; Found from microanalysis: C 55.21, H 6.38, N 9.91.

[$\text{Zn}_4(\text{PhForm})_6\text{O}$].THF (**4.5**)

ZnEt_2 (0.72 mL of a 15 W% solution in toluene; 0.8 mmol) was added by a syringe to a stirring solution of PhFormH (0.23 g; 1.2 mmol) in THF (20mL) using Schlenk line. After 1 hr stirring, the solution was concentrated to ~5 mL, and cooled for one week, causing the formation of colourless crystals of (**4.5**). Yield = 0.58 g (47.7%); M.P. 245-249 °C; IR (crystal oil): ν = 1852 (vw), 1789 (vw), 1723 (vw), 1667 (vw), 1596 (m), 1452 (vs), 1377 (vs), 1337 (vs), 1226 (vs), 1174 (s), 1154 (m), 1079 (s), 1024 (m), 998 (m), 974 (vs), 926 (s), 892 (s), 820 (s), 770 (s), 755 (vs), 695 (vs), 642 (s), 617 (w), cm^{-1} (w); ^1H NMR (C_6D_6 , 303.2 K): δ = 0.11 (s, 2 H, CH_2), 3.35 (s, 2 H, CH_2) (loss half of THF of solvation), 6.65–6.98 (br m, 60H; Ar-H), 8.71 (s, 6 H, NC(H)N). Elemental analysis calcd. (%) for $\text{C}_{82}\text{H}_{74}\text{N}_{12}\text{O}_2\text{Zn}_4$ (M = 1521.01 g/mol): C 64.39, H 4.99, N 11.55; Found from microanalysis: C 64.45, H 4.76, N 11.30.

[Al(PhForm) $_3$] (**4.6**)

A solution of AlMe_3 (1 mL of a 2.0 M solution in toluene; 2 mmol) was added dropwise to a solution of PhFormH ligand (1.17g, 6 mmol) in 20 mL THF under vigorous stirring and flow of nitrogen gas. The clear solution was stirred for 1 hr at ambient temperature. The solution was evaporated to ~10 mL using Schlenk line and cooled slowly. Colourless crystals of the product formed after 2 days. Yield = 0.24 g (39.2%); M.P. 231-235 °C; IR (Nujol oil): ν = 1540 (m), 1463 (vs), 1377 (s), 1286 (m), 1263 (s), 1099 (m), 1024 (w), 974 (vw), 896 (vw), 803 (vw), 761 (w), 721 (vw) and 697 (w) cm^{-1} ; ^1H NMR (C_6D_6 , 303.2 K): δ = 6.97–7.03 (br m, 30H; Ar-H), 8.45 (s, 3 H, NC(H)N). Elemental analysis calcd. (%) for $\text{C}_{39}\text{H}_{33}\text{AlN}_6$ (M = 612.69 g/mol): C 76.45, H 5.42, N 13.71; Found from microanalysis: C 73.59, H 6.06, N 12.79.

X-Ray crystallography

[K(DMForm)(dme)]_∞ (4.1)

C₂₁H₂₉KN₂O₂ (*M* = 380.56 g/mol): triclinic, space group P-1 (no. 2), *a* = 8.8050(18) Å, *b* = 11.029(2) Å, *c* = 12.239(2) Å, α = 66.50(3)°, β = 85.81(3)°, γ = 76.15(3)°, *V* = 1057.9(4) Å³, *Z* = 2, *T* = 173.15 K, μ (MoK α) = 0.267 mm⁻¹, *D*_{calc} = 1.195 g/cm³, 13005 reflections measured (4.766° ≤ 2 θ ≤ 52.732°), 3854 unique (*R*_{int} = 0.0195, *R*_{sigma} = 0.0178) which were used in all calculations. The final *R*₁ was 0.0332 (*I* > 2 σ (*I*)) and *wR*₂ was 0.0829 (all data).

[K₂(PhForm)N(SiMe₃)₂]_∞ (4.2)

C₁₉H₂₉K₂N₃Si₂ (*M* = 433.83 g/mol): triclinic, space group P-1 (no. 2), *a* = 9.6830(19) Å, *b* = 10.887(2) Å, *c* = 12.246(2) Å, α = 99.72(3)°, β = 104.84(3)°, γ = 103.36(3)°, *V* = 1177.9(5) Å³, *Z* = 2, *T* = 293(2) K, μ (MoK α) = 0.512 mm⁻¹, *D*_{calc} = 1.223 g/cm³, 12890 reflections measured (4.828° ≤ 2 θ ≤ 63.918°), 5670 unique (*R*_{int} = 0.0461, *R*_{sigma} = 0.0590) which were used in all calculations. The final *R*₁ was 0.0823 (*I* > 2 σ (*I*)) and *wR*₂ was 0.2374 (all data).

[Na(DMForm)(dme)₂] (4.3)

C₂₅H₃₉N₂NaO₄ (*M* = 223.27 g/mol): monoclinic, space group C2/c (no. 15), *a* = 27.319(6) Å, *b* = 13.891(3) Å, *c* = 15.603(3) Å, β = 117.11(3)°, *V* = 5271(2) Å³, *Z* = 8, *T* = 293(2) K, μ (MoK α) = 0.106 mm⁻¹, *D*_{calc} = 1.125 g/cm³, 47438 reflections measured (3.35° ≤ 2 θ ≤ 63.71°), 7429 unique (*R*_{int} = 0.0293, *R*_{sigma} = 0.0165) which were used in all calculations. The final *R*₁ was 0.0489 (*I* > 2 σ (*I*)) and *wR*₂ was 0.1374 (all data).

[Na(PhForm)(dme)]₂ (4.4)

C₁₇H₂₁N₂NaO₂ (*M* = 308.35 g/mol): monoclinic, space group P2₁/n (no. 14), *a* = 12.1748(8) Å, *b* = 8.0390(5) Å, *c* = 18.0539(11) Å, β = 102.960(3)°, *V* = 1721.98(19) Å³, *Z* = 4, *T* = 296.15 K, μ (MoK α) = 0.100 mm⁻¹, *D*_{calc} = 1.189 g/cm³, 11220 reflections measured (3.684° ≤ 2 θ ≤ 49.99°), 2782 unique (*R*_{int} = 0.0391, *R*_{sigma} = 0.0502) which were used in all calculations. The final *R*₁ was 0.0480 (*I* > 2 σ (*I*)) and *wR*₂ was 0.1274 (all data).

[Zn₄(PhForm)₆O].THF (4.5)

C₈₂H₇₄N₁₂O₂Zn₄ (*M* = 1521.01 g/mol): triclinic, space group P-1 (no. 2), *a* = 14.673(3) Å, *b* = 15.918(3) Å, *c* = 19.353(4) Å, α = 91.90(3)°, β = 102.06(3)°, γ = 101.16(3)°, *V* = 4324.0(16) Å³, *Z* = 2, *T* = 173.15 K, $\mu(\text{MoK}\alpha)$ = 1.144 mm⁻¹, *D*_{calc} = 1.168 g/cm³, 54130 reflections measured (2.158° ≤ 2 θ ≤ 52.744°), 16121 unique (*R*_{int} = 0.0413, *R*_{sigma} = 0.0356) which were used in all calculations. The final *R*₁ was 0.0772 (*I* > 2 σ (*I*)) and *wR*₂ was 0.2595 (all data).

[Al(PhForm)₃] (4.6)

C₃₉H₃₃AlN₆ (*M* = 612.69 g/mol): orthorhombic, space group Pccn (no. 56), *a* = 18.333(4) Å, *b* = 10.794(2) Å, *c* = 16.061(3) Å, *V* = 3178.3(11) Å³, *Z* = 4, *T* = 100.15 K, $\mu(\text{MoK}\alpha)$ = 0.103 mm⁻¹, *D*_{calc} = 1.280 g/cm³, 28588 reflections measured (5.06° ≤ 2 θ ≤ 63.8°), 4529 unique (*R*_{int} = 0.0680, *R*_{sigma} = 0.0371) which were used in all calculations. The final *R*₁ was 0.0483 (*I* > 2 σ (*I*)) and *wR*₂ was 0.1324 (all data).

4.5 References

1. M. Majewski and D. M. Gleave, *J. Organomet. Chem.*, 1994, **470**, 1-16.
2. B. J. Wakefield, *Organolithium methods*, Academic Pr., 1988.
3. A. M. Sapse and P. v. R. Schleyer, *Lithium chemistry: a theoretical and experimental overview*, John Wiley & Sons, 1995.
4. D. M. Grove, G. van Koten, H. J. Ubbels, K. Vrieze, L. C. Niemann and C. H. Stam, *J. Chem. Soc., Dalton Trans.*, 1986, 717-724.
5. J. Barker, M. Kilner and R. O. Gould, *J. Chem. Soc., Dalton Trans.*, 1987, 2687-2694.
6. M. G. Drew and J. D. Wilkins, *J. Organomet. Chem.*, 1974, **69**, 271-278.
7. A. R. Sadique, M. J. Heeg and C. H. Winter, *Inorg. Chem.*, 2001, **40**, 6349-6355.
8. D. Abeysekera, K. N. Robertson, T. S. Cameron and J. A. Clyburne, *Organometallics*, 2001, **20**, 5532-5536.
9. J. A. Schmidt and J. Arnold, *Organometallics*, 2002, **21**, 2306-2313.
10. S. R. Foley, Y. Zhou, G. P. Yap and D. S. Richeson, *Inorg. Chem.*, 2000, **39**, 924-929.
11. P. C. Junk and M. L. Cole, *Chem. Commun.*, 2007, 1579-1590.
12. M. L. Cole, P. C. Junk and L. M. Louis, *J. Chem. Soc., Dalton Trans.*, 2002, 3906-3914.
13. F. A. Cotton, L. M. Daniels and C. A. Murillo, *Inorg. Chem.*, 1993, **32**, 2881-2885.
14. F. A. Cotton, L. M. Daniels, L. R. Falvello and C. A. Murillo, *Inorg. Chim. Acta*, 1994, **219**, 7-10.
15. F. A. Cotton, L. M. Daniels, D. J. Maloney and C. A. Murillo, *Inorg. Chim. Acta*, 1996, **249**, 9-11.
16. F. A. Cotton, L. Daniels, L. Falvello, J. Matonic, C. Murillo, X. Wang and H. Zhou, *Inorg. Chim. Acta*, 1997, **266**, 91-102.
17. F. A. Cotton, L. M. Daniels and C. A. Murillo, *Angew. Chem. Int. Ed.*, 1992, **31**, 737-738.
18. T. Ren, *Coord. Chem. Rev.*, 1998, **175**, 43-58.
19. J. Barker and M. Kilner, *Coord. Chem. Rev.*, 1994, **133**, 219-300.
20. F. A. Cotton, S. C. Haefner, J. H. Matonic, X. Wang and C. A. Murillo, *Polyhedron*, 1997, **16**, 541-550.
21. R. Shannon, *Acta Crystallogr. A*, 1976, **32**, 751-767.
22. C. M. Haar, C. L. Stern and T. J. Marks, *Organometallics*, 1996, **15**, 1765-1784.

23. J. Baldamus, C. Berghof, M. L. Cole, D. J. Evans, E. Hey-Hawkins and P. C. Junk, *J. Chem. Soc., Dalton Trans.*, 2002, 4185-4192.
24. M. P. Coles and R. F. Jordan, *J. Am. Chem. Soc.*, 1997, **119**, 8125-8126.
25. M. P. Coles, D. C. Swenson, R. F. Jordan and V. G. Young, *Organometallics*, 1997, **16**, 5183-5194.
26. S. Dagorne, I. A. Guzei, M. P. Coles and R. F. Jordan, *J. Am. Chem. Soc.*, 2000, **122**, 274-289.
27. D. Kissounko, M. Zabalov, G. Brusova and D. A. Lemenovskii, *Russ. Chem. Rev.*, 2006, **75**, 351.
28. G. Talarico and P. H. Budzelaar, *Organometallics*, 2000, **19**, 5691-5695.
29. J. Grundy, M. P. Coles and P. B. Hitchcock, *J. Organomet. Chem.*, 2002, **662**, 178-187.
30. F. T. Edelmann, *Chem. Soc. Rev.*, 2012, **41**, 7657-7672.
31. C.-C. Chang, J.-H. Chen, B. Srinivas, M. Y. Chiang, G.-H. Lee and S.-M. Peng, *Organometallics*, 1997, **16**, 4980-4984.
32. C. Jones, P. C. Junk, M. Kloth, K. M. Proctor and A. Stasch, *Polyhedron*, 2006, **25**, 1592-1600.
33. L. A. Lesikar and A. F. Richards, *Polyhedron*, 2010, **29**, 1411-1422.
34. M. L. Cole, A. J. Davies, C. Jones, P. C. Junk, A. I. McKay and A. Stasch, *Z. Anorg. Allg. Chem.*, 2015, **641**, 2233-2244.
35. S. Hamidi, H. M. Dietrich, D. Werner, L. N. Jende, C. Maichle-Mössmer, K. W. Törnroos, G. B. Deacon, P. C. Junk and R. Anwander, *Eur. J. Inorg. Chem.*, 2013, **2013**, 2460-2466.
36. H. Gilman, E. Zoellner and W. Selby, *J. Am. Chem. Soc.*, 1933, **55**, 1252-1257.
37. D. Bryce-Smith and E. Turner, *J. Chem. Soc.*, 1953, 861-867.
38. H. Gilman and J. Morton Jr, *Org. React.*, 1954, **8**, 258-304.
39. R. G. Jones and H. Gilman, *Org. React.*, 1951.
40. D. Peterson, *Organometal. Chem. Rev. A*, 1972, **7**, 295.
41. C. G. Screttas and B. R. Steele, *J. Organomet. Chem.*, 1993, **453**, 163-170.
42. A. Hart, *J. Organomet. Chem.*, 1974, **72**, C19.
43. W. E. Parham, L. D. Jones and Y. A. Sayed, *J. Org. Chem.*, 1976, **41**, 1184-1186.
44. W. Trepka and R. Sonnenfeld, *J. Organomet. Chem.*, 1969, **16**, 317-320.
45. F. H. Allen, *Acta Crystallogr. B*, 2002, **58**, 380-388.
46. M. L. Cole, D. J. Evans, P. C. Junk and M. K. Smith, *Chem. Eur. J.*, 2003, **9**, 415-424.

47. M. L. Cole and P. C. Junk, *J. Organomet. Chem.*, 2003, **666**, 55-62.
48. J. Baldamus, C. Berghof, M. L. Cole, D. J. Evans, E. Hey-Hawkins and P. C. Junk, *J. Chem. Soc., Dalton Trans.*, 2002, 2802-2804.
49. M. L. Cole, G. B. Deacon, C. M. Forsyth, P. C. Junk, D. Polo-Cerón and J. Wang, *Dalton Trans.*, 2010, **39**, 6732-6738.
50. M. L. Cole, A. J. Davies, C. Jones and P. C. Junk, *J. Organomet. Chem.*, 2004, **689**, 3093-3107.
51. M. L. Cole, D. J. Evans, P. C. Junk and L. M. Louis, *New. J. Chem.*, 2002, **26**, 1015-1024.
52. M. L. Cole, G. B. Deacon, C. M. Forsyth, K. Konstas and P. C. Junk, *Dalton Trans.*, 2006, 3360-3367.
53. R. M. Roberts, *J. Org. Chem.*, 1949, **14**, 277-284.

Chapter 5

Concluding remarks

5 Concluding remarks

5.1 Concluding remarks

Investigation of the synthesis of novel rare earth bis(aryl)formamidinate complexes and Na, K, Zn and Al formamidinate complexes has yielded 28 new formamidinate compounds. The aim of this thesis was to isolate rare earth bis(aryl)formamidinate of low to moderate steric bulk using the RTP reaction and study the reactivity of the compounds towards the Tishchenko reaction. $[\text{La}(o\text{-TolForm})_3(\text{thf})_2]^1$ has been reported as the best catalyst towards the Tishchenko reaction. One of the aims in this study was to find a replacement for this compound as *ortho*-toluidine, the precursor for synthesizing *o*-TolFormH, is a restricted carcinogenic compound.^{2,3} The idea was to reduce the steric effect of the final compounds by using smaller forms of the bis(aryl)formamidinate ligands to make the metal center more accessible for the incoming substrate so the reactivity of the final compound should be increased. PhFormH is one of the formamidinate ligands that was used in this research as the smallest bis(aryl)formamidinate ligand.

Chapter two presents the results of studying the structure and reactivity of lanthanoid compounds involving PhFormH ligand. As the results of RTP reactions between Ln = Tb (**2.1**), Ho (**2.2**) and Er (**2.3**), compounds with general formula of $[\text{Ln}(\text{PhForm})_3(\text{thf})]$ were synthesized. Using other lanthanoids, Ln=La (**2.4**), Y (**2.5**), Pr (**2.6**), Nd (**2.7**), Sm (**2.8**), Gd (**2.9**), Dy (**2.10**) and Lu (**2.11**), a series of lanthanoid (III) complexes with general formula of $[\text{Ln}(\text{PhForm})_3(\text{thf})_2](\text{THF})_m$ were synthesized. These compounds have three bidentate formamidinates and two coordinated *transoid*-thf molecules in the coordinate sphere of the metal which give the coordination number of eight to the metal centers. The average Ln-N distance of these compounds reduces moving from La to Lu and follows the same trend as the ionic radii of the metal centers as expected for the lanthanoid contraction. Compounds (**2.1**), (**2.2**) and (**2.3**) did not have the same trend for the average Ln-N distance which can be attributed to the lack of one coordinated thf molecule in the structure. A greater coordination number of the Lu complex (**2.11**) compared with (**2.1**), (**2.2**) and (**2.3**) was one of the unusual features that was observed in this research. The standard reaction of converting benzaldehyde to benzyl benzoate was chosen to evaluate the catalytic activity of the compounds. This study revealed that these compounds have good catalytic properties and

can be used for the Tishchenko reaction however they are not as reactive as previously reported for $[\text{La}(o\text{-TolForm})_3(\text{thf})_2]$.¹ Among all of the compounds in chapter two, $[\text{Y}(\text{PhForm})_3(\text{thf})_2](\text{THF})_3$ (**2.5**) showed the highest reactivity and can be considered as a replacement for $[\text{La}(o\text{-TolForm})_3(\text{thf})_2]$.

It is not clear that two extra methyl groups in the *ortho* position of *o*-TolFormH ligand have any effect on the reactivity of the final compound. Another low bulk formamidine ligand with two methyl groups in *ortho* positions, DMFormH, was used to study the reactivity of the synthesized compounds and the results are presented in chapter three. DMFormH has two extra methyl groups in *para* positions which makes this ligand slightly bulkier than *o*-TolFormH however these methyl groups are away from the center of the ligand and expected to have almost no effect on the reaction but should increase solubility in organic solvents. It was found that DMFormH is a suitable ligand to synthesize organo-lanthanoid compounds and it can bind rare-earth elements very well. New lanthanoid (III) compounds of $[\text{Y}(\text{DMForm})_3(\text{thf})]$ (**3.1**), $[\text{Lu}(\text{DMForm})_3(\text{thf})]$ (**3.2**), $[\text{Pr}(\text{DMForm})_3(\text{DMFormH})]$ (**3.3**), $[\text{Ho}(\text{DMForm})_3(\text{DMFormH})]$ (**3.4**), $[\text{Sm}(\text{DMForm})_3(\text{dme})]$ (**3.5**), $[\text{Gd}(\text{DMForm})_3(\text{dme})]$ (**3.6**) and $[\text{Er}(\text{DMForm})_3(\text{dmf})]$ (**3.7**) were synthesized by RTP reactions using DMFormH in various solvents of THF, DME and DMF. The study of reactivities showed $[\text{Y}(\text{DMForm})_3(\text{thf})]$ (**3.1**) has the highest reactivity towards the Tishchenko reaction compared with other bis(aryl)formamidinate compounds synthesized in this research. Considering all the compounds in this research, compounds with Y as the metal center showed higher reactivity than the analogous compounds. The reason is not clear yet, however it seems two methyl groups in *ortho* positions can influence the reactivity of the Y compounds.

It has been reported that ionic radii of the metal center plays an important role in controlling the rate of catalytic conversion of aldehydes.⁴ One of the aims was to compare the reactivity of compounds with the same metal centers and the same ionic radii. Unfortunately, attempts to synthesize pure La compounds using PhFormH or DMFormH ligands to compare the reactivities with $[\text{La}(o\text{-TolForm})_3(\text{thf})_2]$ compound failed mainly due to isolating the very soluble compounds. Comparing the reactivities of compounds involving PhForm (chapter two) with those involving DMForm (chapter three), confirms the notion that RE-bis(aryl)formamidinate complexes with lower steric effect have higher reactivities towards the Tishchenko reaction. As a conclusion, to produce an effective catalyst, ionic radius of the

metal center and steric hindrance of the compound are two important factors that should be considered in tandem.

Chapter four of this thesis presents a structural study of compounds involving PhFormH and DMFormH and some of the main group metals as a small contribution to the main group chemistry involving formamidinates. Chapter four presents several compounds that can be used in catalysis (Zn, Al) or in metathesis chemistry (K, Na). $[\text{K}(\text{DMForm})(\text{dme})]_{\infty}$ (**4.1**), $[\text{K}_2(\text{PhForm})(\text{SiMe}_3)_2]_{\infty}$ (**4.2**), $[\text{Na}(\text{DMForm})(\text{dme})_2]$ (**4.3**), $[\text{Na}(\text{PhForm})(\text{dme})_2]$ (**4.4**), $[\text{Zn}_4(\text{PhForm})_6\text{O}]\cdot\text{THF}$ (**4.5**), and $[\text{Al}(\text{PhForm})_3]$ (**4.6**) are the compounds were synthesized using metallation method.⁵⁻⁷ It was found that DMFormH and PhFormH can form polymeric potassium-formamidinate compounds ((**4.1**) and (**4.2**)). It should be noted that $[\text{K}(\text{DMForm})(\text{dme})]_{\infty}$ (**4.1**) is the first six coordinated potassium bis(aryl)formamidinate crystallographically characterized.⁸ The study shows the reducing the steric effect of the formamidinate can change the bonding mode or structure. In the case of K, it led to a different bonding mode of η^6 in (**4.2**) compared with (**4.1**). In the case of using Na, the structure changed from $[\text{Na}(\text{DMForm})(\text{dme})_2]$ (**4.3**) to $[\text{Na}(\text{PhForm})(\text{dme})_2]$ (**4.4**) which has a different bonding mode of $\mu\text{-}\eta^2\text{:}\eta^1$.

Treating ZnEt_2 with PhFormH gave $[\text{Zn}_4(\text{PhForm})_6\text{O}]\cdot\text{THF}$ (**4.5**) which has an oxide cage structure same as the perviously reported $[\text{Zn}_4(p\text{-TolForm})_6\text{O}]$ compound.⁹ The source of oxygen in the structure is not clear yet but has been attributed to ring opening of thf. $[\text{Al}(\text{PhForm})_3]$ (**4.6**) is the result of treating AlMe_3 with PhFormH. It was found that using different stoichiometries of 1:1, 1:2 and 1:3 has no effect on the reaction and all the stoichiometries give the same compound of $[\text{Al}(\text{PhForm})_3]$ (**4.6**).

Overall this thesis presents a significant contribution to rare earth bis(aryl)formamidinate chemistry and studies bis(aryl)formamidinate compounds involving some of the main group metals.

5.2 References

1. A. Zuyls, P. W. Roesky, G. B. Deacon, K. Konstas and P. C. Junk, *Eur. J. Org. Chem.*, 2008, **4**, 693-697.
2. C. Watanabe, T. Egami, K. Midorikawa, Y. Hiraku, S. Oikawa, S. Kawanishi and M. Murata, *Environ. Health Prev. Med.*, 2010, **15**, 319.
3. Y. Ohkuma, Y. Hiraku, S. Oikawa, N. Yamashita, M. Murata and S. Kawanishi, *Arch. Biochem. Biophys.*, 1999, **372**, 97-106.
4. H. Berberich and P. W. Roesky, *Angew. Chem. Int. Ed.*, 1998, **37**, 1569-1571.
5. H. Gilman and J. Morton Jr, *Org. React.*, 1954, **8**, 258-304.
6. R. G. Jones and H. Gilman, *Org. React.*, 1951.
7. D. Peterson, *Organometal. Chem. Rev. A*, 1972, **7**, 295.
8. F. H. Allen, *Acta Crystallogr. B*, 2002, **58**, 380-388.
9. M. L. Cole, D. J. Evans, P. C. Junk and L. M. Louis, *New. J. Chem.*, 2002, **26**, 1015-1024.

Publications



Review

Rare-earth N,N'-diarylformamidinate complexes

Glen B. Deacon^a, Md Elius Hossain^b, Peter C. Junk^{b,*}, Mehdi Salehisaki^b^aSchool of Chemistry, Monash University, Clayton, Victoria 3800, Australia^bCollege of Science & Engineering, James Cook University, Townsville, Queensland 4811, Australia

ARTICLE INFO

Article history:

Received 17 January 2017

Received in revised form 10 February 2017

Accepted 11 February 2017

Available online 15 February 2017

Keywords:

Lanthanoids

Lanthanoid(II)

Lanthanoid(III)

Lanthanoid(IV)

Formamidinates

ABSTRACT

This comprehensive review covers the progress of rare earth chemistry with formamidinate ligands to date. The ligands involved offer varying steric and electronic effects and focus on the N,N'-bis(aryl)formamidinates. Synthetic pathways to divalent, trivalent and tetravalent complexes, their structural aspects, reactivity and potential applications in catalysis are extensively discussed.

© 2017 Elsevier B.V. All rights reserved.

Contents

1. Introduction	247
2. Formamidinatanlanthanoid complexes	249
2.1. Synthesis	249
2.2. Divalent compounds	251
2.3. Trivalent compounds	252
2.4. Tetravalent compound(s) [34]	264
2.4.1. Synthesis of trivalent complexes that are potential precursor of tetravalent complexes	264
2.4.2. Protolysis of Ce(IV) amides to give Ce(IV) formamidinates	264
3. Catalysis	264
4. Conclusions and outlook	264
Acknowledgements	265
References	265

1. Introduction

Amidinate ligands ($[R^1NCR^2NR^3]^-$) (Fig. 1-1, $R^4 = H$, deprotonated) are anionic ligands which can be modified sterically and electronically to form stable and structurally interesting complexes with metals [1]. Fig. 1-1 shows the general structure of an amidine. Amidines are named based on the acid or amide obtained after hydrolysis [2]. Amidinate complexes have versatile applications in chemical and material sciences [3–6], including as precursors

for atomic layer deposition of rare-earth oxide films [3,4,7] and polymerisation of olefins [5,8]. In the case of $R^2 = H$, the compound is called a formamidine. N,N'-Diarylformamidinate ligands have advantages over amidinate and guanidinate ligands of greater simplicity. This impacts in ease of synthesis whereby formamidines, the proligands are readily prepared and can be easily modulated to vary steric and electronic effects. These can be as varied as anilines available as reactants. The corresponding formamidines open up a wide range of syntheses owing to the acidic N–H. By contrast amidinate and guanidinate ligands are harder to access, and although they have in the C–R and C–NR₂ moieties the opportunity for additional steric and electronic

* Corresponding author.

E-mail address: peter.junk@jcu.edu.au (P.C. Junk).

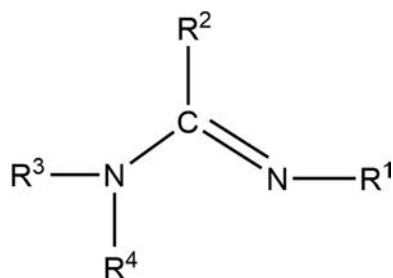
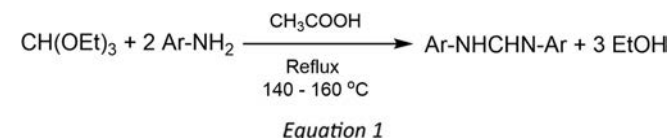


Fig. 1-1. The general structure of an amidine.

modulation, it also brings complexity in distinguishing these effects from those of the N-R groups. The N,N'-diarylformamidinates ((ArN)₂CH⁻, (ArForm⁻)), gives them a special place amongst the amidinate ligands with a wide variety of applications. For example, lanthanoid formamidinates are excellent reagents in catalysing the Tishchenko reaction [9].



There has been a lot of interest in developing N,N'-bis(aryl)formamidinates as ligands [13]. One important use is to kinetically

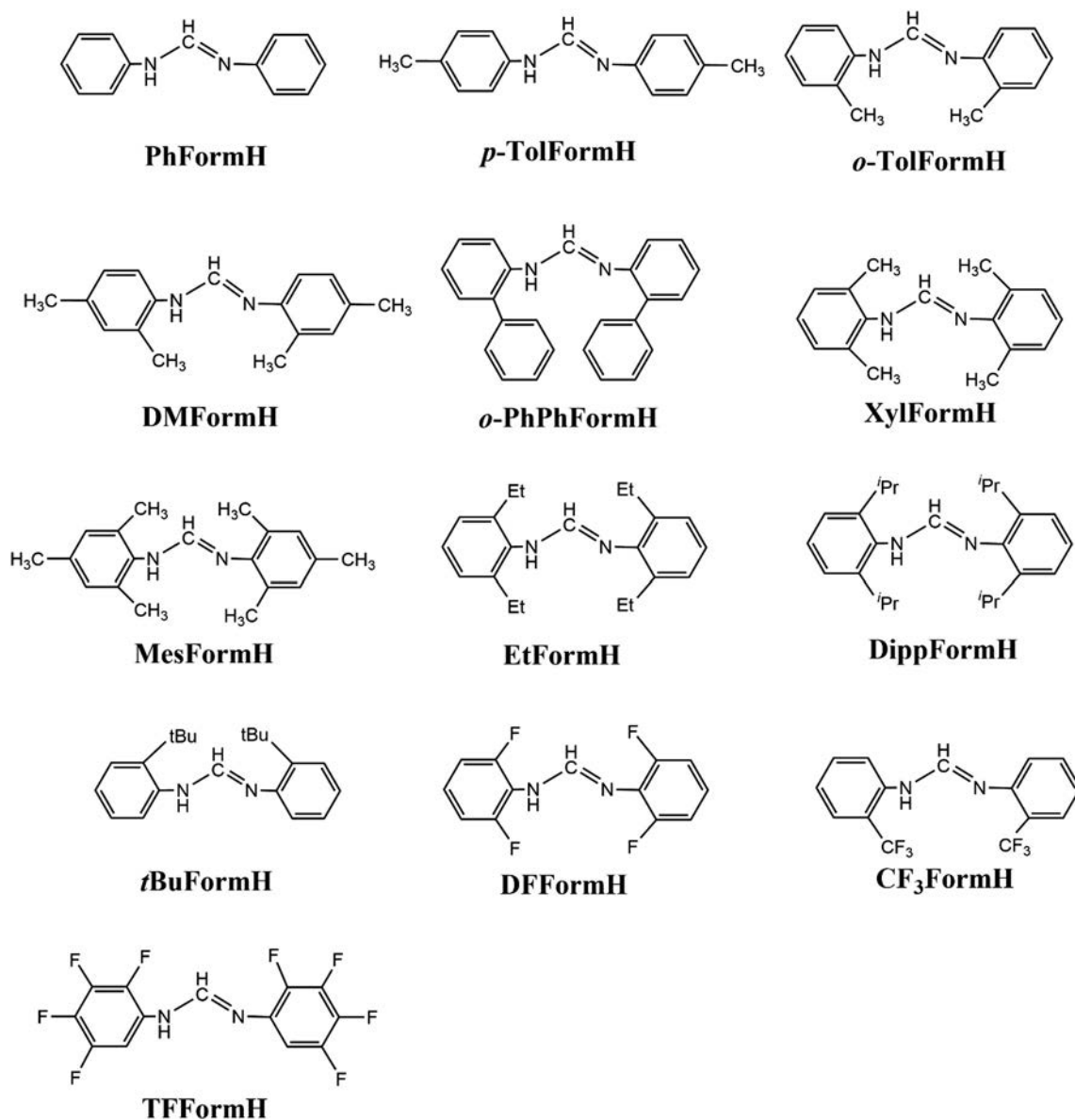


Fig. 1-2. Different Formamidine pro-Ligands.

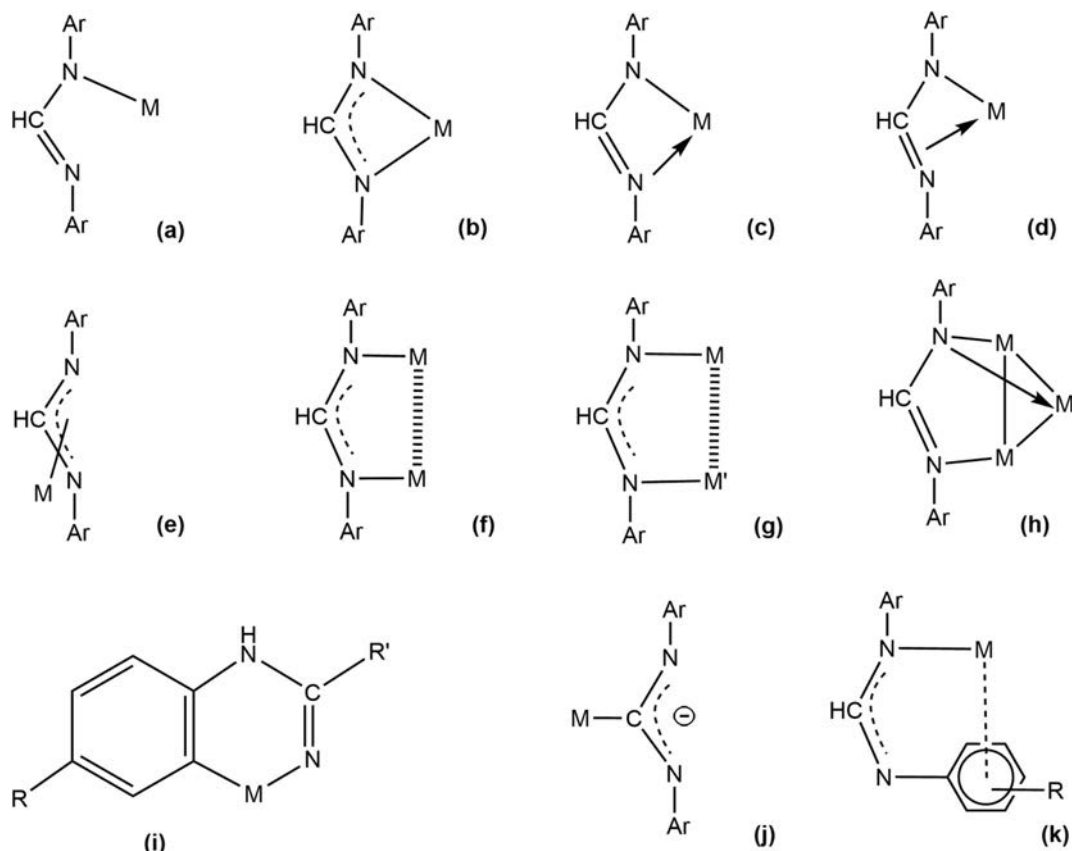


Fig. 1-3. Possible binding modes for N,N'-bis(aryl)formamidinate ligands.

stabilise group 13 hydride complexes by application of bulky ligands [13]. It has also been possible to sterically engineer carbon-fluorine bond activation [14]. Furthermore, they can act as anionic ligand supports for low valent compounds. These ligands bind rare earth metals well with the benefit of variations of the steric bulk and electronic functionality at the N donor atoms [15]. Moreover, rare-earth amidinate complexes have great versatility in material and chemical applications, for example, precursors that are used for atomic layer deposition of rare-earth oxide films [7] or polymerisation of olefins [3]. Fig. 1-2 shows some important types of formamidinate proligands. By using different derivatives of aniline as the precursor, various formamidinate ligands with different steric properties can be prepared. Therefore, different metal-organic compounds with different coordination number can be synthesized by using different formamidines. This can aid in inducing variations in reactivity.

Bis(aryl)formamidinate ligands can display various potential binding modes to metal centers (Fig. 1-3). Infrared and NMR spectroscopy can be used for studying the coordination of metal bis(aryl)formamidinate complexes. However, when more than one binding mode is present and/or the complex exhibits fluxional coordination in solution, the use of these methods is complicated significantly, meaning X-ray crystallography is important in determining the unambiguous structures of these complexes (in the solid state) [13]. Fig. 1-3 illustrates many of the possible bonding modes for the N,N'-bis(aryl)formamidinate ligands including monodentate (a), chelate (b-d), η^3 -allyl (e), bridging (f, g), capping (h), *ortho*-metallation (i), C-bonded (j), and η^6 bonding (k) [2]. Of these bonding modes, symmetric chelation (b) is the most commonly found in RE formamidinate chemistry.

2. Formamidinatolanthanoid complexes

This section presents examples of use of various formamidines to prepare formamidinatolanthanoid complexes.

2.1. Synthesis

Reactive rare earth complexes (organometallics, organoamides including formamidines and organo-oxides) can be synthesized by several reactions. Metathesis (salt elimination), protolysis, redox transmetalation and redox transmetalation/protolysis are the common synthetic routes to prepare rare earth metal-organic compounds.

Metathesis reactions, according to Eq. (2), involve the treatment of a rare earth halide with an alkali metal complex of the ligand [16–18].



M = alkali metal

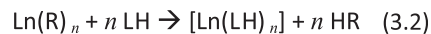
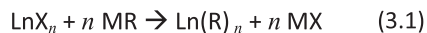
X = halide

Equation 2

In metathesis reactions the choice of lanthanoid halide and alkali metal salt as starting materials is important. For example, in many cases the use of lanthanide trichlorides and lithium salts results in either low yields or unwanted side-products where the

alkali metal is retained forming an 'ate' species, or the alkali metal halide is bound to the lanthanoid complex [18].

Protolysis reactions include treatment of a lanthanoid precursor (LnR_n) with an LH proligand (Eq. (3)).



R = usually $\text{N}(\text{SiMe}_3)_2$, $\text{N}(\text{SiHMe}_2)_2$ or C_6F_5
 $n = 2, 3$
 X = halide

Equation 3

Due to the high solubility of the reactants in common solvents, reaction 3.2 can be performed in the absence of coordinating/donor

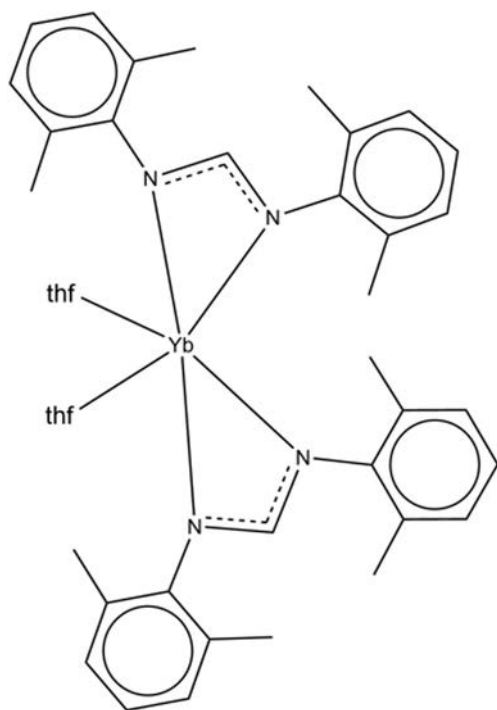


Fig. 2-1. Schematic of the X-ray structure of $[\text{Yb}(\text{XylForm})_2(\text{thf})_2]$ (**1**).

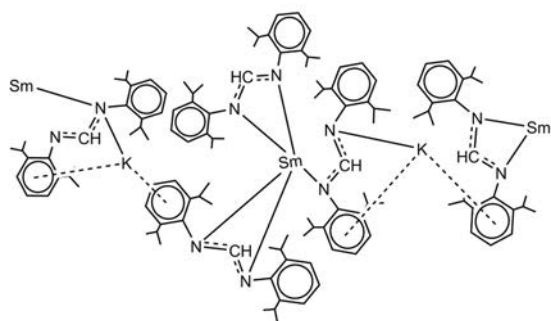


Fig. 2-2. Schematic and the X-ray structure of $[\text{KSm}(\text{DippForm})_3]$ (**10**).

solvents [16]. Thus, this route is a highly versatile approach for the synthesis of homoleptic lanthanoid complexes. Heteroleptic lanthanoid complexes can be synthesized using coordinating/donor solvents [6,19,20]. Protolysis reactions often involve two steps

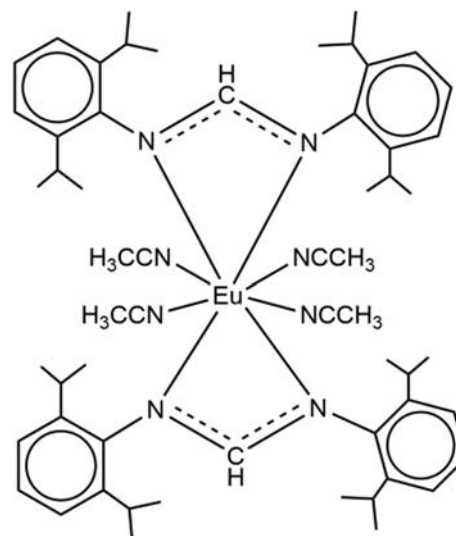


Fig. 2-3. Schematic of the X-ray structure of $[\text{Eu}(\text{DippForm})_2(\text{CH}_3\text{CN})_4]$ (**14**).

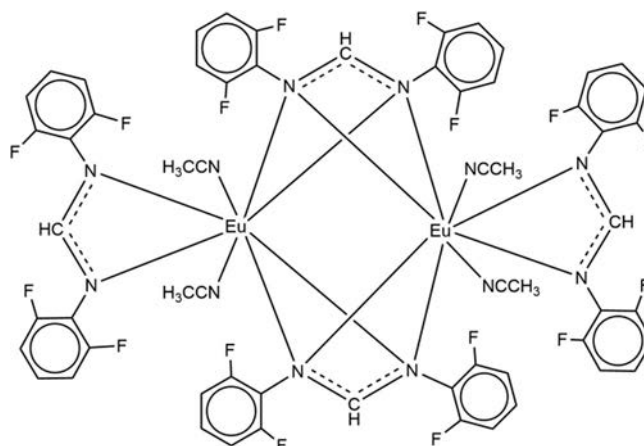
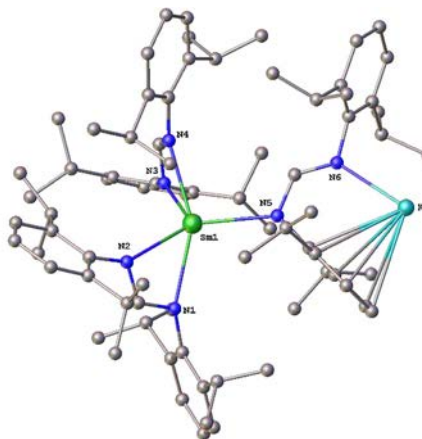


Fig. 2-4. Schematic of the X-ray structure of $[\{\text{Eu}(\text{DFForm})_2(\text{CH}_3\text{CN})_2\}_2]$ (**15**).



which is the main drawback of this method. Each step involves air and/or moisture sensitive compounds, and step 3.1 has the usual potential problems of metathesis reactions.

Redox transmetallation/protolysis (RTP) is another type of reaction for synthesizing rare earth metal-organic compounds. RTP involves the reaction of a rare earth metal with a diarylmercurial such as diphenylmercury [21] or bis(pentafluorophenyl)mercury [14,21–24] and a protic ligand (Eq. (4)).

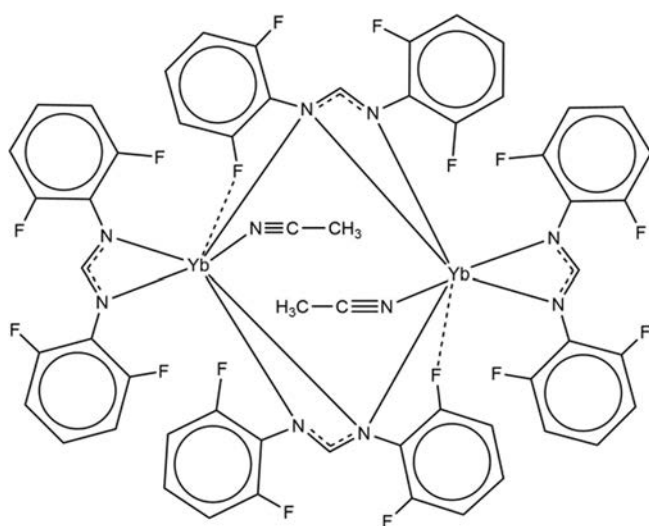
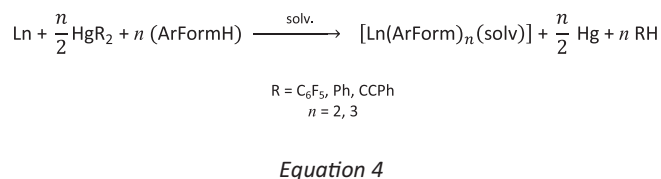


Fig. 2-5. Schematic of the X-ray structure of $[\text{Yb}(\text{DFForm})_2(\text{CH}_3\text{CN})]_2$ (17).

This method is a one-pot procedure. Therefore, compared with metathesis and protolysis synthetic routes, it is more straightforward, particularly since the only air-sensitive material is the lanthanoid metal. The isolation procedure is also straightforward involving a simple filtration to remove excess Ln metal and Hg produced in the reaction. Donor solvents tetrahydrofuran (THF) or 1,2-dimethoxyethane (DME) are normally used in RTP reactions. Reactions in non-donor solvents e.g. toluene normally require more forcing conditions such as heating [25]. Besides using mercury reagents, two or three drops of mercury can be added to the reaction mixture to activate the surface of rare earth metal by formation of an amalgam. Involvement of mercury reagents is the main drawback of this type of reaction since it raises environmental concerns and requires care in handling. $\text{Hg}(\text{C}_6\text{F}_5)_2$ and $\text{Hg}(\text{CPh})_2$ are stronger oxidants compared with diphenylmercury. However, $\text{Hg}(\text{C}_6\text{F}_5)_2$ is more reactive than HgPh_2 and can yield rare $\text{Ln}(\text{Form})_2\text{F}$ complexes after C-F activation of the $\text{Ln}(\text{Form})_2\text{C}_6\text{F}_5$ intermediate species [24]. Performing RTP reactions using diphenylmercury often requires activation of the metal (HgCl_2 or I_2) and heating [21].

2.2. Divalent compounds

Different lanthanoid formamidinate complexes namely $[\text{Yb}(\text{XylForm})_2(\text{thf})_2]$ (1), $[\text{Yb}(\text{EtForm})_2(\text{thf})_2]$ (2), $[\text{Yb}(o\text{-PhPhForm})_2(\text{thf})_2]$ (3), $[\text{Yb}(\text{DippForm})_2(\text{thf})_2]$ (4), $[\text{Yb}(\text{TFForm})_2(\text{thf})_3]$ (5) (which is the result of crystallization of $[\text{Yb}(\text{TFForm})_2(\text{thf})_2]$ (6) from THF), $[\text{Eu}(\text{DippForm})_2(\text{thf})_2]$ (7), $[\text{Yb}(\text{MesForm})_2(\text{thf})_2]$ (8) and $[\text{Yb}(o\text{-TolForm})_2(\text{thf})_2]$ (9) have been prepared by RTP reactions between an excess of a lanthanoid metal, $\text{Hg}(\text{C}_6\text{F}_5)_2$ or HgPh_2 and the corresponding formamidinate ligand [26]. All the compounds are mononuclear. In the case of $[\text{Yb}(\text{TFForm})_2(\text{thf})_3]$ (5) the ytterbium atom is seven coordinate whereas the metal centers of other complexes are six coordinate. The resulting compounds also have chelating N, N'-Form ligands and *cis*-thf donors (Fig. 2-1). The variation in the O-Yb-O angles is an interesting feature which cannot be related to the bulkiness of the Form ligands. The smallest O-Yb-O angles are found in the structures of $[\text{Yb}(\text{DippForm})_2(\text{thf})_2]$ (4) and $[\text{Eu}(\text{DippForm})_2(\text{thf})_2]$ (7) ($75.49(10)^\circ$), and involve the bulkiest

Table 2.2.1
Divalent compounds.

Reaction	Compound/Product	Method	Refs.
$\text{Yb} + \text{XylFormH} + \text{Hg}(\text{C}_6\text{F}_5)_2$ in THF	$[\text{Yb}(\text{XylForm})_2(\text{thf})_2]$ (1)	RTP	[26]
$\text{Yb} + \text{EtFormH} + \text{Hg}(\text{C}_6\text{F}_5)_2$ in THF	$[\text{Yb}(\text{EtForm})_2(\text{thf})_2]$ (2)	RTP	[26]
$\text{Yb} + \text{Ph}_2\text{Hg} + \text{PhPhFormH}$ in THF	$[\text{Yb}(o\text{-PhPhForm})_2(\text{thf})_2]$ (3)	RTP	[26]
$\text{Yb} + \text{DippFormH} + \text{Hg}(\text{C}_6\text{F}_5)_2$ in THF	$[\text{Yb}(\text{DippForm})_2(\text{thf})_2]$ (4)	RTP	[26]
Crystallisation of $[\text{Yb}(\text{TFForm})_2(\text{thf})_2]$ from THF	$[\text{Yb}(\text{TFForm})_2(\text{thf})_3]$ (5)	THF addition	[26]
$\text{Yb} + \text{TFFormH} + \text{Hg}(\text{C}_6\text{F}_5)_2$ in THF	$[\text{Yb}(\text{TFForm})_2(\text{thf})_2]$ (6)	RTP	[26]
$\text{Eu} + \text{DippFormH} + \text{Hg}(\text{C}_6\text{F}_5)_2$ in THF	$[\text{Eu}(\text{DippForm})_2(\text{thf})_2]$ (7)	RTP	[26]
$\text{Yb} + \text{MesFormH} + \text{Hg}(\text{C}_6\text{F}_5)_2$ in THF	$[\text{Yb}(\text{MesForm})_2(\text{thf})_2]$ (8)	RTP	[26]
$\text{Yb} + o\text{-TolFormH} + \text{Hg}(\text{C}_6\text{F}_5)_2$ in THF	$[\text{Yb}(o\text{-TolForm})_2(\text{thf})_2]$ (9)	RTP	[26]
$[\text{Sm}(\text{DippForm})_3] + \text{KC}_8$ in toluene	$[\text{KSm}(\text{DippForm})_3]$ (10)	Reduction	[27]
DippFormNa and $[\text{Sm}(\text{THF})_2]$ in THF or $\text{Sm} + \text{DippFormH} + \text{Hg}(\text{C}_6\text{F}_5)_2$ in THF	$[\text{Sm}(\text{DippForm})_2(\text{thf})_2]$ (11)	Metathesis/ Salt elimination or RTP	[28,29]
$[\text{Yb}(\text{DFForm})_2(\text{CH}_3\text{CN})_2]$ dissolved in PhMe and $[\text{Yb}(\text{DFForm})_2(\text{thf})_3]$ dissolved in PhMe, C ₆ D ₆ , ether	$[\text{Yb}(\text{DFForm})_2]$ (13)	Ligand dissociation	[30]
$\text{Eu} + \text{DippFormH}$ in CH ₃ CN	$[\text{Eu}(\text{DippForm})_2(\text{CH}_3\text{CN})_4]$ (14)	Direct metal synthesis	[30]
$\text{Eu} + \text{DFFormH}$ in CH ₃ CN	$[\text{Eu}(\text{DFForm})_2(\text{CH}_3\text{CN})_2]$ (15)	Direct metal synthesis	[30]
$\text{Yb} + \text{DFFormH} + \text{Hg}$ in CH ₃ CN	$[\text{Yb}(\text{DFForm})_2(\text{CH}_3\text{CN})_2]$ (17)	Direct metal synthesis	[30]
$\text{Yb} + \text{DFFormH} + \text{Hg}$ in mixture of thf and CH ₃ CN	$[\text{Yb}(\text{DFForm})_2(\text{thf})_3]$ (18)	Direct metal synthesis and RTP	[30]
$\text{Yb} + \text{Hg}(\text{Ph})_2 + \text{DippFormH}$ in thf	$[\text{Yb}(\text{DippForm})_2(\text{thf})]$ (20)	RTP and crystallised from thf/hexane	[30]
Dissolution of $[\text{Yb}(\text{DippForm})_2(\text{thf})]$ in CH ₃ CN	$[\text{Yb}(\text{DippForm})_2(\text{CH}_3\text{CN})_3]$ (21)	Solvent exchange	[30]
Crystallisation of $[\text{Yb}(\text{DippForm})_2(\text{CH}_3\text{CN})_3]$ from toluene or hexane	$[\text{Yb}(\text{DippForm})_2(\text{CH}_3\text{CN})_2]$ (22)	Dissociation of ligand	[30]
$\text{Yb} + \text{FFormH} + \text{Hg}(\text{C}_6\text{F}_5)_2$ in THF	$[\text{Yb}(\text{FForm})_2(\text{thf})_2]$ (23)	RTP	[31]
Compound (23) recrystallised from DME	$[\text{Yb}(\text{DFForm})_2(\text{dme})]$ (24)	Recrystallised from dme	[31]

DippForm ligand. Using the least bulky ligand, XylForm, in $[\text{Yb}(\text{XylForm})_2(\text{thf})_2]$ (**1**) gives the next smallest O–Yb–O angle ($78.13(9)^\circ$) and the largest O–Yb–O angle ($87.4(2)^\circ$) is observed in $[\text{Yb}(\text{EtForm})_2(\text{thf})_2]$ (**2**), which has the second bulkiest Form ligand.

The preparation of a new heterobimetallic samarium(II) formamidinate complex and selected reactions of samarium(II) complexes and one samarium(III) formamidinate complex with benzophenone or CS_2 were reported in 2014 [27]. The heterobimetallic formamidinate samarium(II)/potassium complex $[\text{KSm}(\text{DippForm})_3]$ (**10**) was synthesized by the reaction of $[\text{Sm}(\text{DippForm})_3]$ with potassium graphite in toluene at elevated temperature (Fig. 2-2). $[\text{KSm}(\text{DippForm})_3]$ (**10**) and $[\text{Sm}(\text{DippForm})_2(\text{thf})_2]$ (**11**) are the only known divalent formamidinate-samarium species so far reported [28]. In $[\text{KSm}(\text{DippForm})_3]$ (**10**) samarium is five coordinated by two chelating $\kappa(\text{N},\text{N}')$ formamidinate ligands and a one 1κ formamidinate ligand which also binds to potassium by an η^6 -2,6-diisopropylphenyl group and the other N atom.

Reaction of sodium metallated DippForm with $[\text{Sm}(\text{I})_2(\text{thf})_2]$ has been reported as one method to synthesize $[\text{Sm}(\text{DippForm})_2(\text{thf})_2]$ (**11**) compound [29]. During this reaction, another complex, the trivalent samarate $[\text{Na}(\text{thf})_5][\text{Sm}(\text{I})_2(\text{DippForm})_2(\text{thf})]$ (**12**) (see Table 2.3.1) was isolated as a minor co-product.

It has been reported that reaction of Eu and Yb metal with N,N'-bis(2,6-diisopropylphenyl)formamidine or N,N'-bis(2,6-difluorophenyl)formamidine in CH_3CN can be an effective and efficient method of preparing divalent rare earth formamidinate complexes without the need of an organomercurial co-oxidant as in RTP syntheses [31]. Thus, $[\{\text{Yb}(\text{DFForm})_2(\text{CH}_3\text{CN})\}_2]$ (**17**) (Fig. 2-5) (and some $[\text{Yb}(\text{DFForm})_2]$ (**13**) and $[\text{Eu}(\text{DippForm})_2(\text{CH}_3\text{CN})_4]$ (**14**) were synthesized from DFFormH and DippFormH respectively and as a result, the highest coordination number for divalent rare earth ArForm complexes was observed in the latter compound (Fig. 2-3). Using DFFormH as the ligand yields $[\{\text{Eu}(\text{DFForm})_2(\text{CH}_3\text{CN})_2\}_2]$ (**15**) (Fig. 2-4) which has an unusual bridging coordination mode μ -1 $\kappa(\text{N}:\text{N}')$:2 $\kappa(\text{N}:\text{N}')$. This coordination mode is the first for divalent lanthanoid formamidinates and was only recently reported for trivalent formamidinates [15]. This paper reports that using thf in place of CH_3CN with the formamidine ligands yields the trivalent hydroxy-bridged dimer $[\{\text{Eu}(\text{DFForm})_2\text{OH}(\text{thf})\}_2]$ (**16**) establishing the importance of using CH_3CN . Success for these two ligands of disparate acidities and bulk suggests that the method should be widely applicable for most formamidines. The same method is viable for preparing $[\text{Yb}(\text{DFForm})_2(\text{thf})_3]$ (**18**) from CH_3CN and $\text{CH}_3\text{CN}/\text{THF}$ respectively, but activation of Yb by Hg metal is required. Tetrametallic oxide species $[\{\text{Yb}_2(\text{DFForm})_4(\text{O})\}_2]$ (**19**) was synthesized by exposing $[\text{Yb}(\text{DFForm})_2(\text{thf})_3]$ (**18**) to trace amounts of O_2 . This report compares this synthetic method to the RTP reaction which yields $[\text{Yb}(\text{DFForm})_2(\text{thf})_3]$ (**18**) and the lowest coordination number for divalent rare earth ArForm complexes, $[\text{Yb}(\text{DippForm})_2(\text{thf})]$ (**20**), in the case of using Yb as the metal. $[\text{Yb}(\text{DippForm})_2(\text{CH}_3\text{CN})_3]$ (**21**) was crystallised from $[\text{Yb}(\text{DippForm})_2(\text{thf})]$ (**20**) using CH_3CN as the solvent. Another Yb complex $[\text{Yb}(\text{DippForm})_2(\text{CH}_3\text{CN})_2]$ (**22**) can be obtained by evaporation of $[\text{Yb}(\text{DippForm})_2(\text{CH}_3\text{CN})_3]$ (**21**) in CH_3CN and recrystallization from PhMe. The center atoms in $[\{\text{Yb}(\text{DFForm})_2(\text{CH}_3\text{CN})\}_2]$ (**17**) are seven coordinate. They have one CH_3CN and one DFForm terminally bound and an unusual twisted DFForm bridging ligand, because of the close Yb–F bond ($2.626(2)\text{Å}$). Another divalent complex $[\text{Yb}(\text{FForm})_2(\text{thf})_2]$ (**23**) is the result of a RTP reaction between FFormH and an excess Yb metal [31]. Recrystallization of $[\text{Yb}(\text{FForm})_2(\text{thf})_2]$ (**23**) from dme yields another divalent complex $[\text{Yb}(\text{FForm})_2(\text{dme})_2]$ (**24**). All known divalent lanthanoid formamidinate compounds are listed in Table 2.2.1.

2.3. Trivalent compounds

A homoleptic monomer i.e. $[\text{La}(\text{CF}_3\text{Form})_3]$ (**25**) (Fig. 2-6) was obtained from a RTP reaction from CF_3FormH [32]. This compound easily undergoes C–F activation by heating in non-coordinating solvents such as C_6D_6 or PhMe to produce LaF_3 and $[(\text{CF}_3\text{Form})_2(\text{thq})]$ (thq = tetrahydroquinazoline) as the major and $[(\text{CF}_3\text{Form})_2\text{Benz}]$ (Benz = benzamidine) as the minor product. This process can be compared to the $[\text{Yb}(\text{CF}_3\text{Form})_3(\text{thf})]$ (**26**) complex (Fig. 2-7) which

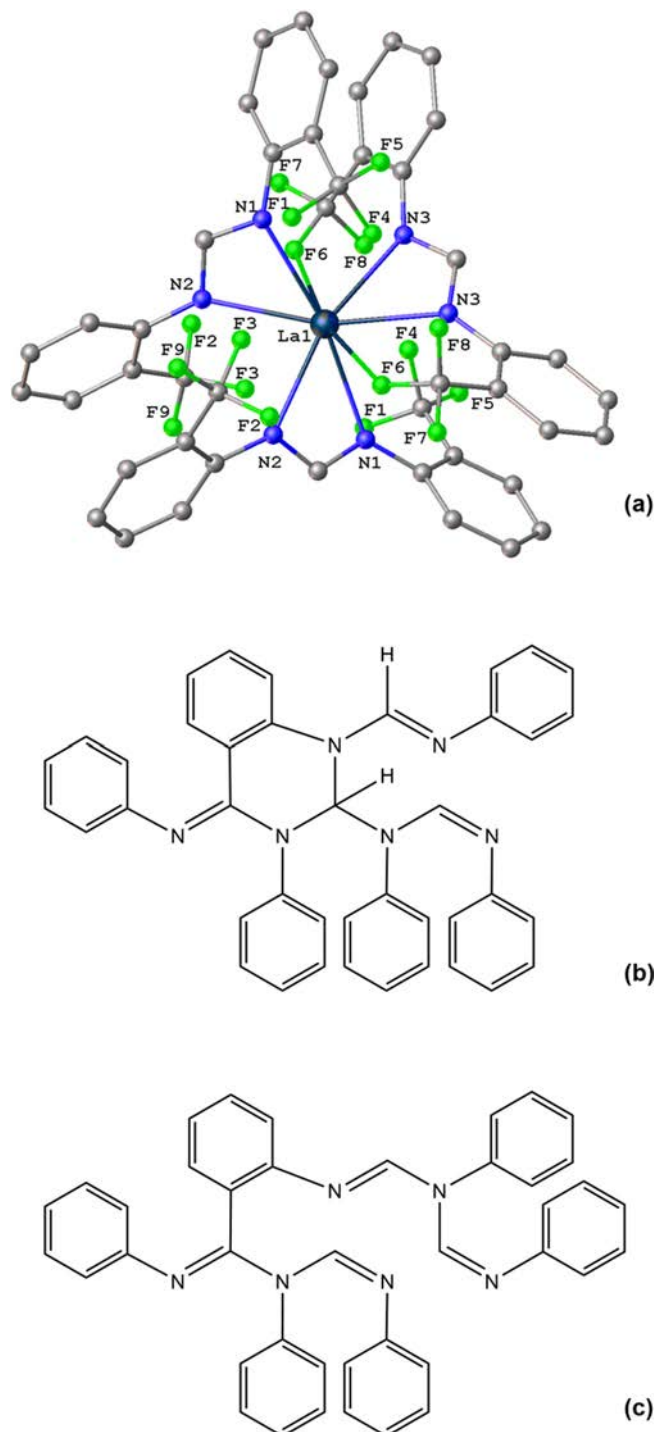


Fig. 2-6. X-ray structure of a) $[\text{La}(\text{CF}_3\text{Form})_3]$ (**25**) and simplified structures of b) $[(\text{CF}_3\text{Form})_2(\text{thq})]$ c) $[(\text{CF}_3\text{Form})_2\text{Benz}]$. All phenyl groups in b) and c) represent *ortho*-trifluoromethylphenyl groups, with the CF_3 groups removed for clarity.

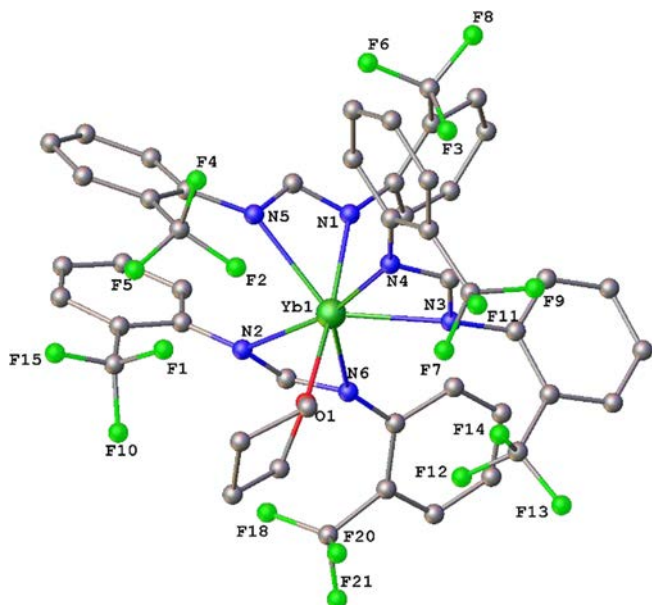


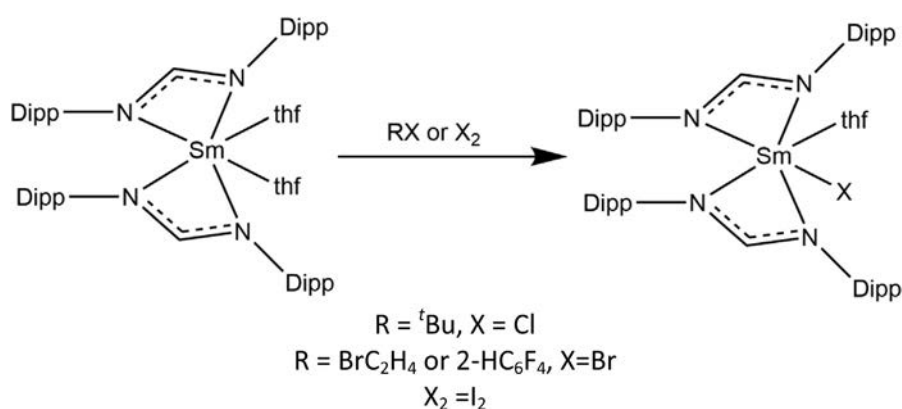
Fig. 2-7. X-ray structure of $[\text{Yb}(\text{CF}_3\text{Form})_3(\text{thf})]$ (**26**).

was synthesized in the same study. $[\text{Yb}(\text{CF}_3\text{Form})_3(\text{thf})]$ (**26**) can be C-F activated using the same method to yield the same compounds but with $[(\text{CF}_3\text{Form})_2\text{Benz}]$ as the major product. However, it has a

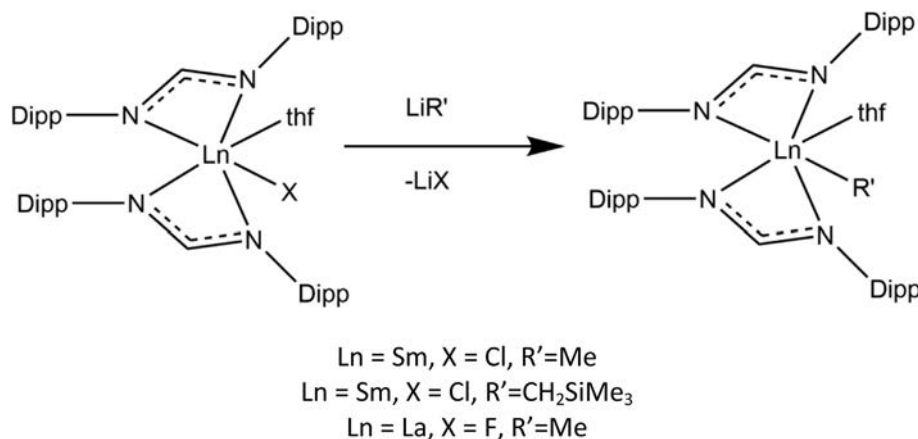
longer activation time perhaps due to the lack of significant Yb-F interactions ($\text{Yb-F} \geq 3.2427(17) \text{ \AA}$) compared with six La-F bonds in **2b**.

The oxidation of $[\text{Sm}(\text{DippForm})_2(\text{thf})_2]$ (**11**) by *tert*-butyl chloride, 1,2-dibromoethane and iodine at ambient temperature led to the formation of the samarium(III) halide complexes $[\text{Sm}(\text{DippForm})_2\text{Cl}(\text{thf})]$ (**27**), $[\text{Sm}(\text{DippForm})_2\text{Br}(\text{thf})]$ (**28**) and $[\text{Sm}(\text{DippForm})_2\text{I}(\text{thf})]$ (**29**) respectively in good yields (Scheme 2-1) [23]. The metathesis reaction of $[\text{Sm}(\text{DippForm})_2\text{Cl}(\text{thf})]$ (**27**) and $[\text{La}(\text{DippForm})_2\text{F}(\text{thf})]$ (**30**) with LiMe and $\text{LiCH}_2\text{SiMe}_3$ resulted in the formation of samarium alkyl complexes $[\text{Sm}(\text{DippForm})_2\text{Me}(\text{thf})]$ (**31**), $[\text{Sm}(\text{DippForm})_2\text{CH}_2\text{SiMe}_3(\text{thf})]$ (**32**) and $[\text{La}(\text{DippForm})_2\text{Me}(\text{thf})]$ (**33**). The complex $[\text{La}(\text{DippForm})_2\text{Me}(\text{thf})]$ (**33**) is the first reported La complex that contains a rare terminal methyl ligand (Scheme 2-2).

Bis(2-bromo-3,4,5,6-tetrafluorophenyl)mercury, DippFormH and Sm were used in a RTP reaction to yield $[\text{Sm}(\text{DippForm})\text{Br}_2(\text{thf})_3]$ (**34**) [23]. The divalent samarium compound, $[\text{Sm}(\text{DippForm})_2(\text{thf})_2]$ (**11**), was used in a redox reaction with diphenylmercury to yield $[\text{Sm}(\text{DippForm})_2(\text{OCH}=\text{CH}_2)(\text{thf})]$ (**35**). $[\text{Sm}(\text{DippForm})_2\text{Cl}(\text{thf})]$ (**27**), $[\text{Sm}(\text{DippForm})\text{Br}_2(\text{thf})_3]$ (**34**) (Fig. 2-8), $[\text{Sm}(\text{DippForm})_2\text{Me}(\text{thf})]$ (**31**), $[\text{Sm}(\text{DippForm})_2\text{CH}_2\text{SiMe}_3(\text{thf})]$ (**32**), $[\text{Sm}(\text{DippForm})_2(\text{OCH}=\text{CH}_2)(\text{thf})]$ (**35**) (Fig. 2-9) and $[\text{La}(\text{DippForm})_2\text{Me}(\text{thf})]$ (**33**) are mononuclear and the coordination number of the central metal is six in all compounds. Formamidinate ligands connect by chelation to the metal atom through two nitrogen donor atoms. Also, it has been reported benzophenone (bp) or halogenating agents like $\text{TiCl}_4(\text{thf})_2$, Ph_3CCl or C_2Cl_6 can be used as



Scheme 2-1. Schematic of the X-ray structure of $[\text{Sm}(\text{DippForm})_2\text{X}(\text{thf})]$. $\text{R} = \text{}^t\text{Bu}$, $\text{X} = \text{Cl}$, $\text{R} = \text{BrC}_2\text{H}_4$ or $2\text{-HC}_6\text{F}_4$, $\text{X} = \text{Br}$, $\text{X}_2 = \text{I}_2$.



Scheme 2-2. Schematic of the X-ray structure of $[\text{Ln}(\text{DippForm})_2\text{R}'(\text{thf})]$. $\text{Ln} = \text{Sm}$, $\text{X} = \text{Cl}$, $\text{R}' = \text{Me}$, $\text{Ln} = \text{Sm}$, $\text{X} = \text{Cl}$, $\text{R}' = \text{CH}_2\text{SiMe}_3$, $\text{Ln} = \text{La}$, $\text{X} = \text{F}$, $\text{R}' = \text{Me}$.

oxidants to synthesize $[\text{Yb}(\text{DFForm})_3(\text{bp})]$ (**36**) and $[\text{Yb}(\text{DFForm})_2\text{Cl}(\text{thf})_2]$ (**37**) from divalent $[\text{Yb}(\text{DFForm})_2(\text{thf})_3]$ (**18**) [30]. $[\text{Yb}(\text{DFForm})_3(\text{thf})]$ (**38**) was also obtained from an RTP reaction in this paper.

It has been reported divalent Yb complexes can induce C-X (X=F, Cl, Br) activation reactions with perfluorodecalin, hexachloroethane or 1,2-dichloroethane, and 1-bromo-2,3,4,5-tetrafluorobenzene, yielding $[\text{Yb}(\text{EtForm})_2\text{F}]_2$ (**39**), $[\text{Yb}(\text{o-PhPhForm})_2\text{F}]_2$ (**40**),

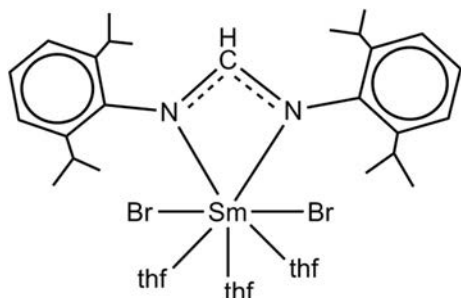


Fig. 2-8. Schematic of the X-ray structure of $[\text{Sm}(\text{DippForm})\text{Br}_2(\text{thf})_3]$ (**34**).

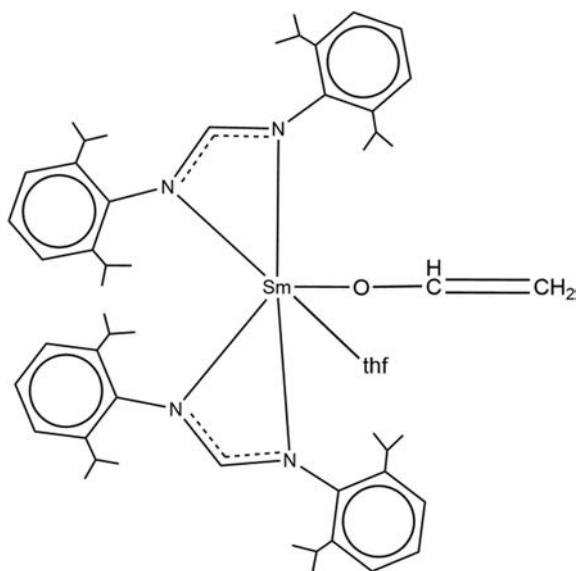


Fig. 2-9. Schematic of the X-ray structure of $[\text{Sm}(\text{DippForm})_2(\text{OCH}=\text{CH}_2)(\text{thf})]$ (**35**).

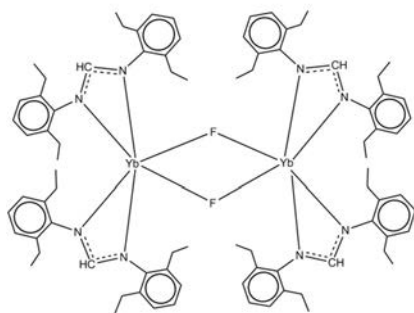
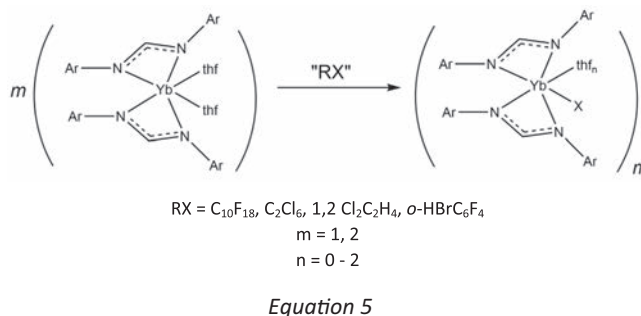


Fig. 2-10. Schematic and the X-ray structure of $[\text{Yb}(\text{EtForm})_2(\mu\text{-F})_2]$ (**39**).

$[\text{Yb}(\text{o-PhPhForm})_2\text{Cl}(\text{thf})_2]$ (**41**), $[\text{Yb}(\text{DippForm})_2\text{Cl}(\text{thf})]$ (**42**) and $[\text{Yb}(\text{DippForm})_2\text{Br}(\text{thf})]$ (**43**) (Eq. (5)) [26].



The coordination number for Yb in $[\text{Yb}(\text{EtForm})_2\text{F}]_2$ (**39**), $[\text{Yb}(\text{DippForm})_2\text{Cl}(\text{thf})]$ (**42**) and $[\text{Yb}(\text{DippForm})_2\text{Br}(\text{thf})]$ (**43**) is six. $[\text{Yb}(\text{EtForm})_2\text{F}]_2$ (**39**) has a dimeric structure containing fluoride-bridges (Fig. 2-10). However, $[\text{Yb}(\text{DippForm})_2\text{Cl}(\text{thf})]$ (**36**) and $[\text{Yb}(\text{DippForm})_2\text{Br}(\text{thf})]$ (**43**) are mononuclear. $[\text{Yb}(\text{o-PhPhForm})_2\text{Cl}]$

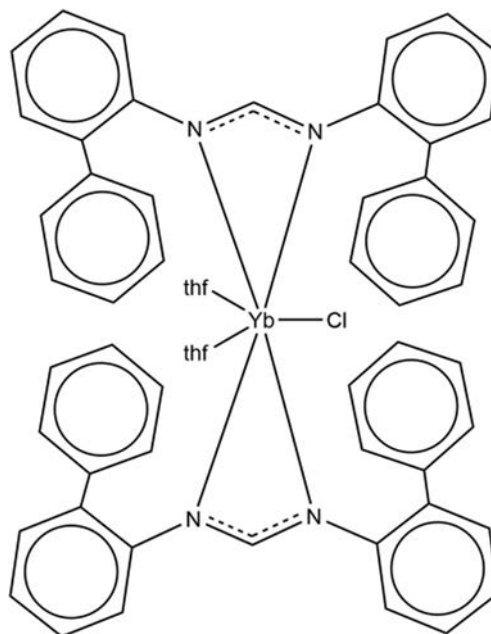
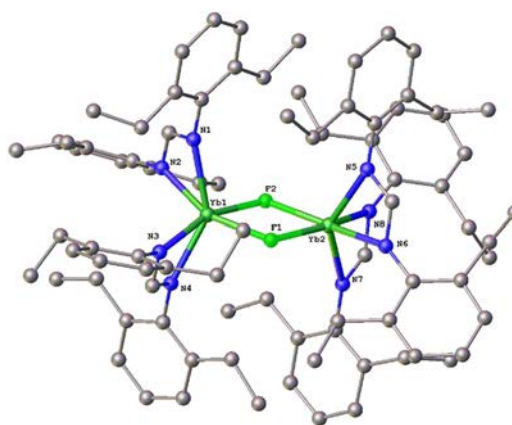
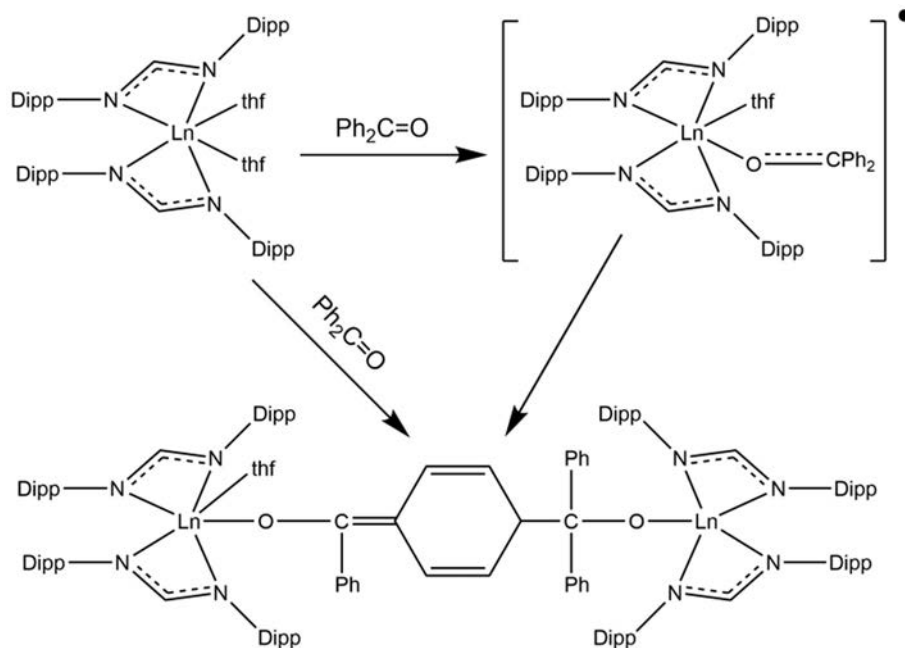
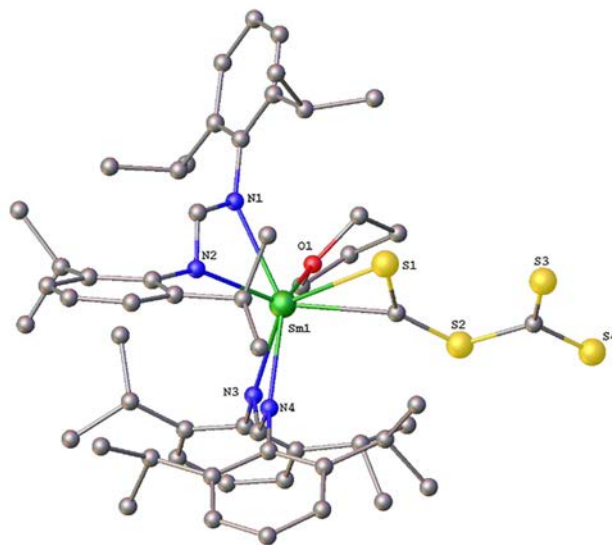
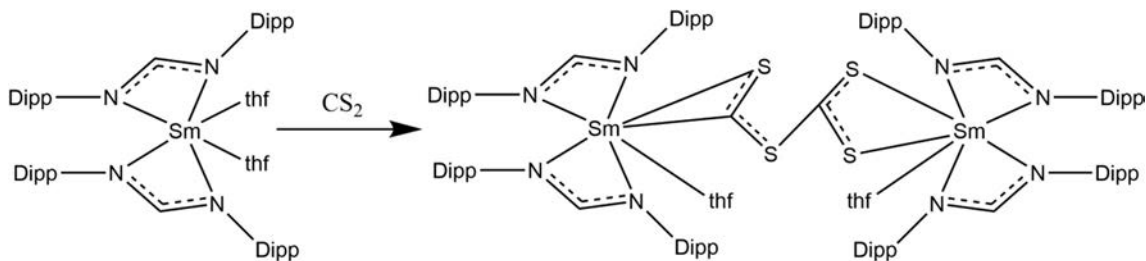


Fig. 2-11. Schematic of the X-ray structure of $[\text{Yb}(\text{o-PhPhForm})_2\text{Cl}(\text{thf})_2]$ (**41**).





Scheme 2-3. Schematic of the X-ray structure of $[\text{Ln}(\text{DippForm})_2(\text{thf})\{\mu\text{-OC}(\text{Ph})=\text{C}(\text{C}_6\text{H}_5)\text{-C}(\text{Ph})_2\text{O}\}\text{Ln}(\text{DippForm})_2]$ (Ln = Sm (**47**), Yb (**48**)).



Scheme 2-4. Schematic and part of the X-ray structures of $[\{\text{Sm}(\text{DippForm})_2(\text{thf})\}_2(\mu\text{-}\eta^2(\text{C},\text{S}):\kappa(\text{S},\text{S}''\text{))-SCSCS}_2)]$ (**49**) highlighting the C_2S_4 fragment.

$(\text{thf})_2]$ (**41**) is a seven coordinated monomeric complex with two chelating formamidinate ligands, a terminal chloride and two THF donors (Fig. 2-11). In the case of using DippFormH and Hg ($2\text{-BrC}_6\text{F}_4$)₂ in RTP reactions, a series of complexes $[\text{Ln}(\text{DippForm})_2\text{-}$

$\text{Br}(\text{thf})]$ (Ln = La (**44**), Nd (**45**)) was synthesized. For comparison purposes, a related complex $[\text{Tb}(\text{DippForm})_2\text{Cl}(\text{thf})_2]\cdot 2.5\text{THF}$ (**46**) was synthesized in this study using a metathesis reaction between TbCl_3 and $\text{Na}(\text{DippForm})$ [26].

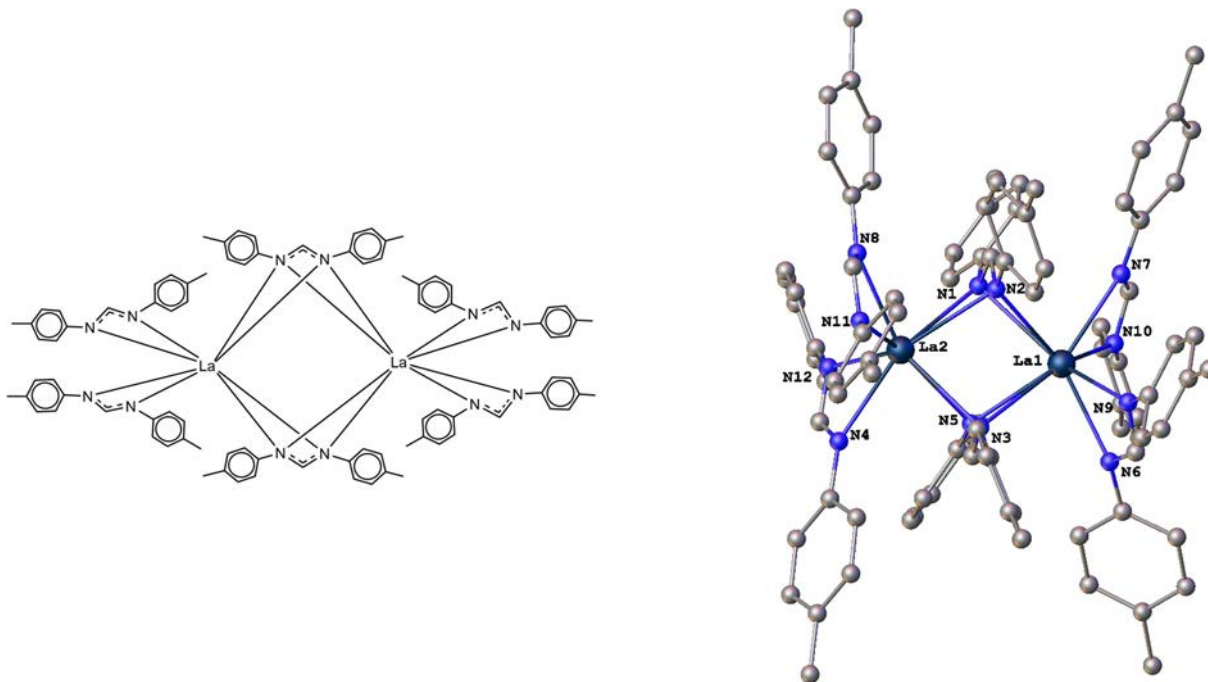


Fig. 2-12. Representative molecular structure of $[\text{La}(\text{p-TolForm})_3]_2$ (**50**).

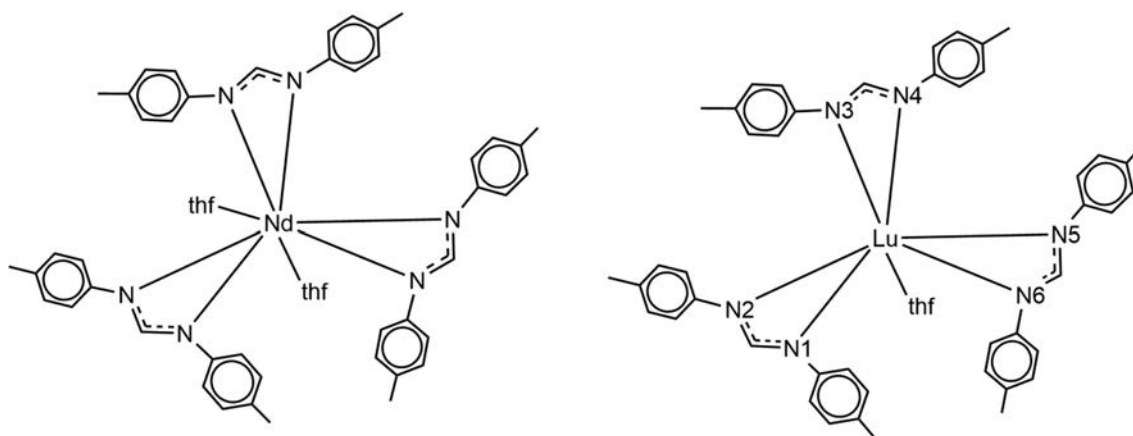


Fig. 2-13. Schematic molecular structures of $[\text{Nd}(\text{p-TolForm})_3(\text{thf})_2] \cdot \text{THF}$ (**56**) (left) and $[\text{Lu}(\text{p-TolForm})_3(\text{thf})] \cdot \text{THF}$ (**57**) (right) exemplifying the lowering of coordination number with lanthanoid size.

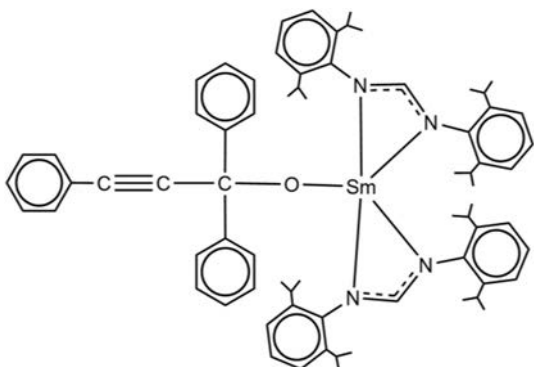


Fig. 2-14. Schematic of the X-ray structures of $[\text{Sm}(\text{DippForm})_2(\text{OC}-(\text{Ph})_2\text{C}_2\text{Ph})]$ (**60**).

The highly unusual $[\text{Sm}(\text{DippForm})_2(\text{thf})\{\mu\text{-OC}(\text{Ph})=(\text{C}_6\text{H}_5)\text{-C}(\text{Ph})_2\text{O}\}\text{Sm}(\text{DippForm})_2]$ (**47**) ($\text{C}_6\text{H}_5 = 1,4\text{-cyclohexadiene-3-yl-6-ylidene}$) compound was reported as the result of the reaction of $[\text{Sm}(\text{DippForm})_2(\text{thf})_2]$ (**11**) with benzophenone [27]. This compound contains rare C-C coupling between a carbonyl carbon and the carbon at the *para* position of a phenyl group of the OCPh_2 fragment. It was also found that the reaction of $[\text{Yb}(\text{DippForm})_2(\text{thf})_2]$ (**4**) with benzophenone gives a similar product (**48**) (Scheme 2-3), with a ketyl complex intermediate considered to be involved.

It was also reported that $[\text{Sm}(\text{DippForm})_2(\text{thf})_2]$ (**11**) reacts with carbon disulfide to form a dinuclear $[\{\text{Sm}(\text{DippForm})_2(\text{thf})_2\}_2(\mu\text{-}\eta^2(\text{C},\text{S}):\kappa(\text{S},\text{S}')\text{-SCSCS}_2)]$ (**49**) complex (Scheme 2-4). This complex has a rare thioformyl carbonotrithioate ($(\text{SCSCS}_2)^{2-}$) bridging ligand.

RTP reactions were carried out between $\text{Hg}(\text{C}_6\text{F}_5)_2$, *p*-TolForm and rare earth metals including La, Ce, Nd, Lu and Sm to yield trivalent lanthanoid formamidates. By using THF as the solvent, compounds were synthesized with the general form of

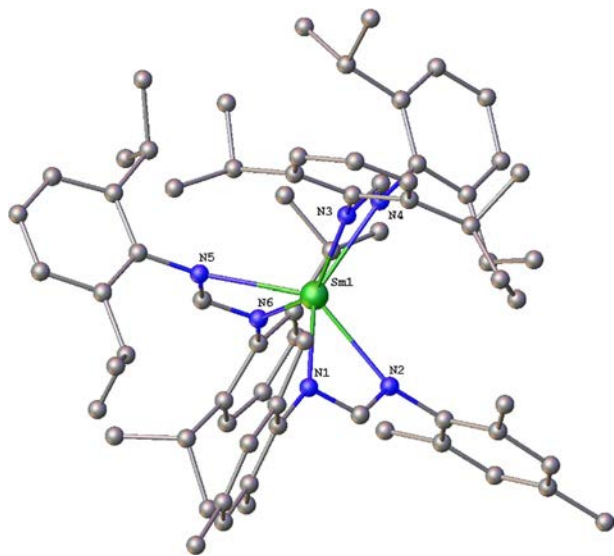


Fig. 2-15. X-ray structure of $[\text{Sm}(\text{DippForm})_2(\text{MesForm})]$ (**62**).

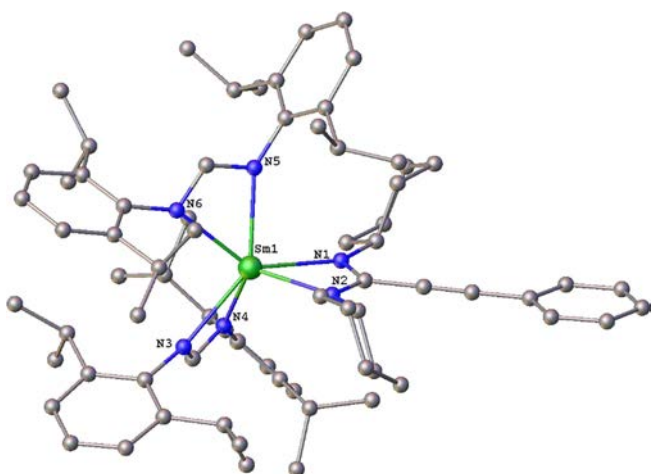


Fig. 2-16. X-ray structure of $[\text{Sm}(\text{DippForm})_2(\text{CyNC}(\text{CPh})\text{NCy})]$ (**65**).

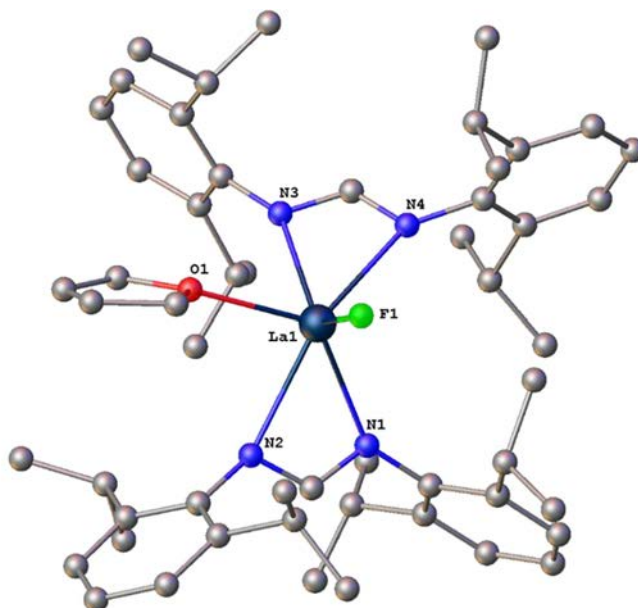
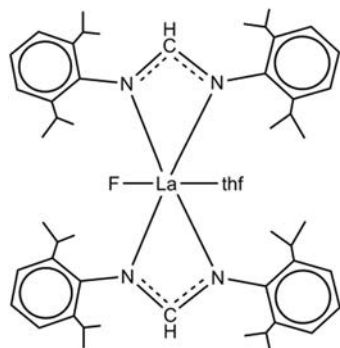


Fig. 2-17. Schematic and the X-ray structure of $[\text{LaF}(\text{DippForm})_2(\text{thf})]$ (**30**).

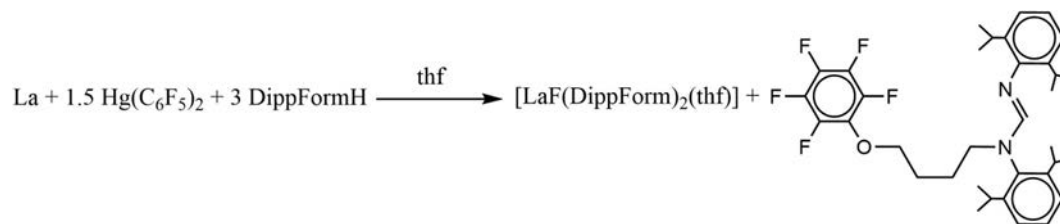
$[\text{Ln}(p\text{-TolForm})_3]$ or $[\text{Ln}(p\text{-TolForm})_3(\text{thf})_2]$ (Ln = rare earth metal). [15] It was the first time that the $\mu\text{-}1\kappa(\text{N},\text{N}')\text{:}2\kappa(\text{N},\text{N}')$ coordination mode had been achieved in trivalent rare earth formamidate chemistry and also discussed previously for the divalent Eu complex $[\{\text{Eu}(\text{DFForm})_2(\text{CH}_3\text{CN})_2\}_2]$ (**15**). Fig. 2-12 shows the X-ray structure of the $[\text{La}(p\text{-TolForm})_3]_2$ (**50**) which is same as the $[\text{Sm}(p\text{-TolForm})_3]_2$ (**51**). The cerium analogue has a similar structure but with an eclipsed rather than a staggered conformation [15]. Two $\mu\text{-}1\kappa(\text{N},\text{N}')\text{:}2\kappa(\text{N},\text{N}')$ bridging and four $\kappa(\text{N},\text{N}')$ terminal $p\text{-TolForm}$ ligands are present in the structure of each dimeric complex.

$[\text{Sm}(p\text{-TolForm})_3(\text{Ph}_3\text{PO})_2]$ (**52**) was synthesized by treating $[\text{Sm}(p\text{-TolForm})_3]$ (**51**) with triphenylphosphine oxide (Ph_3PO) and crystallizing from C_6D_6 . The reaction of DFFormH on $[\text{Sm}(p\text{-TolForm})_3]$ (**51**) was studied using PhMe. As a result of a protolysis reaction and crystallization from THF/hexane, three different complexes, $[\text{Sm}(\text{DFForm})_2(p\text{-TolForm})(\text{thf})_2]$ (**53**), $[\text{Sm}(p\text{-TolForm})_3]_2$ (**51**) and $[\text{Sm}(\text{DFForm})_3(\text{thf})_2]$ (**54**) were isolated. Another complex, $[\text{K}(18\text{-Crown-6})][\text{Sm}(p\text{-TolForm})_4]$ (**55**), was synthesized by reaction of $[\text{Sm}(p\text{-TolForm})_3]$ (**51**) in PhMe in the presence of 18-Crown-6 and a potassium mirror.

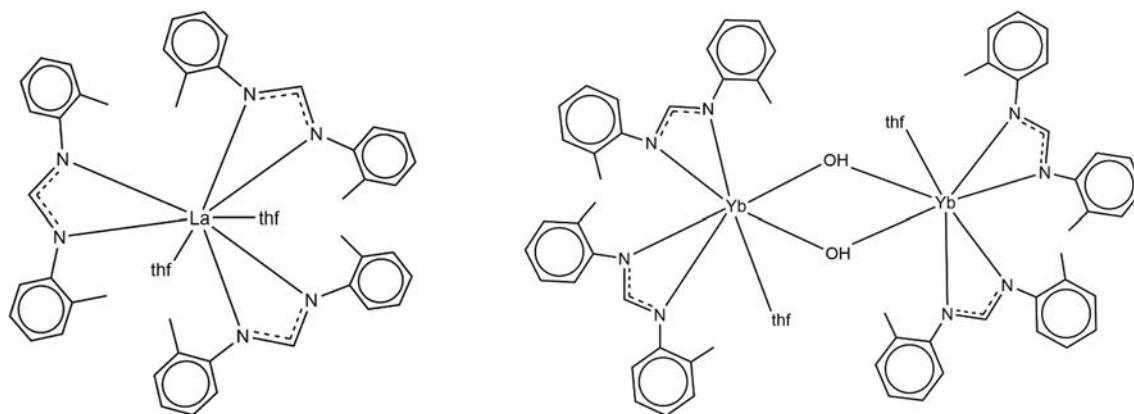
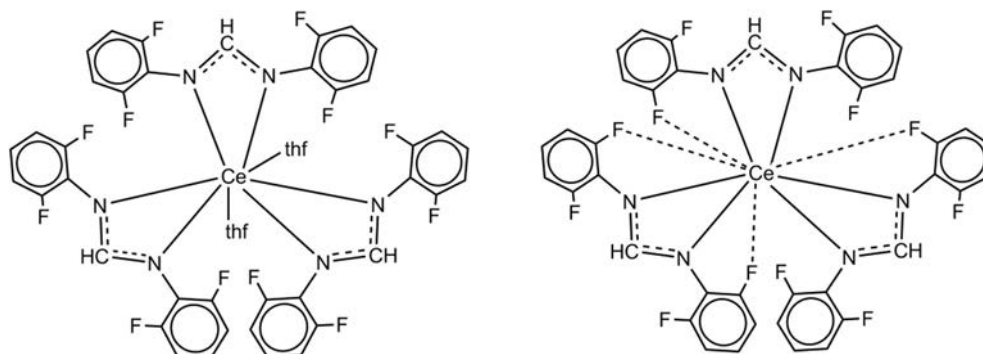
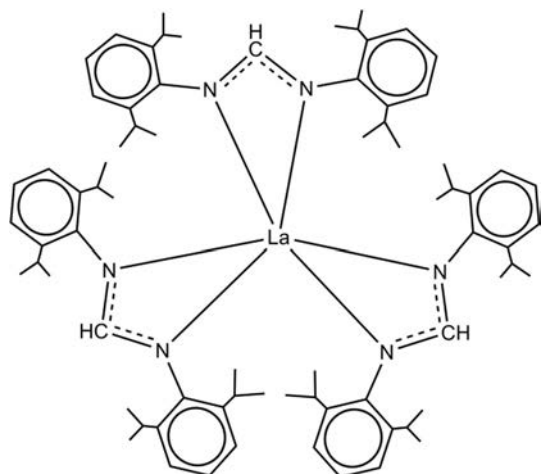
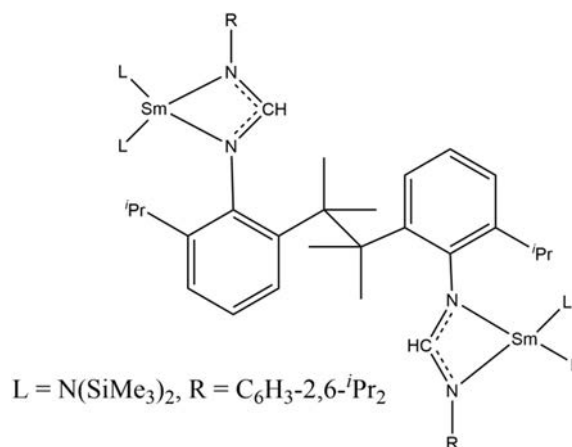
Fig. 2-13 shows the schematic structure for complexes in this study containing Nd (**56**) and Lu (**57**) [15]. The Nd atom is eight coordinated by three bidentate $p\text{-TolForm}$ ligands and two *transoid*-THF ligands ($\text{O}\text{--}\text{Nd}\text{--}\text{O}$: $153.61(6)^\circ$), in a distorted dodecahedral environment. The lutetium atom is seven coordinate with one symmetric ($\text{Lu}\text{--}\text{N}5$: 2.374(4), $\text{Lu}\text{--}\text{N}6$: 2.373(4)) and two asymmetric chelating $p\text{-TolForm}$ ligands ($\text{Lu}\text{--}\text{N}1$: 2.386(4), $\text{Lu}\text{--}\text{N}2$: 2.303(4), $\text{Lu}\text{--}\text{N}3$: 2.358(4), $\text{Lu}\text{--}\text{N}4$: 2.336(4)) and one THF ligand with the reduction in coordination number being a consequence of the lanthanoid contraction.

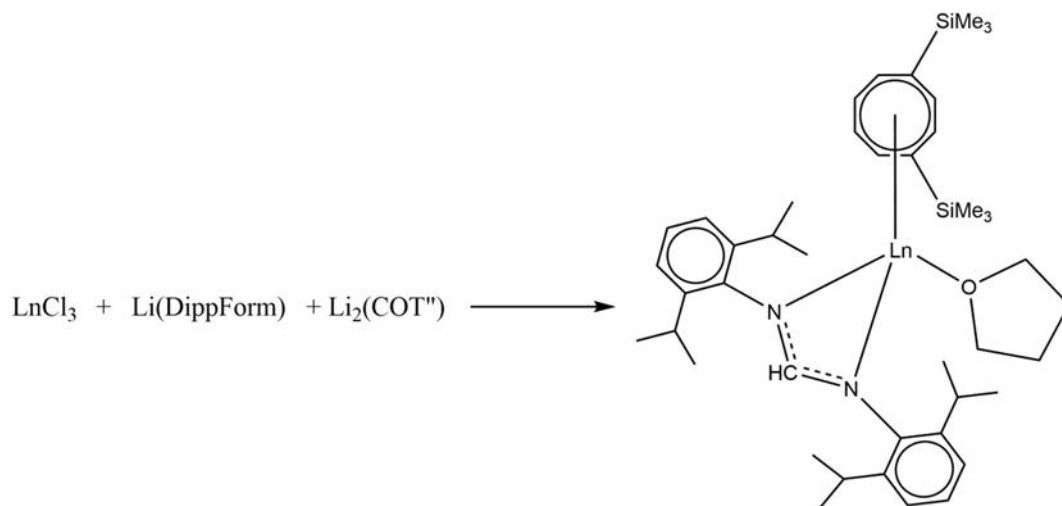
Trivalent $[\text{Sm}(\text{DippForm})_2(\text{CCPh})(\text{thf})]$ (**58**) can activate the $\text{C}=\text{O}$ bond of benzophenone and form $[\text{Sm}(\text{DippForm})_2\{\text{OC}(\text{Ph})_2\text{C}_2\text{Ph}\}(\text{thf})]$ (**59**) with unsolvated $[\text{Sm}(\text{DippForm})_2\{\text{OC}(\text{Ph})_2\text{C}_2\text{Ph}\}]$ (**60**) as a minor product. $\kappa(\text{N},\text{N}')$ -Bonding between a DippForm and samarium exists in all compounds (Fig. 2-14 [27]).

Oxidation of $[\text{Sm}(\text{DippForm})_2(\text{thf})_2]$ (**11**) with different oxidizing agents has been investigated in another study [28]. Oxidation of $[\text{Sm}(\text{DippForm})_2(\text{thf})_2]$ (**11**) with DippNCNDipp in PhMe can yield $[\text{Sm}(\text{DippForm})_3]$ (**61**). Using the less bulky carbodiimide, MesNCNMes, yields the heteroleptic $[\text{Sm}(\text{DippForm})_2(\text{MesForm})]$



Scheme 2-5.

Fig. 2-18. Schematic molecular structures of [La(o-TolForm)₃(thf)₂] (**67**) (left) and [Yb(o-TolForm)₂(μ-OH)(thf)₂] (**85**) (right).Fig. 2-19. Schematic of the X-ray molecular structures of [Ce(DFForm)₃(thf)₂] (**91**) (left) and [Ce(DFForm)₃] (**92**) (right).Fig. 2-20. Schematic of the X-ray structure of [La(DippForm)₃] (**97**).Fig. 2-21. Schematic of the X-ray structure of [((Me₃Si)₂N)₂Sm{μ-(RNC(H)N(Ar-Ar)NC(H)NR)}Sm{N(SiMe₃)₂}₂] (**99**) complex.



Scheme 2-6. Schematic of the X-ray structure of $[\text{Ln}(\text{DippForm})(\text{COT}')(\text{thf})] \cdot \text{C}_7\text{H}_8$ complexes (Ln = Sm (**99**), Yb (**100**)).

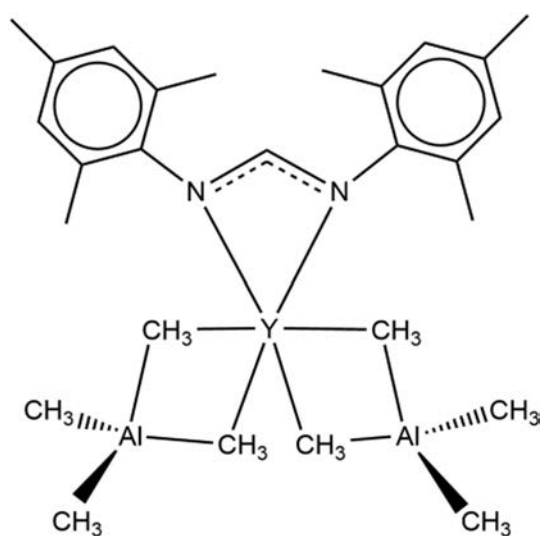


Fig. 2-22. Schematic of the X-ray structure of $[\text{Y}(\text{MesForm})(\text{AlMe}_4)_2]$ (**102**).

(**62**) (Fig. 2-15). It has been found that using *N,N'*-dicyclohexylcarbodiimide (CyNCNCy) as the oxidant in PhMe can yield two complexes, $[\text{Sm}(\text{DippForm})_2(\text{CyNC}(\text{CH}_2\text{Ph})\text{NCy})]$ (**63**) and $[\text{Sm}(\text{DippForm})_2(\text{CyNC}(\text{H})\text{NCy})]$ (**64**) in approximately equal yields, indicating activation of toluene has occurred. However, in the case of using thf as the solvent, only $[\text{Sm}(\text{DippForm})_2(\text{CyNC}(\text{H})\text{NCy})]$ (**64**) can be isolated. In this process an intermediate radical compound can receive a hydrogen atom from the solvent to give a formamidinate ligand. This paper also reports complexes $[\text{Sm}(\text{DippForm})_2(\text{CyNC}(\text{CPh})\text{NCy})]$ (**65**) (Fig. 2-16) and $[\text{Sm}(\text{DippForm})_2(\text{MesNC}(\text{CPh})\text{NMe}_2)]$ (**66**) as the result of the reaction of $[\text{Sm}(\text{DippForm})_2(\text{CPh})(\text{thf})]$ (**58**) with RNCNR (R = Cy, Mes) where the carbodiimide inserts into the Sm–CPh bond.

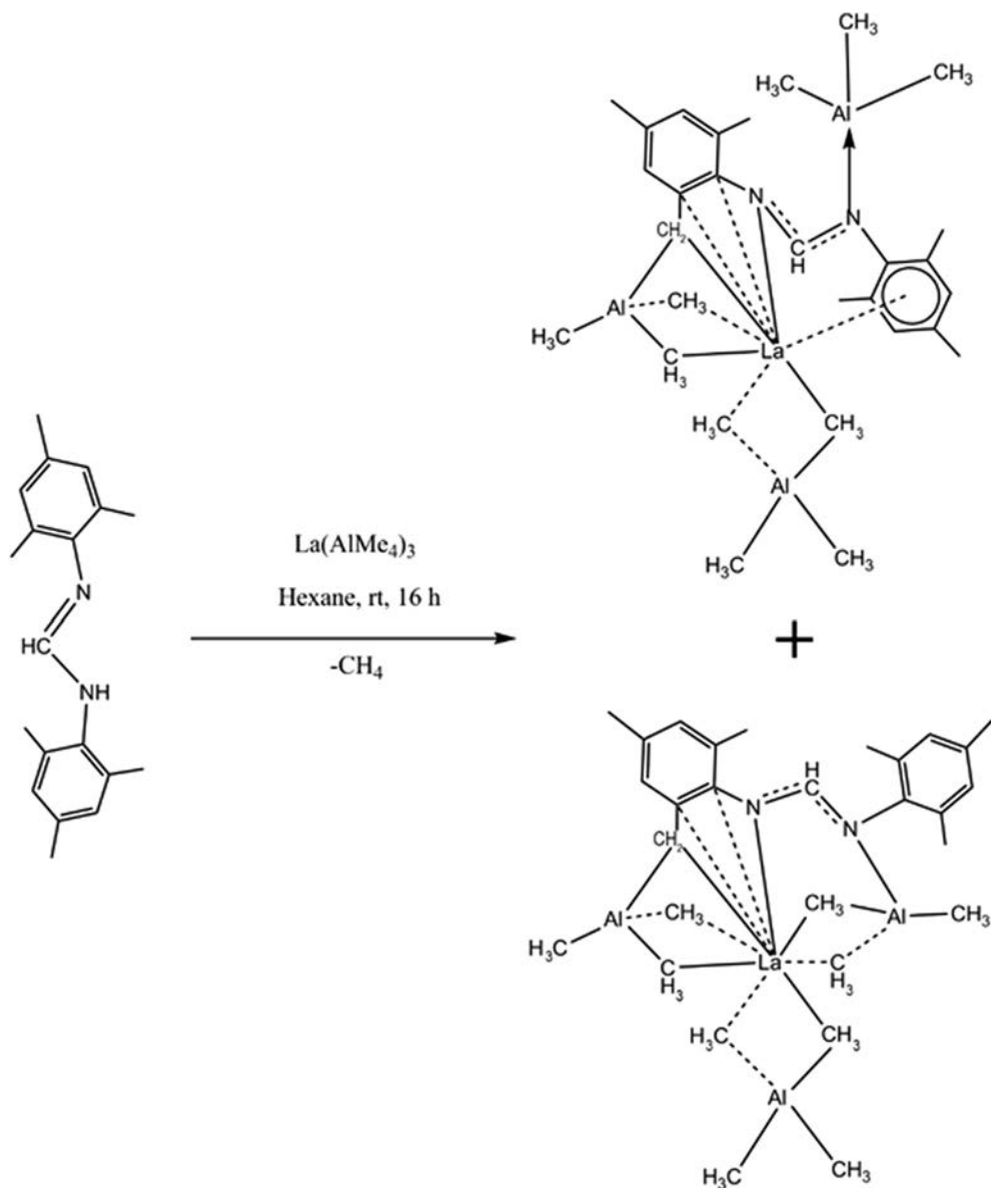
A functionalised formamidine, $\text{DippForm}((\text{CH}_2)_4\text{OC}_6\text{F}_4\text{H}-o)$ and a rare terminal Ln–F bond were formed in an RTP study from DippFormH , lanthanum and $\text{Hg}(\text{C}_6\text{F}_5)_2$ (Scheme 3-5) [14]. The resulting compound, $[\text{LaF}(\text{DippForm})_2(\text{thf})]$ (**30**) (Fig. 2-17), shows that lanthanum is six coordinate and there are two chelating *cisoid* DippForm ligands. The main idea of this study was to use the RTP reaction with bis(pentafluorophenyl)mercury to synthesise a heteroleptic lanthanum fluoride $[\text{La}(\text{L})_2\text{F}]$ complex. This report

shows that the proposed $[\text{Ln}(\text{C}_6\text{F}_5)_2]$ intermediate undergoes C–F activation to yield $[\text{Ln}(\text{F})\text{L}_2]$ and a unique functionalised formamidine, $\text{DippForm}((\text{CH}_2)_4\text{OC}_6\text{F}_4\text{H}-o)$ (Scheme 2-5) which arises from a substituted benzyne, a ring opened thf and DippFormH . In this study elemental lanthanum was used with bis(pentafluorophenyl)mercury and DippFormH in THF in a 1 : 1.5 : 3 stoichiometry.

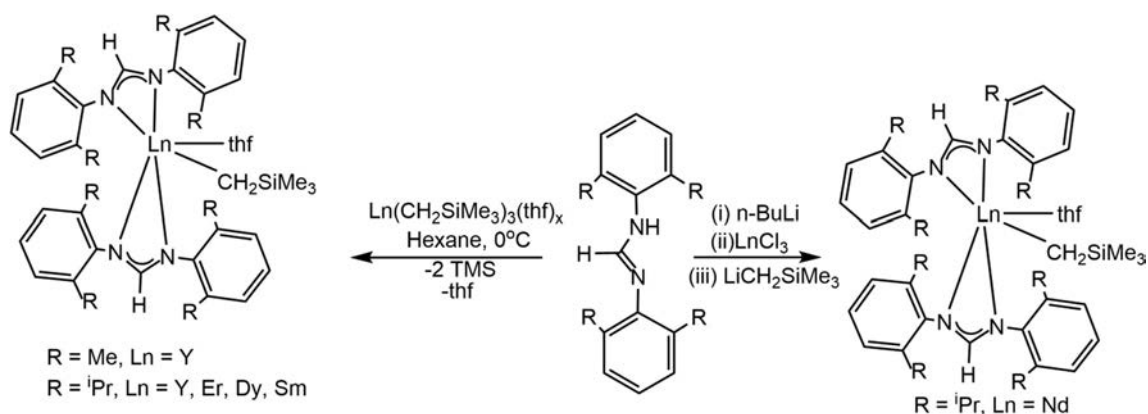
A series of tris(formamidinato)lanthanoid(III) complexes in the form of $[\text{Ln}(\text{Form})_3(\text{thf})_n]$ has been reported as the products of RTP reaction between different lanthanoids and *N,N'*-bis(aryl)formamidine ligands [24]. The *o*-TolFormH ligand was used with La and Er to give $[\text{La}(\text{o-TolForm})_3(\text{thf})_2]$ (**67**) and $[\text{Er}(\text{o-TolForm})_3(\text{thf})]$ (**68**) respectively. $[\text{La}(\text{XylForm})_3(\text{thf})]$ (**69**) and $[\text{Sm}(\text{XylForm})_3]$ (**70**) were synthesized using XylFormH ligand and MesFormH as the proligand yielded $[\text{Ln}(\text{MesForm})_3]$ complexes (Ln = La (**71**), Nd (**72**), Sm (**73**) and Yb (**74**)). In the case of EtFormH, the $[\text{Ln}(\text{EtForm})_3]$ complexes were synthesized (Ln = La (**75**), Nd (**76**), Sm (**77**), Ho (**78**) and Yb (**79**)). The *o*-PhPhFormH ligand gave $[\text{Ln}(\text{o-PhPhFormH})_3]$ complexes (Ln = La (**80**), Nd (**81**), Sm (**82**) and Er (**83**)). In this study, $[\text{Yb}(\text{o-TolForm})_3(\text{thf})]$ (**84**) was isolated from a metathesis reaction route because the RTP reaction consistently gave $[\{\text{Yb}(\text{o-TolForm})_2(\mu\text{-OH})(\text{thf})_2\}]$ (**85**). The La metal center is eight-coordinate in **67** and the molecular unit exhibits two *transoid* THF donor molecules (O–La–O: 157.23 (17)°) (Fig. 2-18 left). In the Yb complex (**85**), each ytterbium center has two chelating *o*-TolForm ligands, one THF molecule and two bridging OH groups giving a seven-coordinate ytterbium atom (Fig. 2-18 right). The ionic radius of Yb^{3+} is smaller than La^{3+} due to the lanthanoid contraction giving the lanthanum complex a higher coordination number than the ytterbium complex [33].

Using DippFormH which is a bulkier ligand, C–F activation occurs to give $[\text{Ln}(\text{DippForm})_2\text{F}(\text{thf})]$ complexes (Ln = La (**30**), Ce (**86**), Nd (**87**), Sm (**88**) and Tm (**89**)) [26]. $[\text{Nd}(\text{DippForm})_2(\text{CPh})(\text{thf})]$ (**90**) was synthesized in this study by using bis(phenylethynyl)mercury ($\text{Hg}(\text{CPh})_2$) rather than $\text{Hg}(\text{C}_6\text{F}_5)_2$ in an RTP reaction and provides evidence for the formation of $[\text{Ln}(\text{Form})_2\text{R}]$ (R = C_6F_5 or CPh) intermediates. $\text{Hg}(\text{CPh})_2$ also was used to prepare $[\text{Sm}(\text{DippForm})_2(\text{CPh})(\text{thf})]$ (**58**) complex by oxidation of $[\text{Sm}(\text{DippForm})_2(\text{thf})_2]$ (**11**).

Three new cerium(III) formamidinate complexes comprising $[\text{Ce}(\text{DFForm})_3(\text{thf})_2]$ (**91**), $[\text{Ce}(\text{DFForm})_3]$ (**92**), and $[\text{Ce}(\text{EtForm})_3]$ (**93**) are the results of a protonolysis reactions between $[\text{Ce}(\text{N}(\text{SiMe}_3)_2)_3]$ and *N,N'*-bis(2,6-difluorophenyl)formamidine (DFFormH) or EtFormH [34]. The unsolvated $[\text{Ce}(\text{DFForm})_3]$ (**92**)



Scheme 2-7. Synthetic pathway and the products for formation of $[\text{La}\{\eta^1(\text{N})\}\eta^6(\text{Ar})\text{-}2\text{-Me}_3\text{AlCH}_2\text{-}4,6\text{-Me}_2\text{C}_6\text{H}_2\text{NCHNMe}_2\}\{\text{AlMe}_3\}\{\text{AlMe}_4\}]$ (**107**) and $[\text{La}\{2\text{-Me}_3\text{AlCH}_2\text{-}4,6\text{-Me}_2\text{C}_6\text{H}_2\text{NCHNMe}_2\}\{\text{AlMe}_3\}\{\text{AlMe}_4\}]_2(\text{C}_6\text{H}_{14})_{1.5}$ (**108**) which cocrystallize 1:1.



Scheme 2-8. Structures of $\text{Ln}_2\text{RECH}_2\text{SiMe}_3\cdot\text{thf}$ [$\text{L} = \text{XylForm}$, $\text{RE} = \text{Y}$ (**113**) and $\text{L} = \text{DippForm}$, $\text{RE} = \text{Y}$ (**113**), **Er** (**114**), **Dy** (**115**), **Sm** (**116**), and **Nd** (**117**)].

Table 2.3.1
Trivalent compounds.

Reaction	Compound	Method	Refs.
[SmI ₂ (THF) ₂] + solution of [Sm(DippForm) ₂ (thf) ₂] in THF	[Na(thf) ₅][Sm(I) ₂ (DippForm) ₂ (thf)] (12)	Redox	[29]
Eu + DFFormH in THF	{[Eu(DFForm) ₂ OH(thf) ₂]} (16)	RTP	[30]
[Yb(DFForm) ₂ (thf) ₃] in PhMe exposed with trace O ₂	{[Yb ₂ (DFForm) ₄ (O) ₂]} (19)	Oxidation	[30]
La + CF ₃ FormH + Hg(C ₆ F ₅) ₂ in THF	[La(CF ₃ Form) ₃] (25)	RT	[32]
Yb + CF ₃ FormH + Hg(C ₆ F ₅) ₂ in THF	[Yb(CF ₃ Form) ₃ (thf)] (26)	RT	[32]
[Sm(DippForm) ₂ (thf) ₂] + (CH ₃) ₃ CCl in PhMe	[Sm(DippForm) ₂ Cl(thf)] (27)	Oxidation	[23]
[Sm(DippForm) ₂ (thf) ₂] + BrCH ₂ CH ₂ Br in PhMe	[Sm(DippForm) ₂ Br(thf)] (28)	Oxidation	[23]
[Sm(DippForm) ₂ (thf) ₂] + I ₂ in PhMe	[Sm(DippForm) ₂ I(thf)] (29)	Oxidation	[23]
[Sm(DippForm) ₂ Cl(thf)] + MeLi in PhMe	[Sm(DippForm) ₂ Me(thf)] (31)	Metathesis	[23]
[Sm(DippForm) ₂ Cl(thf)] + SiMe ₃ CH ₂ Li	[Sm(DippForm) ₂ (CH ₂ SiMe ₃)(thf)] (32)	Metathesis	[23]
[La(DippForm) ₂ F(thf)] + MeLi in PhMe	[La(DippForm) ₂ Me(thf)] (33)	Metathesis	[23]
Sm + Hg(2-BrC ₆ F ₄) ₂ + DippFormH	[Sm(DippForm)Br ₂ (thf) ₃] (34)	RTP	[23]
[Sm(DippForm) ₂ (thf) ₂] and diphenylmercury in toluene	[Sm(DippForm) ₂ (OCH=CH ₂)(thf)] (35)	Oxidation + thf cleavage	[23]
[Yb(DFForm) ₂ (thf) ₃] + BP in DME (crystallised from PhMe)	[Yb(DFForm) ₃ (bp)] (36)	Oxidation and redistribution	[30]
[Yb(DFForm) ₂ (thf) ₃] + TiCl ₄ (thf) ₂ /Ph ₃ CCl in THF	[Yb(DFForm) ₂ Cl(thf) ₂] (37)	Oxidation	[30]
Yb + DFFormH + Hg(C ₆ F ₅) ₂ in THF	[Yb(DFForm) ₃ (thf)] (38)	RTP	[30]
Perfluorodecalin + [Yb(EtForm) ₂ (thf) ₂] in THF	{[Yb(EtForm) ₂ (μ ₂ -F) ₂]} (39)	C–F activation	[26]
Perfluorodecalin + [Yb(<i>o</i> -PhPhForm) ₂ (thf) ₂] in THF	[Yb(<i>o</i> -PhPhForm) ₂ F] ₂ (40)	C–F activation	[26]
Hexachloroethane + [Yb(<i>o</i> -PhPhForm) ₂ (thf) ₂]-2THF in THF	[Yb(<i>o</i> -PhPhForm) ₂ Cl(thf) ₂] (41)	C–Cl activation	[26]
1,2-dichloroethane + [Yb(DippForm) ₂ (thf) ₂] in PhMe	[Yb(DippForm) ₂ Cl(thf)] (42)	C–Cl activation	[26]
Yb + Hg(2-BrC ₆ F ₄) ₂ + DippFormH in THF	[Yb(DippForm) ₂ Br(thf)] (43)	C–Br activation	[26]
Ln + Hg(2-BrC ₆ F ₄) ₂ + DippFormH in THF	[Ln(DippForm) ₂ Br(thf)] (Ln = La (44), Nd (45))	C–Br activation	[26]
[Na-(DippForm)(thf) ₃] + TlCl ₃ in THF	[Tl(DippForm) ₂ Cl(thf) ₂]-2.5THF (46)	Metathesis	[26]
[Sm(DippForm) ₂ (thf) ₂] + Benzophenone in toluene	[Sm(DippForm) ₂ (thf) {μ-OC(Ph)=(C ₆ H ₅)C-(Ph) ₂ O}Sm(DippForm) ₂] (47)	Ketyl rearrangement	[27]
[Yb(DippForm) ₂ (thf) ₂] + Benzophenone in toluene	[Yb(DippForm) ₂ (thf) {μ-OC(Ph)=(C ₆ H ₅)C(Ph) ₂ O}Yb(DippForm) ₂] (48)	Ketyl rearrangement	[27]
[Sm(DippForm) ₂ (thf) ₂] + CS ₂ in C ₆ D ₆	{[Sm(DippForm) ₂ (thf) ₂] ₂ (μ ² -η ² (C,S):κ(S',S'') SCSCS ₂)} (49)	Oxidation	[27]
Ln + <i>p</i> -TolFormH + Hg(C ₆ F ₅) ₂ in THF	[Ln(<i>p</i> -TolForm) ₃] ₂ (Ln = La (50), Ce (96), Sm (51), Nd (127))	RTP	[15]
[Sm(<i>p</i> -TolForm) ₃] ₂ .1/2 thf + Ph ₃ PO in PhMe	[Sm(<i>p</i> -TolForm) ₃ (Ph ₃ PO) ₂] (52)	Bridge splitting	[15]
[Sm(<i>p</i> -TolForm) ₃] ₂ .1/2 thf + DFFormH in PhMe (crystallised from THF/Hexane mixture)	[Sm(<i>p</i> -TolForm)(DFForm) ₂ (thf) ₂] (53)	Bridge splitting	[15]
[Sm(<i>p</i> -TolForm) ₃] ₂ .1/2 thf + DFFormH in PhMe (crystallised from THF/Hexane mixture)	[Sm(DFForm) ₃ (thf) ₂] (54)	Bridge splitting	[15]
KC ₈ + 18-Crown-6 + [Sm(<i>p</i> -TolForm) ₃] ₂ in PhMe	[K(18-Crown-6)][Sm(<i>p</i> -TolForm) ₄] (55)	Attempted reduction	[15]
[Nd(<i>p</i> -TolForm) ₃] ₂ .PhMe dissolved in THF and layered with hexane	[Nd(<i>p</i> -TolForm) ₃ (thf) ₂] (56)	Bridge splitting	[15]
Lu + <i>p</i> -TolFormH + Hg(C ₆ F ₅) ₂ in THF	[Lu(<i>p</i> -TolForm) ₃ (thf)] (57)	RTP	[15]
[Sm(DippForm) ₂ (thf) ₂] + Hg(CPh) ₂ in Toluene	[Sm(DippForm) ₂ (C≡CPh)(thf)] (58)	Oxidation	[24]
[Sm(DippForm) ₂ (CCPh)(thf)] + Benzophenone in toluene	[Sm(DippForm) ₂ (OC(Ph) ₂ C ₂ Ph)(thf)] (59) (major) [Sm(DippForm) ₂ (OC(Ph) ₂ C ₂ Ph)] (60) (minor)	Insertion	[27]
Dissolution of [Na(THF) ₅][SmI ₂ (DippForm) ₂ (THF)] in hexane	[Sm(DippForm) ₃] (61)	Rearrangement	[29]
[Sm(DippForm) ₂ (thf) ₂] + DippNCNDipp in toluene	[Sm(DippForm) ₃] (61)	Oxidation	[28]
MesNCNMes + [Sm(DippForm) ₂ (thf) ₂] in PhMe (crystallised from hexane)	[Sm(DippForm) ₂ (MesForm)] (62)	Oxidation	[28]
N,N'-dicyclohexylcarbodiimide (CyNCNCy) + [Sm(DippForm) ₂ (thf) ₂] in PhMe	[Sm(DippForm) ₂ (CyNC(CH ₂ Ph)NCy)] (63) and [Sm(DippForm) ₂ (CyNC(H)NCy)] (64)	Oxidation	[28]
[Sm(DippForm) ₂ (C≡CPh)(thf)] + N,N'-dicyclohexylcarbodiimide (CyNCNCy) in PhMe	[Sm(DippForm) ₂ (CyNC(C≡CPh)NCy)] (65)	Insertion	[28]
[Sm(DippForm) ₂ (C≡CPh)(thf)] + MesNCNMes in PhMe	[Sm(DippForm) ₂ (MesNC(C≡CPh)NMes)] (66)	Insertion	[28]
La + <i>o</i> -TolFormH + Hg(C ₆ F ₅) ₂ in THF	[La(<i>o</i> -TolForm) ₃ (thf) ₂] (67)	RTP	[24]
Er + <i>o</i> -TolFormH + Hg(C ₆ F ₅) ₂ in THF	[Er(<i>o</i> -TolForm) ₃ (thf)] (68)	RTP	[24]
La + XylFormH + Hg(C ₆ F ₅) ₂ in THF	[La(XylForm) ₃ (thf)] (69)	RTP	[24]
Sm + XylFormH + Hg(C ₆ F ₅) ₂ in THF	[Sm(XylForm) ₃] (70)	RTP	[24]
Ln + MesFormH + Hg(C ₆ F ₅) ₂ in THF	[Ln(MesForm) ₃] (Ln = La (71), Nd (72), Sm (73) and Yb (74))	RTP	[24]
Ln + EtFormH + Hg(C ₆ F ₅) ₂ in THF	[Ln(EtForm) ₃] (Ln = La (75), Nd (76), Sm (77), Ho (78) and Yb (79))	RTP	[24]
Ln + <i>o</i> -PhPhFormH + Hg(C ₆ F ₅) ₂ in THF	[Ln(<i>o</i> -PhPhForm) ₃] (Ln = La (80), Nd (81), Sm (82) and Er (83))	RTP	[24]
YbCl ₃ + <i>o</i> -TolFormLi in THF	[Yb(<i>o</i> -TolForm) ₃ (thf)] (84)	Metathesis	[24]
Yb + <i>o</i> -TolFormH + Hg(C ₆ F ₅) ₂ in THF	{[Yb(<i>o</i> -TolForm) ₂ (μ-OH)(thf) ₂]} (85)	RTP	[24]
Ln + DippFormH + Hg(C ₆ F ₅) ₂ in THF	[Ln(DippForm) ₂ F(thf)] (Ln = La (30), Ce (86), Nd (87), Sm (88) and Tm (89))	RTP + C–F activation	[24]
Nd + DippFormH + Hg(CPh) ₂ in THF	[Nd(DippForm) ₂ (C≡CPh)(thf)] (90)	RTP	[24]
[Ce(N(SiMe ₃) ₂) ₃] + DFFormH in THF	[Ce(DFForm) ₃ (thf) ₂] (91)	Protolysis	[34]
[Ce(N(SiMe ₃) ₂) ₃] + DFFormH in PhMe	[Ce(DFForm) ₃] (92)	Protolysis	[34]
[Ce(N(SiMe ₃) ₂) ₃] + EtFormH in THF	[Ce(EtForm) ₃] (93)	Protolysis	[34]
Oxidation of [Ce(DFForm) ₃ (thf) ₂] with Ph ₃ CCl	[Ce ₃ Cl ₅ (DFForm) ₄ (thf) ₄] (94)	Attempted oxidation	[34]
[Ce(EtForm) ₃] + Ph ₃ CCl in THF	[Ce(EtForm)Cl ₂ (thf) ₃] (95)	Redox	[34]
[La(DippForm) ₂ Me(thf)] + H ₂ C ₃ Ph ₄ in C ₆ D ₆	[La(DippForm) ₃] (97)	–	[23]

(continued on next page)

Table 2.3.1 (continued)

Reaction	Compound	Method	Refs.
[Sm{N(SiMe ₃) ₂ }(THF) ₂] and N,N'-bis(2,6-diisopropylphenyl)carbodiimide in hexane	{[(Me ₃ Si) ₂ N] ₂ Sm{μ-(RNC(H)N(Ar-Ar) (R = C ₆ H ₃ -2,6- ⁱ Pr ₂ ; Ar-Ar = C ₆ H ₃ -2- ⁱ Pr-6-C(CH ₃) ₂ C(CH ₃) ₂ -6'-C ₆ H ₃ -2- ⁱ Pr)NC(H)-NR)}Sm{N(SiMe ₃) ₂ }}] (98)	Oxidation + Radical coupling	[35]
SmCl ₃ + DippFormLi + Li ₂ COT'' in THF	Sm(DippForm)(COT'')(THF) (COT'' = 1,4-bis-(trimethylsilyl)cyclooctatetraenyl dianion) (99)	Metathesis	[36]
YbCl ₃ + DippFormLi + Li ₂ COT'' in THF	Yb(DippForm)(COT'')(THF) (COT'' = 1,4-bis-(trimethylsilyl)cyclooctatetraenyl dianion) (100)	Metathesis	[37]
Y(AlMe ₄) ₃ + EtFormH in hexane	Y(EtForm)(AlMe ₄) ₂ (101)	Protolysis	[20]
Y(AlMe ₄) ₃ + MesFormH in hexane	Y(MesFormAlMe ₃)(AlMe ₄) ₂ (102)	Protolysis	[20]
Ln(AlMe ₄) ₃ + DippFormH in hexane	Ln(DippForm)(AlMe ₄) ₂ (Ln = Y (103), La (105))	Protolysis	[20]
Ln(AlMe ₄) ₃ + tBuFormH in hexane	Ln(tBuForm)(AlMe ₄) ₂ (Ln = Y (104), La (106))	Protolysis	[20]
La(AlMe ₄) ₃ + MesFormH in hexane	[La{η ¹ (N):η ⁶ (Ar)-2-Me ₃ AlCH ₂ -4,6-Me ₂ C ₆ H ₂ NCHNMe ₃ }(AlMe ₃)(AlMe ₄)] (107) and [La(2-Me ₃ AlCH ₂ -4,6-Me ₂ C ₆ H ₂ NCHNMe ₃)(AlMe ₃)(AlMe ₄)](C ₆ H ₁₄) _{1.5}] (108)	Protolysis	[20]
La(AlMe ₄) ₃ + EtFormH in toluene	[La{η ¹ (N):η ⁶ (Ar)-EtFormAlMe ₃ }(AlMe ₄) ₂](C ₇ H ₈) _{1.5} (109)	Protolysis	[20]
Y[N(SiHMe ₂) ₂] ₃ (thf) ₂ + EtFormH in hexane	Y(EtForm)[N(SiHMe ₂) ₂] ₂ (thf) (110)	Protolysis	[20]
Y[N(SiHMe ₂) ₂] ₃ (thf) ₂ + DippFormH in hexane	Y(DippForm)[N(SiHMe ₂) ₂] ₂ (thf) (111)	Protolysis	[20]
Y(CH ₂ SiMe ₃) ₃ (THF) ₂ + XylFormH in Hexane	Y(XylForm) ₂ (CH ₂ SiMe ₃)(thf) (112)	Protolysis	[38]
Ln(CH ₂ SiMe ₃) ₃ (THF) ₂ + DippFormH in Hexane	Ln[DippForm] ₂ (CH ₂ SiMe ₃)(thf) (Ln = Y (113), Er (114), Dy (115), Sm (116))	Protolysis	[38]
n-BuLi + DippFormH + NdCl ₃ + LiCH ₂ SiMe ₃	Nd[DippForm] ₂ (CH ₂ SiMe ₃)(thf) (117)	Metathesis	[38]
Yb + FFormH + Hg(C ₆ F ₅) ₂ in THF	[Yb(FForm) ₃ (thf)] (118)	RTP	[31]
La + FFormH + Hg(C ₆ F ₅) ₂ in THF	[La(FForm) ₃ (thf) ₂].thf (119)	RTP	[31]
Nd + FFormH + Hg(C ₆ F ₅) ₂ in THF	[Nd(FForm) ₃ (thf) _x] (x = 1 (120), x = 2 (121))	RTP	[31]
[La(FForm) ₃ (thf) ₂].thf dissolved in DME	[La(FForm) ₃ (dme)] (122)	Ligand exchange	[31]
Nd + FFormH + Hg(C ₆ F ₅) ₂ in THF (crystallised from diglyme)	[Nd(FForm) ₃ (diglyme)].diglyme (123)	RTP	[31]
Nd + TFFormH + Hg(C ₆ F ₅) ₂ in THF (crystallised from a mixture of DME and toluene)	[Nd(TFForm) ₃ (dme)] (124)	RTP	[31]
[Yb(TFForm) ₂ (thf) ₂] was dissolved in toluene and crystallised from mixture of toluene and hexane	[Yb(TFForm) ₃ (thf) ₂] (125)	-	[31]
[Yb(TFForm) ₂ (thf) ₂] was dissolved in diglyme and crystallised from mixture of toluene and hexane	[Yb(TFForm)(diglyme) ₂][Yb(TFForm) ₄] (126)	-	[31]
[Ce{N(SiHMe ₂) ₂] ₃ (thf) ₂] + [Li{N(SiHMe ₂) ₂ }] + DFFormH in PhMe	[LiCe(DFForm) ₄] (128)	Protolysis	[34]

complex was prepared and isolated from toluene. The THF solvated species [Ce(DFForm)₃(thf)₂] (**93**) (Fig. 2-19), can be formed by adding THF to [Ce(DFForm)₃] (**92**) but this process is irreversible. The absence of THF in the [Ce(DFForm)₃] (**92**) complex may be the main reason for having shorter Ce-N bonds in this complex compared to the Ce-N bonds in [Ce(DFForm)₃(thf)₂] (**93**). The shorter Ce-N bonds in [Ce(DFForm)₃] (**92**) allow fluorine coordination. Because of the coordinating fluorine the C_{ipso}-N-CH angle (126.4(2)–128.3(2)°) is higher compared to the [Ce(DFForm)₃(thf)₂] (**93**) complex (116.1(4)–121.4(4)°). It has been reported another Ce(III) complex [Ce₃Cl₅(DFForm)₄(thf)₄] (**94**) was synthesized by attempted oxidation of [Ce(DFForm)₃(thf)₂] with Ph₃CCl (**93**) while [Ce(EtForm)Cl₂(thf)₃] (**95**) was isolated from a similar reaction of [Ce(EtForm)₃] (**92**).

Moreover, the cerium(III) formamidinate {[Ce(*p*-TolForm)₃]₂] (**96**) was prepared in good yield (96%) using a protolysis reaction between [Ce{N(SiMe₃)₂]₃] and *p*-TolFormH ligand [34]. The structure was determined following an alternative RTP synthesis [15].

Unexpectedly, the homoleptic tris-(formamidinato)lanthanum complex [La(DippForm)₃] (**97**) (Fig. 2-20) was isolated in a very low yield from the ligand exchange reaction of [La(DippForm)₂-Me(thf)] (**33**) with 1,2,3,4-tetraphenylcyclopentadiene [23]. An earlier attempt to prepare this complex by metathesis was unsuccessful [29].

The {(Me₃Si)₂N}₂Sm{μ-(RNC(H)N(Ar-Ar)NC(H)NR)}Sm{N(SiMe₃)₂}] (**98**) complex with a coupled, bis(formamidinate) ligand (Fig. 2-21) was synthesized by reaction of solutions of N,N'-bis(2,6-diisopropylphenyl)carbodiimide and [Sm{N(SiMe₃)₂}(thf)₂] in hexane [35].

It has been reported that [N,N'-bis(2,6-diisopropylphenyl)formamidinato][η⁸-1,4-bis(trimethylsilyl)cyclooctatetraenyl](tetrahydrofuran)samarium(III) toluene monosolvate (**99**) can be synthesized by the treatment of Li(DippForm) with anhydrous samarium

trichloride and Li₂(COT'') [COT'' = 1,4-bis(trimethylsilyl)cyclooctatetraenyl] in thf [36]. The same procedure was also used to synthesize [(COT'')Yb-(DippForm)(thf)] (**100**) (Scheme 2-6) [37].

A series of Y(Form)(AlMe₄)₂ (Form = EtForm (**101**), MesForm (**102**), DippForm (**103**), tBuForm (**104**)) complexes have been synthesized by protolysis of Y(AlMe₄)₃ species (Fig. 2-22). Using the same route and La metal, La(Form)(AlMe₄)₂ (Form = DippForm (**105**), tBuForm (**106**)) complexes can be prepared [20]. Adding La(AlMe₄)₃ to one equivalent of MesFormH in hexane yields a yellow solution, from which the complexes [La{η¹(N):η⁶(Ar)-2-Me₃AlCH₂-4,6-Me₂C₆H₂NCHNMe₃}(AlMe₃)(AlMe₄)] (**107**) and [La(2-Me₃AlCH₂-4,6-Me₂C₆H₂NCHNMe₃)(AlMe₃)(AlMe₄)](C₆H₁₄)_{1.5}] (**108**) have been co-crystallised in a 1:1 ratio and result from C–H activation of a C–Me group of the mesityl moiety. The presence of a methylene ligand is the most interesting structural characteristic of this compound. The methylene ligand increases the coordination saturation of the lanthanum center and helps the η² binding of two aromatic carbon atoms (Scheme 2-7). The same method was used to synthesize [La{η¹(N):η⁶(Ar)-EtFormAlMe₃}(AlMe₄)₂](C₇H₈)_{1.5} (**109**). In this study Y[N(SiHMe₂)₂]₃(thf)₂ was treated with EtFormH and DippFormH in protolysis reactions to yield Y(EtForm)[N(SiHMe₂)₂]₂(thf) (**110**) and Y(DippForm)[N(SiHMe₂)₂]₂(thf) (**111**) respectively.

The coordination number in [La{η¹(N):η⁶(Ar)-2-Me₃AlCH₂-4,6-Me₂C₆H₂NCHNMe₃}(AlMe₃)(AlMe₄)] (**107**) is 10 and this complex contains the η¹(N):η⁶(Ar) binding mode of the metallated Form ligand. The coordination number for the La center in [La(2-Me₃AlCH₂-4,6-Me₂C₆H₂NCHNMe₃)(AlMe₃)(AlMe₄)] (**108**) is nine and AlMe₃ bridges a nitrogen donor atom and the lanthanum atom via two methyl groups. The upper product (Scheme 2-7) can be isolated pure from the filtrate after isolation of the 1:1 mixture.

A series of rare-earth metal monoalkyl complexes of formamidinates, LnL₂CH₂SiMe₃-thf [L₂ = (XylForm)₂, Ln = Y (**112**), L₂ =

(DippForm)₂, Ln = Y (**113**), Er (**114**), Dy (**115**), Sm (**116**), and Nd (**117**) (Scheme 2-8) were synthesized by alkyl elimination or salt metathesis reactions in good yields (64–73%) [38]. These compounds are similar to the reported complexes in another study (see above Scheme 2-2) [23].

Using the FFormH ligand in RTP reactions yielded [Yb(FForm)₃(-thf)] (**118**), [La(FForm)₃(thf)₂].thf (**119**) and [Nd(FForm)₃(thf)_x] (x = 1–2) (**120**, **121**) complexes [31]. These compounds were crys-

talized either from DME or diglyme/hexane to give [La(FForm)₃(dme)] (**122**) and [Nd(FForm)₃(diglyme)]₂.diglyme (**123**) complexes to allow X-ray crystal structural determinations. In an RTP reaction with Nd and after recrystallization from dme, [Nd(TFForm)₃(dme)] (**124**) was isolated. Two other complexes [Yb(TFForm)₃(thf)₂] (**125**) and [Yb(TFForm)(diglyme)₂][Yb(TFForm)₄] (**126**) were synthesized by heating [Yb(TFForm)₂(thf)₃] (**5**) in PhMe and diglyme respectively.

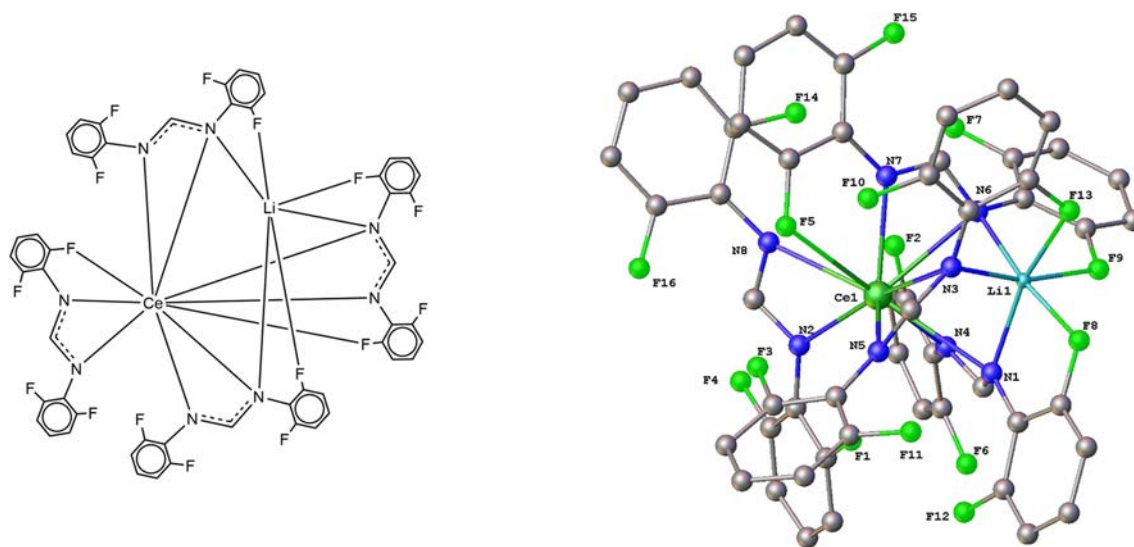
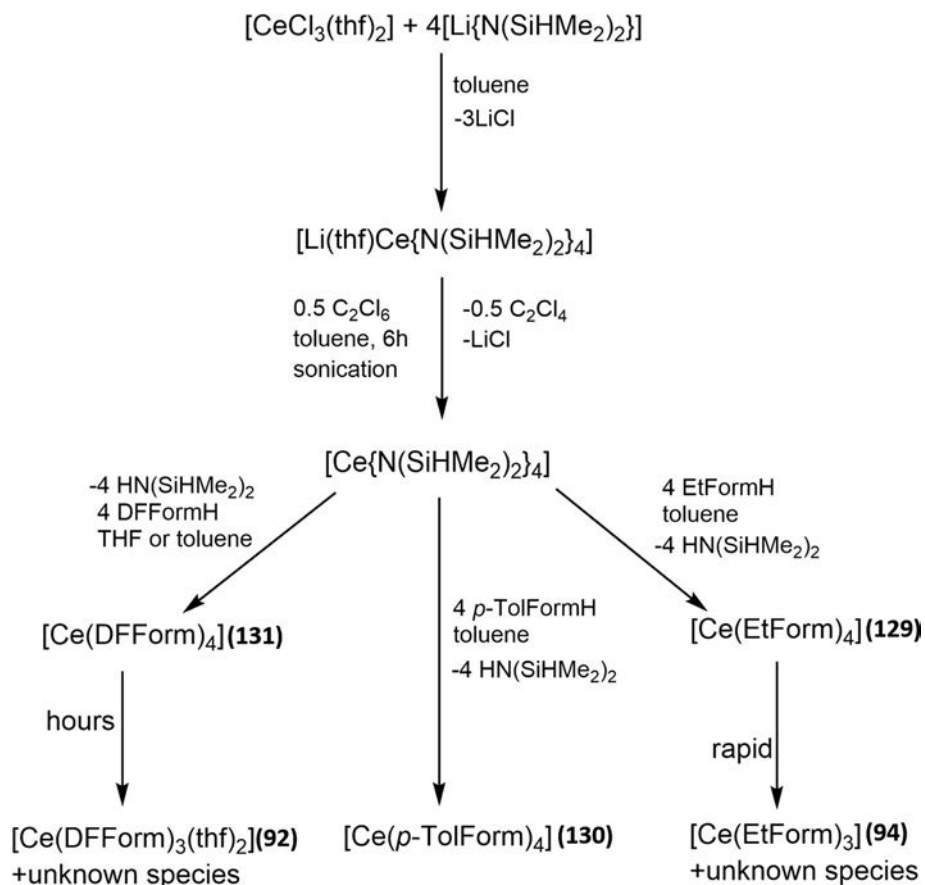


Fig. 2-23. Schematic and the X-ray structure of [LiCe(DFForm)₄] (**128**).



Scheme 2-9. The procedure of making [Ce{N(SiHMe₂)₂}₄] complex and formamidine-promoted protonolysis reactions.

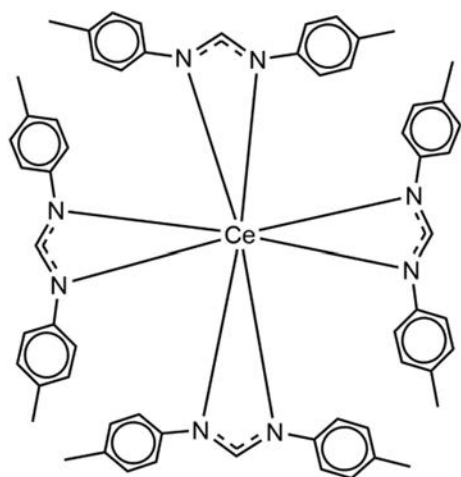


Fig. 2-24. Schematic of the X-ray structure of $[\text{Ce}(\text{p-TolForm})_4]$ (**130**).

All trivalent lanthanoid formamidinato compounds are listed in Table 2.3.1.

2.4. Tetravalent compound(s) [34]

2.4.1. Synthesis of trivalent complexes that are potential precursor of tetravalent complexes

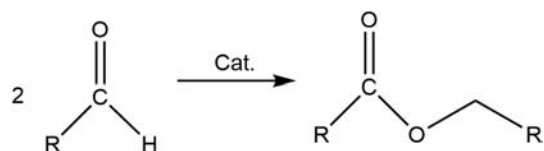
Treating a mixture of $[\text{Ce}\{\text{N}(\text{SiHMe}_2)_2\}_3(\text{thf})_2]$ and $[\text{Li}\{\text{N}(\text{SiHMe}_2)_2\}_2]$ with four equivalents of DFFormH in toluene resulted in the bimetallic cerium lithium complex $[\text{LiCe}(\text{DFForm})_4]$ (**128**). The cerium–lithium bimetallic complex $[\text{LiCe}(\text{DFForm})_4]$ (**128**) was the first reported trivalent rare-earth complex with four coordinating formamidinate ligands. The cerium atom is ten-coordinated, with eight nitrogen and two fluorine donor atoms (Fig. 2-23). The lithium atom is six-coordinate and it has closer fluorine interactions than the bridging lithium–nitrogen bond lengths. Bridging of the ligands to the larger, higher charged cerium atom maybe the main reason for inability of the lithium metal to bind closer to nitrogen. It can be seen that this complex has one terminal formamidinate ligand bound N, N', F to cerium and three formamidinate ligands bridging between cerium and lithium. The bridging formamidinate ligands have one nitrogen bridging Ce and Li, and are bond just to Ce, i.e. the ligands are chelating to Ce and unidentate to Li.

2.4.2. Protolysis of Ce(IV) amides to give Ce(IV) formamidinates

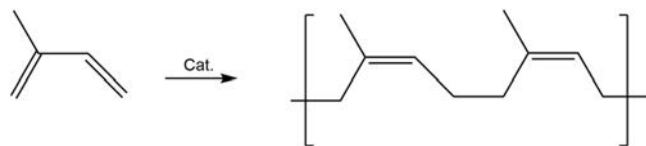
It has been reported [34] that the product of the reaction of $[\text{Ce}\{\text{N}(\text{SiHMe}_2)_2\}_4]$ with DFFormH and EtFormH are cerium(IV) complexes, e.g. $[\text{Ce}(\text{EtForm})_4]$ (**129**), which decompose before possible isolation (Scheme 2-9). Using a protolysis reaction between $[\text{Ce}\{\text{N}(\text{SiHMe}_2)_2\}_4]$ and four equivalents of *p*-TolFormH, the first structurally characterized homoleptic cerium(IV) formamidinate complex $[\text{Ce}(\text{p-TolForm})_4]$ (**130**) was obtained [35]. The coordination number of cerium in this compound is eight (Fig. 2-24). Scheme 2-9 shows the procedure of synthesising $[\text{Ce}\{\text{N}(\text{SiHMe}_2)_2\}_4]$ and the subsequent formamidine-promoted protolysis reactions. However, reaction of $[\text{Ce}\{\text{N}(\text{SiHMe}_2)_2\}_4]$ with bulkier formamidines leads to reduction giving Ce^{III} complexes (Scheme 2-9).

3. Catalysis

A series of tris(formamidinato)lanthanum(III) complexes $[\text{La}(\text{o-TolForm})_3(\text{thf})_2]$ (**57**), $[\text{La}(\text{XylForm})_3(\text{thf})]$ (**59**) and $[\text{La}(\text{EtForm})_3]$ (**65**) (synthesis by RTP reactions [26]–Table 2.3.1) have been



Scheme 3-1. Tishchenko reaction.



Scheme 3-2. Isoprene polymerisation showing only the *cis*-1,4 isomer.

reported to be precatalysts for the Tishchenko reaction. The Tishchenko reaction is the dimerization of an aldehyde to form the corresponding carboxylic ester (Scheme 3-1) and is an industrially important reaction [9]. Generally, aluminum alkoxides have been used as homogeneous catalysts for the Tishchenko reaction. [39–41] However, other catalysts such as boric acid [42] and a few transition-metal complexes have been used in the recent past [43]. Recently, some Mg compounds have been tested as catalysts for the Tishchenko reaction [44]. But these alternative catalysts are often either very expensive (e.g. $[\text{H}_2\text{Ru}(\text{PPh}_3)_2]$) [41] or give low yields (e.g. $\text{K}_2[\text{Fe}(\text{CO})_4]$) [42,44], or they are only reactive under extreme reaction conditions (e.g. boric acid) or slow (e.g. $[(\text{C}_5\text{H}_5)_2\text{-ZrH}_2]$) [43]. The lanthanoid formamidinate compounds are the most active catalyst system ever reported. Catalytic activity increases with reduced steric effect of the formamidinate ligands, with $[\text{La}(\text{o-TolForm})_3(\text{thf})_2]$ (**57**) the most effective, La is the most effective metal.

The catalytic activity of the compounds $[\text{Ln}(\text{Form})(\text{AlMe}_4)_2]$ ($\text{Ln} = \text{Y, La}$; Form = EtForm (**89, 93**), DippForm (**91, 95**)) in isoprene polymerization was investigated by activating them with $[\text{Ph}_3\text{C}][\text{B}(\text{C}_6\text{F}_5)_4]$ or $[\text{PhNMe}_2\text{H}][\text{B}(\text{C}_6\text{F}_5)_4]$. At ambient temperature, polyisoprene of narrow molecular weight distribution ($\text{PDI} < 1.2$) was produced. The stereochemical outcome of the polymerization was dependent on the catalyst; trityl tetrakis(pentafluorophenyl)borate gave *trans*-1,4-selectivity (maximum 87%), while the anilinium borate favours *cis*-1,4-selectivity (maximum 82%) [20]. The general isoprene polymerisation reaction is illustrated in Scheme 3-2 (only the *cis*-1,4 isomer is shown, *trans*-1,4, 1,2 and 3,4 polymers are also possible).

Moreover, a series of rare-earth metal monoalkyl complexes of formamidinates $\text{LnL}_2\text{CH}_2\text{SiMe}_3\cdot\text{thf}$ [$\text{L} = \text{XylForm}$, $\text{Ln} = \text{Y}$, $\text{L} = \text{DippForm}$, $\text{Ln} = \text{Y, Er, Dy, Sm, and Nd}$] were combined with $[\text{Ph}_3\text{C}][\text{B}(\text{C}_6\text{F}_5)_4]$ and alkylaluminium species to test the catalytic activity for isoprene polymerisation. The catalytic activity towards isoprene polymerization provided polyisoprenes with high molecular weight ($M_n > 10^4$) and narrow molecular weight distributions ($\text{PDI} < 2.0$) were obtained. If the catalysts were added in the order $[\text{RE}]/[\text{alkylaluminium}]/[\text{B}(\text{C}_6\text{F}_5)_4]$, 1,4-regioselectivity was reported as high as 98%. However, there was no appreciable selectivity between *cis*-1,4- and *trans*-1,4- isomers in the polymers [38].

4. Conclusions and outlook

The formamidinate complexes of rare earth metals have been reviewed. By varying the metals or the steric and electronic effects of the ligands, the structures and reactivity of the resulting complexes can be widely varied. By using formamidinates with fluorinated substituents on the arene rings, C-F activation can be

promoted. The current review offers many openings to future research involving these easy to prepare ligands, and many other related ligands can be used to provide new reactivity and structures. Unusual oxidation state chemistry for the rare earth metals remains a challenge, e.g. divalent complexes other than Eu(II), Sm(II) and Yb(II) and tetravalent complexes other than Ce(IV). The chemical and catalytic activity of some of these compounds presented has been explored but there still remains much more to be studied.

Acknowledgements

We are grateful to the Australian Research Council (DP160101640) for funding of this project.

References

- [1] F.T. Edelmann, *Adv. Organomet. Chem.*, in: A.F. Hill, M.J. Fink (Eds.), 61, Elsevier Science, 2013, pp. 55–374.
- [2] J. Barker, M. Kilner, *Coord. Chem. Rev.* 133 (1994) 219–300.
- [3] F.T. Edelmann, *Chem. Soc. Rev.* 38 (2009) 2253–2268.
- [4] F.T. Edelmann, *Chem. Soc. Rev.* 41 (2012) 7657–7672.
- [5] F.T. Edelmann, *Adv. Organomet. Chem.*, in: A.F. Hill, M.J. Fink (Eds.), 57, Elsevier Science, 2008, p. 183.
- [6] F.T. Edelmann, D.M. Freckmann, H. Schumann, *Chem. Rev.* 102 (2002) 1851–1896.
- [7] B.S. Lim, A. Rahtu, R.G. Gordon, *Nat. Mater.* 2 (2003) 749–754.
- [8] S. Bambirra, M.W. Bouwkamp, A. Meetsma, B. Hessen, *J. Am. Chem. Soc.* 126 (2004) 9182–9183.
- [9] A. Zuyls, P.W. Roesky, G.B. Deacon, K. Konstas, P.C. Junk, *Eur. J. Org. Chem.* (2008) 693–697.
- [10] M.L. Cole, P.C. Junk, *New. J. Chem.* 29 (2005) 135–140.
- [11] M.L. Cole, G.B. Deacon, C.M. Forsyth, K. Konstas, P.C. Junk, *Dalton Trans.* (2006) 3360–3367.
- [12] R.M. Roberts, *J. Org. Chem.* 14 (1949) 277–284.
- [13] P.C. Junk, M.L. Cole, *Chem. Commun.* (2007) 1579–1590.
- [14] M.L. Cole, G.B. Deacon, P.C. Junk, K. Konstas, *Chem. Commun.* (2005) 1581–1583.
- [15] G.B. Deacon, P.C. Junk, L.K. Macreadie, D. Werner, *Eur. J. Inorg. Chem.* (2014) 5240–5250.
- [16] T.J. Boyle, L.A.M. Ottley, *Chem. Rev.* 108 (2008) 1896–1917.
- [17] N. Bochkarev, L.N. Zakharov, G.S. Kalinina, *Organoderivatives of Rare Earth Elements*, Kluwer Academic Publishers 3 (1995).
- [18] K. Izod, S.T. Liddle, W. Clegg, *Inorg. Chem.* 43 (2004) 214–218.
- [19] D.M. Barnhart, D.L. Clark, J.C. Gordon, J.C. Huffman, R.L. Vincent, J.G. Watkin, B. D. Zwick, *Inorg. Chem.* 33 (1994) 3487–3497.
- [20] S. Hamidi, L.N. Jende, H. Martin Dietrich, C.C. Maichle-Mössmer, K.W. Törnroos, G.B. Deacon, P.C. Junk, R. Anwender, *Organometallics* 32 (2013) 1209–1223.
- [21] G.B. Deacon, C.M. Forsyth, S. Nickel, *J. Organomet. Chem.* 647 (2002) 50–60.
- [22] G.B. Deacon, P.C. Junk, A. Urbatsch, *Aust. J. Chem.* 65 (2012) 802–810.
- [23] M.L. Cole, G.B. Deacon, P.C. Junk, J. Wang, *Organometallics* 32 (2013) 1370–1378.
- [24] M.L. Cole, G.B. Deacon, C.M. Forsyth, P.C. Junk, K. Konstas, J. Wang, *Chem. Eur. J.* 13 (2007) 8092–8110.
- [25] G.B. Deacon, T. Feng, C.M. Forsyth, A. Gitlits, D.C. Hockless, Q. Shen, B.W. Skelton, A.H. White, *J. Chem. Soc. Dalton Trans.* (2000) 961–966.
- [26] M.L. Cole, G.B. Deacon, C.M. Forsyth, P.C. Junk, K. Konstas, J. Wang, H. Bittig, D. Werner, *Chem. Eur. J.* 19 (2013) 1410–1420.
- [27] G.B. Deacon, P.C. Junk, J. Wang, D. Werner, *Inorg. Chem.* 53 (2014) 12553–12563.
- [28] M.L. Cole, G.B. Deacon, C.M. Forsyth, P.C. Junk, D. Polo-Cerón, J. Wang, *Dalton Trans.* 39 (2010) 6732–6738.
- [29] M.L. Cole, P.C. Junk, *Chem. Commun.* (2005) 2695–2697.
- [30] G.B. Deacon, P.C. Junk, D. Werner, *Chem. Eur. J.* 22 (2016) 160–173.
- [31] G.B. Deacon, P.C. Junk, D. Werner, *Polyhedron* 103 (2016) 178–186.
- [32] G.B. Deacon, P.C. Junk, D. Werner, *Eur. J. Inorg. Chem.* (2015) 1484–1489.
- [33] R.D. Shannon, *Acta. Crystallogr. A* 32 (1976) 751–767.
- [34] D. Werner, G.B. Deacon, P.C. Junk, R. Anwender, *Chem. Eur. J.* 20 (2014) 4426–4438.
- [35] G.B. Deacon, C.M. Forsyth, P.C. Junk, J. Wang, *Inorg. Chem.* 46 (2007) 10022–10030.
- [36] A. Edelmann, C.G. Hrib, L. Hilfert, S. Blaurock, F.T. Edelmann, *Acta. Crystallogr. E* 66 (2010) m1675–m1676.
- [37] A. Edelmann, V. Lorenz, C.G. Hrib, L. Hilfert, S. Blaurock, F.T. Edelmann, *Organometallics* 32 (2012) 1435–1444.
- [38] L. Guo, X. Zhu, S. Zhou, X. Mu, Y. Wei, S. Wang, Z. Feng, G. Zhang, B. Deng, *Dalton Trans.* 43 (2014) 6842–6847.
- [39] E. Hawkins, D. Long, F. Major, *J. Chem. Soc.* (1955) 1462–1468.
- [40] F.J. Villani, F. Nord, *J. Am. Chem. Soc.* 69 (1947) 2605–2607.
- [41] I. Lin, A.R. Day, *J. Am. Chem. Soc.* 74 (1952) 5133–5135.
- [42] P.R. Stapp, *J. Org. Chem.* 38 (1973) 1433–1434.
- [43] K. Morita, Y. Nishiyama, Y. Ishii, *Organometallics* 12 (1993) 3748–3752.
- [44] B.M. Day, W. Knowelden, M.P. Coles, *Dalton Trans.* 41 (2012) 10930–10933.